

DISS. ETH NO. 26877

*Mechanistic insights into Endoplasmic Reticulum
functionality and homeostasis*

A thesis is submitted to obtain the degree of
DOCTOR OF SCIENCES ETH ZURICH
(Dr. sc. ETH Zurich)

presented by
CONCETTA GUERRA

MSc Pharmaceutical Biotechnologies, University of Padua
born on *19.10.1992*
citizen of Italy

accepted on the recommendation of
Ulrike Kutay
Maurizio Molinari
Matthias Peter

2020

TABLE OF CONTENTS

1	LIST OF ABBREVIATIONS	9
2	SUMMARY.....	13
3	RIASSUNTO.....	17
4	INTRODUCTION.....	21
4.1	The Endoplasmic Reticulum (ER) as protein factory	21
4.1.1	Architecture and functions of the ER.....	21
4.1.2	Polypeptides entry into the ER	21
4.1.3	N-glycosylation of the nascent polypeptides	23
4.1.4	Protein folding and quality control in the ER	24
4.1.4.1	Polypeptide binding to ER lectins: the CNX/CRT folding cycle	24
4.1.4.2	PQC systems	26
4.1.5	Export of correctly folded proteins from the ER	27
4.2	Catabolic pathways for misfolded proteins clearance.....	28
4.2.1	ER-associated degradation (ERAD)	28
4.2.1.1	Recognition and preparation of misfolded proteins for retro-translocation	29
4.2.1.2	Poly-ubiquitination, retro-translocation and proteasomal degradation..	29
4.2.2	ER-to lysosomes associated degradation (ERLAD)	30
4.3	Rate-limiting reactions in protein folding and ERAD	33
4.3.1	Peptidyl-prolyl bonds isomerization: PPI enzymes	33
4.3.2	Disulfide bonds formation, isomerization and reduction.....	34
4.4	The PDI family.....	36
4.4.1	PDI structure and mechanism of action.....	36
4.4.2	The Thioredoxin-related transmembrane (TMX) protein family	37
4.4.2.1	TMX1.....	38
4.4.2.2	TMX5.....	39

4.4.2.3	Other members of TMX family	40
4.5	ER stress and the Unfolded Protein Response (UPR).....	42
4.5.1	ER proteostasis and UPR induction.....	42
4.5.1.1	IRE1 pathway.....	43
4.5.1.2	ATF6 pathway	44
4.5.1.3	PERK pathway.....	44
4.5.2	How do cells recover after an ER stress: Recov-ER-phagy	45
4.6	Aim of the research projects.....	47
4.6.1	Investigation of Thioredoxin-related transmembrane protein 1 (TMX1) role in ERAD	47
4.6.2	Characterization of Thioredoxin-related transmembrane protein 5 (TMX5)	48
4.6.3	Generation of HaloTag2® chimeras as protein-based tools for the characterization of PQC systems	49
4.6.4	Transcriptional analysis of Recov-ER-Phagy process.....	50
5	PHD RESARCH PROJECTS.....	51
5.1	Thioredoxin-related transmembrane protein 1 (TMX1) as ER reductase acting in ERAD of membrane-bound folding-defective polypeptides	51
5.1.1	Results.....	51
5.1.1.1	TMX1 preferentially associates with membrane-bound folding-defective model substrates.....	51
5.1.1.2	TMX1 establishes mixed disulfides with the membrane-tethered folding- defective substrates BACE457 and NHKCD3δ	54
5.1.1.3	TMX1 preferentially intervenes in ERAD of membrane-anchored folding-defective model substrates	56
5.1.2	Discussion.....	59
5.1.2.1	Thioredoxin-related transmembrane (TMX) protein family.....	59
5.1.2.1.1	TMX1, a membrane-tethered ER reductase.....	59

5.1.2.1.2	TMX1 preferentially associates with folding-defective membrane-protein substrates delaying their degradation	61
5.1.3	Contributions.....	62
5.2	Preliminary characterization of thioredoxin-related transmembrane protein 5 (TMX5), a single-pass type-I member of the PDI protein family.....	63
5.2.1	Results.....	63
5.2.1.1	TMX5, an ER stress unresponsive member of the PDI family.....	63
5.2.1.2	TMX5 is a secreted N-glycosylated protein	64
5.2.1.3	TMX5 forms mixed disulfides with endogenous substrates.....	66
5.2.1.4	Mass spectrometry analysis of TMX5 interacting partners	67
5.2.1.5	TMX5 forms a mixed disulfide with ERp44	69
5.2.1.6	Characterization of TMX5:ERp44 complex.....	71
5.2.1.7	ERp44 regulates the sub-cellular localization of TMX5 through the formation of a mixed disulfide.....	74
5.2.2	Discussion.....	78
5.2.2.1	TMX5, a peculiar member of TMX family	78
5.2.2.1.1	TMX5, a secreted N-glycosylated PDI unresponsive to ER stress..	78
5.2.2.1.2	TMX5, a natural trapping mutant preferentially interacting with ERp44 and membrane-tethered substrates.....	79
5.2.3	Contributions.....	80
5.3	Design and development of HaloTag2®-based protein tools for the study of cellular PQC	81
5.3.1	Results.....	81
5.3.1.1	Generation of HaloTag2® protein chimeras.....	81
5.3.1.2	Biochemical characterization of the HaloTag2®-based protein chimeras	82
5.3.1.3	Intracellular localization of the HaloTag2® protein chimeras	85

5.3.1.4	HyT36 treatment induces BiP binding of the NH-HaloTag2® protein chimeras	89
5.3.1.5	Analysis of the ER stress induction by the HyT36-mediated misfolding of the HaloTag2® protein chimeras	90
5.3.2	Discussion	93
5.3.2.1	Rational of the HaloTag2®-based protein chimeras and the effects of the HyT36-mediated misfolding	93
5.3.3	Contributions.....	96
5.4	Analysis of the transcriptional response underlying Recov-ER-Phagy	97
5.4.1	Results.....	97
5.4.1.1	Concept and design of the “Recov-ER-Phagy” transcriptomic analysis	97
5.4.1.2	RNA-seq data processing and analysis	98
5.4.1.2.1	Gene enrichment analysis of differentially expressed genes	99
5.4.1.2.2	Kinetics reconstruction of the differentially expressed genes	104
5.4.2	Discussion	106
5.4.2.1	Gene enrichment analysis of the differentially expressed genes to unhide the biological processes underlying Recov-ER-Phagy	106
5.4.3	Contributions.....	109
6	CONCLUSIVE REMARKS.....	111
6.1	TMX1 and TMX5, two membrane-tethered PDI family member	111
6.2	HaloTag2® protein chimeras as tools for the characterization of the PQC systems	113
6.3	Analysis of the transcriptional response underlying “RecovER-Phagy” process	114
7	MATERIALS AND METHODS	117
8	APPENDIX	123
9	REFERENCES	141

10 ACKNOWLEDGEMENTS.....163

1 LIST OF ABBREVIATIONS

ATF	Activating transcription factor
ATG	Autophagy related
ATP	Adenosine triphosphate
ATZ	Alpha-1-antitrypsin Z
BACE	Beta-secretase
BiP	Binding immunoglobulin protein
BFA	Brefeldin A
bZIP	Basic leucine zipper domain
CHMP4B	Charged multivesicular body protein 4B
CHOP	C/EBP homologous protein
CNX	Calnexin
COPII	Coat protein complex II
CPA	Cyclopiazonic acid
CRISPR	Clustered regularly interspaced short palindromic repeats
CRT	Calreticulin
Cyp	Cyclophilin
E1	Ubiquitin activating enzyme
E2	Ubiquitin conjugating enzyme
E3	Ubiquitin ligase
EDEM	ER degradation-enhancing α -mannosidase-like protein
eIF2 α	Eukaryotic translation initiation factor 2 α
EL	Endolysosome
EndoH	Endoglycosidase H
ER	Endoplasmic reticulum
ERAD	Endoplasmic reticulum-associated degradation
ERES	Endoplasmic reticulum exit sites
ERGIC	Endoplasmic reticulum-Golgi intermediate compartment

ERLAD	Endoplasmic reticulum-to-lysosome associated degradation
ERManI	ER α 1,2-mannosidase I
ERp44 _{C/S}	ERp44 inactive mutant
ERQC	Endoplasmic reticulum quality control
ERSE	Endoplasmic reticulum stress response element
ESCRT	Endosomal sorting complexes required for transport
FDR	False discovery rate
FKBP	FK506 binding protein
GABARAP	Gamma-aminobutyric acid receptor-associated protein
GADD34	Growth arrest and DNA damage-inducible protein 34
Glc	Glucose
GlcNac	N-acetylglucosamine
GnRHR	Gonadotropin-releasing hormone receptor
GP78	Glycoprotein 78
GRP	Glucose regulated protein
GTP	Guanosine triphosphate
HEK	Human embryonic kidney cells
HERP	Homocysteine-responsive ER-resident ubiquitin-like domain member 1 protein
HRD1	HMG-CoA reductase degradation protein 1
HSP	heat shock protein
HyT36	Hydrophobic tag 36
IRE1	Inositol-requiring enzyme 1
JNK	Jun N-terminal kinase
KO	Knock-out
LC3	Light chain 3
LIR	LC3-interacting region
MAM	Mitochondria-associated membrane
Man	Mannose

MD	Mixed disulfide
MKS	Meckel-Gruber syndrome
MRH	Mannose-6-phosphate receptor homology
MLEC	Malectin
NE	Nuclear envelope
NHK	Null Hong Kong
NPC1	Niemann–Pick type C protein-1
NPL4	Nuclear protein localization protein 4
OS-9	Amplified in osteosarcoma 9
OST	Oligosaccharyltransferase
PDI	Protein disulfide isomerase
PERK	Protein kinase R (PKR)-like endoplasmic reticulum kinase
PNGase	Peptide:N-glycosidase F
PNS	Post-nuclear supernatant
PPI	Peptidyl-prolyl isomerase
PQC	Protein quality control
PTPA	Serine/threonine-protein phosphatase 2A activator
QC	Quality control
rER	Rough endoplasmic reticulum
RIDD	Regulated IRE1-dependent decay of mRNA
RNase	Ribonuclease
RTN	Reticulon
SEC	Secretory protein
sER	Smooth endoplasmic reticulum
SERCA	Sarco/endoplasmic reticulum Ca ²⁺ -ATPase
SNARE	Soluble NSF attachment protein receptor
STX17	Syntaxin 17
SRP	Signal recognition particle
SRPR	Signal recognition particle receptor

TCE	Total cell extract
TGFβ	Transforming growth factor beta
TM	Transmembrane
TMX	Thioredoxin-related transmembrane protein
TMX1 _{C/A}	TMX1 trapping mutant
TMX5 _{C/A}	TMX5 inactive mutant
TRAP	Translocon-associated protein
TRX	Thioredoxin
UFD1	Ubiquitin fusion degradation protein 1
UGGT1	UDP-glucose glycoprotein glucosyltransferase 1
UPR	Unfolded protein response
UPRE	Unfolded protein response element
VAMP8	Vesicle associated membrane protein 8
VCP/p97	Valosin-containing protein
VKOR	Vitamin K epoxide reductase
VPS	Vacuolar protein sorting
WNT	Wingless-related integration site
WT	Wild type
XBP1	X-box binding protein 1
XTP3-B	Endoplasmic reticulum lectin 1
α1AT	Alpha-1-antitrypsin

2 SUMMARY

The endoplasmic reticulum (ER) is a complex organelle divided into different sub-domains that are required for the execution of various functions, such as protein and lipid synthesis, Ca^{2+} storage and drug detoxification. The rough ER (rER), named as such by the presence of membrane-bound ribosomes on the cytosolic side of the ER membrane, is the ER sub-compartment deputed to the production of membrane and secretory proteins in the eukaryotic cells, which constitute about one third of the total cell proteome.

Translocation of the newly synthesized polypeptides into the ER represents the first step in protein biogenesis. Upon ER import, the nascent polypeptide chains are N-glycosylated by the oligosaccharyltransferase complex (OST). The OST complex catalyzes the addition of pre-assembled 14-subunits oligosaccharides ($\text{Glc}_3\text{Man}_9\text{GlcNAc}_2$) on the side chains of asparagine residues within the peculiar N-X-S/T/C consensus sequences. N-glycosylation increases the solubility of the newly synthesized polypeptides and creates binding motifs for the ER resident lectins, which help protein folding process.

As soon as the nascent polypeptides have been N-glycosylated, the last two glucoses are sequentially removed by ER-resident glucosyl hydrolases generating mono-glucosylated polypeptides that enter the calnexin-calreticulin (CNX/CRT) folding cage. CNX and CRT are two ER lectins that specifically recruit ER resident enzymes responsible for the catalysis of protein folding rate-limiting steps. These enzymes belong to the protein disulfide isomerase (PDI) and peptidyl-prolyl isomerase (PPI) families, and catalyze the formation of the correct pattern of disulfide bonds and the isomerization of the peptidyl-prolyl bonds of the maturing polypeptides, respectively.

Once released from the CNX/CRT folding cage, a strict quality control system checks the folding state of the proteins ensuring only the export of the correctly folded proteins via COPII-mediated vesicles, while misfolded polypeptides are retained into the ER and subjected to additional folding attempts. If after extensive folding the polypeptides fail to acquire their native structure, they are labelled as terminally misfolded and degraded. Misfolded proteins degradation can occur through ER-associated degradation (ERAD), which is a complex series of events that comprehends polypeptide recognition, preparation for retro-translocation, poly-ubiquitination and degradation by cytosolic proteasomes. In

this context, PDI members are involved during the preparation of misfolded polypeptides for ERAD catalyzing the disulfide bonds reduction. Misfolded proteins can also form large polymers or aggregates that cannot be retro-translocated across the ER membrane, and thus are sent to the endolysosomal compartment for clearance through a series of events named as ER-to-lysosome associated degradation (ERLAD).

A balanced equilibrium between protein synthesis, folding, export and degradation is fundamental for cells function and health. Perturbations of this equilibrium by cell-intrinsic events or external stimuli can trigger the induction of an ER stress condition. To restore the initial equilibrium, cells evolved a series of transcriptional and translational responses known as unfolded protein response (UPR). UPR activation leads to an up-regulation of ER chaperones, folding and degradative factors, a decreased translation of ER cargo proteins and an expansion of the ER membrane. If the stress condition cannot be resolved, UPR activates cell death-programs. On the other hand, if UPR resolves the ER stress situation, cells activate recovery programs, which efficiently clear excess and/or damaged ER portions generated during the stress phase to restore ER homeostasis. These catabolic pathways, recently named as Recov-ER-Phagy, ensure the delivery of specific ER sub-domains to the endolysosome for clearance ensuring the return to pre-stress conditions.

The four projects presented in this thesis represent a stepwise journey within the ER. Indeed, although different, each of the projects aimed at the characterization of ER function and homeostasis from different perspectives.

In the first project, we dissected the role in ERAD of the thioredoxin related transmembrane (TMX) protein 1 (TMX1), an ER membrane-anchored PDI, member of the TMX subfamily. We demonstrated that the ER reductase TMX1 preferentially intervenes in ERAD of membrane-tethered folding-defective polypeptides, while ignoring the same misfolded ectodomains, when not associated to the ER membrane. These findings confirmed the selectivity of TMX1 towards membrane-anchored protein clients, previously showed for folding-competent substrates, characterizing TMX1 as the first example within the PDI family of topology-specific redox-catalyst acting in both protein folding and degradation.

In the second project, we focused on TMX5, an un-characterized transmembrane PDI that belongs, as TMX1, to the TMX subfamily. We found that TMX5 is a secreted N-glycosylated protein, whose expression is not transcriptionally regulated by ER stress

induction. Through its peculiar active site, TMX5 engages mixed disulfides preferentially with endogenous membrane-bound proteins, in line with what previously demonstrated for TMX1. Additionally, our data showed that TMX5 establishes a mixed disulfide with the soluble PDI ERp44: this interaction relies on a functional ERp44 active site and mediates the retention of TMX5 within the ER, possibly regulating its function.

In the third project, we designed and generated membrane-bound variants of GFP-HaloTag2® as chimeric reporters of protein misfolding to study protein quality control (PQC) systems. HaloTag2® is a modified version of a bacterial chloroalkane dehalogenase, which misfolds upon covalent binding of the cell-permeable hydrophobic chloroalkane-reactive ligand HyT36. The generated GFP-HaloTag2® chimeric substrates are characterized by transmembrane anchors of different length, presence/absence of N-glycans, and HaloTag2® domain facing either the cytosol or the ER lumen. Our data showed that upon misfolding mediated by HyT36 binding, the HaloTag2® protein chimeras expressed in mammalian cells elicit different cellular responses according to their characteristics, being as such an ideal tool for the study of PQC machineries.

For the fourth and last project, we analyzed Recov-ER-Phagy process from the transcriptional point of view. To this aim, we performed a RNAseq analysis of stressed cells and cells at different timepoints during the recovery phase. Gene enrichment analysis of differential expressed genes showed that upon ER stress, cells activate UPR, while down-regulating components of the other ER biosynthetic pathways and genes linked to cells growth. This trend is reversed as soon as the stress stimulus is relieved meaning that cells are recovering. Interestingly, upon initiation of the recovery phase, components of the WNT signaling pathway resulted up-regulated: these genes have been recently shown to regulate the function of proteins belonging to the ESCRT machinery, some of which are involved in Recov-ER-Phagy. Finally, these analyses revealed that most of the components of Recov-ER-Phagy pathway are not transcriptionally regulated, suggesting that this process could be most likely and alternatively regulated by post-transcriptional mechanisms.

All in all, the projects presented in this thesis enlarged our current knowledge on the players and mechanisms regulating ER homeostasis and functionality.

3 RIASSUNTO

Il reticolo endoplasmatico (RE) è un organello complesso suddiviso in diversi sottodomini che svolgono diverse funzioni, come la sintesi di proteine e di lipidi, il deposito di Ca^{2+} e la metabolizzazione di farmaci. Il RE rugoso (RER), così denominato per la presenza di ribosomi legati alla membrana del RE sul lato citosolico, costituisce il compartimento deputato alla biogenesi delle proteine di membrana e secretorie nelle cellule eucariotiche, le quali rappresentano circa un terzo del proteoma totale della cellula.

La traslocazione nel RE rappresenta l'evento iniziale nella sintesi e maturazione delle proteine. Successivamente all'importazione nel RE, le proteine vengono N-glicosilate dalla oligosaccariltransferasi (OST). L'OST catalizza l'aggiunta di un'oligosaccaride costituito da 14 subunità ($\text{Glc}_3\text{Man}_9\text{GlcNAc}_2$) su un residuo di asparagina contenuto all'interno delle specifiche sequenze consenso N-X-S/T/C. Questa modifica aumenta la solubilità delle proteine e crea sequenze specificamente riconosciute da lectine localizzate nel RE, che aiutano le proteine ad acquisire la loro struttura corretta.

La catena oligosaccaridica delle glicoproteine viene successivamente processata da idrolasi del RE generando polipeptidi mono-glucosilati che entrano nel programma di ripiegamento gestito dalle lectine calnexina (CNX) e calreticulina (CRT). CNX e CRT reclutano in modo specifico degli enzimi residenti nel RE responsabili della catalisi di alcune fasi limitanti nel processo di ripiegamento delle proteine. Questi enzimi appartengono alle famiglie delle disolfuro isomerasi (PDI) e peptidil-prolil isomerasi (PPI) e catalizzano rispettivamente la formazione di ponti disolfuro e l'isomerizzazione dei legami peptidil-prolil.

Al termine della fase di ripiegamento, un rigoroso sistema di controllo verifica la struttura delle proteine assicurando che solo le proteine correttamente ripiegate lascino il RE tramite vescicole COPII. Le proteine mal ripiegate vengono trattenute nel RE e sottoposte ad ulteriori tentativi di ripiegamento. Se le proteine non riescono ad acquisire la loro struttura nativa vengono etichettate come prodotti aberranti e degradate. La degradazione può avvenire tramite il processo denominato come *ER-associated degradation* (ERAD), che comprende una serie di eventi come il riconoscimento dei polipeptidi mal ripiegati, la loro linearizzazione per facilitare la retro-traslocazione, la poli-ubiquitinazione e la loro degradazione operata dai proteasomi citosolici. Alcune PDI sono coinvolte durante il

processo di linearizzazione dei polipeptidi mal ripiegati, catalizzando la riduzione dei ponti disolfuro. In alcuni casi, i prodotti aberranti possono formare grandi polimeri o aggregati che non possono essere retro-traslocati attraverso la membrana del RE, e vengono portati al lisosoma per essere degradati attraverso una serie di eventi denominati come *ER-to-lysosome associated degradation* (ERLAD).

Il mantenimento di una situazione di equilibrio tra sintesi, ripiegamento, esportazione e degradazione delle proteine risulta fondamentale per garantire la funzione e la sopravvivenza delle cellule. La perturbazione di questo equilibrio da parte di diversi fattori interni o stimoli esterni può indurre una condizione di stress all'interno del RE. Per risolvere la situazione di stress, le cellule hanno sviluppato una serie di risposte trascrizionali e traslazionali che vanno sotto il nome di *unfolded protein response* (UPR). L'attivazione dell'UPR induce un aumento nella quantità di fattori ripieganti, enzimi e componenti di ERAD, ma anche una ridotta sintesi proteica e un'espansione della membrana del RE. Se lo stress non può essere risolto, l'UPR attiva dei programmi di morte cellulare. Se invece la situazione di stress viene risolta efficientemente, le cellule attivano dei processi catabolici che portano all'eliminazione di porzioni del RE in eccesso e/o danneggiate generate durante lo stress, così da ripristinare l'omeostasi del RE. Questi processi sono stati recentemente denominati come *Recov-ER-Phagy* e assicurano che specifici sottodomini del RE vengano portati al lisosoma affinché siano degradati.

I quattro progetti presentati in questa tesi rappresentano un viaggio a tappe attraverso la caratterizzazione di diversi processi consequenziali che avvengono nel RE. Infatti, sebbene diversi, ciascuno dei progetti mira alla caratterizzazione da diverse prospettive delle funzioni e dei processi deputati al mantenimento dell'omeostasi del RE.

Nel primo progetto, abbiamo analizzato il ruolo in ERAD della proteina TMX1, una PDI legata alla membrana che fa parte della sottofamiglia TMX. Abbiamo dimostrato che TMX1 interviene preferibilmente nell'ERAD di proteine mal ripiegate legate alla membrana, ignorando le loro controparti non associate alla membrana del RE. Questi risultati hanno confermato la selettività di legame di TMX1 nei confronti di proteine di membrana, precedentemente dimostrata nella caratterizzazione del ruolo di TMX1 nel ripiegamento delle proteine. I dati mostrati caratterizzano TMX1 come primo esempio all'interno della famiglia delle PDI di catalizzatore redox che agisce sia nel ripiegamento che nella degradazione di proteine che presentano una determinata topologia.

Nel secondo progetto, abbiamo caratterizzato la proteina TMX5, una PDI legata alla membrana che appartiene, come TMX1, alla sottofamiglia TMX. In questo lavoro abbiamo dimostrato che TMX5 è una proteina N-glicosilata che viene esportata dal RE e non è regolata trascrizionalmente da uno stress del RE. Attraverso il suo peculiare sito attivo, TMX5 stabilisce preferibilmente complessi legati da ponti disolfuro con proteine endogene legate alla membrana, similmente con quanto precedentemente dimostrato per TMX1. Inoltre, i nostri dati hanno mostrato che TMX5 stabilisce un complesso mediato da ponti disolfuro con ERp44, una PDI solubile: questa interazione viene mediata dal sito attivo di ERp44 e induce la ritenzione di TMX5 all'interno del RE, probabilmente regolandone la sua funzione.

Nel terzo progetto, abbiamo costruito varianti chimeriche di GFP-HaloTag2® legate alla membrana come reporter di *misfolding* per studiare i sistemi cellulari che si occupano di controllare la struttura delle proteine. HaloTag2® è una versione modificata di una dealogenasi batterica, che assume una conformazione mal ripiegata a seguito del legame con il ligando idrofobico HyT36. Le chimere GFP-HaloTag2® generate presentano caratteristiche diverse come regioni transmembrana di lunghezza variabile, la presenza o l'assenza di N-glicani e il dominio HaloTag2® rivolto verso il citoplasma o il lume del RE. I nostri dati hanno mostrato che quando le chimere GFP-HaloTag2® espresse in cellule di mammifero vengono mal ripiegate in seguito al legame di HyT36 inducono risposte cellulari diverse in base alle loro caratteristiche chimico-fisiche. A seguito di ciò, esse costituiscono uno strumento ideale per lo studio dei sistemi cellulari deputati al controllo della struttura delle proteine.

Per il quarto e ultimo progetto, abbiamo analizzato dal punto di vista trascrizionale il processo di Recov-ER-Phagy. Per tale scopo, abbiamo eseguito un'analisi RNAseq dei trascritti di cellule stressate e di cellule durante diverse fasi di *recovery* da stress del RE. *Gene enrichment analysis* dei geni differenzialmente espressi ha rivelato che in seguito all'induzione dello stress, le cellule attivano l'UPR e allo stesso tempo riducono l'espressione di componenti legati ad altre vie biosintetiche del RE e di geni collegati alla crescita cellulare. Questa tendenza si inverte non appena lo stimolo che induce lo stress viene alleviato, dimostrando l'entrata delle cellule nella fase di *recovery*. Abbiamo inoltre notato che all'inizio del *recovery* la trascrizione dei componenti del *WNT signaling* risulta indotta: per questi geni è stato recentemente dimostrato che sono in grado di regolare la funzione di componenti della *ESCRT machinery*, alcuni dei quali sono coinvolti nel

processo di Recov-ER-Phagy. Infine, queste analisi hanno rivelato che la maggior parte dei componenti che mediano il processo di Recov-ER-Phagy non sono regolati trascrizionalmente, suggerendo che questo processo potrebbe essere in alternativa regolato da meccanismi post-trascrizionali.

Nel complesso, i progetti presentati in questa tesi ampliano le nostre attuali conoscenze sui fattori e i meccanismi che regolano l'omeostasi e la funzionalità del RE.

4 INTRODUCTION

4.1 The Endoplasmic Reticulum (ER) as protein factory

4.1.1 Architecture and functions of the ER

The Endoplasmic Reticulum (ER) is the largest organelle within eukaryotic cells¹. It is constituted by a series of continuous membranous structures delimiting a common intraluminal space that spans through the cytosol^{2,3}. It is architecturally organized into different specialized sub-compartments defined by the presence of various integral membrane proteins, contact sites with other organelles and the cytoskeleton¹. Its complex structural organization reflects its complexity from the functional point of view. In fact, the existence of specialized sub-domains displaying unique features is required for the accomplishment of many different tasks, from protein and lipid synthesis to calcium storage and drug detoxification¹. Historically, the ER has been divided into smooth (sER) and rough ER (rER), constituted by a network of branched tubules and flat sheets³⁻⁷. Beyond this main division, the ER also includes other specialized sub-domains, such as the nuclear envelope (NE), the contact sites with different organelles⁸ (e.g. mitochondria, peroxisomes, endosomes, lysosomes) and ER exit sites^{1,9}. All in all, the ER architecture displays an high degree of plasticity, where the relative abundance of each sub-compartment is characteristic of a particular cell type and can be remodeled according to the diverse cellular needs^{10,11}.

In general, the sER is mainly constituted by tubular structures¹² and is the site of lipid synthesis¹³, drug metabolism^{14,15} and protein export¹⁶. On the other hand, the rER is constituted by a series of sheet-like structures characterized by the presence of ribosomes bound to its cytosolic side, responsible for its “rough” aspect¹. Its peculiar appearance is a strong clue of rER function: in fact, it is the sub-domain designated for the synthesis and folding of membrane and secretory proteins, which count for about one third of the total proteome in eukaryotic cells¹⁷⁻¹⁹.

4.1.2 Polypeptides entry into the ER

Translocation of the nascent polypeptide chains within the ER is the first step in the biogenesis of membrane-bound and proteins destined to the secretory pathway. This process can occur either co-translationally or post-translationally²⁰, but in both cases it requires the recognition and targeting of the polypeptide to the ER, the association with the

translocation machinery, and eventually its energy dependent import²¹. The first step of targeting is ensured by the presence of a cleavable N-terminal signal sequence within the nascent polypeptide. This signal is typically an amino acid stretch of 15-30 residues composed by an hydrophobic core flanked by a N-terminal positively charged region and a polar uncharged C-terminal region²²⁻²⁷. During co-translational translocation, the signal recognition particle (SRP) recognizes and binds the signal peptide as soon as it emerges from the ribosome²⁸. SRP binding slows down protein translation allowing the mRNA-ribosome-SRP complex to reach the ER surface thanks to the interaction with the SRP receptor (SRPR)²⁸⁻³². The association between SRP and its receptor induces GTP binding and hydrolysis in both proteins²⁰. Consequently, the complex is resolved and the nascent polypeptide chain is transferred to the translocon complex, placed in close proximity to the SRPR^{33,34}. Once completed this step, protein translation re-starts. Alternatively, in post-translational translocation, the polypeptide is fully synthesized within the cytosol, where it is bound by the cytosolic chaperones belonging to the heat shock protein (HSP) family HSP70 and HSP40^{35,36}. These proteins keep the nascent polypeptide chain in a soluble state, preventing its premature folding, and drive its interaction with the translocon complex³⁶.

Membrane insertion and physical translocation of the nascent polypeptide across the ER membrane are accomplished thanks to the translocon complex, that is composed by the heterotrimeric complex SEC61 (SEC61 α 1, SEC61 β and SEC61 γ). The three subunits are spatially organized to build a proteinaceous channel through which the elongating polypeptide slides into the ER^{37,38}. Translocation of some polypeptide chains requires the assistance of additional components, such as the ER luminal chaperone BiP and the membrane translocon-associated protein (TRAP) complex, which bind the nascent polypeptide chain and act as a ratchet driving its unidirectional transport into the ER lumen³⁹⁻⁴². The association between BiP and the polypeptide is facilitated by the J domain containing proteins (e.g. ERj1) and SEC63⁴³, whereas the ATP hydrolysis and the nucleotide exchange activity are ensured by the intervention of SIL1 and GRP170^{44,45}.

Furthermore, SEC61 complex can be complemented by the additional components SEC62 and SEC63 to facilitate post-translational translocation of newly synthesized polypeptides⁴⁶. Others important constituents of the translocation machinery are the signal peptidase complex, which cleaves the signal peptide from the nascent polypeptide⁴⁷, and the oligosaccharyltransferase (OST) complex that catalyzes protein N-glycosylation⁴⁸.

4.1.3 N-glycosylation of the nascent polypeptides

Most of the polypeptides entering the ER are subjected to N-glycosylation^{49,50}. This modification consists in the covalent attachment of a pre-formed sugar moiety made of three glucoses, nine mannoses and two N-acetylglucosamines (Glc₃Man₉GlcNAc₂) to the side chain of an asparagine residue included within a specific consensus sequence (N-X-S/T/C, where X is any amino acid except proline) (**Figure 1**)^{50,51}.

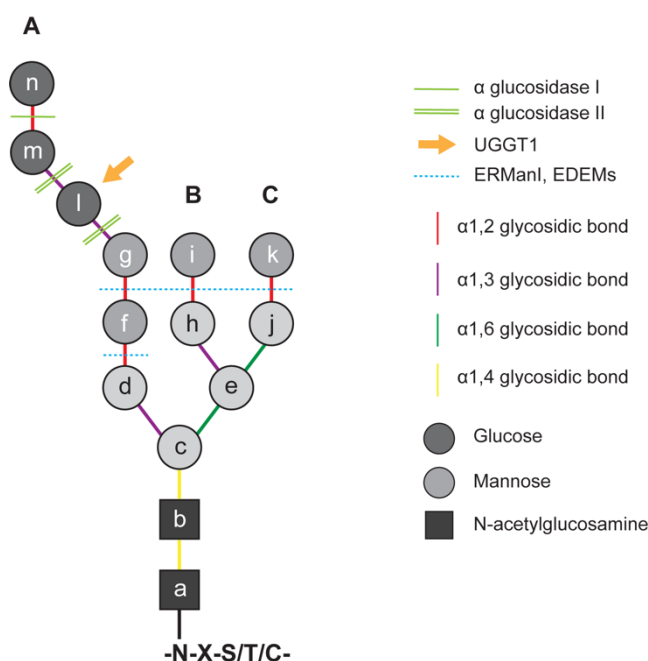


Figure 1: N-glycan structure and processing. (Elaborated from Tannous et al. 2015)

The OST complex catalyzes the transfer reaction of the 14-subunits oligosaccharide from a lipid carrier (i.e. dolichylpyrophosphate) to the amide side chain of the designated asparagine residue^{48,49}. In mammals, the OST complex is a membrane-bound heteromeric structure composed by a catalytic subunit (STT3A or STT3B) and six other proteins (ribophorin I, ribophorin II, OST48, OST4, N33 or MAGT1, and DAD1)^{48,52,53}. While STT3A is involved in N-glycosylation of co-translationally imported polypeptides, its paralogue STT3B catalyzes post-translational N-glycosylation⁵⁴.

N-glycosylation is an highly conserved modification among eukaryotes⁵⁵. It enhances the solubility of the newly synthesized polypeptides, but also stabilizes mature proteins hiding hydrophobic patches or immunogenic sites^{56,57}. In the ER context, N-linked glycans represent crucial signal molecules for protein folding process: indeed, the covalent addition of these oligosaccharides creates binding sites for the ER lectins, which assist glycoproteins

folding⁵⁸⁻⁶⁰. Reflecting its pivotal importance in different cellular processes, impairments within N-glycosylation pathway are at the basis of different human diseases⁶¹.

4.1.4 Protein folding and quality control in the ER

4.1.4.1 Polypeptide binding to ER lectins: the CNX/CRT folding cycle

As soon as the pre-assembled 14-units oligosaccharide is attached to the nascent polypeptide chain, it starts to be processed⁶⁰. The first cleavage operated by the α -glucosidase I removes the outermost α 1,2-linked glucose (**Figure 1**) giving rise to a diglycosylated glycan^{57,62}. Once this moiety has been exposed, it is selectively bound by the ER resident lectin malectin (MLEC) (**Figure 2**, step 1)^{63,64}. MLEC is a single-pass type I protein, which is up-regulated upon ER stress⁶⁴. In complex with ribophorin I, MLEC efficiently binds misfolded glycopeptides retaining them within the ER^{65,66}.

Trimming of the second outermost glucose unit by α -glucosidase II produces a monoglycosylated glycan (**Figure 1**) competent for the binding to the ER lectins calnexin (CNX) and calreticulin (CRT)⁶⁷⁻⁶⁹. This step determines the entry of the polypeptide within the CNX/CRT folding cycle (**Figure 2**, step 2)⁷⁰. CNX is a single pass type I protein, while CRT is its soluble paralogue. These two proteins show a sequence similarity of about 39% and a similar structural organization⁷¹. In fact, they share a N-terminal globular domain containing the lectin binding site, calcium (Ca^{2+}) binding sites and a P-domain, named as such since it is enriched in proline residues^{72,73}. Despite their good degree of similarity, CNX and CRT preferentially bind different subsets of client proteins⁷⁴. Once the maturing polypeptide is bound by CNX/CRT, these proteins recruit in turn, thanks to their P-domains, different ER resident enzymes such as ERp57⁷⁵ (**Figure 2**, step 2b) and Cyclophilin B (CypB)⁷⁶. These two proteins belong to the protein disulfide isomerase (PDI) and peptidyl-prolyl isomerase (PPI) families, respectively, and catalyze two rate-limiting steps during protein folding^{77,78}. While the PPIs promote the isomerization of the peptidyl-prolyl bonds, the members of the PDI family catalyze the formation of the native set of intra- and inter-molecular disulfide bonds within the newly synthesized polypeptides⁵⁸. Both topics will be object of further discussion in **5.3** sub-chapter.

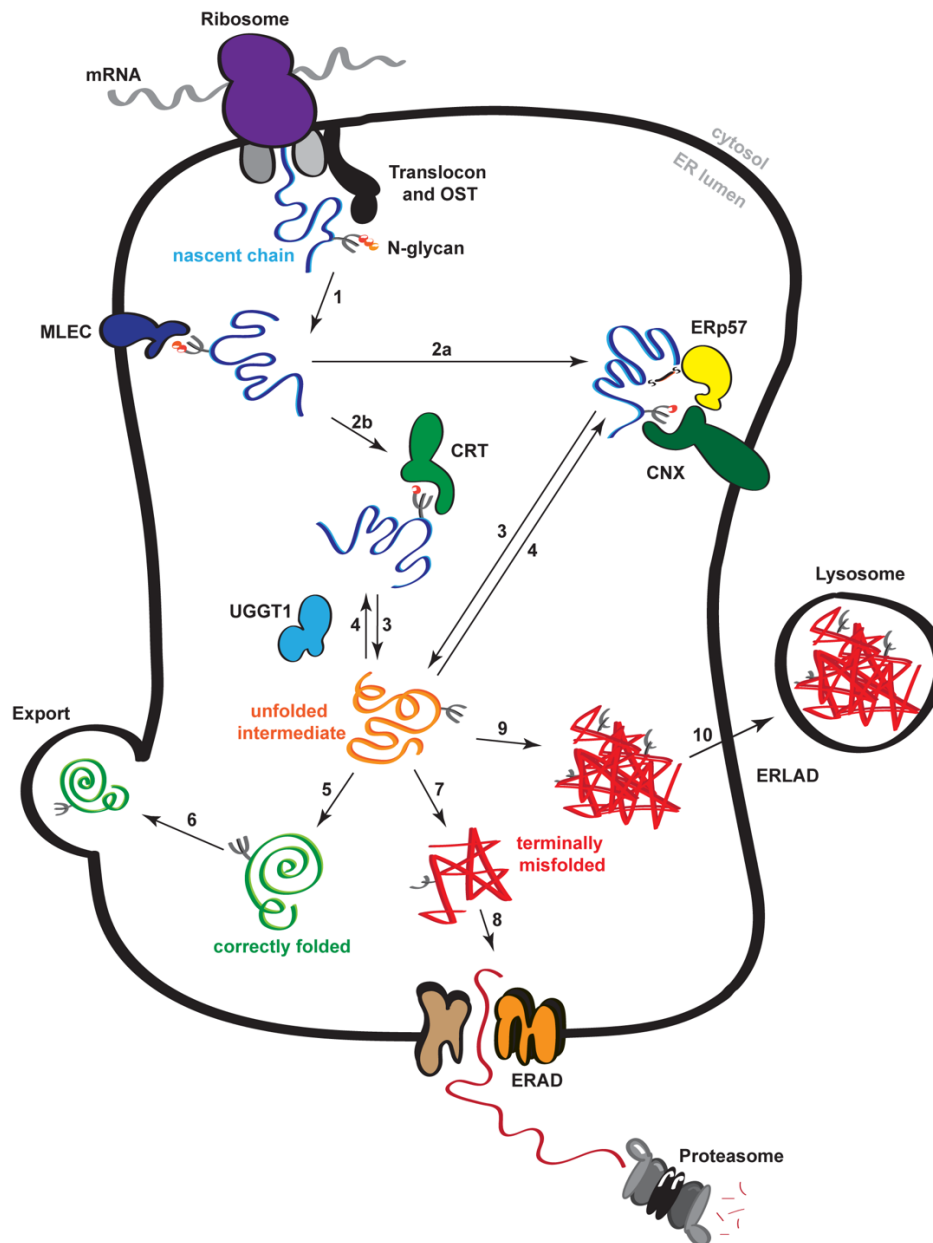


Figure 2: Protein folding and quality control in the ER. As soon as the N-glycan is added by the OST complex to the newly synthesized polypeptide, α -glucosidase I cleaves the outermost glucose allowing MLEC binding (**step 1**). α -glucosidase II removes the second glucose residue. This mono-glucosylated moiety is bound by CNX and CRT (**step 2a and b**), which can recruit in turn ERp57 promoting the formation of the native disulfide bonds (**step 2a**). Removal of the last glucose by the α -glucosidase II causes polypeptide release from CNX/CRT (**step 3**). UGGT1 checks polypeptide folding state and catalyzes the re-glucosylation of the unfolded intermediates to allow their re-association with CNX/CRT (**step 4**). Several cycles of association and dissociation from CNX/CRT can occur to attain polypeptide native structure (**step 3-4**). Once correctly folded (**step 5**), proteins can exit the ER (**step 6**). Polypeptides that fail to achieve their native conformation are labelled as terminally misfolded and their N-glycans are further trimmed upon the removal of the terminal mannose residue (**step 7**) to allow retro-translocation into the cytosol for proteasomal degradation (**step 8**). Misfolded aggregates (**step 9**) that are too large to be retro-translocated across the ER membrane are delivered via vesicular pathways to the lysosome for clearance (**step 10**).

α -glucosidase II is also responsible for the cleavage of the last glucose residue within the N-linked glycans (**Figure 1**)⁶⁷. As such, it determines the release of the protein substrate from CNX and CRT, since these two lectins display very poor affinity for the de-glucosylated species (**Figure 2**, step 3)⁷⁹. Since folding efficiency is not the same for all proteins, it could happen that a particular substrate requires more than a single round in the CNX/CRT folding cycle to reach the native conformation⁸⁰.

4.1.4.2 PQC systems

Only correctly folded proteins can be exported to reach their final destination, while incompletely folded polypeptides are retained within the ER lumen. To ensure this process, cells evolved a sophisticated quality control machinery that is able to discriminate folded from unfolded structures, bind the latter and eventually retaining them in the ER⁸¹. Specific folding sensors check protein frameworks looking for solvent-accessible hydrophobic patches and unpaired cysteine residues, which are characteristic signs of unfolded structures^{82,83}. Once recognized, misfolded proteins can be re-addressed to the folding machinery for further folding attempts. However, if after several rounds the polypeptides fail to achieve their correct conformation, these are recognized and labelled as terminally misfolded, and eventually committed to degradation⁸⁴. The correct working of this mechanism of surveillance is crucial, since the accumulation of aggregated misfolded intermediates or incompletely folded protein complexes can be very dangerous for the cells⁸⁵. Indeed, this phenomenon constitutes the basis of many human diseases^{86,87}.

After protein substrate release from CNX/CRT, the UDP-glucose:glycoprotein glucosyltransferase 1 (UGGT1) checks its folding status⁸⁸. UGGT1 is a soluble ER-resident glycoprotein structurally organized in a N-terminal folding sensor domain and a C-terminal glucosyltransferase domain⁸⁹. The N-terminal folding sensor domain adopts a flexible curved conformation with a central hydrophobic cavity, which recruits high-mannose structures via hydrophobic interactions⁹⁰. Upon recruitment through the N-terminal region, the C-terminal domain of UGGT1 catalyzes the re-addition of the terminal glucose unit (**Figure 1**) to the incompletely folded protein to ensure its re-binding to CNX/CRT and determining in turn its retention in the ER for an additional folding attempt (**Figure 2**, step 4)^{88,89}. Consequent cycles of CNX/CRT binding, glucose trimming by α -glucosidase II and UGGT1-mediated re-glucosylation allow misfolded substrates retention within the ER, while fostering their folding through interactions with ER chaperones and folding

enzymes⁶⁰. In this way, UGGT1 plays the role of the CNX/CRT cycle gatekeeper⁹¹, which determines glycoproteins' fate within the secretory pathway.

Another important checkpoint is represented by the thiol-mediated QC^{83,92}. Since most of the cysteine residues within a protein sequence are paired in disulfide bonds before trafficking through the secretory pathway, the exposure of free cysteines suggests that a protein is not correctly folded. As such, specific ER sensors recognize exposed thiols mediating proteins retention within the ER, in a model suggested by the observation that unassembled IgM subunits exposing C-terminal cysteines in lymphocytes B are not secreted from the ER⁹³.

4.1.5 Export of correctly folded proteins from the ER

Once passed the quality control check (**Figure 2**, step 5), correctly folded proteins can travel through the secretory pathway to reach their final destination. Notably, a post-ER quality control checkpoint has been reported: it is operated by UGGT1 in combination with VCP/p97 and prevents the export to the Golgi of cargo proteins showing native ectodomains, but defects at the level of the transmembrane regions⁹⁴.

Protein export from the ER occurs at specialized sites known as transitional ER or ER exit sites (ERESs) (**Figure 2**, step 6)⁹⁵. Here, cargo proteins are packed into coat protein complex II (COPII) coated vesicles and bud from the ER to reach the Golgi apparatus^{96,97}. Homotypic fusion events between COPII-coated vesicles can occur giving rise to the ER-Golgi intermediate compartment (ERGIC)^{98,99}. Cargo exit from the ER can be a receptor-mediated process, or occur by bulk flow¹⁰⁰. Usually, in the first case, the receptor engages the protein substrate through its glycans or by protein-protein interactions. Indeed, the cleavage of mannose i (**Figure 1**) operated by ERManI¹⁰¹ allows protein interaction with different lectin receptors as ERGIC53, VIPL and VIP36¹⁰². On the other hand, in the bulk flow *modus operandi*, correctly folded proteins diffuse and enter COPII-coated vesicles^{103,104}, while misfolded proteins are retained thanks to the action of ER resident chaperones.

4.2 Catabolic pathways for misfolded proteins clearance

4.2.1 ER-associated degradation (ERAD)

Protein folding is not a completely accurate process. In fact, it has been estimated that about 30% of the newly synthesized proteins are not correctly folded¹⁰⁵ and this rate can incredibly rise in the case of genetic mutations or cellular stresses^{106,107}. An adequate removal of the misfolded proteins is needed to protect ER homeostasis and in turn cells' health. This can happen through the ER-associated degradation, shortly ERAD, which is defined as an highly conserved and complex series of events including a step of recognition of the misfolded substrates, their preparation for retro-translocation, poly-ubiquitination and eventually their degradation by the cytosolic proteasomes (**Figure 3**)¹⁰⁸.

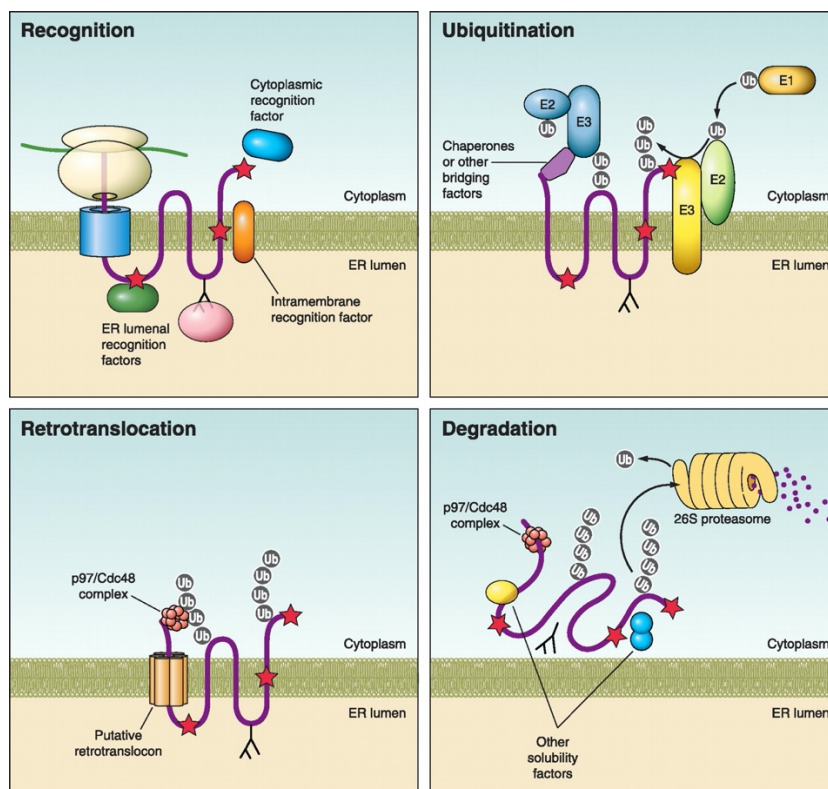


Figure 3: Schematics of the ER-associated degradation steps. Recognition of the misfolded substrate by ER lectins and chaperones, which respectively recognize specific N-glycan structures and exposed hydrophobic patches. **Ubiquitination** of the misfolded substrate catalyzed by the sequential intervention of E1, E2 and E3 enzymes. **Retrotranslocation** is helped by the AAA ATPase VCP/p97 that provides the mechanical force through ATP hydrolysis. Once in the cytosol, the misfolded polypeptide is kept soluble by different cytosolic factors, and then it undergoes de-ubiquitination and de-glycosylation prior proteasomal **degradation**. (From Guerriero and Brodsky 2012)

4.2.1.1 Recognition and preparation of misfolded proteins for retro-translocation

After several unsuccessful cycles of folding, glycoproteins undergo extensive de-mannosylation (**Figure 2**, step 7), which determines the definitive exit from CNX/CRT folding cycle and eventually their recognition as ERAD substrates (**Figure 2**, step 8)¹⁰⁷. The progressive trimming of mannose units starts from the action of ERMAnI that generates a Man₈GlcNAc₂ isomer (**Figure 1**). This moiety is subjected then to further trimming operated by ER degradation-enhancing alpha-mannosidase like (EDEM) 1¹⁰⁹⁻¹¹¹, EDEM2¹¹²⁻¹¹⁴ and EDEM3¹¹⁵. Trimming of the outermost mannose of the branch C exposes the mannose j (**Figure 1**), which is recognized by the ERAD lectins OS-9 and XTP3-B and bound through their mannose-6-phosphate receptor homology (MRH) domains¹¹⁶⁻¹²⁰. This interaction allows the transfer of the misfolded glycoproteins to the dislocation machineries (**Figure 3**, Recognition)^{120,121}.

Recognition and ERAD targeting of non-glycosylated misfolded polypeptides are still less well understood. Interactions of the ERAD lectins OS-9 and XTP3-B with both BiP and GRP94 have been reported, hinting that these ER chaperones could recognize incorrectly folded substrates to directly address them to ERAD.^{116,122}

Recognition and shuttling of misfolded proteins to the dislocon complex are usually followed by a step of substrates preparation^{123,124}. Linearization of the polypeptides structure facilitates their retro-translocation across the ER membrane for ERAD¹²⁵. PDI and PPI family members take care of this step. Indeed, many PDIs and PPIs have been shown to be involved in the reduction of disulfide bonds¹²⁶ and in the cis-trans isomerization of peptidyl-prolyl bonds¹²⁷, respectively, to help the disassembly of the tertiary/quaternary protein structures prior their dislocation and degradation by the cytosolic proteasomes (more details in 5.3). Of note, retro-translocation of misfolded proteins that do not require a step of preparation has been also reported¹²⁸.

4.2.1.2 Poly-ubiquitination, retro-translocation and proteasomal degradation

Retro-translocation of misfolded products to the cytosol for proteasomal degradation relies on dislocation machineries, that are large protein complexes embedded within the ER membrane. Several candidates have been suggested as protein scaffolds forming the channel through which misfolded substrates are extracted from the ER. Among them, we find SEC61¹²⁹, signal peptidases¹³⁰, Derlins 1-3^{131,132} and HRD1¹³³⁻¹³⁵.

The retro-translocation process is coupled with substrates' poly-ubiquitination, a modification that requires the consequent action of different proteins¹⁰⁸. E1 enzymes activate the ubiquitin, which is then transferred to E2 ubiquitin-conjugating enzymes and eventually delivered to E3 ubiquitin-ligases that are responsible for the ubiquitination reaction of selected protein substrates (**Figure 3**, Ubiquitination)^{136,137}. Dislocon complexes are built around the E3 ubiquitin-ligases: in mammalian cells, 24 distinct enzymes have been identified so far¹³⁸, with HRD1¹³⁹ and GP78¹⁴⁰ as the best known members. Other than E3-ligases, retro-translocation machineries rely on the help of adaptor proteins, which allow substrates recognition and regulate the activity of the E3 ligase enzymes. SEL1L is one excellent example: this protein serves as scaffold for the recognition of many protein substrates and stabilizes the HRD1-dislocon based complex^{116,141,142}. Indeed, SEL1L has been shown to interact with the luminal acceptors OS-9, XTP3-B, EDEM1, BiP or GRP94, shuttling protein substrates to the dislocation machinery^{116,122,143,144}. Another important adaptor protein is HERP that, thanks to its short half-life, acts as a regulator of the HRD1-based dislocon assembly and function¹⁴⁵⁻¹⁴⁷. The variety of the players involved in these processes implicates the existence of different alternative dislocation complexes, each one taking rid of a specific subset of misfolded substrates.

Consequently to the poly-ubiquitination, the extraction of the protein substrates from the ER is driven by the action of the AAA ATPase VCP/p97 (**Figure 3**, Retro-translocation)¹⁴⁸. In combination with its co-factors, UFD1 and NPL4, and the ATP hydrolysis, VCP/p97 mediates the unidirectional transport to the cytosol of poly-ubiquitinated clients¹⁴⁸⁻¹⁵⁰. As the substrates emerge from the ER, they are degraded by the 26S cytosolic proteasomes (**Figure 3**, Degradation). The intervention of de-ubiquitinating enzymes (DUBs) and Peptide:N-glycanases (PNGases) ensures an efficient protein transition within the proteasomal pore, allowing its prompt degradation¹⁵¹.

4.2.2 ER-to lysosomes associated degradation (ERLAD)

Since the ER does not contain catabolic devices, the misfolded proteins are retro-translocated within the cytosol and degraded by the cytosolic proteasomes through ERAD¹⁰⁸. However, misfolded proteins can also form polymers or aggregates, that are too large to be dislocated across the ER membrane. These ERAD-resistant proteins are instead delivered to the lysosomes for clearance through an ensemble of autophagic and non-autophagic pathways collectively defined as ER-to-lysosomes-associated degradation

(ERLAD) process^{152,153}. In the literature, many examples of ERAD-resistant misfolded proteins have been reported so far, including β -subunits of the thyrotrophic hormone¹⁵⁴, various mutants of the serpin proteins¹⁵⁵⁻¹⁵⁸, mutant dysferlin¹⁵⁹, endogenous and ectopic expressed collagen¹⁶⁰⁻¹⁶², mutant of the gonadotropin releasing hormone receptor (GnRHR)¹⁶³, the mutant Niemann–Pick type C protein-1 (NPC1)¹⁶⁴, and proinsulin aggregates¹⁶⁵. Similarly to what has been found for ERAD in the past years¹³⁹, description of ERLAD route for handful of these proteins showed that cells evolved different mechanisms to get rid of misfolded polymers or aggregates with different characteristics.

α 1-antitrypsin Z (ATZ) is a mutant form of the serine protease inhibitor α 1-antitrypsin (α 1AT)¹⁵⁵. This protein forms large ERAD-resistant polymers, whose removal from the ER lumen requires the intervention of ERLAD¹⁵⁸. During this process, ATZ polymers are segregated with the help of the ER lectin CNX in specific ER sub-domains, decorated with the ER-phagy receptor FAM134B¹⁵⁸. These sub-domains undergo scission generating single-membrane vesicles containing ATZ polymers, but not CNX. The vesicles are then transported to the endolysosomal compartment, where LC3 is engaged by the LC3 interacting region (LIR) displayed by FAM134B, allowing vesicles docking to the endolysosomes¹⁵⁸. As final step, the intervention of the SNAREs Syntaxin17 (STX17) and Vesicle-associated membrane protein 8 (VAMP8) allows vesicles fusion to release ATZ polymers within the lumen of the endolysosomes for clearance¹⁵⁸.

The same receptor FAM134B is also responsible for the lysosomal degradation of the endogenous misfolded procollagen¹⁶². This occurs through an ERLAD pathway that shows several differences compared to the one described for ATZ¹⁵⁸. As first step, the endogenous misfolded procollagen is recognized by CNX that interacts with FAM134B¹⁶². Afterwards, FAM134B engages LC3 on the autophagosomal membranes, which enwrap ER sub-regions containing both misfolded procollagen and CNX, ensuring their delivery to the endolysosomes for clearance¹⁶². As such, although the intervention of the same receptor, ERLAD degradation of the endogenous misfolded procollagen relies on the formation of double membrane autophagosomes¹⁶², which are dispensable for ATZ delivery to the endolysosomes¹⁵⁸. Of note, a recent work showed that misfolded procollagen degradation can also occur through an alternative microautophagic-like process, where lysosomes directly engulf specialized ER-exit sites containing ectopic procollagen¹⁶¹. However, mechanistic details of this pathway are still not known.

Another ERLAD pathway has been postulated for the degradation of the misfolded proinsulin *Akita* mutant. Although the molecular mechanisms of this pathway are still not clearly defined, it has been shown that the lysosomal clearance of *Akita* aggregates relies on the intervention of the ER-phagy receptor RTN3, which mediates a process that does not require RTN3 functional LIRs¹⁶⁵.

4.3 Rate-limiting reactions in protein folding and ERAD

4.3.1 Peptidyl-prolyl bonds isomerization: PPI enzymes

Polypeptide chains are made by the *ensemble* of different amino acids kept together by peptide bonds. This kind of linkage is naturally planar with the flanking C α that can adopt either a *cis* or a *trans* conformation, where the latter is the most common, since it is energetically favored. This preference is generally true, except in the case of linkages involving a proline residue (i.e. prolyl bond)¹⁶⁶⁻¹⁶⁸. The spontaneous *cis-trans* isomerization of the prolyl bonds is quite slow (in order of hundreds of seconds)¹⁶⁹ and it represents a rate-limiting step in both protein folding^{123,170} and substrates preparation for ERAD¹⁷¹. Thus, the intervention of the peptidyl-prolyl isomerases (PPIs) results crucial (**Figure 4**).

PPI family members are sub-divided into four sub-groups: cyclophilins (Cyps), FK506 binding proteins (FKBPs), parvulins and the serine/threonine-protein phosphatase 2A activator (PTPA)^{58,172-174}. Cyps activity is blocked by the immunosuppressive and anti-rejection drug cyclosporine A, while the FKBPs are inhibited by FK506 and rapamycin¹⁷⁵⁻¹⁷⁷. For PPIs, quite little is known about their substrate's specificity and redundancy. Several studies highlighted that different PPI family members are not in the same protein complex, suggesting that these enzymes could cooperate with different ER chaperones, according to the type of substrate or process in which they are involved^{178,179}.

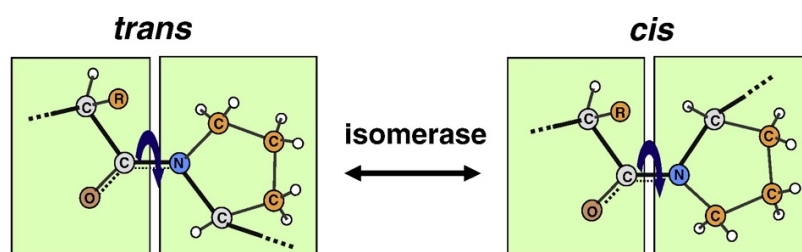


Figure 4: Schematics of peptidyl-prolyl *cis-trans* isomerization catalyzed by the PPI proteins.

(From Hanes 2015)

Interestingly, some members of the FKBPs have a chaperone-like activity in addition to their PPIase function: indeed, these proteins have been shown to bind hydrophobic patches exposed by the misfolded proteins preventing their aggregation^{174,180}.

4.3.2 Disulfide bonds formation, isomerization and reduction

Disulfide bond is defined as a covalent linkage established through an oxidation reaction between the thiol groups of two cysteine residues¹⁸¹. Due to its more oxidizing nature compared to the cytosolic compartment, this reaction is more likely to occur within the ER environment¹⁸², even though disulfide bonds can be also established within the cytosol¹⁸³ or the mitochondria¹⁸⁴. Disulfide bonds formation can occur between two cysteines of the same polypeptide (intramolecular) or of two distinct polypeptides (intermolecular) to form an oligomeric complex. Thus, the formation of disulfide bonds stabilizes tertiary or quaternary protein structures¹⁸⁵. The establishment of the correct set of disulfide bonds does not only require a step of oxidation, but also reduction (i.e. breakage) and isomerization (i.e. shuffling) of mispaired linkages (**Figure 5**)¹⁸⁶.

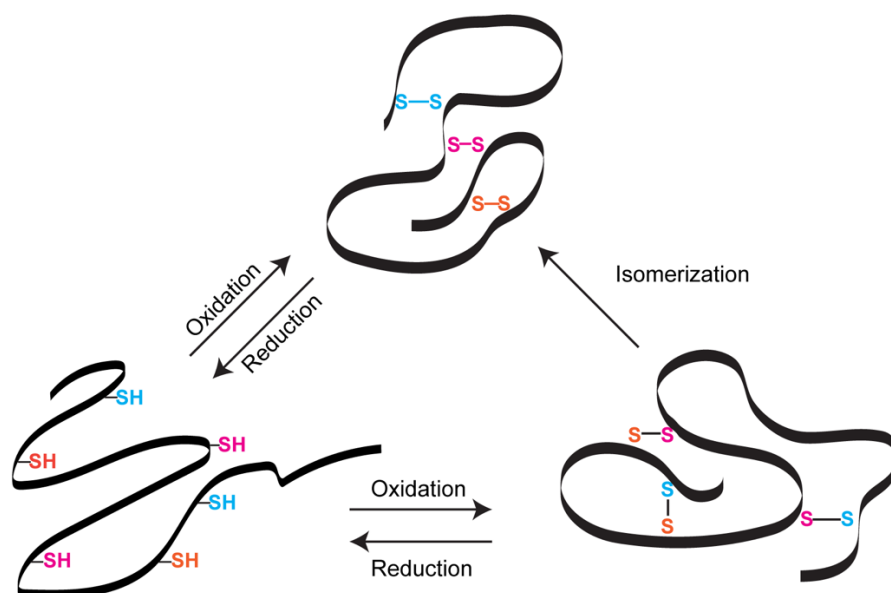


Figure 5: Schematics of disulfide bonds formation. Native disulfide bonds are established through oxidation, reduction and isomerization reactions, which are catalyzed by the PDI family members.

Potentially, a disulfide bond can form between any couple of exposed cysteine residues: as such, greater is the number of cysteines within a polypeptide sequence, greater is the possibility to form non-native disulfide bonds. Thus, their formation constitutes a rate-

limiting step during protein folding and the intervention of protein disulfide isomerase (PDI) enzymes is required to successfully accomplish this task¹⁸⁷.

Besides its critical importance in protein folding, reduction and rearrangement of disulfide bonds have also a pivotal role in substrates preparation prior ERAD. Indeed, other than protein structure stabilization, disulfide bonds can also create large oligomers of misfolded proteins, which do not fit across the retro-translocation channel, and therefore must be reduced by the intervention of PDIs¹⁸⁸.

4.4 The PDI family

4.4.1 PDI structure and mechanism of action

In mammalian cells, more than 20 members of the PDI family have been identified so far⁵⁸ (Table 1). Despite these proteins differ in size, membrane topology and tissue distribution, they have all in common the presence of at least one thioredoxin (TRX)-like domain, which can be either catalytically active (a) or inactive (b)^{186,189}.

Protein	Structure	Active sites	Function
PDI	abb'xa'	CGHC, CGHC	O, R, I, C
ERp57	abb'xa'	CGHC, CGHC	O, R, I
ERp72	a ⁰ abb'xa'	CGHC, CGHC, CGHC	O, R, I
P5	aa'b	CGHC, CGHC	O, R, I
ERp44	abb'	CRFS	Ero1 binding and Thiol QC
ERdj5	Ja''ba ⁰ aa'	CSHC, CPPC, CHPC, CGPC	R
PDIp	abb'xa'	CGHC, CTHC	O, R, I, C
PDILT	abb'xa'	SKQS, SKKC	Ero1 binding
PDIr	ba ⁰ aa'	CSMC, CGHC, CPHC	O, R, I
ERp46	a ⁰ aa'	CGHC, CGHC, CGHC	?
ERp18	a	CGAC	O, VKOR binding
hAGR2	a	CPHS	?
hAGR3	a	CQYS	?
TMX1	at	CPAC	R, VKOR binding
TMX2	ta	SNDC	?
TMX3	abb't	CGHC	O
TMX4	at	CPSC	O, R, VKOR binding
TMX5	at	CRFS	?
ERp29	b	-	?
ERp27	bb'	-	ERp57 binding
N33/Tusc3		CSVC	OST complex subunit
IAP/MagT1		CVVC	OST complex subunit
ERp90		-	ERFAD interactor

Table 1: PDI family. a, active TRX-like domain; b, inactive TRX-like domain; x, linker domain; J, J-domain; t, transmembrane domain. The active site composition of each PDI is shown in the third column. O, oxidation; R, reduction; I, isomerization; C, chaperone activity.

Little is known about the function of the inactive **b**-type, for which several studies suggested a role as substrate binding site¹⁹⁰. Type-**a** TRX-like domain is characterized by an active site usually containing a CXXC motif: the cysteine residues constitute the redox active core, while the surrounding residues influence the pKa of the cysteines, determining the local redox potential and in turn the overall activity of the PDI as oxidase or reductase¹⁹¹. As working model, the N-terminal cysteine of the CXXC active site performs a nucleophilic attack towards a thiol group of a protein substrate, forming a transient reaction intermediate between the PDI and the substrate known as mixed-disulfide (MD), while the intervention of the C-terminal cysteine resolves the interaction¹⁹¹. Several PDIs do not display a classical CXXC active site within their TRX-like domains (**Table 1**). Indeed, alternative active sites missing either the N-terminal or the C-terminal cysteine have been found. PDIs missing the N-terminal cysteine are unable to perform the nucleophilic attack, and thus they result catalytically inactive^{192,193}. Instead, proteins lacking the C-terminal cysteine within the active site sequence can still perform a nucleophilic attack towards a substrate protein, resulting in the formation of a MD: however, this interaction is stabilized, since it can be resolved only by the intervention of an external thiol group supplied by other PDIs or by the protein substrate itself¹⁹⁴.

Many members of the PDI family possess an ER stress responsive (ERSE) motif¹⁹⁵ within their promoter region, which is responsible for their upregulation upon ER stress induction, hinting an important role of some PDIs during UPR (see 4.5)¹⁹⁴. Considering their differences in structural organization, size and active site composition, it is likely that PDIs are not broadly equivalent and that each of them would act as a reaction catalyst towards a select group of substrates, and also in different cellular processes. However, the absence of relevant phenotypes in individual PDIs knock-out models let hypothesize about a functional redundancy¹⁸⁹.

4.4.2 The Thioredoxin-related transmembrane (TMX) protein family

Most of the members of the PDI family are soluble proteins. One exception is represented by a small sub-group known as thioredoxin-related transmembrane (TMX) proteins, which counts five transmembrane proteins (TMX1, TMX2, TMX3, TMX4 and TMX5) (**Figure 6**)¹⁹⁶. TMX proteins are characterized by a N-terminal ER signal peptide, one or more transmembrane regions of variable length and one type-**a** TRX-like domain displaying different active site sequences¹⁹⁴. Among the five members, TMX1 represents the best described, while TMX5 is the least characterized.

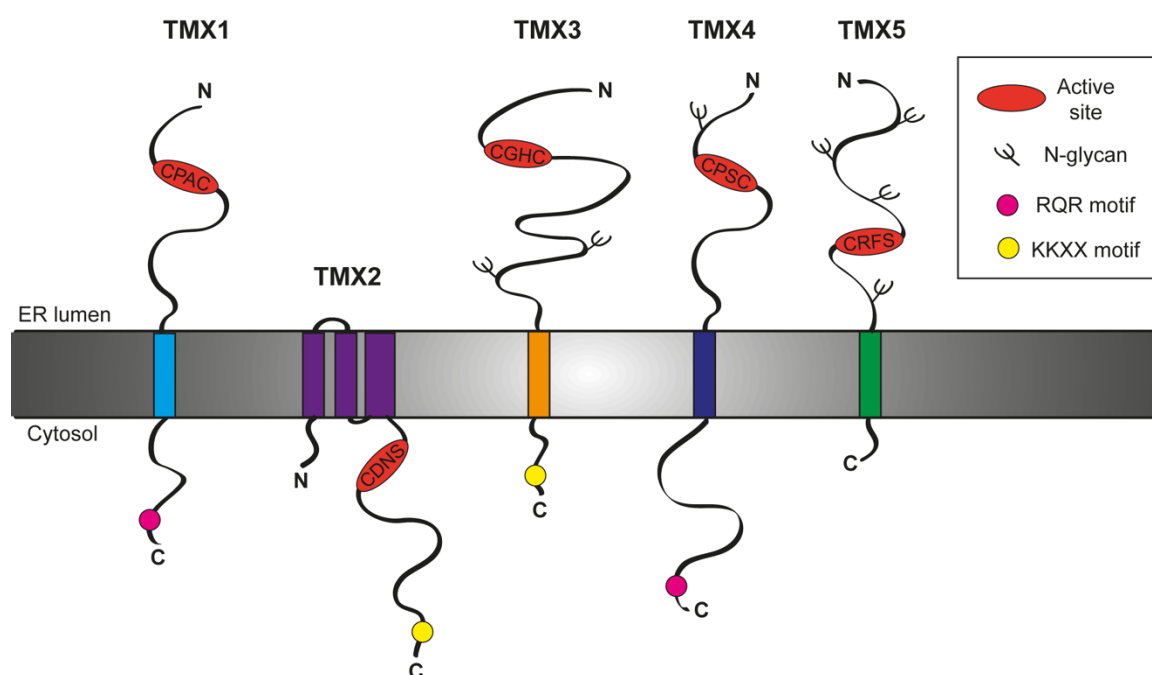


Figure 6: Schematic representation of TMX family members. Active site composition, topology, N-glycosylation state and retention motifs are shown in the scheme.

4.4.2.1 TMX1

TMX1 has been identified in 2001¹⁹⁷ in a screening among the responsive genes for TGF- β ¹⁹⁸. It is a non-glycosylated protein of 281 amino acids¹⁹⁷. It possesses a large N-terminal luminal domain and a C-terminal cytosolic portion lacking a canonical ER retention signal¹⁹⁷. Alternatively, it has been proposed that an RQR motif within the C-terminal tail mediates its ER retention and localization¹⁹⁹. TMX1 harbors a TRX-like domain within its N-terminal region, which contains a non-canonical CPAC active site¹⁹⁷. The presence of a proline in position 2 indicates a role of TMX1 as reductase¹⁹¹. Indeed, TMX1 reduces insulin disulfides *in vitro*¹⁹⁷, and *in vivo* is predominantly found in the reduced form²⁰⁰. Moreover, its overexpression enhances the cytotoxicity of the type 2 ribosome-inactivating proteins ricin and abrin, which require a reduction step in the ER prior retro-translocation of the catalytic subunit within the cytosol²⁰¹.

Unlike other members of the PDI family, TMX1 does not contain an ERSE motif within its promoter region¹⁹⁴, and indeed it is not up-regulated upon ER stress²⁰². Notably, it has been shown that TMX1 is reversibly oxidized upon ER stress induced by brefeldin A (BFA)

treatment: BFA unbalances protein export from the ER, leading to the accumulation of unfolded substrates and the consequent induction of an ER stress; in this condition, TMX1 results oxidized in a reversible manner, suggesting a role as redox gatekeeper to cope with protein overload²⁰³. TMX1 expression is ubiquitous with the highest levels in liver, kidney, lungs and placenta¹⁹⁷. Consistent with its high expression in liver, TMX1 knockout mice exhibit no evident defects, as in cellular culture, except for an higher susceptibility to liver damage upon treatment with lipopolysaccharides (LPSs)²⁰⁴. An important interactor of TMX1 is VKOR, a membrane bound co-factor of the ER electron transfer pathway. The high expression of VKOR in liver tissue suggested its possible role as redox partner for TMX1²⁰⁵.

TMX1 is the first member of the PDI family showing a topology-specific behavior in protein folding, preferentially binding folding-competent membrane-tethered substrates²⁰⁶. Thanks to the exploitation of a trapping-mutant version, it has been demonstrated that TMX1 establishes mixed disulfides with membrane-bound clients selectively delaying their maturation and secretion²⁰⁶. TMX1 also forms a functional complex with CNX^{202,206}, that is mediated by the transmembrane regions²⁰². Additionally, this functional complex is stabilized by the presence of protein substrates, suggesting that TMX1 recruits its membrane-bound clients through cooperative interaction with the ER lectin CNX²⁰⁶.

In addition to its role in protein folding, TMX1 seems also to act as a regulator of the Ca²⁺ homeostasis. Indeed, palmitoylation of two cysteine residues within its C-terminal region determines TMX1 targeting to the MAM, i.e. contact sites between ER and mitochondria. In this context, TMX1 binds the Ca²⁺-ATPase SERCA2b decreasing its activity and increasing in turn the calcium flux from the ER to the mitochondria²⁰⁷.

4.4.2.2 TMX5

TMX5 (also known as TXNDC15) is a poorly characterized member of the TMX family that has been identified in 2003²⁰⁸. It is a single-pass type I protein of 360 amino acids with four predicted N-glycosylation sites and no ER retention signal. As the other TMX proteins, it harbors one type-**a** TRX-like domain within its N-terminal region. Of note, this domain displays a non-canonical CRFS active site: this sequence characterizes TMX5 as a natural trapping-mutant protein, suggesting a distinct role of this protein compared to the other family members.

Recently mutations within TMX5 sequence have been associated to several perinatally lethal autosomal recessive ciliopathies, as the Meckel syndrome (MKS). In particular, frame-shift and missense mutations that alter the overall protein expression or lead to the production of a truncated protein version, have been reported²⁰⁹⁻²¹¹.

4.4.2.3 Other members of TMX family

Beyond TMX1 and TMX5, other three proteins belong to the TMX protein family. TMX2 is non-glycosylated protein of 296 amino acids. It has been identified in 2003 and its expression is ubiquitous, with the highest levels in brain, liver, kidney, heart and pancreas¹⁹³. Despite it has been predicted as a single-pass type II protein¹⁹³, it has been recently shown that TMX2 is a multi-span transmembrane protein with both the N- and the C-termini facing the cytosol²¹². Its C-terminal domain harbors a KKDK retention signal and a TRX-like domain¹⁹³. The latter contains a peculiar SNDC active site sequence that, lacking of the canonical N-terminal cysteine, results catalytically inactive as oxidoreductase²¹². TMX2 can be localized in the nuclear outer membrane²¹² or at the MAM upon palmitoylation²⁰⁷. Its alternative localization suggests that TMX2 could be involved in different processes: indeed, at the nuclear envelope, TMX2 interacts with the importin- β and the GTPase Ran to maintain the nucleocytoplasmic Ran protein gradient, and ensure in turn an efficient nuclear import of the importin- β cargo proteins²¹². On the other hand, palmitoylated TMX2 interacts with the Ca²⁺ pump SERCA2b regulating calcium flux at the MAM²¹³. Interestingly, TMX2 results up-regulated upon oxidative stress, but not upon ER stress, hypoxia or heat shock induction²¹². Moreover, TMX2 knockout experiment in primary neurons demonstrated its protective function from ER stress²¹⁴, while missense mutations have been recently associated to human patients with microlissencephaly and brain developmental abnormalities^{213,215}.

TMX3 is a single-pass type I protein of 454 amino acids that has been identified in 2005²¹⁶. It displays a large N-terminal luminal domain containing two N-glycosylation sites²¹⁷ and a short C-terminal cytosolic tail harboring a KKKD retention sequence²¹⁶. TMX3 is not up-regulated upon ER stress and it is broadly expressed in all human tissues, with the highest levels in heart and skeletal muscle²¹⁶. TMX3 contains 3 TRX-like domains, one type-**a** characterized by a canonical CGHC active site, responsible for TMX3 behavior as oxidase in vitro, and two enzymatically inactive type-**b** domains²¹⁸. Preliminary studies suggested a protective role of TMX3 in mice models for Huntington's disease²¹⁹.

TMX4 is a single-pass type I protein of 349 amino acids and it is considered the paralogue of TMX1²²⁰. It has been identified in 2010²²⁰ and contains one N-glycosylation site within its N-terminal region¹⁹⁹. As TMX1, TMX4 lacks a canonical cytosolic ER retention signal, but it displays the di-arginine RQR motif¹⁹⁹. Consistent with the lack of an ERSE motif within its promoter region, TMX4 is not up-regulated upon ER stress induction²²⁰. TMX4 has a non-canonical CPSC active site sequence within its type-a TRX-like domain²²⁰: similarly to TMX1, this sequence contains a proline in position 2, which destabilizes the disulfide state and favors the di-thiol reduced form of the active site^{191,221}. Consistently, also TMX4 acts as reductase in vitro²²⁰ and it weakly interacts with VKOR²⁰⁵. TMX4 knockdown has no effects on degradation of ERAD substrates²²⁰, suggesting that it is not involved in this pathway, or that other proteins may compensate its absence. More interestingly, it has been shown that TMX4 interacts with CNX and ERp57, suggesting a role as reductase within the folding pathway²²⁰.

4.5 ER stress and the Unfolded Protein Response (UPR)

4.5.1 ER proteostasis and UPR induction

ER proteostasis is defined as the capacity to keep cell's proteome in the proper quantity and quality²²². Its maintenance is of crucial importance to ensure cells, tissues and organisms functionality and health²²³. A sustained inward flux of nascent polypeptides can overwhelm the folding capacity of the ER, leading to an accumulation of unfolded proteins, and eventually to an unbalanced ER proteostasis²²⁴. Other conditions that can perturb ER proteostasis include exogenous stimuli as nutrient deprivation, hypoxia, alterations in temperature or redox conditions, drugs, attacks by pathogens, but also endogenous events such gene mutations, cell differentiation and aging. These perturbations alter the normal function of the ER leading to a condition of ER stress²²⁵⁻²²⁸. In this situation, a series of transcriptional and translational events are activated in order to restore ER proteostasis. This program goes under the name of Unfolded Protein Response, or shortly UPR²²⁹. During UPR, genes encoding for ER chaperones and folding enzymes^{230,231}, components of the export machinery²³², together with enzymes dedicated to lipid synthesis²³³⁻²³⁵, are transcriptionally up-regulated. Concomitantly, general translation of ER cargo proteins is repressed^{236,237}, while ER turnover is increased to clear damaged ER sub-regions or stockpile of misfolded proteins generated during the stress^{153,238}. The overall meaning of these measures aims to resolve the overwhelming pressure on the ER allowing the return to its homeostatic conditions. If the stress cannot be alleviated and resolved, the prolonged UPR brings to the activation of cell-death programs^{239,240}.

In mammalian cells, the UPR activation is orchestrated by the action of three ER stress sensors embedded within the ER membrane: the kinase/RNase inositol-requiring protein 1 (IRE1)²⁴¹, the activating transcription factor 6 (ATF6)²⁴² and the protein kinase RNA-like ER kinase (PERK)²³⁶. The mechanisms leading to the activation of these sensors are still not completely understood. One hypothesis, defined as competition model, is that the ER chaperone BiP binds at steady state the luminal domains of the stress sensors, keeping them inactive. Upon misfolded proteins accumulation within the ER lumen, these compete for BiP binding, causing its detachment from the sensors' luminal domains and the consequent UPR cascade activation²⁴³⁻²⁴⁸. Another hypothesis is represented by the model of direct binding, according which misfolded proteins directly bind the luminal domains of the sensors leading to their activation²⁴⁹⁻²⁵¹. In this case, BiP regulates the shutdown of the response by binding to the sensors' luminal domains²⁴⁸.

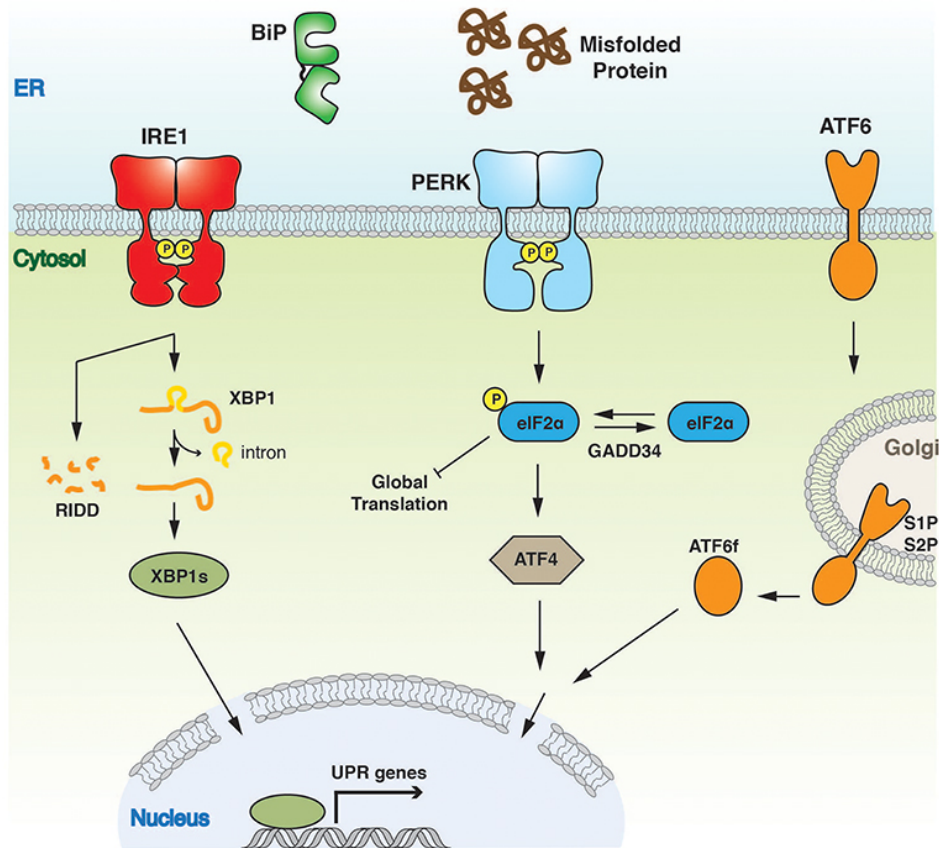


Figure 7: The three branches of the unfolded protein response (UPR). IRE1, PERK, and ATF6 represent the UPR stress sensors that mediate the activation of the transcriptional and the translational responses aiming to the restoration of the ER homeostasis.

4.5.1.1 IRE1 pathway

Identified as ER stress sensor in the late 1980s, IRE1 represents the only UPR branch conserved from yeast to human. In metazoan, two distinct isoforms of IRE1 have been described: IRE1 α , whose expression is ubiquitous and its knockout is embryonal lethal²⁵²; IRE1 β , which has an expression restricted to the respiratory and the gastrointestinal tracts and no particular phenotypes are observed if knocked out in mice models^{253,254}. As such, IRE1 α represents the most studied isoform²⁵⁵.

IRE1 α is a single-pass type I membrane protein with a N-terminal luminal stress sensor domain and a C-terminal cytosolic region containing both serine/threonine kinase and endoribonuclease (RNase) activities^{224,256,257}. Upon activation, IRE1 α oligomerizes and undergoes trans-autophosphorylation, enabling its RNase activity that is responsible for the

unconventional splicing of XBP1 mRNA²⁵⁸⁻²⁶². Spliced XBP1 (sXBP1) encodes for a transcription factor, which translocates into the nucleus to promote the transcription of genes involved in protein folding and secretion, ERAD and lipid synthesis^{230,231,263}. sXBP1 mediates this process through binding to ER stress response elements (ERSE)¹⁹⁵, ERSE II²⁶⁴ and UPR elements (UPRE)²⁶⁵ that are present within the promoter region of the target genes. RNase activity of IRE1 α is also responsible for the so called regulated IRE1-dependent decay (RIDD)²⁶⁶: during this process, ribosomal RNAs²⁶⁷, mRNAs²⁶⁸⁻²⁷⁰ and miRNAs^{271,272} are degraded to smooth the pressure on the ER biosynthetic compartment.

In case of sustained UPR, IRE1 α activates a signaling cascade leading to cell death²⁷³. In particular, this occurs through an uncontrolled RIDD activity that ends up with the degradation of anti-apoptotic miRNAs^{271,272}, but also through the activation of c-Jun N-terminal kinase (JNK) and apoptosis by a phosphorylation cascade^{274,275}.

4.5.1.2 ATF6 pathway

ATF6 has two isoforms in vertebrates, ATF6 α and ATF6 β , with the first showing stronger transcriptional activity *in vivo*²⁷⁶. ATF6 α is a single-span type II membrane glycoprotein, which displays a basic leucine zipper (bZIP) motif within its N-terminal cytosolic region²⁴². Interestingly, upon ER stress burden, ATF6 α is transported to the Golgi compartment²⁷⁷ where it is sequentially processed by two endopeptidases site-1 (S1P) and site-2 (S2P)^{243,278}. Their action results in the release within the cytosol of the bZIP domain (known as ATF6f), which upon nuclear translocation acts as a transcription factor. Indeed, ATF6f binds to ERSE¹⁹⁵ and ERSE II²⁷⁹ motifs to mediate the transcription mainly of ER folding enzymes and ERAD factors.

4.5.1.3 PERK pathway

PERK is a single-pass type I protein and represents the third branch of the UPR. Upon activation, it oligomerizes and undergoes trans-autophosphorylation within its cytosolic portion²⁸⁰. Moreover, PERK phosphorylates the eukaryotic initiation factor 2 α (eIF2 α), inhibiting its activity as translation initiation factor and thus leading to a decreased general translation^{236,237,281,282}. Interestingly, P-eIF2 α selectively promotes the translation of the activating transcription factor 4 (ATF4)^{283,284}, a transcription factor whose targets are genes encoding for proteins involved in folding process, amino acid metabolism, autophagy, anti-oxidant response and apoptosis²⁸⁵⁻²⁸⁸. Sustained activation of PERK branch can lead to cell death²⁸⁹. In fact, ATF4 also induces the expression of C/EBP homologous protein

(CHOP)²⁹⁰, a transcription factor controlling the expression of different pro-apoptotic genes²⁹¹. Another target gene of ATF4 is growth arrest and DNA damage–inducible 34 (GADD34), which mediates eIF2 α de-phosphorylation and decreases in turn PERK signaling^{292,293}.

4.5.2 How do cells recover after an ER stress: Recov-ER-phagy

Perturbations of ER homeostasis, due to different endogenous and exogenous stimuli, induce a condition of ER stress that triggers the activation of the UPR to adapt the cellular homeostasis to the changing conditions²⁹⁴. UPR activation leads to the ER expansion in order to accommodate and dilute the accumulated misfolded proteins, but also many ER chaperones and folding enzymes are synthesized during this phase²³⁴. If the ER stress is successfully resolved, the excess machinery and membranes previously generated have to be cleared in order to restore organelle pre-stress volume, content and activity^{295,296}. In this context, we recently demonstrated that upon resolution of an ER stress, specific ER subdomains are delivered to the endolysosomal compartment for clearance through a selective ER-phagy process, named as Recov-ER-phagy²⁹⁷. Specifically, this pathway is mediated by SEC62, an ER resident component of the post-translational protein translocation machinery²⁹⁷. Upon ER stress resolution, SEC62 acts as an ER-phagy receptor allowing the delivery of excess ER portions to the endolysosomes (ELs) for clearance²⁹⁷. SEC62 possesses an LC3 interacting region (LIR) that is required for its function as ER-phagy receptor, but not for its role in protein translocation²⁹⁷. Interestingly, Recov-ER-phagy does not rely on the hierarchical intervention of the functional complexes ensuring macro-autophagy²⁹⁸. Indeed, while the engagement of the LC3 lipidation machinery results indispensable, Recov-ER-phagy does not require the intervention of both the autophagosomal biogenesis machinery and the SNAREs proteins, which are typically involved in autophagosomes-ELs fusion events²⁹⁸. We recently showed that Recov-ER-phagy occurs via piecemeal micro-autophagic like process: ER portions containing SEC62 and decorated with LC3 are directly engulfed by the ELs via membrane invagination process²⁹⁸. These events rely on the intervention²⁹⁸ of the ESCRT-III component CHMP4B and the accessory AAA+ ATPase VPS4A, which typically catalyze membrane inward invagination processes²⁹⁸.

4.6 Aim of the research projects

4.6.1 Investigation of Thioredoxin-related transmembrane protein 1 (TMX1) role in ERAD

Mammalian ER contains more than 20 members of the PDI protein family. These enzymes are responsible for the formation of the correct set of intra- and inter-molecular disulfide bonds, which represents a rate-limiting step during protein folding process. Additionally, PDIs are also involved in the reduction of disulfide bonds within misfolded substrates to facilitate their dislocation across the ER membrane for ERAD. The reasons for a high degree of redundancy, as well as PDI substrate preferences, are still poorly understood. PDI family mainly comprises soluble members with one exception represented by a sub-group named thioredoxin-related transmembrane (TMX) proteins, whose members are five membrane-bound PDIs. TMX1 represents the first identified TMX family member for which a role in protein folding has been demonstrated. TMX1 forms functional complexes with CNX preferentially intervening during the maturation of cysteine-containing membrane-tethered proteins. These evidences characterized TMX1 as the first example of topology-specific redox-catalyst in living cells. Interestingly, it has been also reported in literature an involvement of TMX1 in the reduction of the toxins ricin and abrin prior their retro-translocation across the ER membrane. This evidence together with its reductase nature suggested a role of TMX1 in ERAD.

The aim of this project was to investigate TMX1 involvement in ERAD. The exploitation of a trapping mutant version of TMX1 (TMX1_{C/A}) allowed to demonstrate that TMX1 preferentially forms mixed disulfides with membrane-bound folding-defective protein substrates selectively delaying their degradation.

These data have been published as follows (see Appendix):

The reductase TMX1 contributes to ERAD by preferentially acting on membrane associated folding-defective polypeptides.

Guerra C, Brambilla Pisoni G, Soldà T, Molinari M.

Biochem Biophys Res Commun. 2018 Sep 5;503(2):938-943.
doi:10.1016/j.bbrc.2018.06.099. Epub 2018 Jun 22.

4.6.2 Characterization of Thioredoxin-related transmembrane protein 5 (TMX5)

TMX5 is the less characterized member of the TMX family. It is a single-span type I protein containing one TRX-like domain within its luminal region. The peculiar CRFS active site displayed within its TRX-like domain characterizes TMX5 as a natural trapping mutant protein. Information about TMX5 are limited to structural annotations. Indeed, the unique data available in the literature link TMX5 mutations to the development of a rare ciliopathy, known as Meckel-Gruber syndrome (MKS).

In this thesis, we aimed to preliminary characterize TMX5 protein. We showed that TMX5 is a N-glycosylated protein, whose expression is not regulated by ER stress induction. In contrast with the other TMXs, TMX5 exits the ER to travel along the secretory pathway. Moreover, its active site allows the formation of mixed disulfides with endogenous proteins with a preference for membrane-tethered substrates. Additionally, TMX5 interacts with ERp44 establishing a disulfide-bonded complex: this interaction requires a functional ERp44 active site and determines TMX5 retention within the ER.

4.6.3 Generation of HaloTag2® chimeras as protein-based tools for the characterization of PQC systems

Maintenance of cell proteome in appropriate quantity and quality is crucial for cells viability and health. Indeed, accumulation of unfolded intermediates or misfolded proteins within cells is linked to the development of many human diseases. To cope with failures in protein folding, cells possess different quality control systems to allow the recognition of misfolded polypeptides, eventually leading to their degradation.

The aim of this project was to design and develop HaloTag2® protein-based tools for the characterization of the PQC pathways. HaloTag2® is a mutated version of a bacterial haloalkane dehalogenase, which misfolds upon covalent binding to the hydrophobic chloroalkane reactive ligand HyT36. I built a palette of membrane-tethered GFP-HaloTag2® protein substrates with different characteristics (i.e. length of the transmembrane anchor, presence/absence of N-glycans, HaloTag2® domain in the cytosol or in the ER lumen) to determine the consequences of domain misfolding on protein secretion and cells homeostasis. HyT36-mediated misfolding of the HaloTag2® chimeras elicited different responses according to the properties of the single proteins. Indeed, HyT36 treatment induces a decrease in protein levels of the luminal HaloTag2® protein chimeras. The same treatment does not affect protein levels of the HaloTag2® protein chimeras displaying the misfolded domain on the cytosolic side. This is due to the recognition of the luminal misfolded moieties by the ER quality control through BiP. As direct consequence of BiP engagement, upon HyT36 treatment, the secreted luminal HaloTag2® chimeras lose the plasma membrane staining, while leaving unaffected the sub-cellular localization of the secreted chimera harboring the HaloTag2® domain within the cytosolic region. Additionally, analysis of the BiP transcript levels showed the induction of an ER stress and the consequent UPR activation upon HyT36-mediated misfolding of the luminal HaloTag2® protein chimeras. In the view of these results, the developed HaloTag2® protein chimeras represent reliable tools for the study of the PQC pathways.

4.6.4 Transcriptional analysis of Recov-ER-Phagy process

ER homeostasis perturbations caused by different endogenous and exogenous stimuli, can lead to ER stress and UPR activation. Upon ER stress relief, cells activate ill-defined recovery programs that mediate the removal of excess and/or damaged ER portions produced during the stress phase and the re-establishment of the ER homeostasis. These recently identified catabolic pathways have been defined as Recov-ER-Phagy. During this process, the translocon subunit SEC62 acts as the ER-phagy receptor that ensures the lysosomal degradation of select ER sub-regions. In detail, on a resolution of an ER stress, SEC62 recruits components of the autophagic machinery through its LC3-interacting region (LIR) mediating the delivery of selected ER portions to the endolysosomal compartment for clearance. Recov-ER-Phagy occurs via piecemeal micro-ER-phagy mechanism, during which the ER sub-domains to be degraded are directly engulfed by the endolysosomes in a process relying on the ESCRT-III component CHMP4B and the accessory AAA+ ATPase VPS4A. Even though, genetic tools as KO and CRISPR cell lines allowed the individual dissection of the required components of Recov-ER-Phagy pathway, there are still many points to be understood.

Here, we aimed to transcriptionally characterize Recov-ER-Phagy process. As such, we performed an RNA-seq analysis to monitor transcripts variations during the different phases of Recov-ER-Phagy. In particular, we analyzed the transcriptome of untreated cells, of cells treated for 12h with CPA to induce an ER stress, and of cells at different timepoints after CPA wash-out (i.e., during the recovery phase). From these analyses, we obtained a time-resolved description of the transcriptional events and pathways that cells are activating or suppressing to counteract the perturbations of the ER homeostasis and successfully ride the recovery phase.

5 PHD RESEARCH PROJECTS

5.1 Thioredoxin-related transmembrane protein 1 (TMX1) as ER reductase acting in ERAD of membrane-bound folding-defective polypeptides

5.1.1 Results

5.1.1.1 TMX1 preferentially associates with membrane-bound folding-defective model substrates

TMX1 is a transmembrane ER-resident member of the PDI protein family. It harbors one TRX-like domain displaying a non-canonical CPAC active site¹⁹⁷ (**Figure 1A**). As for other PDIs, the substitution of the C-terminal resolving cysteine of the TMX1 active site with an alanine (TMX1_{C/A}) traps the mixed disulfide intermediate in the reductive pathway, thus stabilizing the interaction with the client proteins (**Figures 1A-C**). In the recent years, the exploitation of its trapping mutant version allowed the characterization of TMX1 as the first example of topology-specific redox-catalyst selectively acting during productive folding of membrane-bound clients²⁰⁶.

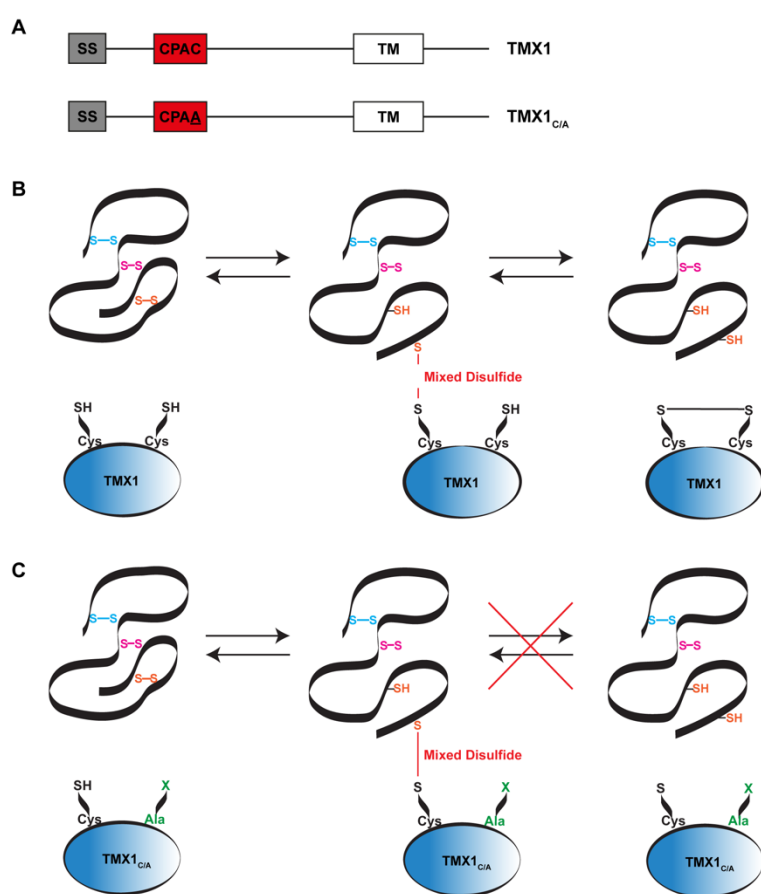


Figure 1: TMX1 wild-type vs trapping mutant. A, TMX1 and TMX1_{C/A} constructs are shown together respectively with wild-type and trapping-mutant active sites (red boxes). SS, signal sequence; TM, transmembrane region. B and C, Schematic representation of the disulfide bonds reduction catalyzed by TMX1. Mixed disulfide intermediate formation mediated by the nucleophilic attack of the N-terminal active site cysteine on a substrate disulfide bond is shown. The resulting intermediate is resolved thanks to the intervention of the C-terminal active site cysteine on the mixed disulfide. The replacement of the C-terminal resolving cysteine of TMX1 with an alanine residue substantially stabilizes mixed disulfide reaction intermediate between the enzyme and its substrate.

To date, a possible role of TMX1 in ERAD is suggested by circumstantial evidences. Indeed, the proline residue in position 2 of the TMX1 active site contributes to its redox attitude, driving the potential towards substrate reduction, thus hinting a role as ER reductase¹⁹¹. Additionally, its overexpression increases the cytotoxicity of the type-2 ribosome inactivating proteins abrin and ricin, two toxins that require a step of reduction prior retro-translocation from the ER to the cytosol where they act²⁰¹.

To study TMX1 contribution in the reduction of ERAD substrates prior degradation, we exploited two couples of folding-defective model substrates (**Figure 2A**): the first is represented by the single-span type I, pancreatic splice form of the beta secretase BACE457 and BACE457 Δ , its soluble variant obtained ablating the transmembrane C-terminal domain¹²⁴; the second couple is composed by the soluble disease-causing mutant form of the alpha-1-antitrypsin inhibitor (NHK) and NHKCD3 δ , a membrane-tethered version obtained adding the CD3 δ transmembrane domain to the NHK C-terminal portion⁹⁴. HEK293 cells were mock-transfected (EV for empty vector **Figure 2B**, lane 1), transfected with a plasmid for the expression of a V5-tagged version of the trapping mutant TMX1_{C/A} alone (**Figure 2B**, lane 2), or in combination with the HA-tagged versions of BACE457 (**Figure 2B**, lane 3), BACE457 Δ (**Figure 2B**, lane 4), NHK (**Figure 2B**, lane 5) and NHKCD3 δ (**Figure 2B**, lane 6). Cells were lysed and the ectopically expressed folding-defective substrates were immunisolated from the post nuclear supernatants (PNSs) using an anti-HA antibody. The immunocomplexes were then separated in a reducing SDS-PAGE and transferred on a PVDF membrane. The upper part of the membrane was probed with an anti-HA antibody to reveal the presence of the model ERAD substrates (**Figure 2B**, upper panel), while the portion below 40kDa was probed with an anti-V5 antibody to assess the co-immunoprecipitation of TMX1_{C/A} (**Figure 2B**, lower panel).

This experiment revealed that TMX1_{C/A} strongly associates with both folding-defective membrane-tethered BACE457 and NHKCD3 δ (**Figure 2B**, lanes 3 and 6, respectively), and much less with their soluble counterparts BACE457 Δ and NHK (**Figure 2B**, lanes 4 and 5, respectively). These findings were additionally supported by the reciprocal experiment (**Figure 2C**), where upon immunisolation of the ectopically expressed TMX1_{C/A}-V5 using an anti-V5 antibody (**Figure 2C**, lower panel), both the membrane-tethered BACE457 and NHKCD3 δ were abundantly co-precipitated compared with their soluble forms BACE457 Δ and NHK (**Figure 2C**, lane 3 vs 4 and lane 5 vs 6, upper panel).

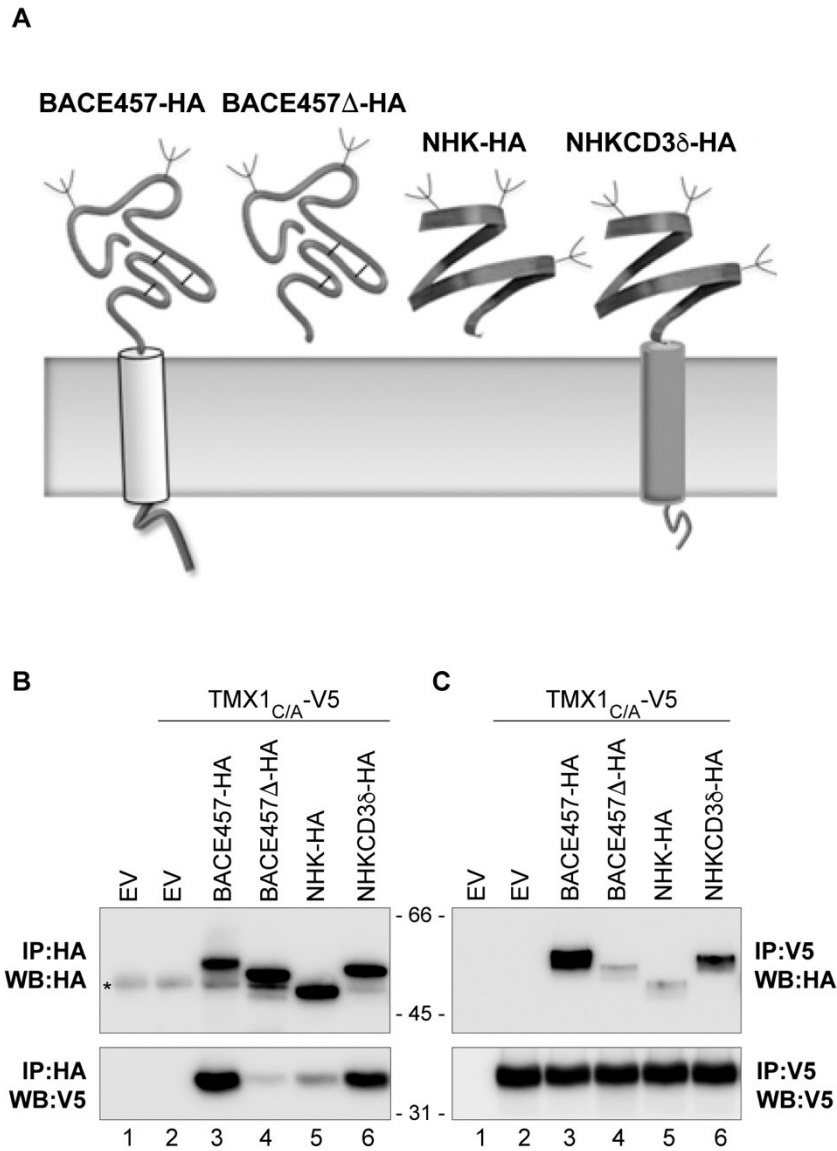


Figure 2: TMX1_{C/A} association with ERAD model substrates. **A**, Schematic of the model ERAD folding-defective substrates used in the experiments. **B**, HEK293 cells were transfected with an empty vector (EV, lane 1), with the V5-tagged TMX1_{C/A} alone (lane 2), or in combination with the HA-tagged BACE457, BACE457Δ, NHK or NHKCD3δ (lanes 3-6). After cells lysis, the HA-tagged substrates were immunisolated from the PNS and revealed by WB with an anti-HA antibody (upper panel). Using an anti-V5 antibody, the co-precipitation of TMX1_{C/A} has been revealed (lower panel). **C**, V5-tagged TMX1_{C/A} was immunisolated from the same PNS of panel **B** using the anti-V5 antibody conjugated agarose beads to check the association of TMX1 with the HA-tagged model folding-defective proteins (upper panel). As control, TMX1_{C/A} immunisolated was checked using an anti-V5 antibody (lower panel). *, cross-reaction due to the heavy chains antibody recognized by the secondary antibody in WB.

All in all, these data confirm the preferential association of TMX1 with membrane-bound protein substrates previously demonstrated for folding-competent substrates²⁰⁶, and extend its binding specificity to folding-defective membrane-tethered polypeptides that are committed to ERAD.

5.1.1.2 TMX1 establishes mixed disulfides with the membrane-tethered folding-defective substrates BACE457 and NHKCD3 δ

Functional interactions between PDIs and protein substrates implies the formation of mixed disulfides as reaction intermediates^{299,300}. To directly determine the establishment of mixed disulfides between TMX1 and the folding-defective substrates, HEK293 cells were transfected and lysed to isolate the PNSs as described in the previous paragraph. TMX1-containing complexes were immunoprecipitated from the PNSs using an anti-V5 antibody and then separated by SDS-PAGE under both non-reducing and reducing conditions. Western blot analysis of the non-reduced samples with an anti-V5 antibody, confirmed the immunoprecipitation of TMX1_{C/A} (**Figure 3A**, lanes 2-6, shown with a lane) and revealed the presence of disulfide-bounded complexes containing TMX1_{C/A} (**Figure 3A**, lanes 2-6 above 45kDa). Notably, TMX1_{C/A} alone engages mixed disulfides with cysteine-containing endogenous substrates (**Figure 3A**, lane 2). Upon the co-expression of TMX1_{C/A} with the folding-defective model substrates, the pattern of the disulfide-bounded complexes positive for TMX1_{C/A} changed (**Figure 3A**, lane 2 vs 3-6). In particular, this phenotype appears clearly evident when TMX1_{C/A} is co-expressed with the two membrane-tethered folding-defective substrates BACE457 and NHKCD3 δ (**Figure 3A**, lanes 3 and 6).

Upon BACE457-HA co-expression, TMX1_{C/A}-V5 establishes a high molecular weight complex of about 90kDa that is positive for both the anti-V5 (**Figure 3A**, lane 3, arrow MD1_T for TMX1 component (T) of Mixed Disulfide 1) and the anti-HA components (**Figure 3B**, lane 3, arrow MD1_B for BACE457 component (B) of Mixed Disulfide 1). This complex is disassembled when the same sample is analyzed under reducing conditions (**Figures 3C and 3D**, lane 3), meaning that it represents the mixed disulfide between TMX1_{C/A} and BACE457. Similarly, upon NHKCD3 δ -HA co-expression, TMX1_{C/A}-V5 forms two distinct complexes of about 116 and 160kDa, which are positive for both the anti-V5 (**Figure 3A**, lane 6, arrows MD2_T for TMX1 component (T) of Mixed Disulfide 2) and the anti-HA components (**Figure 3B**, lane 6, arrows MD2_N for NHKCD3 δ component (N) of Mixed Disulfide 2). Moreover, both complexes are resolved under reducing conditions (**Figures 3C and 3D**, lane 6), confirming that TMX1_{C/A} engages NHKCD3 δ into two distinct disulfide-bounded complexes, representing TMX1-s-s-NHKCD3 δ and TMX1-s-s-NHKCD3 δ -s-s-NHKCD3 δ , according to their electrophoretic mobility. In contrast, TMX1_{C/A} does not establish distinct mixed disulfides with the soluble folding-defective model substrates BACE457 Δ and NHK (**Figures 3A and 3B**, lanes 4 and 5).

Altogether, these data demonstrate that the selective interaction of TMX1 with membrane-tethered folding-defective polypeptides involves the establishment of mixed disulfide reaction intermediates.

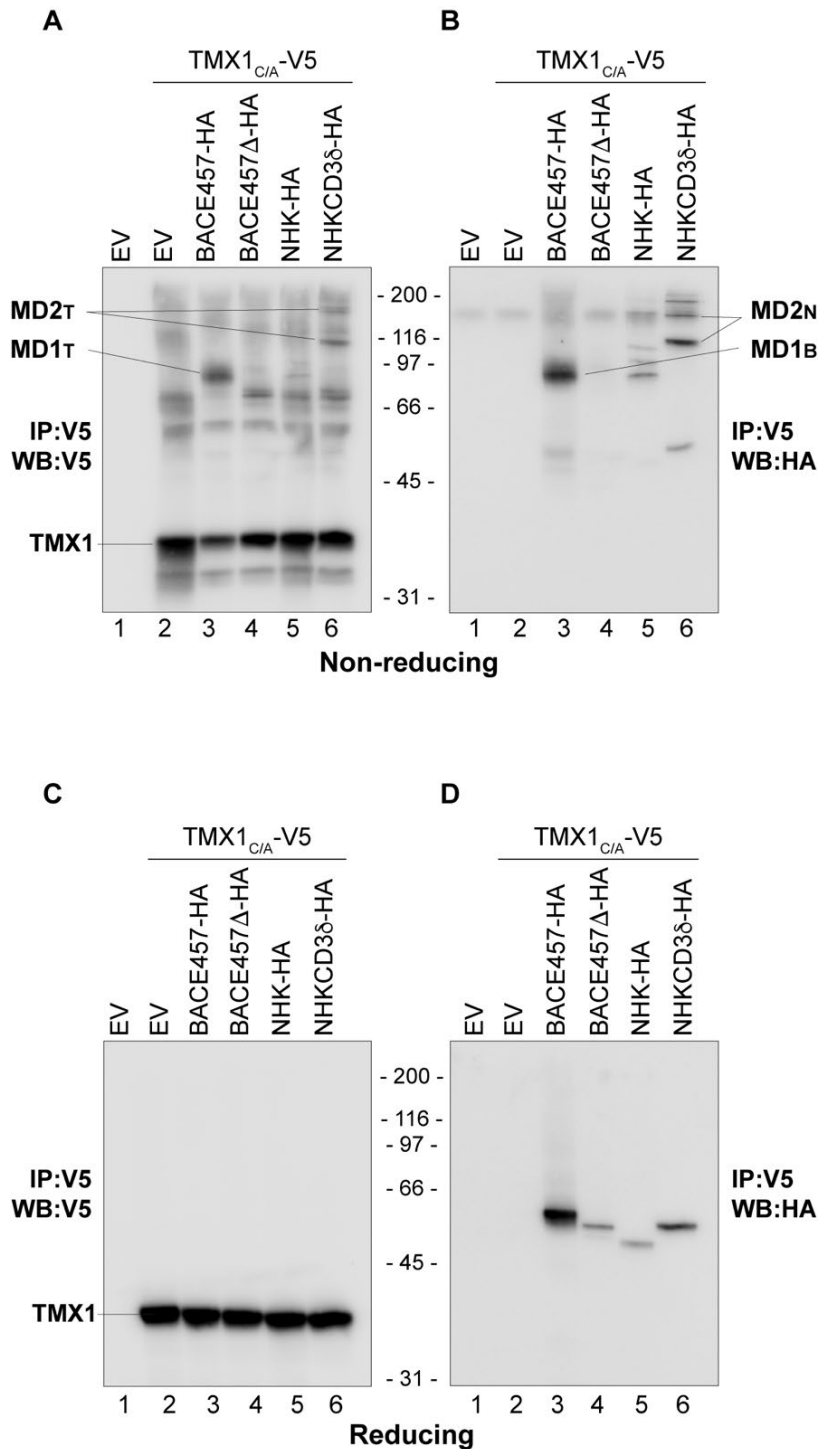


Figure 3: TMX1_{C/A} forms mixed disulfides with BACE457 and NHKCD38. **A**, HEK293 cells were transfected with an empty vector (EV, lane 1), with a V5-tagged version of TMX1_{C/A} alone (lane 2), or in combination with the HA-tagged BACE457, BACE457Δ, NHK or NHKCD38 (lanes 3-6). After cells lysis, the complexes containing TMX1_{C/A}-V5 were immunoprecipitated from the PNSs using anti-V5 conjugated agarose beads. Protein complexes were separated by SDS-PAGE under non-reducing conditions and analyzed by WB using an anti-V5 antibody to reveal TMX1_{C/A} signal. **B**, The same membrane of panel **A** was probed with an anti-HA antibody after stripping to detect the coprecipitation of the HA-tagged substrates. **C**, Same as panel **A**, but the V5-containing complexes were separated under reducing conditions. **D**, The same membrane of panel **C** was probed with an anti-HA antibody after stripping to check the coprecipitation of the HA-tagged substrates. MD1_T for TMX1 component (T) of Mixed Disulfide 1; MD1_B for BACE457 component (B) of Mixed Disulfide 1; MD2_T for TMX1 component (T) of Mixed Disulfide 2; MD2_N for NHKCD38 component (N) of Mixed Disulfide 2.

5.1.1.3 TMX1 preferentially intervenes in ERAD of membrane-anchored folding-defective model substrates

Misfolded proteins may require a step of linearization prior retro-translocation into the cytosol for proteasomal degradation¹²³. This step includes the intervention of some PDIs, which reduce intra- and inter-molecular disulfide bonds¹²⁶, facilitating the dislocation of the misfolded substrates across the ER membrane. The non-canonical active site of TMX1 with a proline in position 2 supports its role as ER reductase and suggests in turn its possible function as reductase acting in ERAD. To assess TMX1 role as ERAD reductase, we examined the effect of TMX1_{C/A} expression on the degradation of the select folding-defective model substrates. HEK293 cells were transfected with the previously described HA-tagged ERAD model substrates (**Figure 2A**) in combination either with an EV or with TMX1_{C/A}-V5. Afterwards, cells were metabolically labelled upon 15 minutes incubation with ³⁵S-methionine/cysteine, and then chased at different timepoints to follow the decay of the radioactive signal and thus monitor the degradation of the folding-defective model substrates. To this extent, after cells lysis, the ERAD substrates were immunoprecipitated from the PNSs using an anti-HA antibody and separated by SDS-PAGE under reducing conditions. The radiolabeled proteins were finally visualized by autoradiography.

The co-expression of TMX1_{C/A} with the membrane-anchored BACE457 significantly delays its degradation (**Figure 4A**, lanes 1-4 vs 5-8, and **Figure 4B** for quantification). Conversely, the overexpression of TMX1_{C/A} does not affect the clearance of the soluble BACE457Δ (**Figure 4C**, lanes 1-4 vs 5-8, and **Figure 4D** for quantification). On the same line, the degradation of the soluble NHK is not affected upon TMX1_{C/A} overexpression (**Figure 5A**, lanes 1-4 vs 5-8, and **Figure 5B** for quantification), whereas the clearance of the same cysteine-containing ectodomain tethered to the membrane, NHKCD3δ, results significantly delayed (**Figure 5C**, lanes 1-4 vs 5-8, and **Figure D** for quantification). Consistently with the previous data (**Figures 2B and C, 3C and D**), TMX1_{C/A} strongly associates with both membrane-tethered ERAD substrates BACE457 (**Figure 4A**, lanes 5-8) and NHKCD3δ (**Figure 5C**, lanes 5-8), whereas the interaction results weaker in the case of the soluble ERAD model proteins BACE457Δ (**Figure 4C**, lanes 5-8) and NHK (**Figure 5A**, lanes 5-8). All in all, these evidences demonstrate that the ER reductase TMX1 selectively intervenes during the degradation of membrane-anchored ERAD model substrates.

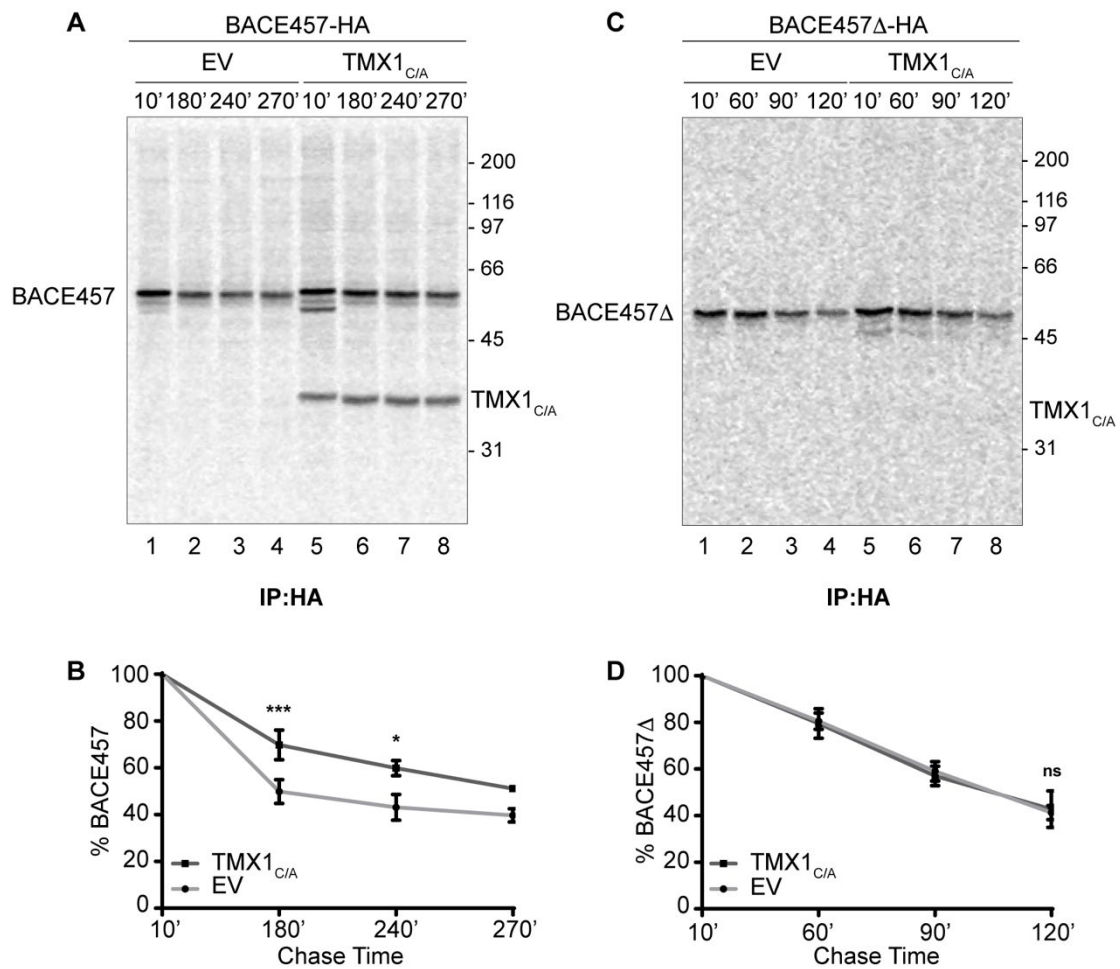


Figure 4: TMX1_{C/A} selectively delays the clearance of BACE457. **A**, HEK293 cells were transfected with the HA-tagged BACE457 in combination with an empty vector (EV, lanes 1-4), or with the V5-tagged TMX1_{C/A} (lanes 5-8). Cells were metabolically labelled with ³⁵S-methionine/cysteine for 15 minutes and chased for 10, 180, 240, or 270 minutes. The radiolabeled HA-tagged BACE457 was immunoprecipitated using an anti-HA antibody to monitor its degradation. **B**, Quantification of panel A. Error bars: SDs of six independent experiments for 180 min, three independent experiments for 240 and two for 270 min chase. For 180 and 240 min chase points, significance was analyzed by unpaired t-test; *p < 0.05; ***p < 0.001. **C**, Same as panel A for the HA-tagged BACE457Δ. **D**, Quantification of panel C. Error bars: SDs of two independent experiments for 60 and 90 min chase, and three independent experiments for 120 min chase time. For 120 min chase point, significance was analyzed by unpaired t-test; ns not significant.

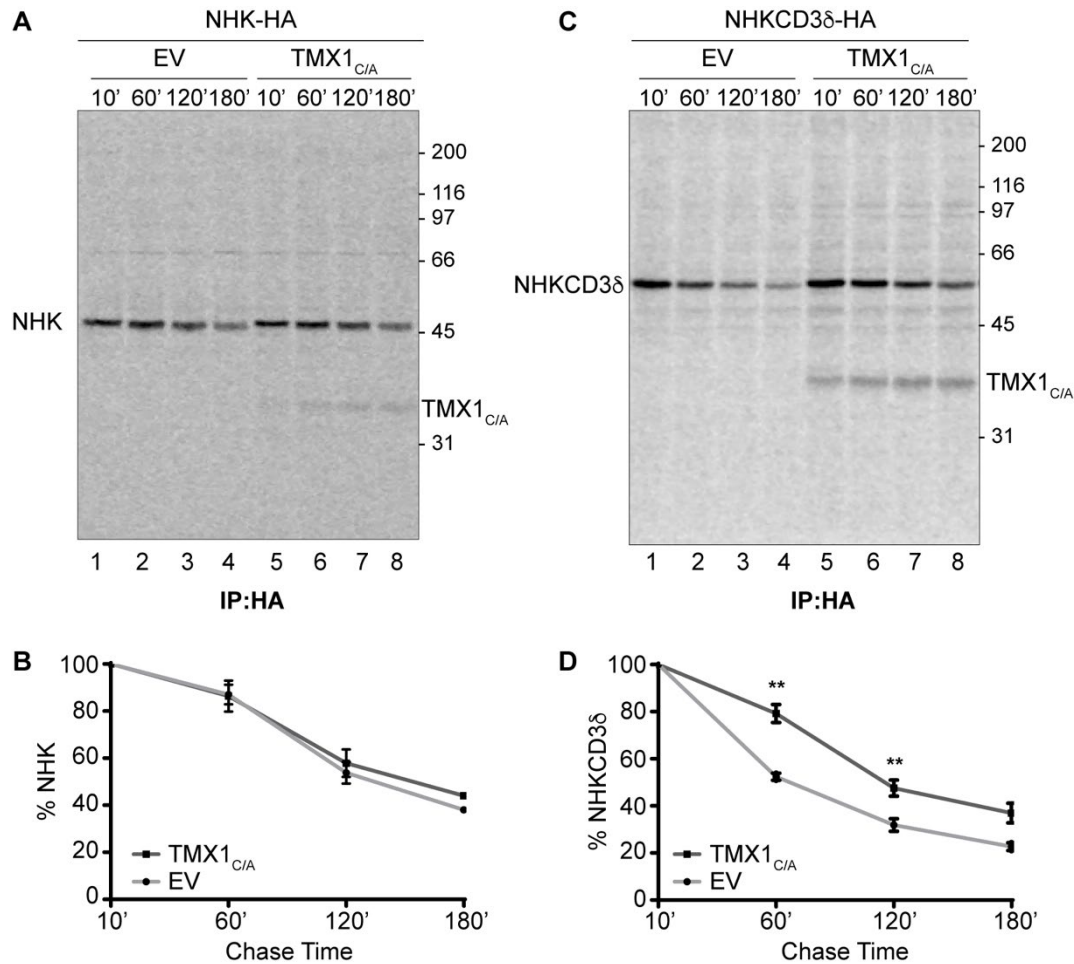


Figure 5: TMX1_{C/A} selectively delays the clearance of NHKCD3δ. **A**, HEK293 cells were transfected with the HA-tagged NHK in combination with an empty vector (EV, lanes 1-4), or with the V5-tagged TMX1_{C/A} (lanes 5-8). Cells were metabolically labelled with ³⁵S-methionine/cysteine for 15 minutes and chased for 10, 60, 120, or 180 minutes. The radiolabeled HA-tagged NHK was immunoprecipitated using an anti-HA antibody to monitor its degradation. **B**, Quantification of panel A. Error bars: SDs of two independent experiments for 60 and 120 min chase points. **C**, Same as panel A for NHKCD3δ. **D**, Quantification of panel C. Error bars: SDs of three independent experiments for 60 and 120 min chase, and of two independent experiments for 180 min chase time. For 60 and 120 min chase points, significance was analyzed by unpaired t-test. *p < 0.05; **p < 0.01; ***p < 0.001.

5.1.2 Discussion

The mammalian ER contains more than 20 PDIs, which catalyze the reduction, the oxidation and the isomerization of disulfide bonds to ensure the correct folding of nascent polypeptides and the efficient ERAD of misfolded by products¹⁹⁴. PDIs have as common feature the presence of at least one TRX-like domain, harboring an active site sequence that is crucial for the enzymes' function¹⁹¹. Other than this, PDI family is quite heterogenous, since its members display differences in the number of TRX-like domains, active site composition, topology and structural arrangement. These divergences easily bring to the hypothesis that each PDI would specifically act in a different process or with a different substrate specificity, thus justifying the co-existence of so many PDIs within the ER¹⁹⁴. However, the individual roles and contributions of each PDI are still lost in the fog. This aspect is not of easy investigation as it could seem: indeed, *in vivo* studies using knockout mice models usually do not give clear phenotypes, since the depletion of one PDI could be compensated by the intervention of other proteins^{301,302}. As such, even though a redox activity has been proven for many PDIs^{186,191,194}, there is still a long way to go to assess the individual functions of each PDI in a cellular environment.

5.1.2.1 Thioredoxin-related transmembrane (TMX) protein family

Most of the PDI family members are soluble proteins. One exception is represented by the TMX family, a sub-group of five membrane-tethered proteins (TMX1, TMX2, TMX3, TMX4 and TMX5)^{189,197,212,216,220}. They are characterized by the presence of an ER signal sequence and one type-a TRX-like domain. Manual annotations and preliminary studies about TMX proteins highlighted some differences among the members: first of all, these proteins display different active site sequences^{197,212,216,220}; moreover, TMX1 and TMX2 possess palmitoylation sites within their cytosolic tails²⁰⁷, whereas TMX3, TMX4 and TMX5 harbor a variable number of N-glycosylation sites within their N-terminal luminal domains^{218,220}. These evidences would suggest that functional diversification could exist even in a small protein family, meaning that each of the TMX proteins could be specialized in a precise function, according their structural features. This hypothesis is still far from being confirmed since clear experimental data for all TMXs are not available.

5.1.2.1.1 TMX1, a membrane-tethered ER reductase

TMX1 represents the first identified and also the best characterized member of the TMX protein family. It is a non-glycosylated protein, which contains one type-a TRX-like domain¹⁹⁷. This domain displays a non-canonical CPAC active site¹⁹⁷, whose peculiar

composition is an important hint of TMX1 role in cells: the proline residue in position 2 destabilizes the disulfide state of the active site and favors instead the di-thiol reduced form, thus suggesting a role for TMX1 as ER reductase¹⁹¹. Indeed, TMX1 is mainly found reduced *in vivo*²⁰² and it is able to reduce insulin disulfides *in vitro*¹⁹⁷. As for other members of the PDI protein family, additional information about TMX1 function came from the exploitation of its trapping mutant version, in which the C-terminal cysteine of the active site has been replaced with an alanine (TMX1_{C/A}). As definition of trapping mutant suggests, TMX1_{C/A} is able to establish a mixed disulfide through its N-terminal cysteine, but the interaction cannot be quickly resolved because of the lack of the second cysteine residue, and thus protein substrates result stably trapped in a mixed disulfide reaction intermediate. Recently, the exploitation of the trapping mutant version allowed to demonstrate that TMX1 selectively acts during productive folding of membrane-tethered protein substrates²⁰⁶. In details, through the formation of functional complexes with the ER lectin CNX, TMX1 preferentially engages mixed disulfides with membrane-tethered client substrates intervening during their folding²⁰⁶.

Other than protein folding, PDI family members, as the well-known PDI³⁰³ and ERdj5¹²⁶, can also act in ERAD to catalyze the reduction of disulfide bonds within misfolded substrates facilitating their dislocation across the ER membrane³⁰⁴. The reductase nature of TMX1 makes this protein a good candidate for a role in ERAD. An additional hint in this direction is provided by the evidences that TMX1 overexpression in mammalian cells enhances cytotoxicity of abrin and ricin, two type 2 ribosome-inactivating proteins, which require a step of reduction before being retro-translocated into the cytosol, where they act as toxins²⁰¹.

Considering this prior knowledge, during my PhD, I investigated the role of TMX1 as ER reductase intervening in ERAD, demonstrating that it preferentially establishes mixed disulfides with membrane-anchored ERAD model substrates, while ignoring the same misfolded cysteine-containing ectodomains if detached from the membrane. Moreover, TMX1_{C/A} overexpression significantly delayed the degradation of the membrane-tethered ERAD model substrates. These findings defined TMX1 as the first example of topology-specific ER redox-catalyst intervening in both productive folding and ERAD.

5.1.2.1.2 TMX1 preferentially associates with folding-defective membrane-protein substrates delaying their degradation

Protein topology constitutes a crucial characteristic in determining protein interactions and engagement in different processes, as protein folding and degradation. Indeed, one excellent example is represented by the two ER lectins CNX and CRT, which preferentially engage different protein substrates, according to their distinct topology^{74,305-308}. Evidences that topology matters have been also reported for ERAD, where misfolded soluble proteins exhibit a preference towards HRD1-based dislocon for their disposal^{121,309}. A previous work from our lab demonstrated the selectivity of TMX1 towards membrane-tethered protein clients in the context of protein folding²⁰⁶. The data collected in this thesis show that TMX1 keeps its preference for membrane-anchored protein substrates also in the case of folding-defective ERAD clients. The molecular mechanism through which TMX1 can distinctly act in both protein folding and ERAD of membrane-bound proteins are still unknown. In this context, the most probable hypothesis would be represented by the association of TMX1 with different partners. Indeed, for protein folding process, TMX1 intervention relies on the formation of a functional complex with the ER lectin CNX. Thus, the association of TMX1 with alternative ER chaperones could determine a different sub-ER localization, such as near the dislocation machinery to support its role in ERAD. Interestingly, the interaction between TMX1 and CNX occurs through their transmembrane regions²⁰²: on this basis, it could be envisioned that for its function in ERAD, TMX1 would interact via transmembrane with membrane-tethered components of the dislocon machinery rather than engage soluble factors.

Another important determinant for protein-protein interaction is constituted by N-glycosylation. In this context, it still remains to be determined if TMX1 could also engage mixed disulfides with non-glycosylated protein substrates, since the only evidences available show the association of TMX1 with both folding-competent and folding-defective N-glycosylated substrates. It is quite likely that also in this context, the binding of TMX1 to alternative partners would allow the choice between different clients, as glycosylated or non-glycosylated proteins. In support to this hypothesis, its cooperative binding to the ER lectin CNX easily explains the activity of TMX1 on N-glycosylated substrates during protein folding.

5.1.3 Contributions

I was involved in the conceptualization and development of this research project. I realized all the figures contained in this section, except panels **5A** and **5C**.

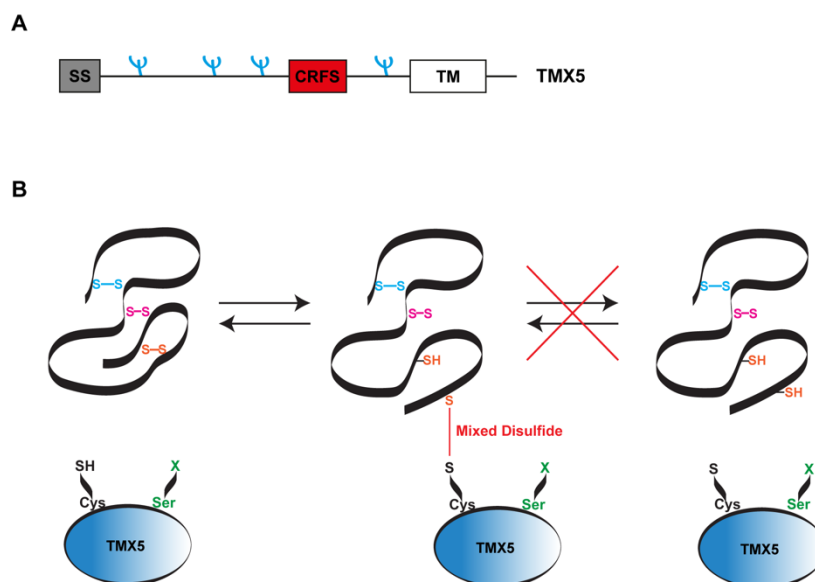
5.2 Preliminary characterization of thioredoxin-related transmembrane protein 5 (TMX5), a single-pass type-I member of the PDI protein family

5.2.1 Results

5.2.1.1 TMX5, an ER stress unresponsive member of the PDI family

TMX5 is a poorly characterized PDI belonging to the TMX subfamily. It is a single-pass type I protein, which harbors one type-a TRX-like domain within its N-terminal luminal side, containing a peculiar non-canonical CRFS active site (**Figure 6A**). The expression of different PDI family members, such as PDI, ERp57, ERdj5 and ERp44, is transcriptionally regulated by ER stress induction^{186,310-312}.

Figure 6: TMX5, a natural trapping mutant PDI. **A**, TMX5 construct is shown together with the active site sequence (red box) and the four putative N-glycosylation sites (blue symbols). SS, signal sequence; TM, transmembrane region. **B**, Schematic representation of the formation of the mixed disulfide between TMX5 and a substrate protein. N-terminal cysteine of TMX5 active site performs a nucleophilic attack on a thiol-group of a client protein establishing a mixed disulfide that results substantially stabilized by the lack of the C-terminal cysteine within its active site.



To verify if TMX5 is transcriptionally up-regulated upon induction of an ER stress, HEK293 cells were mock-treated with DMSO or treated with 5 $\mu\text{g}/\text{mL}$ tunicamycin for 17h. Tunicamycin is a N-glycosylation inhibitor commonly used in literature to trigger ER stress³¹³. After treatment, cells were lysed, and the RNA was collected. Transcript levels of TMX5 were determined by Quantitative Real-Time PCR (qPCR). The levels of sXbp1 and BiP transcripts were also checked, as positive control of ER stress induction.

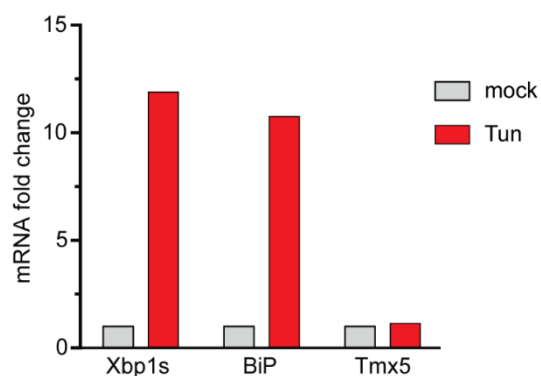


Figure 7: TMX5 is not up-regulated upon ER stress induction. HEK293 cells were mock treated (DMSO) or treated with the ER stress inducer tunicamycin for 17h. After cell lysis, transcripts were isolated and analyzed by qPCR to check TMX5 levels. sXbp1 and BiP transcripts were used as positive control of ER stress induction.

Upon tunicamycin treatment, transcript levels of sXbp1 and BiP had an increase of more than 10 folds (**Figure 7**), indicating the induction of an ER stress. Interestingly, the levels of TMX5 transcript were not affected (**Figure 7**). Thus, similarly to the other TMXs, these data reveal that TMX5 is not transcriptionally regulated upon ER stress induction.

5.2.1.2 TMX5 is a secreted N-glycosylated protein

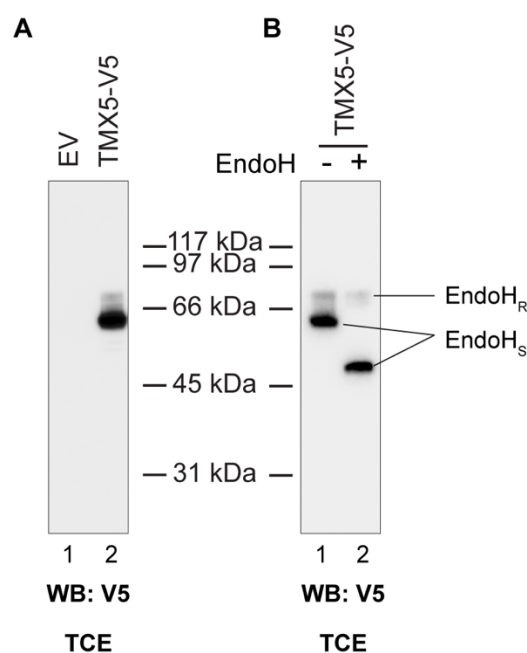
In order to characterize TMX5, we prepared a plasmid for the expression in mammalian cells of a V5-tagged version of TMX5. HEK293 were mock-transfected with an empty vector (EV, **Figure 8A**, lane 1) or with a plasmid for the expression of TMX5-V5 (**Figure 8A**, lane 2). After cell lysis, the collected PNSs were separated by reducing SDS-PAGE and the proteins were then transferred on a PVDF membrane. Western blot analysis using an anti-V5 antibody was used to reveal the expression of V5-tagged TMX5.

Comparison between mock-transfected and TMX5 transfected samples (**Figure 8A**, lane 1 vs 2) revealed the expression of the recombinant V5-tagged protein. In particular, the anti-V5 antibody specifically recognized a main band slightly below 66kDa and a smear just above. This is compatible with the fact that other than a TRX-like domain, TMX5 also contains four putative N-glycosylation sites within its N-terminal luminal region (**Figure 6A**).

To determine N-glycosylation state of TMX5, we performed a biochemical assay using the Endoglycosidase H (EndoH) enzyme, which cleaves the N-linked oligosaccharides of proteins localized within the ER allowing their definition as EndoH sensitive. N-glycosylated proteins exiting the ER undergo further glycan processing and modification

that make EndoH cleavage site no more accessible. As such, these proteins are described as EndoH resistant. The PNS of cells transfected with the TMX5-V5 from the previous experiment was mock-treated (**Figure 8B**, lane 1) or subjected to EndoH treatment (**Figure 8B**, lane 2). After enzymatic digestion, the samples were separated by reducing SDS-PAGE and the proteins were then transferred on a PVDF membrane. Western blot analysis using an anti-V5 antibody was performed to reveal TMX5-V5 signal.

Figure 8: TMX5-V5 expression in mammalian cells and EndoH treatment. **A**, HEK293 were transfected with an empty vector (lane 1) or with a plasmid for the expression of the TMX5-V5 (lane 2). Cells were lysed and the collected PNSs were subjected to SDS-PAGE under reducing conditions. After electrophoretic migration, proteins were transferred on a PVDF membrane that was probed with an anti-V5 antibody to reveal TMX5-V5 signal. **B**, Same PNS of cells transfected with the TMX5-V5 of panel **A** was mock-treated (lane 1) or treated with the EndoH (lanes 2) for 1 h at 37°C. The samples were then separated by SDS-PAGE under reducing conditions, and the proteins were transferred on a PVDF membrane. Western blot analysis was performed using an anti-V5 antibody. EndoH_R, for TMX5 EndoH resistant fraction; EndoH_S, for TMX5 EndoH sensitive fraction.



The comparison between the mock-treated and the EndoH-treated samples showed that TMX5-V5 has both a major EndoH sensitive fraction and a less abundant EndoH resistant fraction (**Figure 8B**, lane 1 vs 2). Indeed, the EndoH treatment induced a shift in the electrophoretic migration of the main band of about 10-15kDa (**Figure 8B**, lane 1 vs 2, EndoH_S arrows for EndoH sensitive fraction), which is compatible with the presence of the four predicted N-glycans. Moreover, upon EndoH treatment, the smeared bands above 66kDa did not change their electrophoretic migration (**Figure 8B**, lane 1 vs 2, EndoH_R arrows for EndoH resistant fraction), indicating the existence of a TMX5-V5 EndoH resistant fraction that exits from the ER. All in all, this experiment showed that TMX5 is a secreted N-glycosylated protein, compatibly with the lack of a retention signal within its sequence.

5.2.1.3 TMX5 forms mixed disulfides with endogenous substrates

Functional ER oxidoreductases are characterized by the presence of at least one type-a TRX-like domain displaying a CXXC active site, where the N-terminal cysteine residue performs a nucleophilic attack towards a thiol of a client protein establishing a mixed disulfide. This reaction intermediate is very short living, since it is quickly resolved by the C-terminal cysteine residue of the active site. TMX5 contains a peculiar CRFS active site, which is missing the C-terminal cysteine residue (**Figure 6A**). As such, it can be defined as a natural trapping mutant, since it could theoretically establish a mixed disulfide with a substrate protein thanks to its N-terminal cysteine, but this interaction could be resolved only by the intervention of an external cysteine residue supplied by other PDIs or by the protein substrate itself. As result, the mixed disulfides involving TMX5 and its cargo proteins are likely to be more stable than the mixed disulfides formed by other PDIs displaying the conventional CXXC active site (**Figure 6B**).

To verify the ability of TMX5 to trap protein substrates in disulfide bonded complexes, HEK293 cells were mock-transfected with an empty vector (EV, **Figure 9**, lanes 1 and 3) or transfected with the TMX5-V5 (**Figure 9**, lanes 2 and 4). Cells were lysed and TMX5-V5 was immunisolated from the PNSs using anti-V5 antibody-conjugated agarose beads. The immunisolated complexes were separated by SDS-PAGE under both non-reducing and reducing conditions and then transferred on a PDVF membrane. A western blot analysis with an anti-V5 antibody was performed to reveal TMX5-V5 signal.

The immunoblotting of the PVDF membrane with an anti-V5 antibody confirmed the immunoisolation of TMX5-V5 (**Figure 9**, arrows), but more interestingly it also revealed few bands at high molecular weight positive for TMX5-V5, under non-reducing conditions (**Figure 9**, lane 2, red box). These bands correspond to the mixed disulfides engaged by TMX5 with endogenous proteins, since these complexes were disassembled under reducing conditions, where only the monomeric TMX5 was detected (**Figure 9**, lane 4). The absence of bands in the mock-transfected samples (**Figure 9**, lanes 1 and 3) confirmed the specificity of the anti-tag antibody. All together, these evidences show that the natural trapping-mutant TMX5 is able to establish high molecular weight disulfide-bonded complexes with endogenous proteins.

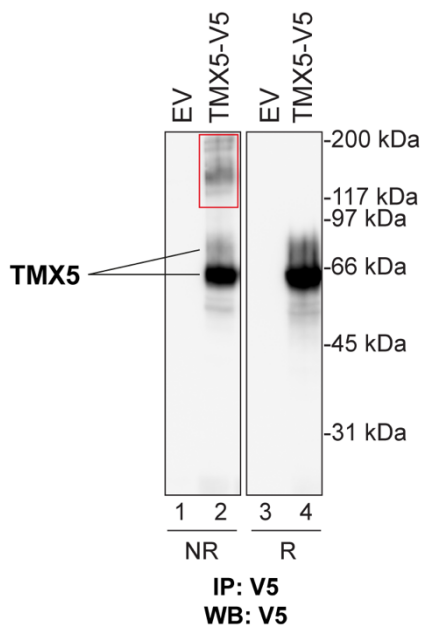
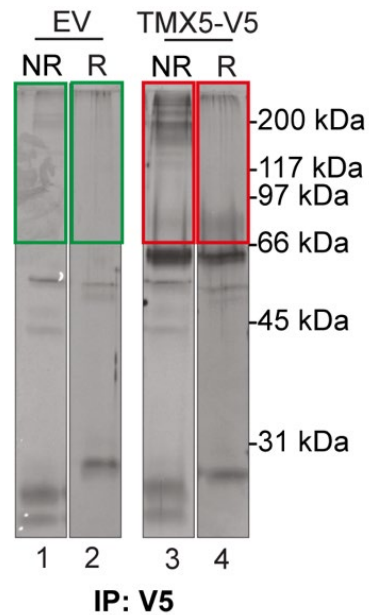


Figure 9: TMX5 forms mixed disulfides with endogenous proteins. HEK293 cells were transfected with an empty vector (EV) or with TMX5-V5. The PNSs were immunoprecipitated using anti-V5 antibody-conjugated agarose beads. The proteins were separated by SDS-PAGE under both non reducing and reducing conditions and then transferred on a PVDF membrane, which was probed with an anti-V5 antibody to reveal TMX5-V5 signal.

5.2.1.4 Mass spectrometry analysis of TMX5 interacting partners

For many PDI family members, interactomic analyses allowed the characterization of their client proteins as well as their potential role in a cellular context. To identify the endogenous substrates of TMX5, we expressed TMX5-V5 in HEK293 cells and analyzed by mass spectrometry analysis the endogenous proteins interacting with TMX5. In details, HEK293 cells were mock-transfected with an empty vector (EV, **Figure 10**, lanes 1 and 2) or transfected with the V5-tagged TMX5 (**Figure 10**, lanes 3 and 4). After cell lysis, the collected PNSs were immunoprecipitated twice using anti-V5 antibody-conjugated agarose beads. The immunisolated complexes were then separated by SDS-PAGE under both non-reducing and reducing conditions. The proteins were then revealed by silver staining and all the bands above 66kDa were cut (**Figure 10**, green boxes for EV, red boxes for TMX5-V5) and analyzed by mass spectrometry (in collaboration with Dr. Manfredo Quadroni, UNIL). TMX5 partners were identified from the results of two independent experiments.

Figure 10: Preparative gel for the mass spectrometry analysis of the TMX5 interacting partners. HEK293 cells were mock-transfected with an empty vector or transfected with the TMX5-V5. Cells were lysed and the collected PNSs were subjected to a double immunoprecipitation using anti-V5 antibody-conjugated agarose beads. After separation by SDS-PAGE under both non-reducing and reducing conditions, the isolated complexes were visualized by silver staining. The bands shown in the colored boxes were cut and analyzed by mass spectrometry.



As first step, the mass spectrometry data were filtered excluding the non-specific hits that were identified in mock-transfected samples (**Figure 10**, lanes 1 and 2 vs 3 and 4). Results were further refined leaving out the hits that were found to interact with TMX5 under both non-reducing and reducing conditions, in order to keep only the proteins establishing disulfide-bonded complexes with TMX5. These interactomic analyses show that TMX5 preferentially associates with membrane-tethered endogenous substrates (**Table 1**), similarly to what previously shown for TMX1²⁰⁶, another member of the TMX protein family. Surprisingly, endogenous ERp44 was identified among the strongest partners of TMX5 (**Table 1**). ERp44 is a soluble and well-characterized member of the PDI family³¹². It harbors one catalytically active TRX-like domain, which comprises a CRFS active site sequence³¹², similarly to TMX5. Through its active site, ERp44 intervenes during the thiol-mediated protein quality control, preventing the release of immature or misfolded proteins within the secretory pathway⁸³. Additionally, ERp44 mediates the retention within the ER of the oxidoreductase ERO1L- α , thus modulating its function as redox-regulator³¹⁴. As ERO1L- α , TMX5 does not contain any retention signal. Thus, given the role of ERp44, we decided to better characterize the interaction between TMX5 and ERp44.

Gene Name	Protein Name	Entry no.	Luminal Cys	Protein description
ERp44	Endoplasmic reticulum resident protein 44	Q9BS26	6	Soluble
LTF	Lactotransferrin	P02788	32	Soluble
HLA-C	HLA class I histocompatibility antigen, C alpha chain	P10321	5	Single-pass TM
HLA-A	HLA class I histocompatibility antigen, A alpha chain	P04439	4	Single pass TM
EXTL3	Exostosin-like 3	O43909	17	Single pass TM
TMEM30A	Cell cycle control protein 50A	Q9NV96	6	Multi-pass TM
ITM2C	Integral membrane protein 2C	Q9NQX7	5	Single pass TM
HS6ST2	Heparan-sulfate 6-O-sulfotransferase 2	Q96MM7	15	Single pass TM
ITM2B	Integral membrane protein 2B	Q9Y287	5	Single pass TM
DOLPP1	Dolichyldiphosphatase 1	Q86YN1	1	Multi-pass TM
VKORC1L1	Vitamin K epoxide reductase complex subunit 1-like protein 1	Q8N0U8	2	Multi-pass TM
DIPK2A	Divergent protein kinase domain 2A	Q8NDZ4	12	Soluble

Table 1: Endogenous disulfide-interacting partners of TMX5 identified by MS analysis. The resulted hits are reported in the table according the decreasing number of the identified peptides.

5.2.1.5 TMX5 forms a mixed disulfide with ERp44

As first step, we verified by biochemical analyses the interaction between TMX5 and ERp44 identified by mass spectrometry. HEK293 cells were transfected with the TMX5-V5 in combination with an empty vector (EV, **Figure 11A**, lane 1) or with the HA-tagged version of ERp44 (**Figure 11A**, lane 2). Cells were lysed, the PNSs were collected and separated by reducing SDS-PAGE. The proteins were then transferred on a PVDF membrane, which was probed with either an anti-V5 antibody or an anti-HA antibody to check both the expression of TMX5-V5 and HA-ERp44, respectively. The same PNSs were then immunoprecipitated using anti-V5 antibody-conjugated agarose beads or with an anti-HA antibody (**Figure 11B and C**). The immunisolated complexes were separated by SDS-PAGE under both non-reducing and reducing conditions, and transferred on PVDF membranes. The immunocomplexes isolated with the anti-V5 were then immunoblotted

with an anti-HA antibody to assess the co-precipitation of ERp44 (**Figure 11B**). On the other hand, the immunocomplexes isolated with the anti-HA were immunoblotted with an anti-V5 antibody to check the co-precipitation of TMX5-V5 (**Figure 11C**).

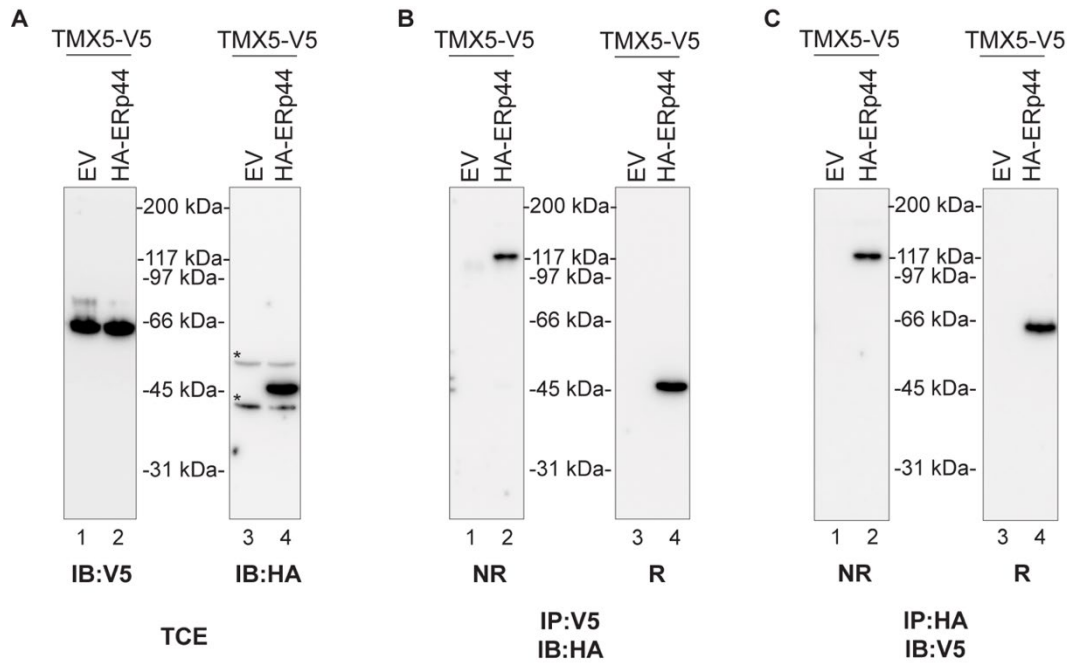


Figure 11: TMX5 establishes a mixed disulfide with ERp44. **A**, HEK293 cells were transfected with the TMX5-V5 in combination with an empty vector (EV) or with the HA-ERp44. Cells were lysed to collect the PNSs that were separated by SDS-PAGE under reducing conditions. After electrophoretic separation, the proteins were transferred on a PVDF membrane that was probed either with an anti-V5 antibody or with an anti-HA antibody to check the expression of TMX5 and ERp44, respectively. **B**, The same PNSs of panel **A** were immunoprecipitated using anti-V5 antibody-conjugated agarose beads. The immunocomplexes were separated by SDS-PAGE under both non-reducing and reducing conditions and then transferred on a PVDF membrane. The immunoblotting with an anti-HA antibody was performed to verify the co-precipitation of ERp44. **C**, The same PNSs of panel **A** were immunoprecipitated with an anti-HA antibody. The immunoprecipitated complexes were separated by SDS-PAGE under both non-reducing and reducing conditions and then transferred on a PVDF membrane. Western blot analysis using an anti-V5 antibody was performed to assess the co-precipitation of TMX5.

The immunoprecipitation of TMX5-V5 upon the co-expression of HA-ERp44 revealed the presence of a complex around 117kDa under non-reducing conditions, which is positive for the HA-ERp44 (**Figure 11B**, lane 2). This complex resulted disassembled when the same sample was separated under reducing conditions, suggesting its disulfide bonded nature (**Figure 11B**, lane 4). The immunoprecipitation of HA-ERp44 under non-reducing

conditions revealed a complex positive for TMX5-V5 with the same electrophoretic mobility (**Figure 11C**, lane 2). This complex was disassembled when the same sample was separated under reducing conditions, where only the monomeric TMX5-V5 was detected (**Figure 11C**, lane 4). Of note, HA-ERp44 forms mixed disulfides with the EndoH sensitive (i.e., ER-localized) fraction of TMX5-V5 (**Figure 11C**, lane 4). As specificity control, the interaction was absent when the TMX5-V5 was expressed in combination with an empty vector (**Figure 11B and C**, lanes 1 and 3). These results confirmed mass spectrometry data showing the formation of a mixed disulfide between TMX5 and ERp44. Moreover, this interaction selectively involves the EndoH sensitive fraction of TMX5, suggesting that the complex between ERp44 and TMX5 is localized within the ER.

5.2.1.6 Characterization of TMX5:ERp44 complex

Both TMX5 and ERp44 display the CRFS sequence within their active site, which is responsible for the engagement of protein substrates through the N-terminal cysteine residue. To determine the direct involvement of the active sites of both TMX5 and ERp44 in the formation of the TMX5:ERp44 mixed disulfide, we took advantage of their inactive mutant versions, in which the N-terminal cysteine of TMX5 and ERp44 was replaced with an alanine (TMX5_{C/A}) (**Figure 12A**) or with a serine (ERp44_{C/S}) (**Figure 12B**), respectively. HEK293 cells were transfected with the V5-tagged TMX5 or with its mutant TMX5_{C/A}-V5 alone or in combination with the HA-ERp44 or with its mutant HA-ERp44_{C/S} (**Figures 13A and B**). Cells were lysed, and the collected PNSs were separated by reducing SDS-PAGE. The proteins were then transferred on a PVDF membrane, which was probed with both an anti-V5 (**Figure 13A**) and an anti-HA (**Figure 13B**) antibody to check the ectopic expression of both the V5- and the HA-tagged proteins. The same PNSs were then immunoprecipitated using anti-V5 antibody-conjugated agarose beads (**Figures 13C and D**). The isolated protein complexes were separated by SDS-PAGE under both non-reducing and reducing conditions and then transferred on PVDF membranes. Finally, the immunisolated complexes were analyzed by western blot with both an anti-V5 (**Figure 13C**) and an anti-HA (**Figure 13D**) antibody to check the formation of a mixed disulfide.

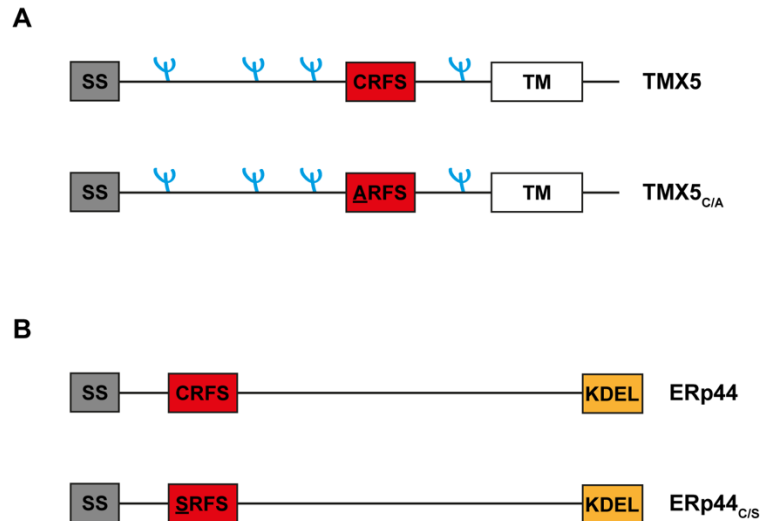


Figure 12: Schematic representation of TMX5 and ERp44 WT and inactive mutant constructs. A, TMX5 and TMX5_{C/A} constructs are shown together with the WT and the mutated active site sequences (red box, mutated amino acid underlined) and the four putative N-glycosylation sites (blue symbols). SS, signal sequence; TM, transmembrane region. B, ERp44 and ERp44_{C/S} constructs are represented indicating the WT and the mutated active site sequences (red box, mutated amino acid underlined). SS, signal sequence; KDEL, retrieval signal.

As previously shown, TMX5 engages mixed disulfides with endogenous substrates (**Figure 9**, lane 2, **Figure 13C**, lane 1). Interestingly, the mutation of the TMX5 active site (TMX5_{C/A}) abolished the formation of mixed disulfides with endogenous clients (**Figure 13C**, lane 2). Upon co-expression of both the WT versions of the two PDIs, the mixed disulfide between TMX5 and ERp44 was detected under non-reducing conditions (**Figure 13C and D**, lane 3), while the complex was disassembled when the same samples were separated under reducing conditions (**Figure 13C and D**, lane 9). Upon co-expression of TMX5 together with the ERp44_{C/S} mutant, the mixed disulfide was not detectable (**Figure 13C and D**, lane 4), hinting a direct role of the active site of ERp44 in the formation of the TMX5:ERp44 complex. On the same line, when the TMX5_{C/A} mutant was expressed in combination with the WT ERp44, the establishment of the disulfide-bonded complex between the two PDIs was not affected (**Figure 13C and D**, lane 5), while upon co-expression of the two mutants, TMX5_{C/A} and ERp44_{C/S}, the formation of the mixed disulfide was abolished (**Figure 13C and D**, lane 6). All in all, these evidences indicate that the formation of a TMX5:ERp44 disulfide bonded complex mainly relies on a functional ERp44 active site, whereas the active site of TMX5 is dispensable for the engagement of ERp44, but is required for the establishment of mixed disulfides with endogenous client substrates.

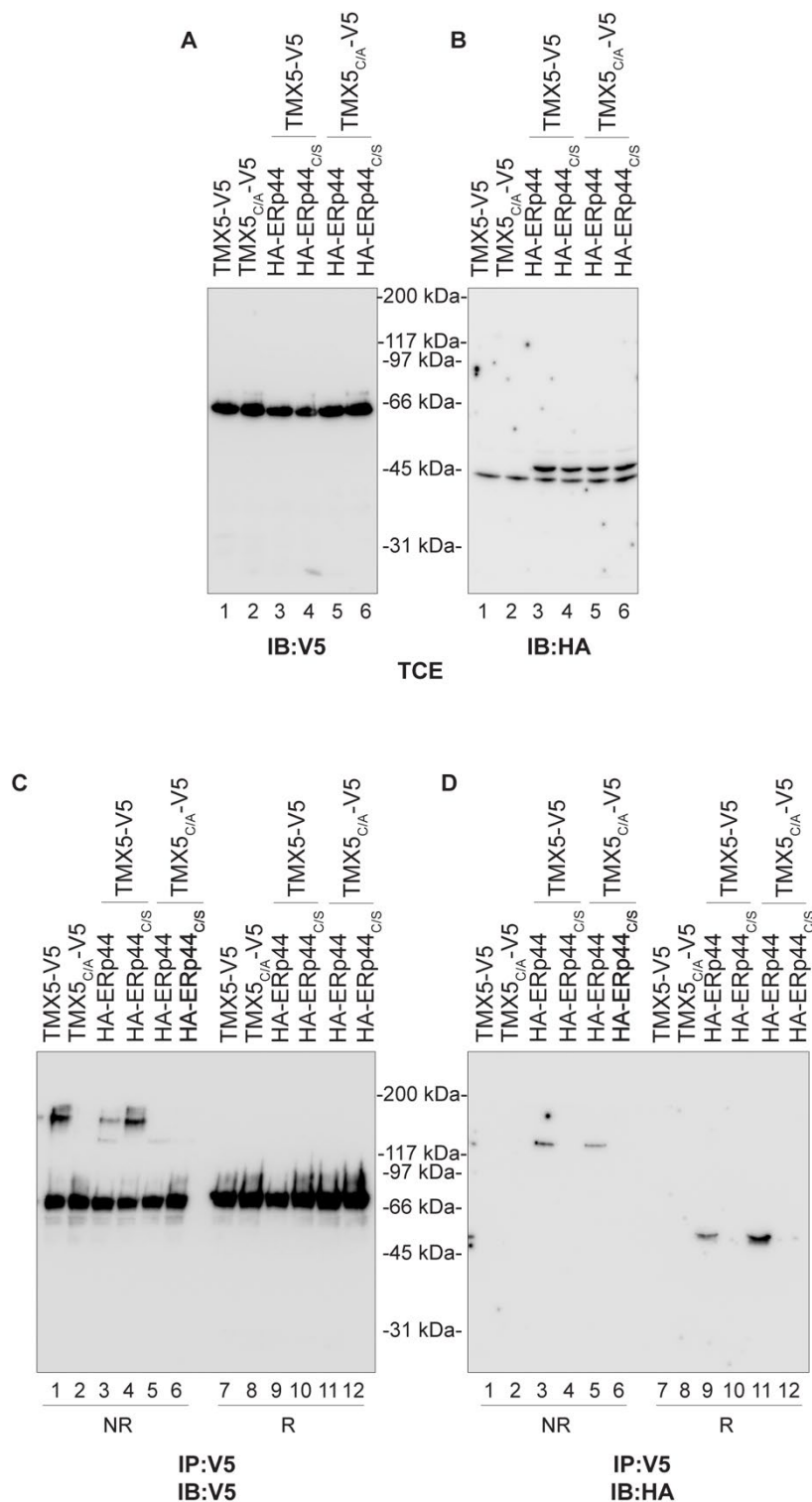


Figure 13: Characterization of the TMX5:ERp44 complex. **A**, HEK293 cells were transfected with the WT TMX5 or the mutant TMX5_{CIA} alone or in combination with the WT ERp44 or the mutant ERp44_{C/S}. After cells lysis, the PNSs were collected and separated by SDS-PAGE under reducing conditions. The proteins were transferred on a PVDF membrane that was probed with an anti-V5 antibody to check the expression of both WT TMX5 and its mutant TMX5_{CIA}. **B**, Same as panel **A**, but the membrane was immunoblotted with an anti-HA antibody to check the expression of WT ERp44 and its mutant ERp44_{C/S}, respectively. **C**, The PNSs of panel **A** were immunoprecipitated using anti-V5 antibody-conjugated agarose beads. The protein complexes were separated by SDS-PAGE under both non-reducing and reducing conditions and then transferred on a PVDF membrane, which was probed with an anti-V5 antibody. **D**, Same as panel **C**, but the membrane was immunoblotted using an anti-HA antibody.

5.2.1.7 ERp44 regulates the sub-cellular localization of TMX5 through the formation of a mixed disulfide

ERp44 is a soluble PDI family member harboring a C-terminal KDEL retrieval signal, which has been found to cycle between ER and ERGIC compartment to operate thiol-mediated-retention of misfolded proteins⁸³. Moreover, ERp44 is responsible for the retention within the ER of the oxidoreductase ERO1L- α , modulating its function as redox regulator³¹⁴. Given the role of ERp44 together with the evidences indicating that it interacts with the EndoH sensitive fraction of TMX5 (**Figure 11C**, lane 4), we decided to investigate if the formation of a mixed disulfide between TMX5 and ERp44 could regulate the sub-cellular localization of TMX5.

To this aim, HEK293 cells were seeded on poly-Lys coated glass coverslips and then transfected with the V5-tagged WT TMX5 or with its V5-tagged mutant TMX5_{C/A} alone (**Figure 14**) or in combination with the WT HA-ERp44, or with the mutated HA-ERp44_{C/S} (**Figures 16 and 17**). As control, cells were also single-transfected with the WT HA-ERp44 and its mutant HA-ERp44_{C/S} (**Figure 15**). Seventeen hours after transfection, cells were fixed, permeabilized and then stained with an anti-V5 and an anti-HA antibody to reveal the intracellular localization of TMX5 and ERp44, respectively. Cells were also stained for the endogenous proteins CNX and giantin, which were exploited as markers of the ER and the Golgi apparatus, respectively.

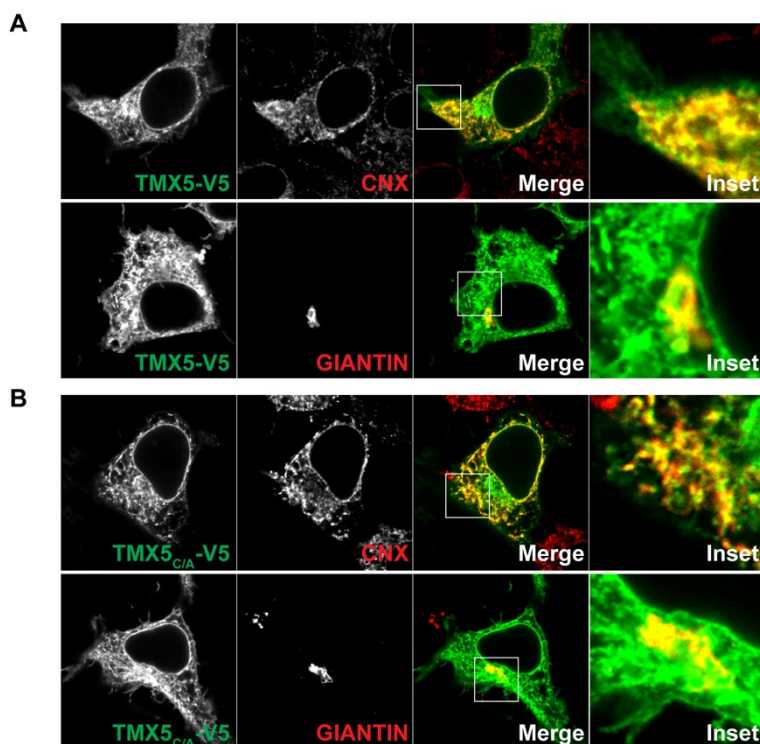
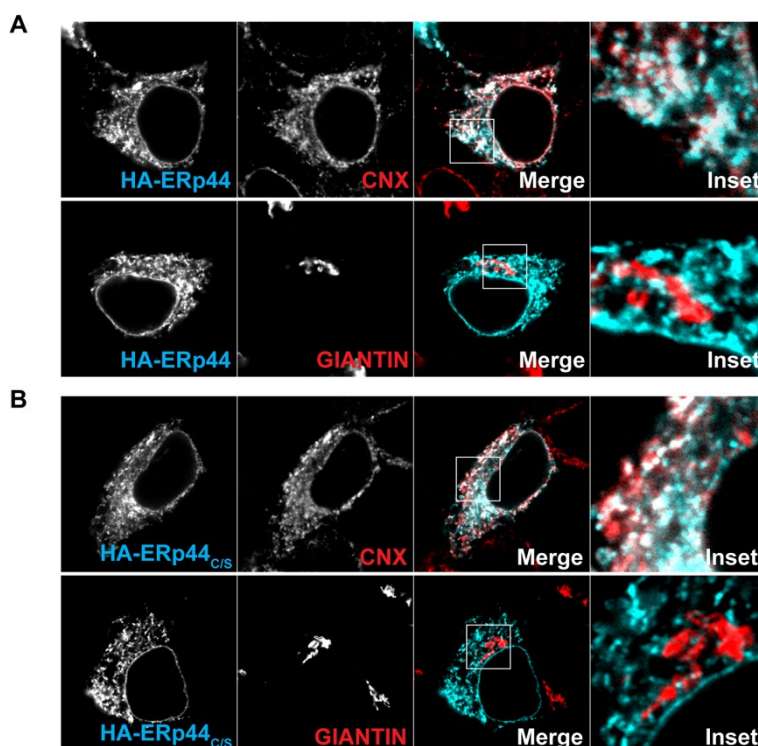


Figure 14: Intracellular localization of TMX5-V5 and TMX5_{C/A}-V5. A, HEK293 cells were seeded on poly-Lys coated coverslips and transfected with TMX5-V5. After fixing, cells were permeabilized and stained with an anti-V5 antibody in combination with an anti-CN X or an anti-giantin antibody as markers of the ER and the Golgi apparatus, respectively. B, Same as panel A, but cells were transfected with TMX5_{C/A}-V5.

Figure 15: Intracellular localization of HA-ERp44 and HA-ERp44_{C/S}. A, HEK293 cells were seeded on poly-Lys coated coverslips and transfected with HA-ERp44. After fixing, cells were permeabilized and stained with an anti-HA antibody in combination with an anti-CNX or an anti-giantin antibody as markers of the ER and the Golgi apparatus, respectively. B, Same as panel A, but cells were transfected with HA-ERp44_{C/S}.



Ectopically expressed TMX5-V5 resulted localized within the ER, but also in the Golgi compartment and at the plasma membrane (**Figure 14A**). These results are in line with the lack of an ER retention signal within the sequence of TMX5, but also with the previous data indicating the existence for TMX5 of an EndoH resistant fraction (**Figure 8B**). Interestingly, the mutation within the active site of TMX5 did not affect its overall sub-cellular localization: indeed, TMX5_{C/A} showed a co-localization with CNX and giantin, and a plasma membrane staining (**Figure 14B**). Consistently with the data reported in the literature, both ectopically expressed WT ERp44 and ERp44_{C/S} localized mainly in the ER (**Figure 15**).

Upon co-expression of ERp44, TMX5 resulted localized within the ER (**Figure 16A**), whereas the co-expression of its mutant ERp44_{C/S} did not affect the sub-cellular distribution of TMX5 (**Figure 16B**). On the same line, when mutant TMX5_{C/A} was expressed together with WT ERp44, it resulted mainly localized in the ER (**Figure 17A**). Upon co-expression of the two mutants PDIs, the route of TMX5_{C/A} to the plasma membrane was restored (**Figure 17B**). All together, these data show that the formation of a mixed disulfide between TMX5 and ERp44 determines the sub-cellular localization of TMX5, suggesting a possible mechanism for the regulation of the TMX5 function through its retention within the ER mediated by ERp44.

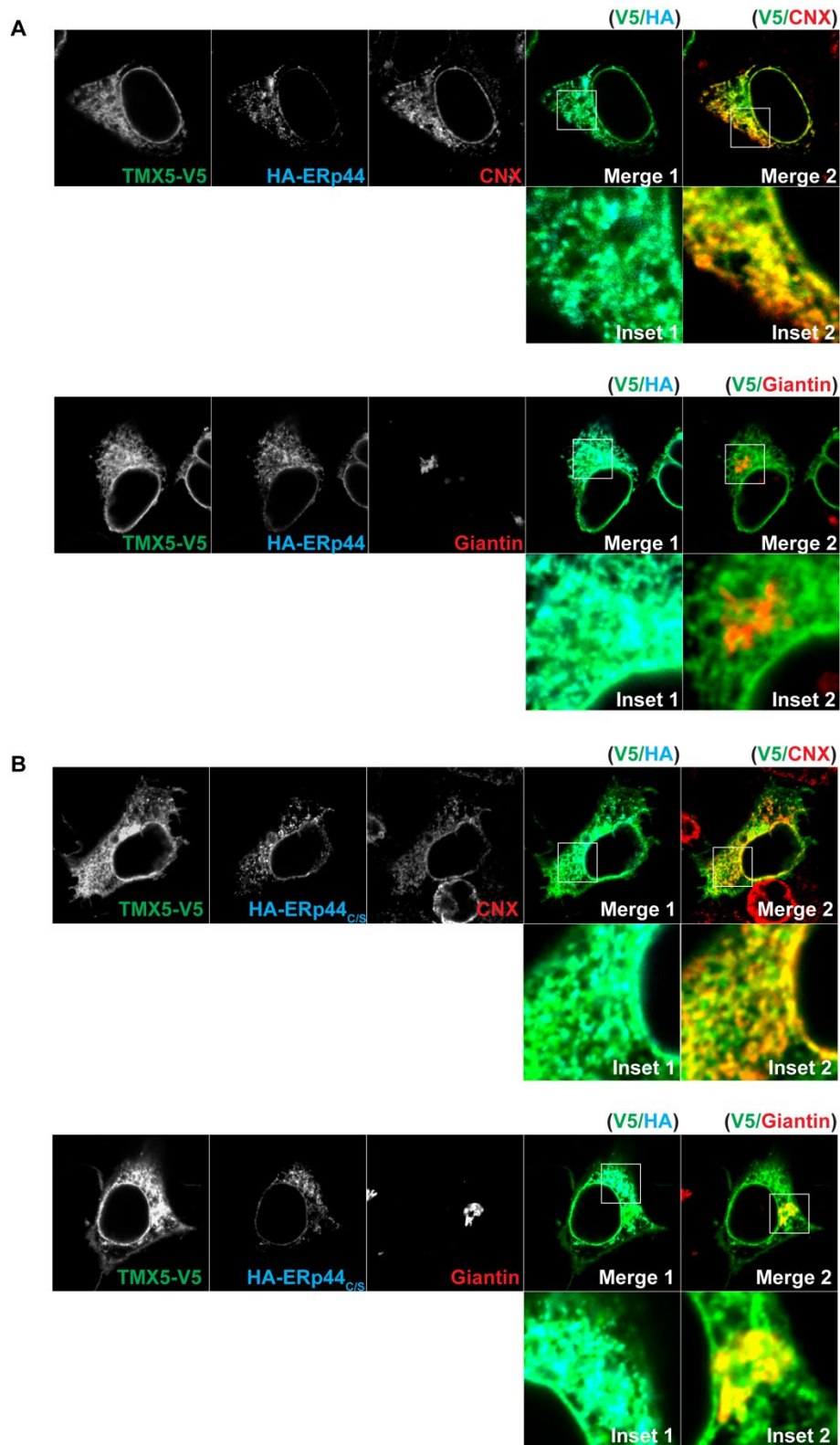


Figure 16: The expression of ERp44, but not of its mutant ERp44_{CIS} affects the sub-cellular localization of TMX5.
A, HEK293 cells were seeded on poly-Lys coated coverslips and co-transfected with TMX5-V5 and HA-ERp44. After fixing, cells were permeabilized and stained with both an anti-V5 and an anti-HA antibody in combination with an anti-CN_X (upper panel) or an anti-giantin (lower panel) antibody as markers of the ER and the Golgi apparatus, respectively.
B, Same as panel A, but cells were co-transfected with TMX5-V5 and HA-ERp44_{CIS}.

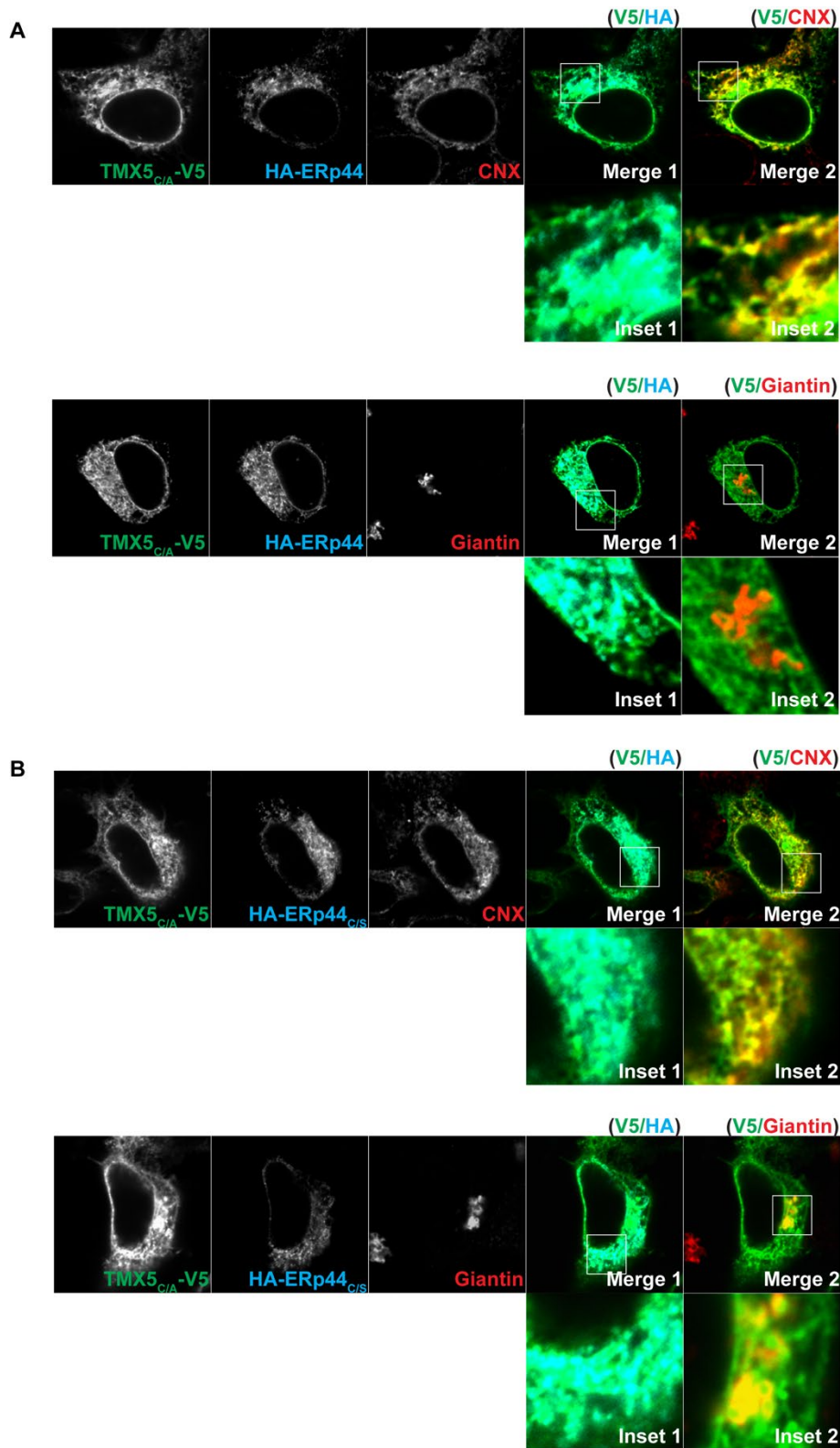


Figure 17: The expression of ERp44, but not of its mutant ERp44_{C/S} affects the sub-cellular localization of TMX5_{C/A}. **A**, HEK293 cells were seeded on poly-Lys coated coverslips and co-transfected with TMX5_{C/A}-V5 and HA-ERp44. After fixing, cells were permeabilized and stained with both an anti-V5 and an anti-HA antibody in combination with an anti-CN_X (upper panel) or an anti-giantin (lower panel) antibody as markers of the ER and the Golgi apparatus, respectively. **B**, Same as panel A, but cells were co-transfected with TMX5_{C/A}-V5 and HA-ERp44_{C/S}.

5.2.2 Discussion

5.2.2.1 TMX5, a peculiar member of TMX family

TMX5 is the youngest and the less characterized member of the TMX protein family. It is a type I protein, whose N-terminal region is characterized by four putative N-glycosylation sites and one type-a TRX-like domain. In this domain resides its greatest peculiarity: indeed, TMX5 displays a non-canonical CRFS active site, where the lack of the C-terminal cysteine residue makes TMX5 a natural trapping mutant. Interestingly, the same active site is shared by ERp44, a soluble member of the PDI protein family that is involved in thiol-mediated protein quality control³¹⁵. The only evidences available in literature about TMX5 report the existence of different mutations linked to the development of the Meckel-Gruber syndrome (MKS)^{210,211,316}, a rare perinatally lethal autosomal recessive ciliopathy.

In this thesis, a preliminary characterization of TMX5 is provided. In particular, the collected data showed that TMX5 is a N-glycosylated and ER stress unresponsive protein that travels along the secretory pathway, differently from the other TMXs. Moreover, it is able to engage mixed disulfides with endogenous proteins with a preference for membrane-tethered substrates. Finally, TMX5 forms a mixed disulfide with ERp44: this association relies on a functional active site of ERp44 and mediates the retention of TMX5 within the ER.

5.2.2.1.1 TMX5, a secreted N-glycosylated PDI unresponsive to ER stress

Different members of the PDI protein family are characterized by the presence of an ER stress responsive element (ERSE) within their promoter region, which is responsible for their transcriptional up-regulation upon ER stress¹⁹⁴. The data available in the literature indicate that TMX1, TMX2, TMX3 and TMX4 do not display any ERSE motif and are not up-regulated upon ER stress induction^{194,202,212,216,220}. On the same line, TMX5 resulted transcriptionally unresponsive to ER stress. This evidence might suggest that TMX5 would not have a role in the alleviation of the ER stress burden. Alternatively, it could also be possible that the expression of TMX5 would be post-transcriptionally regulated.

N-glycosylation is a post-translational modification that has an important role in both protein folding and targeting to different sub-cellular or extracellular sites. This modification also determines an increase in protein solubility and stabilizes the protein structures hiding hydrophobic stretches^{56,317}. Biochemical analyses showed that TMX5 is an N-glycosylated member of the TMX family, in addition to TMX3²¹⁶ and TMX4²²⁰.

Moreover, consistently with the lack of an ER retention signal within its cytosolic tail, TMX5 possesses an EndoH resistant fraction. This observation was further confirmed by the immunofluorescence analyses showing that TMX5 is localized within the ER, the Golgi apparatus and at the plasma membrane. Interestingly, the other members of the TMX family are all ER resident proteins: as such, these findings could suggest a possible peculiar role of TMX5 within the secretory pathway.

5.2.2.1.2 TMX5, a natural trapping mutant preferentially interacting with ERp44 and membrane-tethered substrates

TMX5 possesses a TRX-like domain within its luminal N-terminal region. This domain displays a peculiar CRFS active site that characterizes TMX5 as natural trapping mutant protein. Western blot analysis under non reducing conditions demonstrated that TMX5 is able to establish mixed disulfides with endogenous proteins. Additionally, mass spectrometry analyses suggested that TMX5 preferentially interacts with membrane-tethered endogenous proteins, similarly to what previously reported for TMX1²⁰⁶. This could hint that the topology of the PDI would represent itself a discriminant for the engagement of topology-specific protein substrates. The future characterization of the association between TMX5 and its substrates will be crucial to determine its possible role in the thiol-mediated protein quality control. Surprisingly, the same mass spectrometry analyses also pointed out a disulfide bonded complex between TMX5 and ERp44, a soluble PDI that intervenes during the thiol-mediated protein quality control³¹⁵. The exploitation of inactive mutant versions of both TMX5 and ERp44 allowed to determine that the formation of the mixed disulfide between the two PDIs relies on a functional ERp44 active site. Indeed, the mutation of the active site of TMX5 did not affect the establishment of the TMX5:ERp44 mixed disulfide, but it only abolished the formation of the disulfide-bonded complexes between TMX5 and endogenous client proteins. Immunofluorescence analyses of the sub-cellular localization of TMX5 showed its retention within the ER upon co-expression of ERp44. These results are consistent with the role of ERp44 in the retention of ERO1L- α within the ER³¹⁴, but also with our data showing that ERp44 associates with the EndoH sensitive fraction of TMX5. Considering these evidences, it could be hypothesized that the formation of the mixed disulfide between TMX5 and ERp44 regulates TMX5 function, through the modulation of its intracellular localization.

The similarity of the TMX5 active site with the one displayed by ERp44, together with the data hinting the preferential interaction of TMX5 with membrane-tethered endogenous

proteins, might suggest a possible role of TMX5 in the thiol-mediated quality control of membrane-bound proteins. In this context, TMX5 interaction with ERp44 would be crucial: in fact, since TMX5 lacks an ER retention motif within its sequence, ERp44 binding could mediate the retrieval of TMX5 and its trapped substrate to the ER lumen, thus regulating its function.

5.2.3 Contributions

I was involved in the conceptualization and development of this research project. For this section, I analyzed mass spectrometry data and realized respectively **Figures 6, 7, 8A, 12, 14-17**.

5.3 Design and development of HaloTag2®-based protein tools for the study of cellular PQC

5.3.1 Results

5.3.1.1 Generation of HaloTag2® protein chimeras

Maintenance of the cellular proteome integrity is crucial for cell health and viability. Indeed, the accumulation of unfolded intermediates and misfolded proteins within the cells represents the basis of many rare and inherited pathologies including neuro-degenerative diseases³¹⁸. To deal with this, cells have evolved protein quality control (PQC) systems to ensure the recognition and the consequent degradation of incorrectly folded and mis-localized polypeptides³¹⁹.

To enlarge our knowledge about PQC mechanisms within the secretory pathway, we designed and generated membrane-bound variants of the GFP-HaloTag2® as chimeric reporters of protein misfolding, exploiting basic strategies of plasmid DNA cloning. HaloTag2® is a modified variant of a bacterial haloalkane dehalogenase³²⁰, that is able to misfold upon the covalent binding to a cell-permeable hydrophobic chloroalkane-reactive ligand (**Figure 18A**), named HyT36³²¹ (**Figure 18B**).

All the HaloTag2® protein chimeras are characterized by a GFP molecule within the ER lumen and an HA-tag facing the cytosol (**Figure 18C and D**), in order to allow proteins detection in biochemical and immunofluorescence assays. To introduce variability among the misfoldable protein substrates, we attached the HaloTag2® moiety to two different transmembrane anchors made of respectively 17 (TM17) and 22 (TM22) amino acids to ensure differential protein localization (**Figure 18C and D**). Indeed, based on the available literature on the transmembrane anchors, proteins characterized by short transmembrane regions are retained within ER, also in the absence of a retention signal³²². On the other hand, long transmembrane anchors allow proteins release and trafficking along the secretory pathway³²².

Additionally, the misfoldable HaloTag2® domain was placed either at the cytosolic (**Figure 18C and D**, CH for C-terminal cytosolic side) or at the ER luminal side (**Figure 18C and D**, NH for N-terminal cytosolic side) of both TM17 and TM22, in order to allow the induction of protein misfolding in different cellular compartments. We also introduced N-glycosylation sites within the ER luminal domains of the chimeric proteins (**Figure 18C**

and D, GFP-NH-TM17 and GFP-NH-TM22). As such, we obtained a palette of misfoldable HaloTag2®-based protein chimeras characterized by different chemical-physical properties.

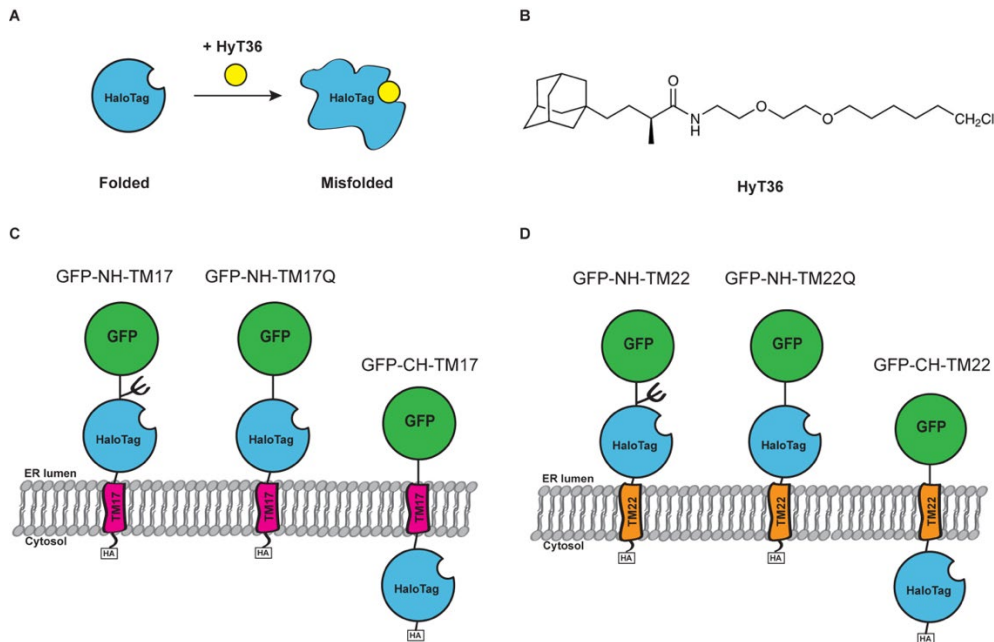


Figure 18: Schematics of the HaloTag2® misfolding and of the generated protein chimeras. **A**, Model of the HyT36-mediated HaloTag2® misfolding. **B**, Chemical structure of HyT36, the small molecule used to destabilize HaloTag2® protein chimeras. This representation was taken from Raina et al 2014. **C**, Schematic representation of the TM17-HaloTag2® protein chimeras. **D**, Schematic representation of the TM22-HaloTag2® protein chimeras.

5.3.1.2 Biochemical characterization of the HaloTag2®-based protein chimeras

As first step, to characterize the HaloTag2® protein chimeras and check the effects of the HyT36-mediated destabilization, HEK293 cells were transfected with an empty vector (EV, **Figure 19A**, lanes 1 and 2) or with the generated HaloTag2® constructs (**Figure 19A**, lanes 3 and 4, **and 19B-F**). Seventeen hours after transfection, cells were mock-treated with DMSO or treated with the destabilizing ligand HyT36. After six hours of treatment, cells were lysed and the collected PNSs were separated by reducing SDS-PAGE. After electrophoretic migration, the proteins were transferred on a PVDF membrane that was probed with an anti-GFP antibody to reveal the expression of the HaloTag2® protein chimeras. As loading control, immunoblotting analysis of the GAPDH levels was also performed.

Considering the modular construction of the HaloTag2® chimeras and the MW of the single domains, we estimated their apparent MW in about 70kDa. Indeed, immunoblotting

analysis with an anti-GFP antibody showed that all protein chimeras migrate near 66kDa, thus not too much far from our predictions (**Figure 19A**, lane 3, and **Figure 19B-F**, lane 1). The treatment with HyT36 of the cells transfected with the different chimeras resulted in a decreased protein signal for the substrates harboring the misfolded HaloTag2® within the ER lumen (**Figure 19A**, lane 3 vs 4, **Figure 19B, D and E**, lane 1 vs 2), while no effects could be seen for the chimeras displaying the HaloTag2® domain towards the cytosol (**Figure 19C and F**, lane 1 vs 2).

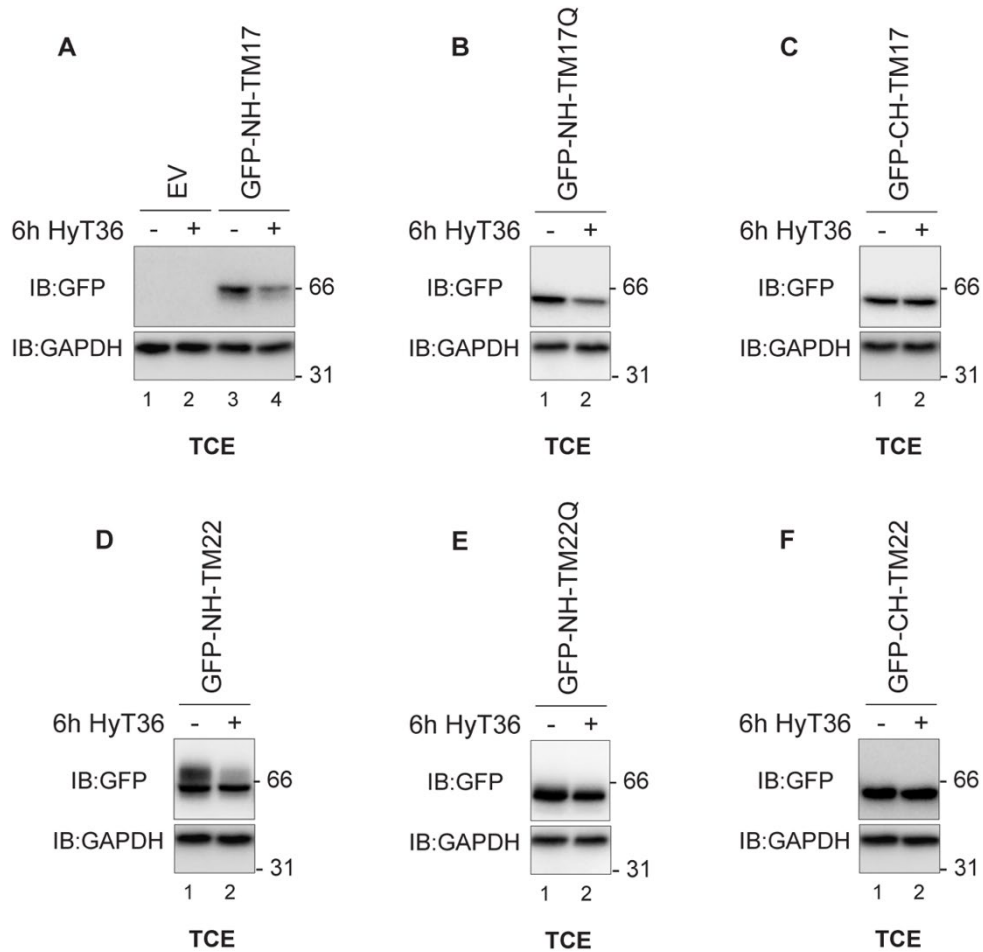


Figure 19: HaloTag2® protein chimeras expression +/- HyT36 ligand. **A**, HEK 293 cells were transfected with an empty vector (EV) or transfected with GFP-NH-TM17. Seventeen hours after transfection, cells were mock-treated with DMSO or incubated with 10µM HyT36 for six hours. After treatment, cells were lysed to collect the PNSs. The proteins were separated by SDS-PAGE under reducing conditions and then transferred on a PVDF membrane. Western blot analysis with an anti-GFP antibody was used to reveal the GFP-HaloTag2® protein chimera. Anti-GAPDH immunoblotting was performed as loading control. **B**, Same as panel **A**, but cells were transfected with GFP-NH-TM17Q. **C**, Same as panel **A**, but cells were transfected with GFP-CH-TM17. **D**, Same as panel **A**, but cells were transfected with GFP-NH-TM22. **E**, Same as panel **A**, but cells were transfected with GFP-NH-TM22Q. **F**, Same as panel **A**, but cells were transfected with GFP-CH-TM22.

Additionally, immunoblotting analysis revealed a unique band for all the HaloTag2® protein chimeras (**Figure 19B, C, E and F**, lanes 1 and 2) except for GFP-NH-TM17 and GFP-NH-TM22 (**Figure 19A**, lanes 3 and 4, **and Figure 19D**, lanes 1 and 2). Indeed, GFP-NH-TM17 displayed a main band at 66kDa and a smear just below (**Figure 19A**, lanes 3 and 4), whereas GFP-NH-TM22 displayed a strong signal just below 66kDa and smeared signals above and below the main band (**Figure 19D**, lanes 1 and 2). Since both GFP-NH-TM17 and GFP-NH-TM22 harbor a N-glycosylation site within their luminal domain (**Figure 18B and C**), these evidences are compatible with the presence of different glycosylated forms at steady state. As such, EndoH and PNGaseF treatment of the PNSs of cells transfected with GFP-NH-TM17 induced a shift in protein electrophoretic migration (**Figure 20A**): intriguingly, the electrophoretic mobility of this protein changed in the same way in both treatments (**Figure 20A**, lanes 1 vs 2 and 3) indicating that it is an ER resident N-glycosylated protein. Interestingly, the enzymatic digestion of GFP-NH-TM22 revealed a distinct susceptibility to the EndoH and the PNGaseF cleavage (**Figure 20B**): in fact, the EndoH treatment induced a shift in the electrophoretic migration only of the main band below 66kDa, indicating the existence of an EndoH resistant fraction (**Figure 20B**, lane 1 vs 2), that is then efficiently processed upon PNGaseF treatment (**Figure 20B**, lane 1 vs 3). This is due to the different cleavage specificity of the two enzymes: while the EndoH removes poorly complex N-glycans belonging to proteins localized within the ER, the PNGaseF cleaves also complex N-glycans resulting from their further processing in the Golgi apparatus. These findings confirm that due to the nature of its TM22, GFP-NH-TM22 is a N-glycosylated protein that exits from the ER.

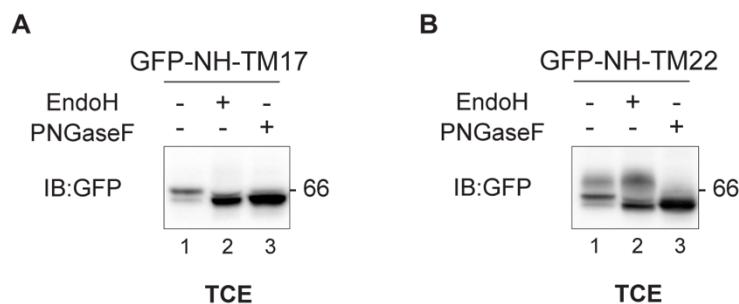


Figure 20: EndoH and PNGaseF treatment of GFP-NH-TM17 and GFP-NH-TM22. **A**, The PNSs of cells transfected with GFP-NH-TM17 were mock-treated or incubated with either EndoH or PNGaseF for 1h at 37°C. After treatment, proteins were separated by reducing SDS-PAGE and transferred on a PVDF membrane. Immunoblotting with an anti-GFP antibody was performed to reveal the signal of the GFP-HaloTag2® chimera. **B**, Same as panel **A**, but the PNSs of cells transfected with GFP-NH-TM22 was used.

All in all, these data show that the levels of the HaloTag2® protein chimeras at steady state result differentially affected upon HyT36 treatment: indeed, the chimeras displaying the HaloTag2® moiety within the ER lumen have a decreased overall level, while their sisters with the same misfolded domain facing the cytosol are not affected. Moreover, the EndoH and the PNGaseF assays confirmed that both GFP-NH-TM17 and GFP-NH-TM22 are N-glycosylated proteins, but thanks to their different transmembrane regions, the first one is resident within the ER, whereas the latter has an EndoH resistant fraction, which exits from the ER.

5.3.1.3 Intracellular localization of the HaloTag2® protein chimeras

To characterize their intracellular localization, Flp-In NIH-3T3 mouse fibroblasts were stably transfected with the HaloTag2® protein chimeras (**Figures 21 and 22**) (see **Materials and Methods** section). Cells were seeded on alcian blue coated glass coverslips and then were mock-treated with DMSO (**Figure 21A, C and E, and Figure 22A, C and E**), or treated with the HyT36 ligand (**Figure 21B, D and F, and Figure 22B, D and F**). After 12h of treatment, cells were fixed, permeabilized and stained using either the anti-CNX (**Figures 21 and 22**, upper panels) or the anti-giantin (**Figures 21 and 22**, lower panels) antibody as endogenous markers respectively for the ER and the Golgi compartment. The HaloTag2® protein chimeras were visualized without staining thanks to the fluorescence of the GFP molecule placed within the constructs.

Immunofluorescence analysis of the TM17-HaloTag2® chimeras revealed the co-localization of the GFP signal with CNX, but not with giantin (**Figure 21A, C and E**), indicating that these three proteins are localized within the ER, consistently with the characteristics of their transmembrane anchor³²². Notably, the treatment with HyT36 did not affect the localization pattern of the TM17-HaloTag2® protein chimeras (**Figure 21B, D and F**). Conversely, the TM22-based HaloTag2® protein chimeras co-localized with both CNX and giantin (**Figure 22A, C and E**). Moreover, these proteins also stained the plasma membrane (**Figure 22A, C and E**). These data are consistent with the previous reports about transmembrane anchors, indicating that the proteins harboring a long transmembrane region, as TM22, are able to exit from the ER and travel along the secretory pathway³²². Interestingly, the HyT36-induced misfolding caused a change in the localization pattern of both the TM22 chimeras displaying HaloTag2® moiety within the ER lumen: indeed, the plasma membrane staining of GFP-NH-TM22 and GFP-NH-TM22Q was lost upon the treatment with HyT36 (**Figure 22B and D**). On the contrary, the

intracellular localization of GFP-CH-TM22 was not affected (**Figure 22F**). These data are in line with what previously emerged for GFP-NH-TM22: indeed, western blot analysis highlighted a decreased level of its EndoH resistant fraction upon the treatment with HyT36 (**Figure 19D**, lane 1 vs 2).

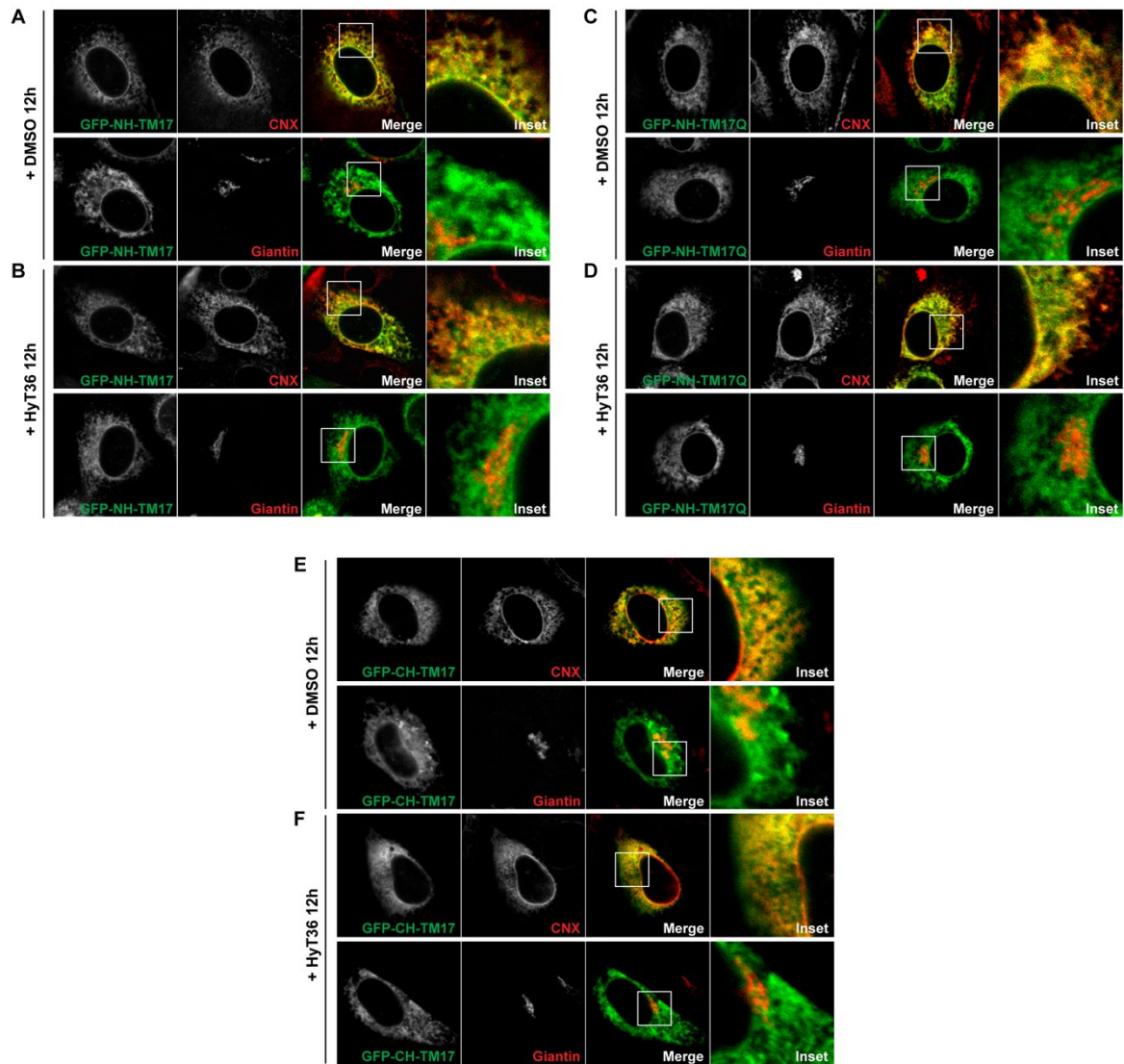


Figure 21: Intracellular localization of the TM17-based HaloTag2® protein chimeras. A, Flp-In NIH-3T3 cells stably transfected with GFP-NH-TM17 were seeded on alcian blue coated coverslips and mock-treated with DMSO for 12h. After fixation and permeabilization, cells were stained either with an anti-CN X (upper panel) or an anti-giantin antibody (lower panel). Coverslips were analyzed by confocal microscopy. B, Same as A, but the cells were treated with HyT36 for 12h. C, Same as A, but for Flp-In NIH-3T3 cells stably transfected with GFP-NH-TM17Q. D, Same as C, but the cells were treated with HyT36 for 12h. E, Same as A, but for Flp-In NIH-3T3 cells stably transfected with GFP-CH-TM17. F, Same as E, but the cells were treated with HyT36 for 12h.

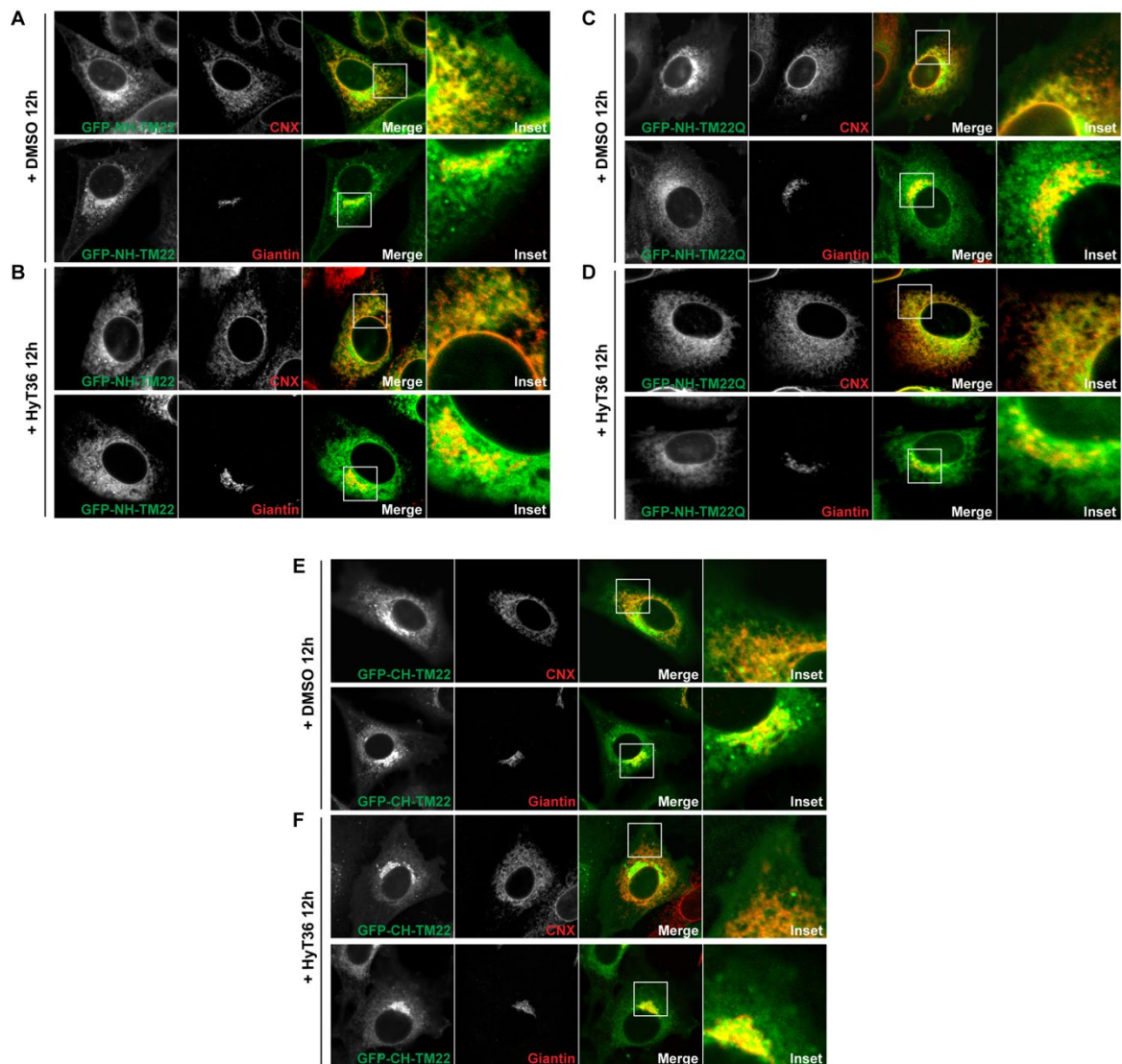


Figure 22: Intracellular localization of the TM22-based HaloTag2® protein chimeras. **A**, Flp-In NIH-3T3 cells stably transfected with GFP-NH-TM22 were seeded on alcian blue coated coverslips and mock-treated with DMSO for 12h. After fixation and permeabilization, cells were stained either with an anti-CN_X (upper panel) or an anti-giantin antibody (lower panel). Coverslips were analyzed by confocal microscopy. **B**, Same as **A**, but the cells were treated with HyT36 for 12h. **C**, Same as **A**, but for Flp-In NIH-3T3 cells stably transfected with GFP-NH-TM22Q. **D**, Same as **C**, but the cells were treated with HyT36 for 12h. **E**, Same as **A**, but for Flp-In NIH-3T3 cells stably transfected with GFP-CH-TM22. **F**, Same as **E**, but the cells were treated with HyT36 for 12h.

As control, we also performed an immunofluorescence analysis of the stably transfected Flp-In NIH-3T3 cells incubated with a fluorescent HaloTag[®] ligand (i.e. PBI5030) instead of the destabilizing ligand HyT36 (**Figure 23**). As such, treatment with PBI5030 did not change the intracellular localization of any of the HaloTag2[®] protein chimeras (**Figure 23**), confirming that the effect on GFP-NH-TM22 and GFP-NH-TM22Q localization (**Figure 22B and D**) is the direct consequence of the HyT36-mediated misfolding.

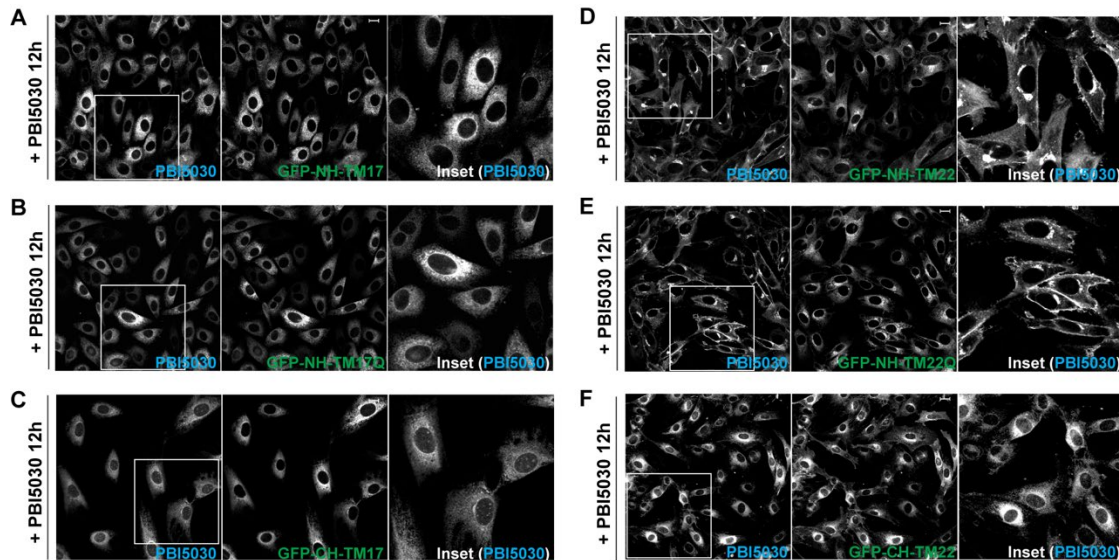


Figure 23: Intracellular localization of the HaloTag2[®] protein chimeras with the fluorescent ligand PBI5030. **A**, Flp-In NIH-3T3 cells stably transfected with GFP-NH-TM17 were seeded on alcian blue coated coverslips and incubated with the fluorescent ligand PBI5030. After 12h, cells were fixed and analyzed by confocal microscopy. **B**, Same as **A**, but for Flp-In NIH-3T3 cells stably transfected with GFP-NH-TM17Q. **C**, Same as **A**, but for Flp-In NIH-3T3 cells stably transfected with GFP-CH-TM17. **D**, Same as **A**, but for Flp-In NIH-3T3 cells stably transfected with GFP-NH-TM22. **E**, Same as **A**, but for Flp-In NIH-3T3 cells stably transfected with GFP-NH-TM22Q. **F**, Same as **A**, but for Flp-In NIH-3T3 cells stably transfected with GFP-CH-TM22.

All together, these data showed that consistently with the intrinsic properties of the transmembrane, the TM17-based HaloTag2[®] chimeras are ER resident proteins. Additionally, their localization is not affected by the binding of HyT36. On the other hand, the TM22-based HaloTag2[®] chimeras stain the ER, the Golgi apparatus and are displayed at the plasma membrane, but upon the treatment with HyT36, only the luminal HaloTag2[®]-TM22 chimeras lose the plasma membrane staining, suggesting that the misfolded HaloTag2[®] domain is efficiently recognized by the ER quality control, eventually preventing the release of the chimeras in the secretory pathway.

5.3.1.4 HyT36 treatment induces BiP binding of the NH-HaloTag2® protein chimeras

Previous evidences reported in literature showed that the HyT36-induced misfolding of an ER resident GFP-HaloTag2® soluble protein triggers its binding to BiP and its consequent degradation³²³. BiP is an ER luminal chaperone that recognizes misfolded proteins thanks to the exposition of hydrophobic stretches allowing their degradation through ERAD³²⁴. Considering the previous data, we hypothesized that the decrease in protein levels of the chimeras harboring the HaloTag2® within the ER lumen (NH-HaloTag2® protein chimeras) upon the treatment with HyT36 could be due to BiP recognition and binding. To confirm this hypothesis, the same PNSs of **6.3.2** paragraph were immunoprecipitated using an anti-GFP antibody and the immunisolated complexes were separated by reducing SDS-PAGE. After electrophoretic migration, the proteins were transferred on a PVDF membrane that was analyzed by western blot to assess the co-precipitation of BiP. After stripping, the same membrane was probed with an anti-GFP antibody to check the immunoisolation of the HaloTag2® protein chimeras.

Western blot analysis of BiP co-precipitation showed that all chimeric proteins bind a certain amount of BiP at steady state (**Figure 24A**, lane 3, **Figures 24B-F**, lane 1). Interestingly, upon treatment with HyT36, BiP binding visibly increased in the case of the chimeras displaying the HaloTag2® within the ER lumen (**Figure 24A**, lane 3 vs 4, **Figure 24B, D and E**, lane 1 vs 2). On the contrary, BiP co-precipitation did not change upon the HyT36-induced misfolding of the HaloTag2® constructs with the misfolded domain facing the cytosol (**Figure 24C and F**, lane 1 vs 2). As specificity control, an anti-GFP immunoprecipitation was also performed in the mock-transfected samples (**Figure 24A**, lanes 1 and 2). These data suggest that as for the ER resident soluble GFP-HaloTag2® protein³²³, the binding of HyT36 destabilizes the HaloTag2® and this destabilization is detected by the ER quality control through BiP only when the misfolded moiety is localized within the ER lumen. BiP could then commit the destabilized HaloTag2® protein chimeras to degradation, justifying their decreased levels at steady state (**Figure 19A**, lane 3 vs 4, **and Figure 19B, D and E**, lane 1 vs 2).

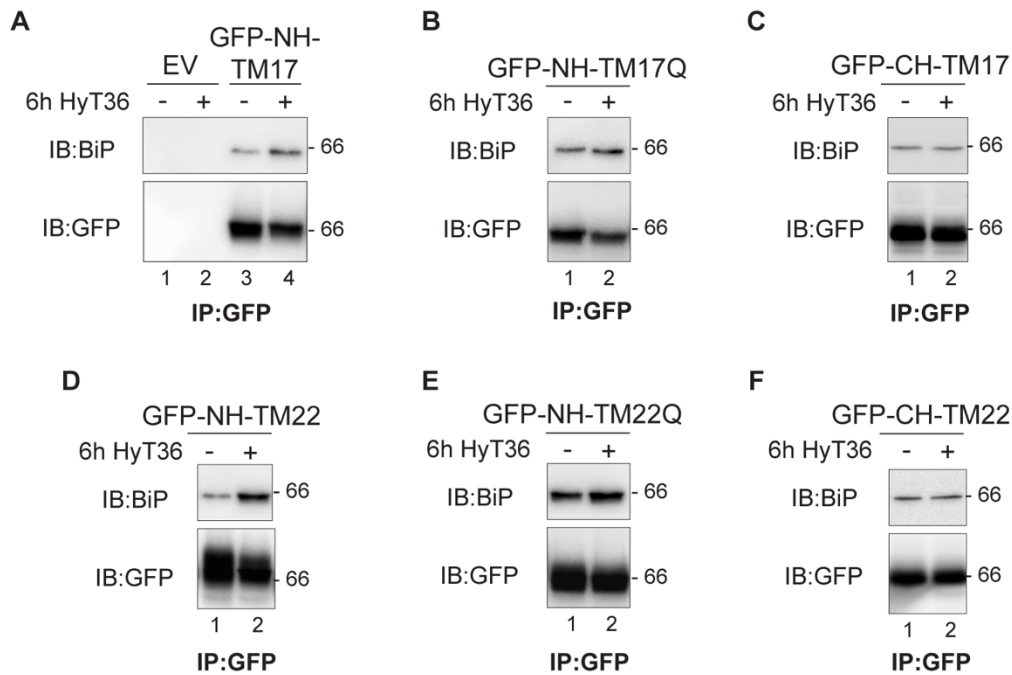


Figure 24: Effect of the HyT36-induced misfolding on BiP binding of the HaloTag2® protein chimeras. **A**, the PNSs of cells transfected with an empty vector (EV) or with GFP-NH-TM17 were immunoprecipitated using an anti-GFP antibody. The isolated protein complexes were then separated by SDS-PAGE under reducing conditions and transferred on a PVDF membrane. Immunoblotting analysis using an anti-KDEL antibody was performed to reveal the co-precipitation of BiP. After stripping, the same membrane was probed with an anti-GFP antibody to check the levels of the HaloTag2® chimera. **B**, Same as **A**, but using the PNSs of cells transfected with GFP-NH-TM17Q. **C**, Same as **A**, but using the PNSs of cells transfected with GFP-CH-TM17. **D**, Same as **A**, but using the PNSs of cells transfected with GFP-NH-TM22. **E**, Same as **A**, but using the PNSs of cells transfected with GFP-NH-TM22Q. **F**, Same as **A**, but using the PNSs of cells transfected with GFP-CH-TM22.

5.3.1.5 Analysis of the ER stress induction by the HyT36-mediated misfolding of the HaloTag2® protein chimeras

The accumulation of misfolded products within the ER can induce ER stress, which results in the activation of the UPR aiming to restore the ER homeostasis²²⁴. Recently, it has been shown that the HyT36-mediated misfolding of the soluble ER resident GFP-HaloTag2® moiety induces ER stress³²³. Thus, to assess if the generated membrane-tethered HaloTag2® chimeras are able to trigger the UPR activation, the transcripts of the stably transfected Flp-In NIH-3T3 cells were analyzed upon treatment with HyT36. In details, Flp-In NIH-3T3 cells stably transfected with the HaloTag2® protein chimeras were plated and incubated with the HyT36 ligand for 6h. Cells were lysed to collect total RNA. The transcript levels of BiP were determined by qPCR. The treatment of mock Flp-In NIH-3T3

cells with 5 μ g/mL tunicamycin for 6h was used as positive control of ER stress induction, whereas the same cells treated with HyT36 for 6h were used as negative control.

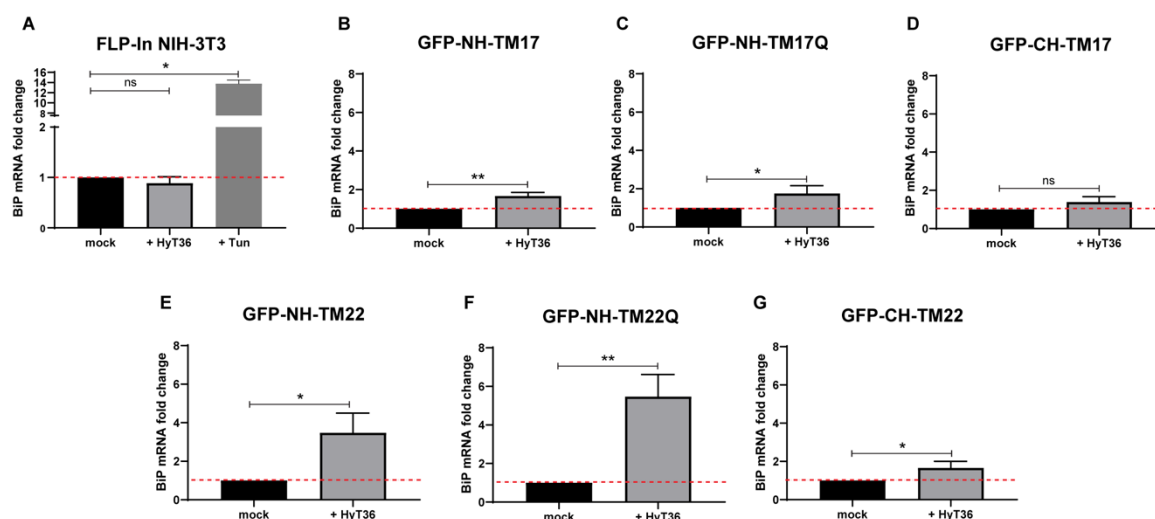


Figure 25: Analysis of the BiP transcript levels upon HyT36-mediated misfolding of the HaloTag2[®] protein chimeras. **A**, FLP-In NIH-3T3 cells were mock-treated with DMSO, treated with 10 μ M HyT36 or 5 μ g/mL tunicamycin for 6h. After lysis, the RNA was collected and used to analyze the transcript levels of BiP by qPCR. **B**, FLP-In NIH-3T3 cells stably expressing GFP-NH-TM17 were mock-treated with DMSO or treated with 10 μ M HyT36 for 6h. Cells were lysed, and the RNA was collected and used to analyze the BiP transcripts by qPCR. **C**, Same as **B**, but for FLP-In NIH-3T3 cells stably expressing GFP-NH-TM17Q. **D**, Same as **B**, but for FLP-In NIH-3T3 cells stably expressing GFP-CH-TM17. **E**, Same as **B**, but for FLP-In NIH-3T3 cells stably expressing GFP-NH-TM22. **F**, Same as **B**, but for FLP-In NIH-3T3 cells stably expressing GFP-NH-TM22Q. **G**, Same as **B**, but for FLP-In NIH-3T3 cells stably expressing GFP-CH-TM22. Error bars: mean and SDs of three independent experiments for all panels. Significance was analyzed by unpaired t-test; *p < 0.05; **p < 0.01

The treatment of mock FLP-In NIH-3T3 cells with HyT36 did not induce any change in BiP transcript levels (**Figure 25A**). On the other hand, a strong up-regulation of the BiP transcripts was detected upon tunicamycin treatment of the same cells (**Figure 25A**). The treatment with HyT36 of the cells expressing the HaloTag2[®] chimeras with the misfolded domain within the ER lumen affected BiP transcript levels but at different extents (**Figure 25B, C, E and F**). Indeed, BiP transcripts were slightly but significantly induced upon the treatment with HyT36 of FLP-In NIH-3T3 cells expressing GFP-NH-TM17 and GFP-NH-TM17Q (**Figure 25B and C**). For their counterparts built around a TM22 scaffold, the induction of BiP resulted much stronger (**Figure 25E and F**), even though the response was not even near to the one induced by the treatment with tunicamycin (**Figure 25A**).

Interestingly, this comparison underlines once more that chemical ER stress inducers trigger an exacerbate response, which is quite far from a more physiological landscape of an ER stress induced by protein misfolding³²⁵. Additionally, for both the TM17 and the TM22 chimeras harboring the HaloTag2® within the ER lumen, the HyT36 induced misfolding of the N-glycosylated versions (GFP-NH-TM17 and GFP-NH-TM22) triggered a lower up-regulation of BiP transcripts compared to their un-glycosylated counterparts (GFP-NH-TM17Q and GFP-NH-TM22Q) (**Figure 25B vs C, Figure 25E vs F**): this would be due to the fact that the oligosaccharide tree could sterically hinder the misfolded domain, impeding its recognition by the ER quality control. Notably, HyT36-mediated destabilization of GFP-CH-TM17 did not induce any statistically significant change in BiP transcript levels (**Figure 25D**). On the other hand, the treatment with HyT36 of FLP-In NIH-3T3 cells expressing GFP-CH-TM22 slightly affected BiP transcripts (**Figure 25G**): even though this response resulted significant, its entity was not comparable to the one induced by its counterparts displaying the HaloTag2® towards the ER (**Figure 25E-F vs 25G**). All together these data indicate that the HyT36 induced misfolding of the membrane-tethered HaloTag2® chimeras triggers an ER stress response when the misfolded domain is placed within the ER lumen. Moreover, this protein-misfolding dependent response results milder compared to the ER stress induced by treating the cells with a chemical compound as tunicamycin.

5.3.2 Discussion

Cells can be compared to a swiss clock, where every little gear is perfectly fitted and works together to ensure the perfect timing. Any damage within this system can lead to catastrophic consequences. Indeed, in cells an unbalanced proteostasis due to the accumulation of misfolded proteins can cause many different rare and invalidating diseases³¹⁸. To avoid this fate, the nature evolved protein quality control (PQC) systems that monitor the proteome health and take care of the misfolded proteins ensuring their clearance³¹⁹. As such, the dissection of these mechanisms results crucial and constitutes the unique weapon to contrast the diseases caused by perturbations in cell proteostasis.

During my PhD, I designed and developed protein-based tools for the characterization of the PQC pathways. To this aim, the HaloTag2® system was exploited: this domain was generated by mutating a bacterial enzyme to covalently bind chloroalkane reactive ligands³²⁰. According to the nature of the ligands, HaloTag2® can be used for different purposes, such as cell imaging and protein purification³²⁰. In this work, I took advantage from the capacity of the HaloTag2® to become misfolded upon the covalent binding of an hydrophobic chloroalkane reactive ligand (i.e. HyT36)³²¹. Using the HaloTag2® as a scaffold, I build a palette of membrane-tethered protein substrates able to elicit PQC systems response.

5.3.2.1 Rational of the HaloTag2®-based protein chimeras and the effects of the HyT36-mediated misfolding

From the less to the most complex organism, the nature evolved proteins displaying a large variety of different features. Indeed, proteins are the results of complex structural 3D arrangements, whose formation is driven by the information contained within its primary sequence. As such, these molecules can be either soluble or anchored to cells membrane through a transmembrane anchor, build around one or more domains of different length, present post-translational modifications such as N-glycosylation, and either be localized in a specific cellular compartment or spread in different sub-regions. This great variability is crucial for cells functionality: in fact, it allows the construction of a complete army of soldiers able to ensure the plasticity needed from the cells to carry out all the different processes indispensable for the survival. Given proteins diversification, the cells developed systems of quality control in order to efficiently recognize misfolded structures displayed by proteins with different characteristics.

Relying on studies showing that transmembrane domains of 17 residues retain membrane proteins within the ER while their elongation by 5 residues promotes secretion³²², the HaloTag2® domain was modified by introducing two different transmembrane anchors of 17 (TM17) and 22 residues (TM22). Trying to emulate the nature variability, the HaloTag2® was alternatively placed either at the cytosolic or at the ER luminal side of the two transmembrane anchors, allowing the induction of protein misfolding in different cellular compartments. Moreover, N-glycosylated variants of the chimeras were also prepared.

To assess if these HaloTag2® protein chimeras could be exploited as tools for the dissection of the cellular PQC systems, biochemical, immunofluorescence and transcriptional analyses were performed. Biochemical analyses of the HaloTag2® protein chimeras expressed in mammalian cells revealed that the binding of the HyT36-destabilizing ligand induces different outcomes according the HaloTag2® orientation: indeed, the proteins displaying the HaloTag2® within the ER lumen showed a decreased level at steady state, upon treatment with HyT36; the same treatment did not induce any change for the chimeras harboring the same misfolded domain towards the cytosol. These data suggest that the luminal quality control efficiently recognizes misfolded moieties independently from their glycosylation state or transmembrane anchor. In addition, immunoprecipitation analyses showed that the recognition of the luminal misfolded moieties is due to the action of the ER chaperone BiP: in fact, upon HyT36 treatment, BiP co-precipitation increased in the case of the luminal HaloTag2® protein chimeras, while being unaffected in the case of the chimeras exposing the same misfolded domain towards the cytosol.

The differences between luminal and cytosolic HaloTag2® protein chimeras were also confirmed by the immunofluorescence analyses. Consistently with the characteristics of the TM17, all the GFP-HaloTag2®-TM17 proteins were localized in the ER and the treatment with HyT36 did not change this pattern. Conversely, the GFP-HaloTag2®-TM22 chimeras were localized in the ER, in the Golgi apparatus and at the plasma membrane: the treatment with HyT36 did not induce any change when the misfolded HaloTag2® domain was displayed on the cytosolic side; differently, both the N-glycosylated and the non-glycosylated luminal TM22 HaloTag2® chimeras lost the plasma membrane staining upon the HyT36-mediated destabilization. Notably, incubation of the same cells with a

fluorescent HaloTag-ligand (i.e. PBI5030) confirmed that this phenotype was due to the specific effect of the HyT36 binding.

It should be taken into consideration that the differential responses between luminal and cytosolic HaloTag2® chimeras could be also a matter of timing: indeed, it could be possible that extending HyT36 treatment, also the levels of the cytosolic HaloTag2® chimeras would change as well as their intracellular localization; as such, this would indicate that the luminal and the cytosolic quality controls have different kinetics of recognition, with the first one being faster and with a lower activation threshold.

Finally, since sensing of the misfolded proteins by the ER quality control could be associated with an ER stress induction and consequently to the UPR activation, transcriptional up-regulation of the stress inducible ER chaperone BiP was checked for all HaloTag2® protein chimeras. This experiment showed a mild but significant UPR induction for GFP-HaloTag2®-TM17 chimeras displaying the misfolded moiety within the ER lumen upon HyT36 treatment, while no differences were detected for their counterpart harboring the HaloTag2® within the cytosol. On the other hand, for the HaloTag2®-TM22 chimeras, a strong and significant BiP induction upon the HyT36 induced misfolding was detected when the HaloTag2® moiety faced the ER lumen. Interestingly, a slight but significant BiP up-regulation was also detected for the cytosolic GFP-HaloTag2®-TM22 chimera. These data indicate that the misfolding within the ER luminal domain is sensed by the ER quality control and triggers an ER stress. Moreover, compatibly with differences in protein features, BiP transcripts were induced at different extents. Indeed, for both the two couples of protein chimeras with luminal HaloTag2®, the non-glycosylated versions induced a higher response compared to their N-glycosylated counterparts. This could hint that the oligosaccharide tree could disfavor through steric hindrance the recognition of the misfolded moiety, thus resulting in a small elicited UPR. Of note, the HyT36-mediated misfolding of any of the HaloTag2® protein chimeras failed to reproduce the strong BiP up-regulation observed upon cells treatment with the chemical ER stress inducer tunicamycin: this evidence interestingly highlights as the HaloTag2® system could reproduce a condition of physiological ER stress; indeed, the usage of chemical compounds to induce ER stress elicits an exacerbate UPR activation, that it is not comparable to the one induced by protein misfolding³²⁵.

All in all, the data collected in this thesis demonstrated that the developed HaloTag2® protein chimeras represent an optimal tool to dissect the PQC systems. The analyses of the transcripts and proteins fluctuations induced by the misfolding of the different HaloTag2® chimeras would allow the dissection of the unique cellular responses characteristics of each misfolded proteins. Moreover, these tools would be also instrumental for the characterization of the machineries required for the degradation of different protein substrates. Indeed, given the great variety of proteins involved in ERAD and the current evidences reported in the literature, it has been postulated that different dislocon complexes take care of different protein substrates. Even though, ERAD is a hot topic since many years, the mechanisms as well as the effectors required for the degradation of non-glycosylated proteins still remain to be assessed. In this context, the comparison of the interacting partners of the misfolded N-glycosylated and non-glycosylated HaloTag2® substrates would be useful. Finally, considering the great plasticity of this HaloTag2® system, it could be also exploited for the targeting of misfoldable protein substrates to the mitochondria or the nuclear envelope in order to widely characterize the cells' responses to protein misfolding in different cellular compartment. As such, the future exploitation of the designed HaloTag2® protein chimeras will lead to the dissection of different crucial aspects of cells functionality and homeostasis.

5.3.3 Contributions

I was involved in the conceptualization and development of this research project and I realized all the figures contained in this section.

5.4 Analysis of the transcriptional response underlying Recov-ER-Phagy

5.4.1 Results

5.4.1.1 Concept and design of the “Recov-ER-Phagy” transcriptomic analysis

Upon cessation of an ER stress, mammalian cells activate ill-defined recovery programs to clear damaged and/or excess ER produced during the stress and thus restore the ER homeostasis. These catabolic pathways have been recently named as “Recov-ER-Phagy” and rely on the intervention of the translocon subunit SEC62²⁹⁷. In details, SEC62 acts as the ER-phagy receptor that, on resolution of an ER stress, exposes its LC3-interacting region (LIR) to engage some components of the autophagic machinery and eventually ensure the degradation of select ER sub-domains via piecemeal micro-ER-phagy process²⁹⁸. Even though, the components of the machinery required for Recov-ER-Phagy are current object of individual dissection with the help of genetic tools (e.g., KO and CRISPR cell lines), this process is still missing many information, since it is relatively of recent discovery. As such, we decided to study the transcriptional profile of Recov-ER-Phagy to enlarge the knowledge on the overall process, and dissect any possible transcriptional regulation underlying this pathway.

To this extent, we took advantage of the previously established protocol for stress/recovery induction²⁹⁷ and performed an RNA-seq analysis in Mouse Embryonic Fibroblast (MEF) cells to monitor transcripts variations during Recov-ER-Phagy process (in collaboration with Andrea Rinaldi, IOR genomic facility, Bellinzona, Switzerland). In details, MEF cells were exposed to cyclopiazonic acid (CPA), a reversible inhibitor of the SERCA Ca²⁺ pump, to induce the UPR. After 12h of treatment, the CPA was withdrawn to initiate the recovery phase. To follow the transcripts variations among time, the RNA was collected from untreated cells, or stressed cells after 12h of CPA treatment, and from cells at three different timepoints during the recovery phase, respectively 2h, 6h and 12h after CPA wash out. The RNA from 3 independent experiments was then processed and subjected to RNA-seq.



Figure 26: Schematics of the experimental set-up of stress/recovery induction. MEF cells were treated with CPA for 12h, then the compound is washed out and cells are grown in normal culture media. For transcriptomic analysis, the RNA was collected from untreated cells, or cells treated with CPA for 12h, and at 2h, 6h and 12h after CPA washout. Modified from Fumagalli et al 2016.

5.4.1.2 RNA-seq data processing and analysis

Raw counts obtained by RNA-seq analysis were transformed using regularized log-transformation and then filtered using the DESeq2 pipeline, excluding genes expressed at very low level, which can lead to non-reliable results when performing differential-expression analysis. As such, 17029 genes were found as highly reliable. On these genes, differential-expression analyses were performed to define the groups of genes whose expression was significantly ($FDR \leq 0.05$) modified during each of the established timepoints. In details, comparison of untreated cells with stressed cells (12h CPA treatment) and cells during 2h, 6h and 12h of recovery, revealed that CPA treatment induced the biggest changes in the pattern of the differentially expressed genes both as number level (1614, of which 702 up-regulated and 912 down-regulated) and as the largest fold changes (**Figure 27**, first column). Instead, during the recovery phase, the differences in transcripts expression shrank indicating that cells are returning to steady state conditions (**Figure 27**).

Interestingly, Recov-ER-Phagy receptor Sec62 did not result significantly differentially expressed in all the analyzed conditions. Any significant transcriptional regulation was also not detected for the other required genes (Atg4b, Atg5, Atg7, Atg16L1, Chmp4b, Gabarap, Gabarap12 and Vps4a)^{297,298}, with the exception of the ATG8 ubiquitin like-proteins Gabarap11, Map1lc3a and Map1lc3b, which were slightly but significantly up-regulated after 12h of CPA treatment. These data would suggest that the expression of the components of the Recov-ER-Phagy machinery could be mainly post-transcriptionally regulated, or that alternatively this pathway could be regulated by changes in protein-protein interactions.

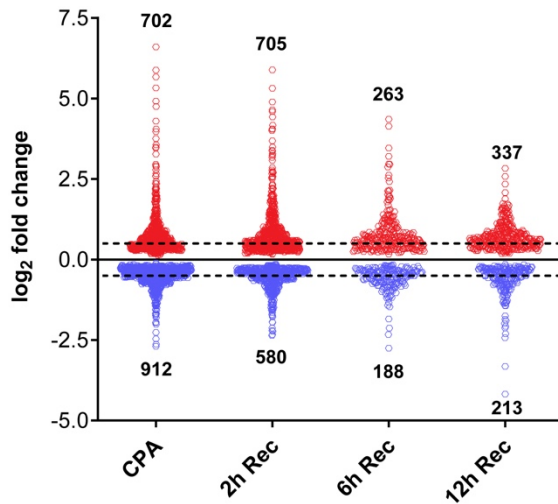


Figure 27: Distribution of fold changes from RNA-seq. Numbers on top and bottom show the number of the significantly up- and down-regulated transcripts (FDR ≤ 0.05) in each condition, dashed lines show the $\pm 0.5 \log_2$ fold change.

5.4.1.2.1 Gene enrichment analysis of differentially expressed genes

To define the transcriptional landscape of Recov-ER-Phagy, differentially expressed genes filtered for each timepoint were subjected to pathways and gene ontology enrichment analyses. Before the analyses, four main groups of differentially expressed genes were defined. The first group was obtained from the comparison between stressed and untreated cells. The other three groups originated from the individual comparison of each of the recovery timepoints (2h, 6h and 12h respectively) with the transcripts data obtained in stressed cells. The selected gene lists were then filtered for FDR values ≤ 0.05 . Moreover, for each group, significantly up-regulated genes were filtered using as parameter a \log_2 fold change value greater than or equal to 0.5, whereas the significantly down-regulated were obtained filtering for a \log_2 fold change value less than or equal to -0.5. The selected groups of genes were finally subjected to pathways and gene ontology enrichment analyses exploiting Enrichr online tool. The results were filtered for a p-value ≤ 0.05 and represented using GraphPad software.

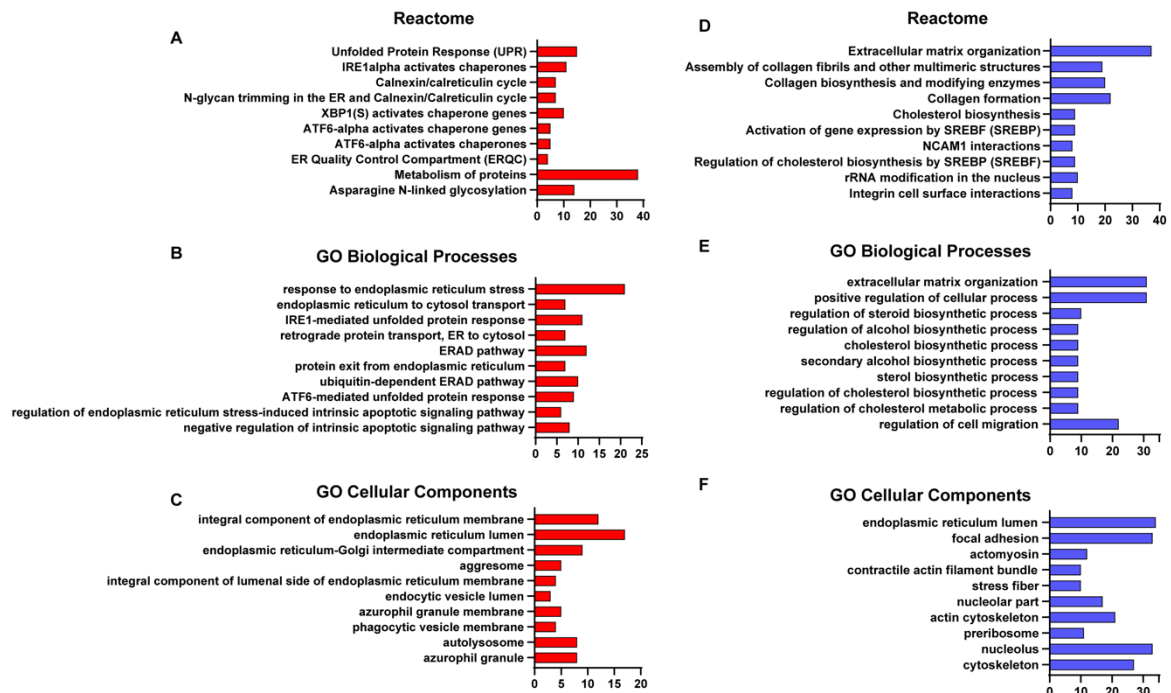


Figure 28: Gene set enrichment analysis of differentially expressed genes after 12h of CPA treatment. A, Box plot representation of the top significant ($p\text{-value} \leq 0.05$) Reactome terms associated to the up-regulated transcripts. Results are represented from the top to the bottom according increasing p-values. Bottom axis shows the number of the genes found for each term. B, Same as A, but displaying the GO Biological Processes. C, Same as A, but displaying the GO Cellular Components. D, Box plot representation of the top significant ($p\text{-value} \leq 0.05$) Reactome terms associated to the down-regulated transcripts. Results are represented from the top to the bottom according increasing p-values. Bottom axis shows the number of the genes found for each term. E, Same as D, but displaying the GO Biological Processes. F, Same as D, but displaying the GO Cellular Components.

Consistently with the induction of an ER stress, analysis of the differentially expressed genes upon CPA treatment revealed the up-regulation of genes belonging to the UPR, and in particular linked to protein folding and ERAD pathways (**Figure 28A-C**). Interestingly, the ER proteins regulated by the UPR branches ATF6 and IRE1 were identified among the most significant (**Figure 28A and B**). On the other hand, down-regulated genes fitted in the pathways of extracellular matrix organization, cell adhesion, cholesterol and collagen biosynthetic pathways (**Figure 28D-F**), which are characteristics of the fibroblast cell type³²⁶. Fibroblasts are the major source of extracellular matrix proteins, that are mainly synthesized within the ER³²⁷. Down-regulation of the genes linked to these pathways is a direct consequence of the ER stress induction, since in these conditions the synthesis of ER cargo proteins is strongly suppressed in favor of chaperones, folding and degradative factors.

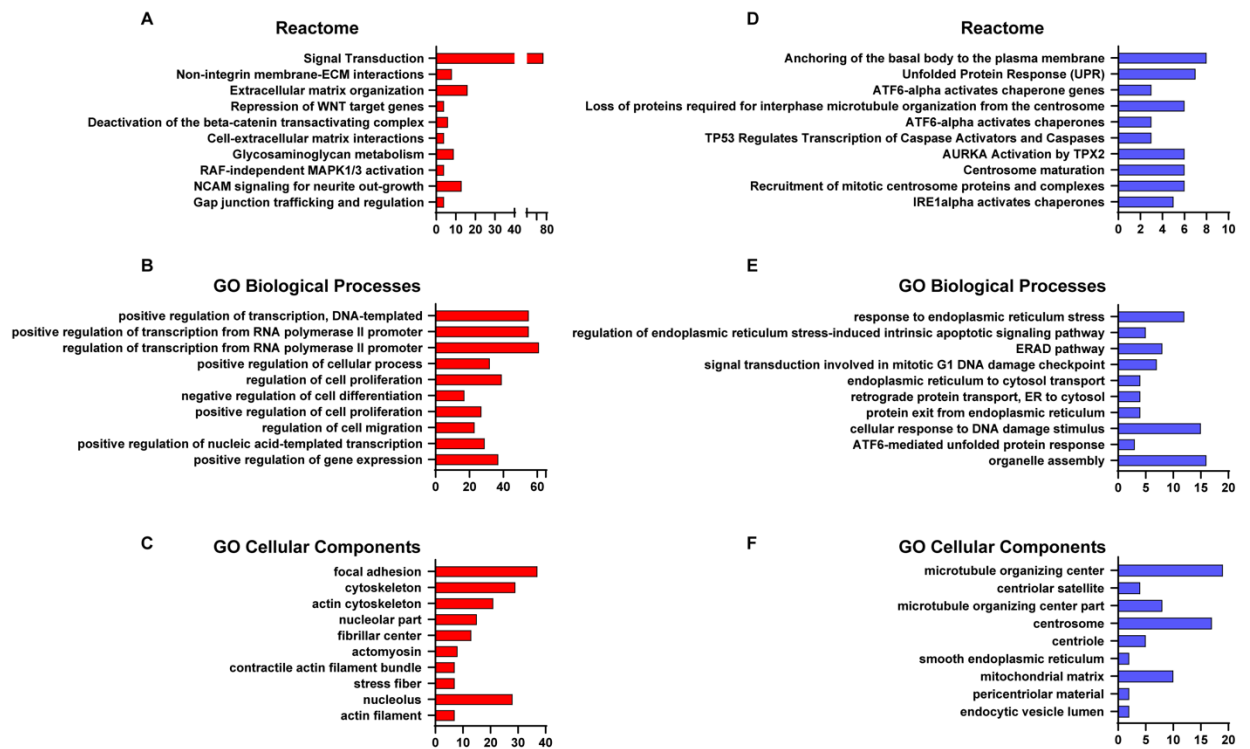


Figure 29: Gene set enrichment analysis of the differentially expressed genes after 2h from CPA wash out. **A**, Box plot representation of the top significant ($p\text{-value} \leq 0.05$) Reactome terms associated to the up-regulated transcripts. Results are represented from the top to the bottom according increasing p-values. Bottom axis shows the number of the genes found for each term. **B**, Same as **A**, but displaying the GO Biological Processes. **C**, Same as **A**, but displaying the GO Cellular Components. **D**, Box plot representation of the top significant ($p\text{-value} \leq 0.05$) Reactome terms associated to the down-regulated transcripts. Results are represented from the top to the bottom according increasing p-values. Bottom axis shows the number of the genes found for each term. **E**, Same as **D**, but displaying the GO Biological Processes. **F**, Same as **D**, but displaying the GO Cellular Components.

During the first recovery timepoint (2h after CPA wash out), constituents of nucleolus, cytoskeleton and focal adhesions resulted up-regulated (**Figure 29C**). These genes are directly correlated to different cellular processes such as DNA transcription, cell proliferation and migration (**Figure 29A and B**). As sign of initiation of the recovery phase, components of the UPR were found among the down-regulated genes, as well as factors linked to cell cycle arrest and apoptosis signaling (**Figure 29D-F**). In line with what previously reported in literature²⁹⁷, these data indicate that compatibly with the reversible nature of the CPA compound, cells start to recover as soon as the stress stimulus is relieved.

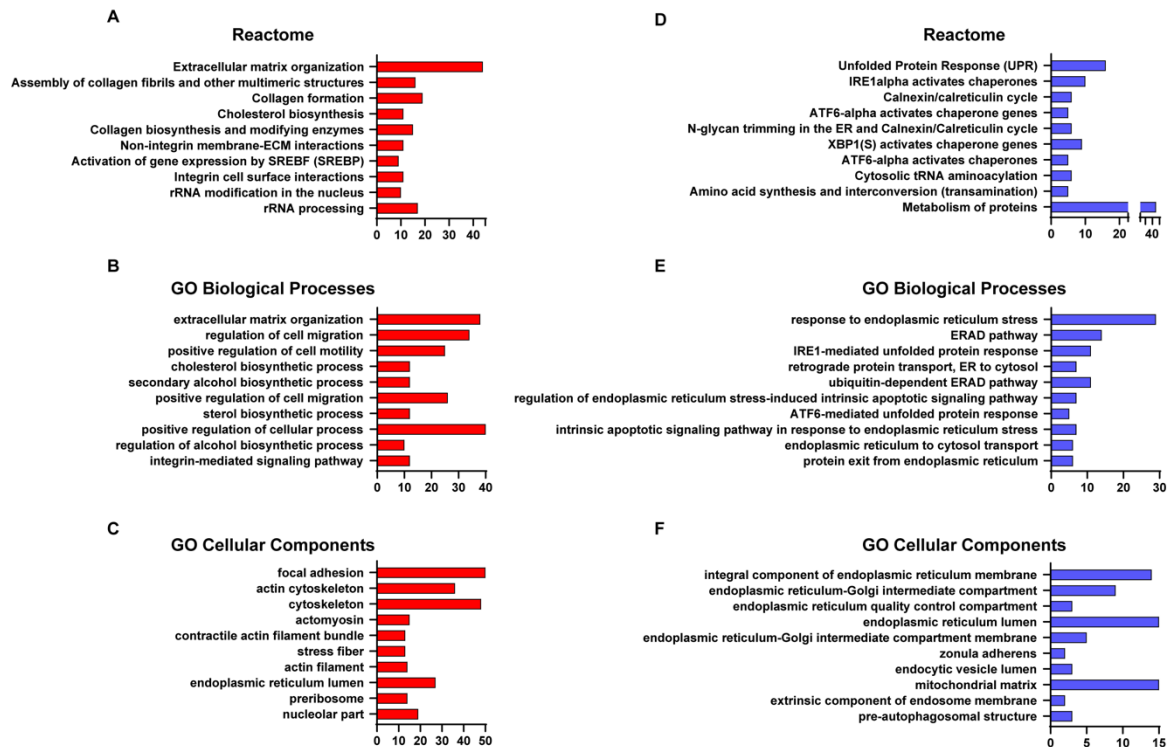


Figure 30: Gene set enrichment analysis of the differentially expressed genes after 6h from CPA wash out. A, Box plot representation of the top significant ($p\text{-value} \leq 0.05$) Reactome terms associated to the up-regulated transcripts. Results are represented from the top to the bottom according increasing p-values. Bottom axis shows the number of the genes found for each term. B, Same as A, but displaying the GO Biological Processes. C, Same as A, but displaying the GO Cellular Components. D, Box plot representation of the top significant ($p\text{-value} \leq 0.05$) Reactome terms associated to the down-regulated transcripts. Results are represented from the top to the bottom according increasing p-values. Bottom axis shows the number of the genes found for each term. E, Same as D, but displaying the GO Biological Processes. F, Same as D, but displaying the GO Cellular Components.

After 6h from CPA wash out, constituents of the extracellular matrix, collagen and cholesterol biosynthetic pathways were up-regulated as well as genes involved in ribosomal RNA processing and modification (**Figure 30A-C**). As showed for the previous timepoint (**Figure 29D-F**), down-regulated genes after 2h from CPA wash out were mainly belonging to the UPR (**Figure 30D-F**). Finally, the transcriptional signature of the last analyzed timepoint (12h from CPA wash out) was similar to the one emerged in the previous (**Figure 31**).

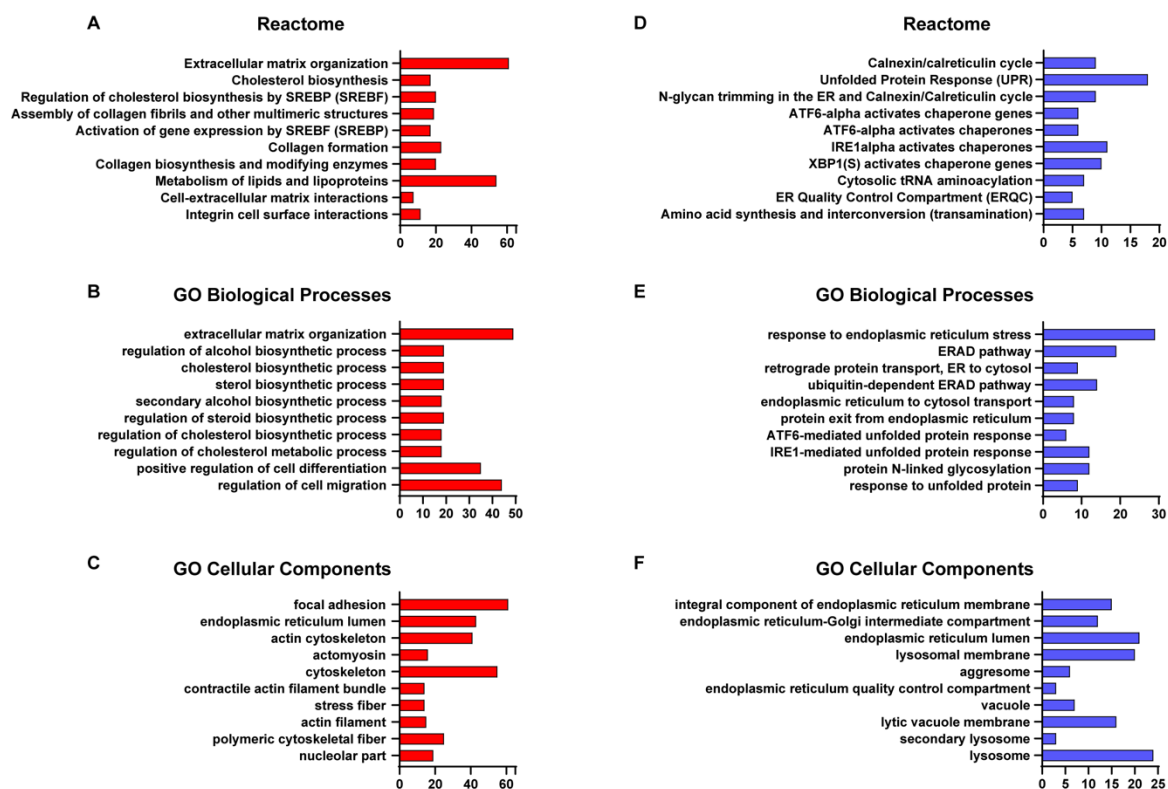


Figure 31: Gene set enrichment analysis of the differentially expressed genes after 12h from CPA wash out. A, Box plot representation of the top significant ($p\text{-value} \leq 0.05$) Reactome terms associated to the up-regulated transcripts. Results are represented from the top to the bottom according increasing p-values. Bottom axis shows the number of the genes found for each term. B, Same as A, but displaying the GO Biological Processes. C, Same as A, but displaying the GO Cellular Components. D, Box plot representation of the top significant ($p\text{-value} \leq 0.05$) Reactome terms associated to the down-regulated transcripts. Results are represented from the top to the bottom according increasing p-values. Bottom axis shows the number of the genes found for each term. E, Same as D, but displaying the GO Biological Processes. F, Same as D, but displaying the GO Cellular Components.

Interestingly, the overall pattern of the up- and down-regulated genes of these last two timepoints within the recovery process (**Figure 30 and 31**) constitutes the specular portrait of the genes differentially expressed upon CPA treatment (**Figure 28**). This suggests that the ER stress burden has been relieved and thus the organelle can re-start the biosynthetic functions previously paused. Moreover, the analysis of the cellular components showed the down-regulation of the genes linked to the lysosomal compartment after 12h from CPA wash out (**Figure 31F**). Manual analysis of these genes revealed that most of them were slightly up-regulated (under $0.5 \log_2$ fold change threshold) after 12h of CPA treatment, confirming the previous evidences reported in literature that ER stress can also regulate the expression of the lysosomal genes ³²⁸. The downregulation of the lysosomal components

after 12h from CPA wash out indicates that the clearance of the excess ER subdomains took place, and there is no more need of lysosome spare parts.

All in all, we obtained a picture of the transcriptional dynamics underlying Recov-ER-Phagy: in fact, these analyses gave us a step-by-step description of the pathways and processes that cells are activating or suppressing to counteract the homeostasis perturbation and successfully ride the recovery phase. However, these data failed to reveal a direct transcriptional regulation of Recov-ER-Phagy process, rather suggesting the existence of post-transcriptional mechanisms of regulation.

5.4.1.2.2 Kinetics reconstruction of the differentially expressed genes

After gene enrichment analysis, data were clustered to build a kinetical representation of the most differentially expressed genes. In details, all genes displaying a \log_2 fold change ≥ 1.5 or ≤ -1.5 with an $FDR \leq 0.05$ in at least one of the four conditions analyzed (stress, 2h, 6h or 12h recovery) were selected. The filtered genes were then manually clustered according their \log_2 fold change variations among time into four kinetics group, which can be summarized in genes up-regulated upon CPA treatment (**Figure 32A**, 12h CPA), up-regulated at 2h of recovery (**Figure 32B**, 2h Rec), up-regulated during the recovery phase (with the highest peak at 12h of recovery) (**Figure 32C**, Up Rec), and down-regulated during the recovery phase (with the lowest peak at 12h recovery) (**Figure 32D**, Down Rec). The four clusters were then subjected to gene enrichment analysis using Enrichr online tool, and the resulting associated GO Biological Processes are shown in **Table 2**.

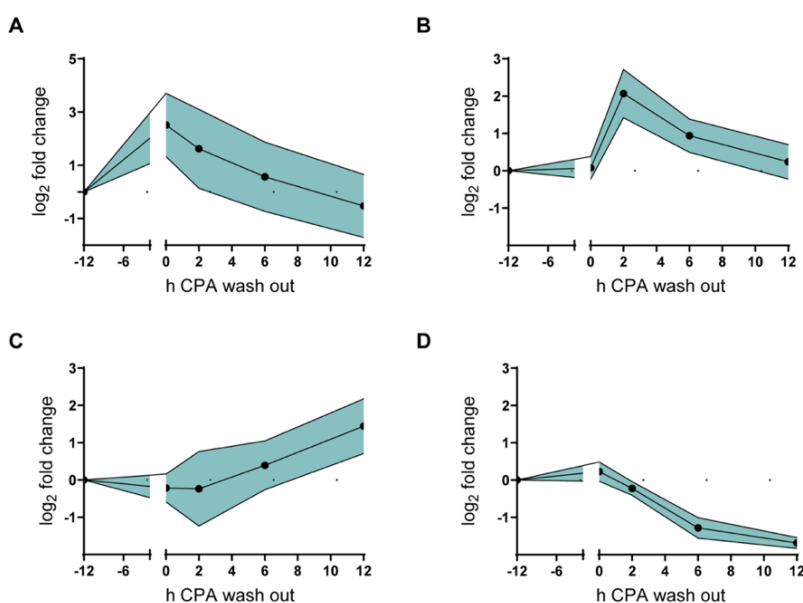


Figure 32: Representation of the selected differentially expressed genes kinetics. **A**, Plot of the differentially expressed genes with a trend of up-regulation after 12h of CPA treatment (i.e. ER stress induction). **B**, Plot of the differentially expressed genes up-regulated at 2h after CPA wash out. **C**, Plot of differentially expressed genes gradually up-regulated during the recovery phase. **D**, Plot of the differentially expressed genes progressively down-regulated during the recovery phase.

As expected, the genes clustered in the first group (**Figure 32A**) belonged to the UPR (**Table 2**), while the genes with a peak of up-regulation at 2h of recovery (**Figure 32B**) were mainly associated to cell growth and motility, but also to the WNT signaling pathway (**Table 2**). Indeed, two main components of the canonical WNT pathway, Wnt11 and Lef1, were found strongly up-regulated at 2h of recovery. Even though WNT signaling has been classically associated to cell growth, differentiation and embryogenesis, recent reports in the literature suggest a role in the activation of endocytosis, pinocytosis and lysosomal degradation through the modulation of the ESCRT machinery³²⁹. Strikingly, Recov-ER-phagy degrades select ER sub-domains via piecemeal micro-ER-phagy process that relies on the intervention of CHMP4B, an ESCRT-III component, and the accessory AAA+ ATPase VPS4A in its final steps. These data could be a hint that the transcriptional regulation of the WNT pathway would be functional to Recov-ER-Phagy process through the modulation of the function of the ESCRT machinery. Similarly to the previous group, the association to cell motility and growth signatures was also found for the genes with an up-regulation peak at 12h of recovery (**Figure 32C** and **Table 2**), whereas genes down-regulated during the recovery phase (**Figure 32D**) were linked to the amino acid biosynthetic process (**Table 2**).

12h CPA	GO Biological Processes	p-value
1	ATF6-mediated unfolded protein response	0.002e-5
2	Response to endoplasmic reticulum stress	0.001e-4
3	IRE1-mediated unfolded protein response	0.006e-2
4	Maintenance of protein localization in endoplasmic reticulum	0.005e-1
5	Response to unfolded protein	0.005e-1

Up Rec	GO Biological Processes	p-value
1	regulation of cell migration	0.006e-1
2	hyaluronan biosynthetic process	0.004
3	positive regulation of cell motility	0.004

2h Rec	GO Biological Processes	p-value
1	Positive regulation of cell motility	0.002e-1
2	Wnt signaling pathway, calcium modulating pathway	0.002e-1
3	Positive regulation of cell migration	0.003e-1
4	Positive regulation of cell growth	0.002
5	Wnt signaling pathway	0.002

Down Rec	GO Biological Processes	p-value
1	cellular amino acid biosynthetic process	0.007e-2
2	sulfur compound catabolic process	0.001e-1
3	carboxylic acid biosynthetic process	0.001e-1
4	sulfur compound biosynthetic process	0.001
5	negative regulation of cell cycle phase transition	0.002

Table 2: Gene enrichment analysis of the selected differentially expressed genes. The differentially expressed genes were clustered according their kinetics and then subjected to gene enrichment analysis. For each group (12h CPA, 2h Rec, Up Rec, and Down Rec) the resulting associated GO Biological Process terms are shown together with their p-values.

All in all, these kinetical analyses portrayed the most important cellular processes taking place during Recov-ER-Phagy. Moreover, these data suggested a possible role of the WNT pathway in the regulation of the endolysosomal engulfment of ER portions through ESCRT machinery during the last steps of Recov-ER-Phagy.

5.4.2 Discussion

An unbalanced ER homeostasis caused by the accumulation of misfolded proteins can lead to the induction of an ER stress, which activates the UPR²²⁴. UPR can be defined as a series of transcriptional and translational measures that the cells put in place to resolve the ER stress situation³³⁰. Among these events, the up-regulation of ER chaperones and folding enzymes, ERAD factors and components of the protein export machinery, together with a general repression of the translation of cargo proteins are the most known³³⁰. Upon relief of the stimuli inducing the ER stress, the return to pre-stress homeostatic conditions is allowed by the activation of a catabolic pathway ensuring the clearance of excess and/or damaged ER portions. This recently identified process goes under the name of Recov-ER-Phagy²⁹⁷. Mechanistically, upon the cessation of an ER stress stimulus, the translocon component SEC62 performs its alternative activity as ER-phagy receptor: indeed, SEC62 shows its LIR, allowing the recruitment of some components of the autophagic machinery to promote the delivery of select ER sub-regions to the endolysosomes for clearance²⁹⁷. In details, the genetic dissection of Recov-ER-Phagy pathway showed that this process occurs via a piecemeal micro-ER-Phagy process during which, specific ER portions are directly engulfed by the endolysosomes²⁹⁸. The engulfment step requires the activity of CHMP4B and VPS4A, which are an ESCRT-III component and an accessory AAA+ ATPase, respectively²⁹⁸.

During my PhD, I realized a transcriptomic analysis of Recov-ER-Phagy process in order to dissect changes among time of the transcriptional landscape underlying this pathway. As such, RNA-seq analyses of stressed cells and cells at different timepoints during the recovery phase were performed. Gene enrichment analyses of the differentially expressed genes allowed then to characterize the dynamics of the biological processes driving the cells out from the stress burden.

5.4.2.1 Gene enrichment analysis of the differentially expressed genes to unhide the biological processes underlying Recov-ER-Phagy

From over 17000 genes emerged from the RNA-seq, the significantly differentially expressed genes for each of the analyzed conditions were subjected to gene enrichment analyses. This analysis clearly pointed out that the genes up-regulated after 12h of CPA treatment belonged to the classical ER stress signature (e.g. ER chaperone and folding

enzymes, ERAD pathway...). Notably, these hits mainly clustered into the genes regulated by the UPR branches ATF6 and IRE1: this could be explained with the fact that CPA is a mild stressor compared to tunicamycin or other chemical compounds, which are able to elicit stronger responses and in turn to activate PERK, an ER stress transducer commonly linked to the activation of cell death pathways³³¹. On the other hand, the down-regulated genes mainly belonged to pathways of extracellular matrix organization, cell adhesion, cholesterol and collagen production. 2h after CPA wash-out (2h recovery) genes linked to cell proliferation and growth, transcription and RNA processing were up-regulated, whereas ER stress players, cycle arrest and apoptotic factors resulted down-regulated. Compatibly with the reversible nature of the CPA as SERCA inhibitor, the overall picture of this timepoint indicates that the recovery phase is starting quite rapidly after the drug wash out. Both the last two recovery timepoints of 6h and 12h were characterized by the up-regulation of constituents of the extracellular matrix, collagen and cholesterol biosynthetic pathways, genes involved in ribosomal RNA processing and modification, and by a massive down-regulation of the UPR players and of the apoptotic signaling pathway. The transcriptional signature of these last two timepoints reminds the one belonging to cells treated with CPA for 12h but in a reversed manner. Interestingly, after 12h of incubation with CPA, cells paused biosynthetic activities as collagen and cholesterol production, which represents the major pathways within fibroblasts³²⁶. At the same time, the ER stress players expression is heavily pushed. These evidences would suggest that in order to strong counteract the unbalance of the ER homeostasis, this organelle suppresses the other parallel activities to alleviate the overall burden. On the same line, the following up-regulation of the previous suspended biosynthetic pathways after 6h and 12h from CPA wash out would be the sign of a successful recovery. In the same direction, after being slightly up-regulated upon CPA treatment, different lysosomal components were found down-regulated after 12h from CPA wash out: indeed, this kind of response at this timepoint could suggest that Recov-ER-Phagy process efficiently took place, and lysosome spare proteins are no more needed.

To maturate a different perspective of the RNA-seq data, the statistically significant differentially expressed genes were clustered into four groups according to their trends across the various timepoints. These four groups were constituted by genes up-regulated after 12h of CPA treatment, genes with an up-regulation peak at 2h of recovery, genes up-regulated and down-regulated during the recovery phase, respectively. Gene enrichment

analysis showed that genes clustered in the first group belonged to the UPR. Instead, genes up-regulated after 2h from CPA washout were linked to cell growth and motility similarly to the genes showing an up-regulation peak at 12h of recovery. Finally, genes down-regulated during the recovery phase mainly belonged to the amino acid biosynthetic process: interestingly, the down-regulation of such genes would be a direct consequence of the shutdown of the UPR. Indeed, during the stress phase, the synthesis of ER chaperones and folding enzymes would require a supply of brick units to sustain their production, which are no more needed when the emergency is faded (aka recovery accomplishment). Notably, components of the WNT pathway were found among the genes linked to cell growth and proliferation that were up-regulated at 2h after CPA wash out. This finding results quite interesting since different players of the canonical WNT pathway were recently found to be implicated in the activation of events of endocytosis, pinocytosis and lysosomal degradation³²⁹. In particular, they were described to regulate the function of some components of the ESCRT machinery³²⁹. Considering the prior knowledge indicating that Recov-ER-Phagy process relies on CHMP4B and VPS4A for the final step of lysosomal engulfment²⁹⁸, a role of the WNT pathway in this context could be easily envisioned. Thus, it could be important in the future to determine if members of the WNT pathway would have a role in the regulation of the final steps of Recov-ER-Phagy process.

Recently the genetic dissection of Recov-ER-Phagy allowed to describe some components of its machinery. Indeed, this process requires the translocon component and ER-phagy receptor SEC62, the ATG8 ubiquitin like-proteins, different components of the LC3 lipidation machinery (ATG4B, ATG5, ATG7, ATG16L1), the ESCRT-III CHMP4B, and the accessory AAA+ ATPase VPS4A^{297,298}. Interestingly, none of these components were significantly differentially expressed in any of the examined conditions, with the exception of the ATG8 ubiquitin like-proteins Gabarapl1, Map1lc3a and Map1lc3b, that resulted slightly up-regulated after 12h of CPA treatment. On this basis, future studies will be important to determine if the expression of any of the required components would rather be post-transcriptionally regulated. An alternative hypothesis for the regulation of Recov-ER-Phagy pathway would be linked to protein-protein interactions: indeed, rather than changes in expression levels, Recov-ER-Phagy players function could be regulated according to the engaged partners. This hypothesis results probable since for the cells would be quite convenient to have proteins already in place to readily support the initiation of Recov-ER-Phagy process.

All in all, these analyses described the transcriptional landscape of the biological processes characterizing the Recov-ER-Phagy background. Moreover, these data offered new perspectives and points of future analysis, as for example the possible contribution of WNT pathway, to enlarge the mechanistic dissection of the Recov-ER-Phagy process.

5.4.3 Contributions

I was involved in the conceptualization and realization of this research project. I prepared the samples for RNA-seq, analyzed the data and realized all the figures contained in this section, except **Figure 32**.

6 CONCLUSIVE REMARKS

The ER is a complex organelle that, thanks to its structural organization, is able to accomplish many tasks¹. Among them, one of the major is represented by the production of membrane and secretory proteins¹, which can be defined as a stepwise process requiring the intervention of different machineries for its successful accomplishment. Once synthesized and imported within the ER, the polypeptide chains undergo folding process assisted by different ER chaperones and folding enzymes³³². Quality control systems monitor the folding state of the newly synthesized polypeptides to allow only correctly folded proteins to exit from the ER³³³. Proteins that fail to achieve their native conformation are recognized as misfolded and targeted to degradation³⁰⁴. Efficient clearance of misfolded proteins is crucial for the maintenance of the ER homeostasis and in turn for cell health³¹⁸. In the case of genetic mutations or environmental stresses the amount of misfolded proteins can drastically increase outperforming the degradative capacity¹⁰⁸. This can lead to an accumulation of misfolded proteins within the ER, that causes a perturbation of the ER homeostasis and triggers the induction of ER stress conditions²²⁴. As backup plan, nature evolved the UPR, during which ER chaperones, folding and degradative factors are drastically up-regulated to empower both folding and degradation processes with the aim to restore the ER homeostasis²²⁴. Once stress burden is relieved, the activation of catabolic programs (aka Recov-ER-Phagy) mediates the lysosomal removal of excess ER previously generated allowing the return to pre-stress conditions^{297,298}.

During my PhD studies, I had the opportunity to work on different research projects, that even so diverse, all focused on the dissection of crucial aspects of the ER functionality and homeostasis from different perspectives.

6.1 TMX1 and TMX5, two membrane-tethered PDI family member

In the first two sections of this thesis, I focused on the characterization of TMX1 and TMX5, two membrane-tethered members of the PDI family. PDIs are enzymes that catalyze the oxidation, the reduction and the isomerization of the disulfide bonds to ensure both efficient protein folding of newly synthesized polypeptides and ERAD of misfolded proteins¹⁸⁶. This family comprises more than 20 members, which show different tissue distribution, topology and structural organization³³⁴. Although, this represent a hint of different client specificity and individual roles in both protein folding and degradation¹⁹⁶,

experimental evidences for many PDIs are still missing. TMX1 is the first identified member of the TMX protein family¹⁹⁷, which comprises other four transmembrane proteins (TMX2, TMX3, TMX4 and TMX5). TMX1 is a single-pass type I protein displaying one type-a TRX-like domain within its luminal region, which contains a non-canonical CPAC active site¹⁹⁷. The peculiar composition of its active site together with the published data proposed TMX1 as an ER reductase^{197,201,202,335}. Recently, a role of TMX1 in protein folding has been reported: in this context, TMX1 forms functional complexes with the ER lectin CNX preferentially intervening during the productive folding of membrane-tethered proteins²⁰⁶. These findings made TMX1 the first example among the PDI family members to act as topology-specific redox-catalyst²⁰⁶. The data collected in this thesis expanded the knowledge about TMX1 role demonstrating its selective intervention during ERAD of membrane-tethered misfolded-proteins. Indeed, the exploitation of TMX1 trapping mutant version (TMX1_{C/A}) allowed to show that TMX1 preferentially engages mixed disulfides with folding-defective membrane-anchored proteins, confirming its topology specificity previously shown for its role in protein folding²⁰⁶. Consequently to mixed disulfides establishment, TMX1_{C/A} selective delayed ERAD of membrane-bound folding-defective substrates. As such, TMX1 represents the first example of topology-specific redox catalyst acting in both folding process and ERAD of membrane-anchored substrates. What still remain to be assessed is if TMX1 can also engage membrane substrates showing different characteristics, as non-glycosylated proteins. Moreover, the mechanisms regulating TMX1 intervention either in protein folding or in ERAD are still poorly understood (for detailed discussion see section **5.1.2**).

Among the TMX family members, TMX5 represents the youngest and the less characterized. It is a single-pass type I protein, which harbors one type-a TRX-like domain within its luminal portion showing a peculiar CRFS active site. This sequence characterizes TMX5 as natural trapping mutant protein, hinting a possible role in thiol-mediated protein quality control. In this thesis, we realized a preliminary characterization of TMX5 showing that it is a N-glycosylated and ER stress unresponsive PDI. Moreover, in contrast with the other members of the TMX family that are all localized within the ER^{197,199,212,216}, TMX5 is a secreted protein that selectively engages a mixed disulfide with ERp44, a soluble member of the PDI family³¹². Interestingly, the formation of a TMX5:ERp44 disulfide bonded complex relies on a functional ERp44 active site. In contrast, the active site of TMX5 is dispensable to engage ERp44, but it required to establish mixed disulfides with

endogenous client proteins. Finally, the analysis of TMX5 intracellular localization revealed that the interaction with ERp44 determines the retention of TMX5 within the ER. Given the role of ERp44 in the retention of the ER oxidoreductase ERO1L α ³¹⁴, the findings reported in this thesis hint at a possible role of ERp44 in the regulation of TMX5 function, through the modulation of its intracellular localization (for detailed discussion see section 5.2.2).

6.2 HaloTag2® protein chimeras as tools for the characterization of the PQC systems

In the third section of this thesis, I reported the design and development of HaloTag2® protein chimeras as tools for the dissection of the PQC systems. PQC can be defined as the ensemble of the mechanisms that surveil on protein folding status ensuring the recognition and the degradation of misfolded proteins³³³. The failure of these mechanisms can lead to an unbalanced ER homeostasis also leading to severe human diseases³¹⁸. Thus, the dissection of the PQC dynamics would be fundamental for the understanding of many conformational diseases.

HaloTag2® is a mutated version of a bacterial chloroalkane dehalogenase, which is able to covalently bind chloroalkane reactive ligands³²⁰. According to the molecular properties of these ligands, HaloTag2® can be exploited for different aims, such as imaging analysis and protein purification³²⁰. Interestingly, the binding of an adamantane-based hydrophobic ligand (i.e. HyT36) is able to induce the misfolding of the HaloTag2®^{323,336}. I exploited this property to generate a palette of membrane-tethered misfoldable GFP-HaloTag2® substrates suitable for the study of cells PQC systems. To this aim, based on the evidences showing that short transmembrane domains of 17 residues retain membrane proteins within the ER while longer anchors of 22 residues promote proteins secretion³²², the HaloTag2® domain was attached to a transmembrane of 17 (TM17) or 22 residues (TM22). Moreover, to allow protein misfolding in different cellular compartments, the HaloTag2® was placed either within the ER lumen or towards the cytosol. Finally, to emulate the diversification of the cellular proteome, N-glycosylated versions of the HaloTag2® protein chimeras were also prepared.

Biochemical characterization upon HyT36-induced misfolding showed that the HaloTag2® protein chimeras displaying the misfolded domain within the ER lumen are recognized by the ER quality control through BiP binding. This explained the decrease in protein levels of the luminal HaloTag2® chimeras. On the contrary, the misfolding of the HaloTag2® mediated by HyT36 did not affect both BiP binding and protein levels of the chimeras displaying the misfolded domain within the cytosol. Additionally, HyT36 treatment affected the intracellular localization of the secreted TM22 luminal HaloTag2® chimeras inducing the loss of the plasma membrane staining, whereas no effects were revealed, upon the same treatment with HyT36, for the TM22 HaloTag2® chimera displaying the misfolded domain within the cytosol. Finally, the misfolding of the luminal HaloTag2® chimeras induced by HyT36 binding triggered an ER stress induction, which was revealed upon analysis of BiP transcript levels. Notably, the entity of the induced responses varied among the different chimeras but was not comparable to the strong UPR induction triggered by cells treatment with the chemical ER stress inducer tunicamycin. All in all, the diversity of the elicited responses indicates that the generated HaloTag2® protein chimeras constitute the reliable tools for the dissection of the PQC pathways. (for detailed discussion see **5.3.2**)

6.3 Analysis of the transcriptional response underlying “RecovER-Phagy” process

In the fourth and last section of this thesis, I focused on how cells recover from an ER stress, in particular describing the transcriptional events underlying Recov-ER-Phagy pathway. The term Recov-ER-Phagy has been recently coined to describe the catabolic process that is activated by the cells upon relief of an ER stress stimulus and mediates the lysosomal clearance of excess and/or damaged ER portions to restore organelle pre-stress homeostasis²⁹⁷. Recov-ER-Phagy process relies on the translocon component SEC62 that upon cessation of an ER stress acts as an ER-phagy receptor: indeed, SEC62 exposes its LIR domain, which in turn recruits some components of the autophagic machinery to deliver select ER portions to the endolysosomal compartment for clearance²⁹⁷. Recently, Recov-ER-Phagy has been mechanistically described as a micro-autophagic like process, where the ER sub-domains to be degraded are directly engulfed by the endolysosomes in a

process that relies on the intervention of the ESCRTIII component CHMP4B and the accessory AAA+ ATPase VPS4A²⁹⁸.

In this thesis, I report a time-resolved transcriptional analysis of the Recov-ER-Phagy pathway. To this aim, RNA-seq analysis was performed to monitor transcripts fluctuations during the different phases. In details, I analyzed transcripts from untreated cells, cells treated for 12h with CPA to induce an ER stress, and cells during three different timepoints after CPA wash-out (i.e., 2h, 6h and 12h during the recovery phase). In particular, gene enrichment analysis performed on the differentially expressed genes revealed how cells put all the efforts to contrast the ER stress, strongly up-regulating genes linked to the UPR after 12h of CPA treatment, while down-regulating the main cells biosynthetic pathways to alleviate the burden on the ER. As soon, as the stimulus is relieved (CPA wash out), cells enter the recovery phase inverting the previous transcriptional tendency and promoting cell growth. Among the genes earlier up-regulated during the recovery phase, components of the WNT pathway emerged: other than its canonical function in cell growth and proliferation, the activation of the WNT signaling has been recently associated to a functional regulation of the ESCRT machinery components³²⁹. Since some members of the ESCRT machinery are required in the final steps of lysosomal engulfment²⁹⁸, this evidence could suggest an indirect regulation of Recov-ER-Phagy process through the WNT signaling pathway. Additionally, the transcriptional analyses revealed no significant variations in the transcript levels of the Recov-ER-Phagy required genes (Atg4b, Atg5, Atg7, Atg16L1, Chmp4b, Gabarap, Gabarapl2, Sec62 and Vps4a)^{297,298}, with the unique exception of the ATG8 ubiquitin like-proteins Gabarapl1, Map1lc3a and Map1lc3b, which were slightly but significantly up-regulated following CPA treatment. This could indicate that Recov-ER-Phagy process is not directly regulated at transcriptional levels, rather suggests the existence of post-translational systems of regulation (for detailed discussion see **5.4.2**).

7 MATERIALS AND METHODS

Expression plasmids and chemicals

Plasmid encoding for V5-tagged TMX1_{C/A} is described in²⁰⁶. Plasmids encoding for the membrane-bound and soluble HA-tagged BACE457 are described in¹²⁴. Plasmids encoding for HA-tagged NHK and HA-tagged NHKCD3 δ are described in⁹⁴. Gene encoding for TMX5-V5 was subcloned in pcDNA3.1(-) plasmid. V5-tagged TMX5_{C/A} was generated by site mutagenesis from TMX5-V5. Plasmids encoding for ERp44-HA and ERp44_{C/S}-HA are described in³¹⁵. Plasmids for the expression of HaloTag2[®] protein chimeras in pcDNA5 FRT/TO vector were generated from ERHT, FP-17 and FP-22 plasmids described respectively in^{322,323}. All HaloTag2[®] protein chimeras contained the 30 amino acids signal sequence from prolactin followed by sfGFP at the N-terminus and an HA-tag at the C-terminus. For GFP-NH-TM17 generation, HaloTag2[®] was amplified from ERHT and inserted at the N-terminus following the sfGFP. Subsequently TM17 was amplified from FP-17 and inserted between the HaloTag2[®] and the HA-tag. GFP-NH-TM17Q was generated by site directed mutagenesis from GFP-NH-TM17. For GFP-CH-TM17 generation, TM17 was amplified from FP-17 and inserted at the N-terminus following the sfGFP. Subsequently, HaloTag2[®] was amplified from ERHT and inserted between TM17 and HA-tag. GFP-NH-TM22 was generated by replacing the TM17 of GFP-NH-TM17 with the TM22 amplified from FP-22. GFP-NH-TM22Q was generated by site directed mutagenesis from GFP-NH-TM22. GFP-CH-TM22 was generated replacing the TM17 of GFP-CH-TM17 with the TM22 amplified from FP-22. Tunicamycin (Sigma-Aldrich) was used at a final concentration of 5 μ g/mL. CPA (Sigma-Aldrich) and HyT36 (kindly gifted by Crews C.) were used at a final concentration of 10 μ M. PBI5030 (kindly gifted by Van Anken E.) was used at a final concentration of 1 μ M.

Cell lines and transient transfection

MEF and HEK293 cell line were cultured in DMEM supplemented with 10% fetal bovine serum (FBS). Flp-In NIH-3T3 cell line was cultured in DMEM supplemented with 10% fetal calf serum (FCS). All cell lines were grown at 37°C, 5% CO₂. HEK293 cells were plated on 3.5/6cm poly-Lys coated dishes and transfected with 1.5 μ g/2.25 μ g of total

plasmid DNA using jetPrime® reagent (Polyplus transfection). Experiments were performed 17h after transfection.

Generation of stable transfected Flp-In NIH-3T3 cell lines

Mock FLP-In NIH-3T3 cells (Invitrogen) were plated on 6cm dishes in DMEM supplemented with 10% FCS and co-transfected with a ratio 9:1 of the pOG44 plasmid (Invitrogen) and the GFP-HaloTag2® protein chimera plasmids in pcDNA-5FRT/TO using Lipofectamine® 2000 transfection reagent (Invitrogen). The day after transfection, cells were split in 10cm dishes. Two days after transfection, the medium was changed with addition of 150µg/mL of hygromycin (Invitrogen). Hygromycin-resistant clones were picked after 10 days. Gene expression was verified by western blot.

Cell lysis and western blots

Cells were washed with ice-cold phosphate-buffered saline (PBS) supplemented with 20 mM N-ethylmaleimide (NEM) and then lysed with 2% CHAPS (Anatrace) in HEPEP-buffered saline, pH 6.8, containing 20 mM NEM and protease inhibitors for 20 min on ice. Post-nuclear supernatants (PNSs) were collected by centrifugation at 4°C and 10,000g for 10 min. Samples were denatured and reduced in sample buffer containing 100mM dithiothreitol (DTT) for 5 min at 95°C. After denaturation, samples were subjected to SDS-PAGE. Proteins were transferred to PVDF membranes using the Trans-Blot® Turbo™ Transfer System (Bio-Rad). Membranes were blocked with 10% (w/v) non-fat dry milk (Bio-Rad) for 10 min and then incubated with primary antibodies (see primary antibody list at the end of this chapter) for 2h and HRP-conjugated secondary antibodies or Protein A for 45 min. Membranes were developed using the Luminata™ Forte ECL detection system (Millipore) or the Western Bright™ Quantum (Advansta), and signals were acquired with the ImageQuant LAS 4000 system (GE Healthcare Life Sciences), or with the Amersham Imager 680 system (GE Healthcare Life Sciences), or with the Fusion FX system (Vilber). Membrane stripping for probing additional antigens was done using Re-Blot Plus Strong Solution (Millipore) according manufacturer's instructions.

Metabolic labelling and immunoprecipitations

Cells were washed with pre-warmed PBS and then pulse labeled with 0.1mCi of [³⁵S]-methionine/cysteine in DMEM, 50 mM Hepes, 1% Glutamax for 15 min at 37°C. Labeling medium was removed and cells were chased in DMEM containing 5 mM non-labeled methionine and cysteine. Cells were lysed and PNSs were collected as described above. For immunoprecipitations, PNSs were incubated with protein A beads (Sigma-Aldrich, 1:10, w/v swollen in PBS) and anti-HA antibody, or with protein G beads (VWR, 1:10, w/v swollen in PBS) and anti-GFP antibody, or with Anti-V5 Agarose Affinity Gel conjugated beads (Sigma-Aldrich) for 2h at 4°C. After extensive washing with 0.5% CHAPS in HEPES-buffered saline, pH 7.4, beads were dried. Dried beads were resuspended in sample buffer without (non-reducing) or with 100mM DTT (reducing conditions) and denatured at 95°C for 5 min. After denaturation, samples were subjected to SDS-PAGE. Gels were dried and exposed to autoradiography films (GE Healthcare Life Sciences). Films were scanned with the Typhoon™ FLA 9500 and images were analyzed for quantification with ImageQuant software (Molecular Dynamics, GE Healthcare Life Sciences).

EndoH and PNGaseF treatments

PNSs were denatured following manufacturer's instructions. After denaturation, PNSs were split into three aliquots and incubated in the absence, or in the presence of 5 mU of EndoH or PNGaseF for 1h at 37°C. Samples were then separated by reducing SDS-PAGE and analyzed by western blot.

Silver staining and Mass Spectrometry

Confluent HEK293 cells transfected with an empty vector (EV) or with V5-tagged TMX5 were washed with PBS and 20 mM NEM. Cells were lysed with 2% CHAPS (Anatrace) in HEPES-buffered saline, pH 6.8, containing 20 mM NEM and protease inhibitors for 20 min on ice. After centrifugation at 4°C and 10,000g for 10 min, PNSs were collected and immunoprecipitated twice with Anti-V5 Agarose Affinity Gel conjugated beads (Sigma-Aldrich).

For Silver staining, immunoprecipitated samples were separated by SDS-PAGE under either non-reducing or reducing conditions. Gel was fixed in a 40% EtOH, 10% Acetic Acid solution for 1-4h at room temperature (RT), and then washed in 30% EtOH for 20 min. After rinsing the gel in H₂O for 20 min, it was sensitized with 0.02% Na₂S₂O₃ for 1 min and then washed three times in H₂O. Gel was incubated in 0.2% AgNO₃ for 20 min and then rinsed three times in H₂O. Staining was revealed incubating the gel in a solution containing 3% Na₂CO₃, 0.05% formaldehyde. When the adequate degree of staining was achieved, gel was rinsed in H₂O and the reaction was stopped washing the gel in 5% Acetic Acid. Gel images were acquired with Fusion FX system (Vilber).

For Mass Spectrometry, immunoprecipitates were washed three times with lysis buffer and then the beads were dried. Dried beads were sent to the Protein Analysis Facility, University of Lausanne (Lausanne, Switzerland) for processing and Mass Spectrometry analysis.

RNA extraction, qPCR and RNAseq

Total RNA was extracted using a GenElute™ Mammalian Total RNA Miniprep Kit (Sigma-Aldrich) following the manufacturer's instructions.

For qPCR analyses, cDNA was synthesized using SuperScript II RT (Invitrogen) and oligo(dT) (Invitrogen) following the manufacturer's instructions starting with 2 µg of total RNA. qPCRs were performed using BioTool™ 2x SYBR Green qPCR master mix (BioTool) according to the manufacturer's instructions. Briefly, for each reaction, 5 µl of cDNA were mixed with 10 µl of SYBR Green master mix, 3.6 µl of H₂O, and 0.4 µl of reference ROX dye. This mixture was added to the 96-well plate and 1 µl of 10 µM primer mixture was pipetted. qPCRs were run on a QuantStudio3 machine (Applied Biosystems) and data analysis was performed using the QuantStudio Design and Analysis Software (Applied Biosystems). Statistical significance was assessed using Prism (GraphPad Software) statistical tests as described in the figure legends.

For RNAseq, total RNA was treated with On-Column DNase I digestion set (Sigma-Aldrich) following manufacturer's instructions. Samples were sent to IOR Genomics Facility (Bellinzona, Switzerland) for processing and RNAseq analyses.

Indirect immunofluorescence

HEK293 and FLP-In NIH-3T3 cells were plated respectively on poly-Lys and on alcian blue-coated glass coverslips and treated according to the experimental setups. Cells were washed twice in PBS and fixed for 20 min at RT with 3.7% formaldehyde in PBS. Cells were then incubated for 15 min at RT with a permeabilization solution (PS) containing 0.05% saponin, 10% goat serum, 10 mM HEPES, 15 mM glycine, pH 7.4. Cells were incubated with the primary antibodies in PS for 90 min, washed for 15 min in PS, and then incubated with Alexa Fluor-conjugated secondary antibodies in PS for 30 min. Finally, cells were rinsed with PS and H₂O and mounted with Vectashield® (Vector Laboratories) supplemented with DAPI. Confocal pictures were acquired using a Leica TCS SP5 microscope with a 63.0 x 1.40 Oil UV objective. Images were processed and mounted using FIJI, Adobe Photoshop and Illustrator software.

List of the primary antibodies

Antibody	Specie	Dilution	Manufacturer
HA	Rabbit	WB: 1:3000	Sigma-Aldrich (H6908)
HA	Mouse	IF: 1:100	Santa Cruz (sc-7392)
V5	Mouse	WB: 1:5000	Invitrogen (R960-25)
V5	Rat	IF: 1:100	Abcam (Ab206571)
GFP	Rabbit	WB: 1:1500	Abcam (ab290)
Giantin	Rabbit	IF: 1:100	BioLegend (924302)
CNX	Rabbit	IF: 1:100	Gifted by A. Helenius
KDEL (827)	Mouse	WB: 1:700	Stressgen (ADI-SPA-827)
GAPDH	Mouse	WB: 1:30000	Merck Millipore (MAB374)

List of the secondary antibodies

Antibody	Specie	Dilution	Manufacturer
Mouse Kappa-HRP	Goat	WB: 1:20000	SouthernBiotech (1050-05)
HRP-proteinA	-	WB: 1:20000	Abcam (101023)
Rabbit IgG (H+L)-HRP conjugate	Goat	WB: 1:10000	BioRad (1706515)
Rabbit (Alexa Fluor® 568 conjugated)	Goat	IF: 1:300	Thermo Fischer (A-11011)
Rat (Alexa Fluor® 647 conjugated)	Goat	IF: 1:300	Thermo Fischer (A-21247)
Mouse (Alexa Fluor® 488 conjugated)	Goat	IF: 1:300	Jackson ImmunoResearch (115-545-166)

8 APPENDIX

CURRICULUM VITAE

CONCETTA GUERRA

Address Via San Bernardino 2, 6500 Bellinzona, Switzerland
Phone +41 764838855 | **E-mail** concetta.guerra.19@gmail.com
Date of birth 19 October 1992 | **Nationality** Italian

EDUCATION

Institute for Research in Biomedicine, Bellinzona (Switzerland)
Enrolled at ETH Zurich, Department of Biology, Zurich (Switzerland)
PhD Student **01/2017 - 06/2020**
Supervisor: Dr. Maurizio Molinari

University of Padua, Padua (Italy)
Master Degree in Pharmaceutical Biotechnologies **10/2014 - 10/2016**
Score: 110/110 cum Laude
Thesis: *Preliminary characterization of thioredoxin-related transmembrane protein 5 (Tmx5), a type-I member of the protein disulfide isomerases superfamily.*
Supervisors: Dr. Dorianna Sandonà and Dr. Maurizio Molinari

University of Padua, Padua (Italy)
Bachelor Degree in Biotechnology **09/2011 - 09/2014**
Score: 103/110
Thesis: *Muscle fiber-type identification by immunohistochemistry of dystrophic murine diaphragms after treatment with nutraceuticals.*
Supervisor: Prof. Luisa Gorza

High School Liceo Scientifico "Publio Virgilio Marone", Carpino (Italy)
Scientific Diploma **09/2006 - 07/2011**
Score: 100/100

WORK EXPERIENCE

University of Padua, Padua (Italy)
Conference "JOB - Job Opportunities in Biotechnology" **10/2015**
Planner and conference chairman

University of Padua, Padua (Italy)
Full-time collaboration at the interactive scientific exhibition "Sperimentando" **04/2015 – 05/2015**
Guide for the chemistry section, realization of scientific experiments adapted to the audience

University of Padua, Padua (Italy)
Part-time collaboration at Administrative Office of Math Department **03/2014 – 09/2014**
Office work and front office activity

University of Padua, Padua (Italy)

Part-time collaboration at Authority for Surveillance of Administrative Action 05/2013 – 07/2013

Front office activity and Customer satisfaction service

PUBLICATIONS

Guerra C., Brambilla Pisoni G., Solda' T., Molinari M. (2018) **The reductase TMX1 contributes to ERAD by preferentially acting on membrane-associated folding-defective polypeptides.** *Biochem Biophys Res Commun.* 2018;503(2):938–943

Loi M., Fregno I., **Guerra C.**, Molinari M. (2018) **Eat it right: ER-phagy and recovER-phagy.** *Biochem Soc Trans.* 46(3):699–706

REVIEWED ARTICLES IN F1000

Molinari M and **Guerra C**: F1000Prime Recommendation of [Sandoz PA et al., *PLoS Biol* 2019 17(12):e3000553].
In F1000Prime, 22 Jan 2020; 10.3410/f.737107331.793569835

Molinari M and **Guerra C**: F1000Prime Recommendation of [Arigoni-Affolter I et al., *Sci Adv* 2019 5(11):eaax8930].
In F1000Prime, 03 Jan 2020; 10.3410/f.736999664.793569013

MEETINGS AND CONFERENCES

IRB Student Retreat 2017, Weggis (CH),
MAY 8th-10th 2017

Poster presentation: **“DISSECTING THE ROLE OF TMX1 IN ER-ASSOCIATED DEGRADATION”**

Introductory Course in Microbiology and Immunology 2018, Zurich (CH),
JANUARY 24th-26th, 2018

Oral presentation: **“‘MISFOLDABLE’ HALOTAG® PROTEIN CHIMERAS TO DISSECT MECHANISMS REGULATING CELLULAR PROTEOSTASIS”**

IRB Student Retreat 2018, Einsiedeln (CH),
MAY 2nd-4th, 2018

Poster presentation: **“INVESTIGATING THE ROLE OF TMX1 IN ER-ASSOCIATED DEGRADATION”**

Microbiology and Immunology Retreat (ETH-ZH), Visp (CH),
AUGUST 23rd-25th 2018

Poster presentation: **“INVESTIGATION OF CELLULAR RESPONSES UPON PERTURBATION OF ER HOMEOSTASIS WITH ‘MISFOLDABLE’ HALOTAG® PROTEIN CHIMERAS”**

Endoplasmic Reticulum Function in Health and Disease, Embo Workshop, Lucca (IT),
OCTOBER 21st-25th 2018

Poster presentation: **“CHARACTERIZATION OF CELLULAR RESPONSES ON PERTURBATION OF ER HOMEOSTASIS USING ‘MISFOLDABLE’ HALOTAG® PROTEIN CHIMERAS”**

IRB Student Retreat 2019, Weggis (CH),
APRIL 8th-10th 2019

Oral presentation: **“DISSECTION OF CELLULAR RESPONSES ON PERTURBATION OF ER HOMEOSTASIS USING ‘MISFOLDABLE’ HALOTAG® PROTEIN CHIMERAS”**

PERSONAL SKILLS

LANGUAGES

Italian – mother tongue

English – speak fluently and read/write with high proficiency

IT SKILLS

Good command of Mac OS/Windows suites

Proficient with MS Word, Excel, and PowerPoint

Good user of Adobe Creative Suite, GraphPad and ImageJ

Basic user of Scaffold platform for MS data analysis

Social media manager for @MolinariLab Twitter account

PERSONAL INTERESTS AND ACTIVITY

Interests: Music, Cooking and Art

Sports: Latin Dance, Jogging and Hiking

PUBLICATIONS

During my PhD, I published one research article and a review:

Research article

The reductase TMX1 contributes to ERAD by preferentially acting on membrane-associated folding-defective polypeptides

Authors: Guerra C, Brambilla Pisoni G, Soldà T, Molinari M.

Published in Biochemical and Biophysical Research Communications,

2018;503(2):938-943. doi:10.1016/j.bbrc.2018.06.099

Review

Eat It Right: ER-phagy and recovER-phagy

Authors: Loi M, Fregno I, Guerra C, Molinari M.

Published in Biochemical Society Transactions,

2018;46(3):699-706. doi:10.1042/BST20170354

The reductase TMX1 contributes to ERAD by preferentially acting on membrane-associated folding-defective polypeptides

Concetta Guerra ^{a, b}, Giorgia Brambilla Pisoni ^{a, c}, Tatiana Soldà ^a, Maurizio Molinari ^{a, c, *}

^a Università della Svizzera italiana (USI), Faculty of Biomedical Sciences, Institute for Research in Biomedicine, Bellinzona, Switzerland

^b Eidgenössische Technische Hochschule Zürich, Department of Biology, Zurich, Switzerland

^c Ecole Polytechnique Fédérale de Lausanne (EPFL), School of Life Sciences, CH-1015 Lausanne, Switzerland

ARTICLE INFO

Article history:

Received 1 June 2018

Accepted 19 June 2018

Available online 22 June 2018

Keywords:

Endoplasmic reticulum

ER-Associated degradation

Oxido-reductase

Protein folding and quality control

TMX1

Ubiquitin proteasome system

ABSTRACT

The Endoplasmic Reticulum (ER) is site of production of secretory and membrane proteins in eukaryotic cells. The ER does not contain catabolic devices and misfolded proteins generated in its lumen must be dislocated across the ER membrane before clearance by cytosolic proteasomes (ER-Associated Degradation, ERAD). How misfolded proteins are dislocated across the ER membrane is a matter of controversy. For example, it remains to be established if polypeptide unfolding is always required. If unfolding is a pre-requisite for dislocation as emerging evidences seem to indicate, it is likely that the incorrect set of disulfide bonds established during unsuccessful folding-attempts that precede selection for ERAD must be reduced to eliminate tertiary and quaternary structures that could hamper dislocation. The lumen of the mammalian ER contains more than 20 members of the PDI family, a handful of which plays a role in ERAD. Here we add the atypical, membrane-bound reductase TMX1 to this list and we show that TMX1 preferentially acts on membrane-tethered folding-defective polypeptides essentially ignoring the same misfolded ectodomains, when not associated to the ER membrane. As such, TMX1 is the first example of a topology-specific client protein redox catalyst acting both in the folding and in the degradative pathways.

© 2018 Elsevier Inc. All rights reserved.

1. Introduction

TMX1 is a membrane-associated member of the PDI superfamily [1]. It has originally been involved in quality control of major histocompatibility complex class I heavy chain [2] and systematic analysis revealed preferential association of TMX1 with newly synthesized polypeptides tethered at the ER membrane [3]. Consistently, expression of the trapping mutant TMX1_{CJA} carrying the active site cysteine59 to alanine point mutation that hampers substrate release, substantially delays folding and secretion of membrane proteins, leaving unaffected secretion of corresponding ectodomains detached from the ER membrane [3]. TMX1 displays a proline residue at position 2 of the catalytic site (CPAC) and is predominantly in the reduced form in the ER lumen, where it is expected to function as a reductase [1,4]. Reduction of intra- and

inter-molecular disulfide bonds is a crucial preparative reaction for dislocation of misfolded polypeptides across the ER membrane and proteasomal degradation [5,6]. To date, of the over 20 PDI family members, an involvement in misfolded protein clearance from the mammalian ER has been reported for PDI [7,8], ERdj5 [9], ERp57 and ERp72 [10], TXNDC11 [11] and PDI A6 [12]. Thus, as for catalysis of the oxidative polypeptide folding processes, also the ER-resident redox machinery involved in preparation of misfolded polypeptides for ER-associated degradation is highly redundant [13,14]. Both the mode of action and the substrate specificity of the various PDI family members is only starting to be understood [3,15] and no information is available on ERAD substrate specificity of ER-resident reductases. In this work, we verify if the reductase TMX1 plays a role in clearance of folding-defective polypeptides from the mammalian ER and, in this case, if it maintains the preference for

* Corresponding author. Università della Svizzera italiana (USI), Faculty of Biomedical Sciences, Institute for Research in Biomedicine, Bellinzona, Switzerland.
E-mail address: maurizio.molinari@rbs.usi.ch (M. Molinari).

membrane-bound substrates, which characterizes its activity in red/ox-dependent protein folding pathways [3].

2. Material and methods

2.1. Antibodies and expression plasmids

Antibodies to HA tag and anti-V5 Agarose Affinity Gel conjugated beads were from Sigma. Antibody against V5 tag was from Invitrogen. Plasmids encoding for V5-tagged TMX1_{C/A}, the membrane-bound and soluble HA-tagged BACE457, HA-tagged NHK and HA-tagged NHKcd3δ are described in Refs. [3,8,16].

2.2. Cell lines and transient transfection

HEK293 were cultured in DMEM supplemented with 10% FBS and grown at 37 °C and 5% CO₂. Cells were plated on poly-lysine-coated 3.5/6 cm culture dishes and transfected with 1.5 μg/2.25 μg of total plasmid DNA using jetPrime® reagent (Polyplus transfection). Seventeen hours after transfection, cells were used for the experiments.

2.3. Cell lysis, immunoprecipitations and western blots

Cells were washed with ice-cold PBS/20 mM N-ethylmaleimide (NEM). Lysis was performed with 2% CHAPS (Anatrace) in HEPES-buffered saline, pH 6.8, containing 20 mM NEM and protease inhibitors for 20 min on ice. Lysates were subjected to centrifugation at 4 °C and 10000 g for 10 min and post-nuclear supernatants (PNS) were collected.

For immunoprecipitations, PNS were incubated with protein A beads (Sigma, 1:10, w/v swollen in PBS) and anti-HA antibody, or with Anti-V5 Agarose Affinity Gel conjugated beads for 2 h at 4 °C. Samples were then washed with 0.5% CHAPS in HEPES-buffered saline, pH 7.4, and then dried. Dried beads were resuspended in sample buffer without (non-reducing) or with 100 mM DTT (reducing conditions) and boiled at 95 °C for 5 min. After denaturation, samples were subjected to SDS-PAGE.

Proteins were transferred to PVDF membranes using the Trans-Blot® Turbo™ Transfer System (Bio-Rad). Membranes were blocked with 10% (w/v) non-fat dry milk (Bio-Rad) in TBS-T and stained with primary antibodies diluted in TBS-T followed by HRP-conjugated secondary antibodies or Protein A diluted in TBS-T. Stained proteins were revealed using the Luminata™ Forte ECL detection system (Millipore) and signals were detected using ImageQuant LAS 4000 system (GE Healthcare Life Sciences) in the standard acquisition mode. If needed, membrane stripping for probing additional antigens was done using Re-Blot Plus Strong Solution (Millipore) following manufacturer's instructions.

2.4. Metabolic labeling

Cells were washed with pre-warmed phosphate buffered saline (PBS) and then pulse labeled with 0.1 mCi of [³⁵S]-methionine/cysteine in DMEM, 50 mM Hepes, 1% Glutamax for 15 min at 37 °C. Labeling medium was removed and cells were chased in DMEM supplemented with 5 mM non-labeled methionine and cysteine. Cells were lysed, PNS were collected and used for immunoprecipitations as described before. Samples were subjected to SDS-PAGE, gels were dried and exposed to autoradiography films (GE Healthcare, Fuji). Films were scanned with the Typhoon™ FLA 9500 (Software Version 1.0) and images were analyzed using the

ImageQuant software (Molecular Dynamics, GE Healthcare).

2.5. Graphs and statistical analysis

Graphical representations and statistical significance assessed by un-paired *t*-test were performed using Prism (GraphPad software).

3. Results and discussion

3.1. TMX1 preferentially associates with membrane-bound folding-defective polypeptides

A mass spectrometry analysis revealed a preferential association of TMX1 with endogenous single pass type I, single pass type II and multipass membrane polypeptides [3]. Selectivity for membrane-bound, disulfide-bond containing polypeptides over corresponding ectodomains detached from the ER membrane was maintained for ectopically expressed folding-competent model proteins [3]. The replacement of the resolving cysteine of oxidoreductase's active sites traps mixed disulfides in the reductive pathway [15]. For TMX1, the substitution of cysteine at position 59 with alanine (TMX1_{C/A}) stabilizes covalent complexes with substrates [3]. Consistent with a topology-specific action of TMX1, intraluminal expression of TMX1_{C/A} delayed secretion of membrane-bound polypeptides, leaving unaffected secretion of the corresponding ectodomains when detached from the ER membrane [3].

To verify if TMX1 plays a role in ERAD, we essentially applied the same experimental protocols, but used folding-defective polypeptides as model substrates. We first checked whether TMX1 associates with membrane-bound and/or soluble folding-defective polypeptides. To this end, 4 different HA-tagged model ERAD substrates were co-expressed with V5-tagged TMX1_{C/A} in human embryonic kidney HEK293 cells: the type I, pancreatic splice form of the beta secretase BACE457 and BACE457Δ, a soluble variant thereof obtained on ablation of the transmembrane C-terminal domain [8], the soluble disease-causing mutant form of the secretory protein alpha-1-antitrypsin inhibitor (NHK) and NHKCD3δ, a membrane-tethered variant thereof obtained on addition of the CD3δ transmembrane domain at the C terminus of NHK [16] (Fig. 1A). Cells were lysed, and the folding-defective polypeptides were immunoprecipitated from postnuclear supernatants (PNS) with an anti-HA antibody (Fig. 1B). The immunocomplexes were separated by reducing polyacrylamide gel electrophoresis and were subsequently transferred on PVDF membranes. The upper part of the PVDF membrane containing polypeptides larger than about 40 kDa was probed with an anti-HA antibody to confirm the immunoprecipitation of the individual folding-defective polypeptide from the PNS (Fig. 1B, IP:HA/WB:HA, lanes 3–6). The lower part of the PVDF membrane was probed with an anti-V5 antibody to reveal the co-precipitation of the V5-tagged TMX1_{C/A} (Fig. 1B, IP:HA/WB:V5, lanes 3–6). The experiment shows that TMX1_{C/A} co-precipitates with the membrane-tethered BACE457 (Fig. 1B, lower part, lane 3) and NHKCD3δ (lane 6), but much less with their soluble forms BACE457Δ (lane 4) and NHK (lane 5). Altogether, these data confirm the preference of TMX1 for folding-competent membrane-tethered polypeptides vs. their soluble variants [3] and extend the binding-specificity of TMX1 to folding-defective, membrane-bound polypeptides that must be selected for ERAD. These conclusions were supported by the reciprocal experiment (Fig. 1C), where the TMX1_{C/A}:ERAD substrate complexes were immunoprecipitated from detergent lysates with anti-V5 antibody

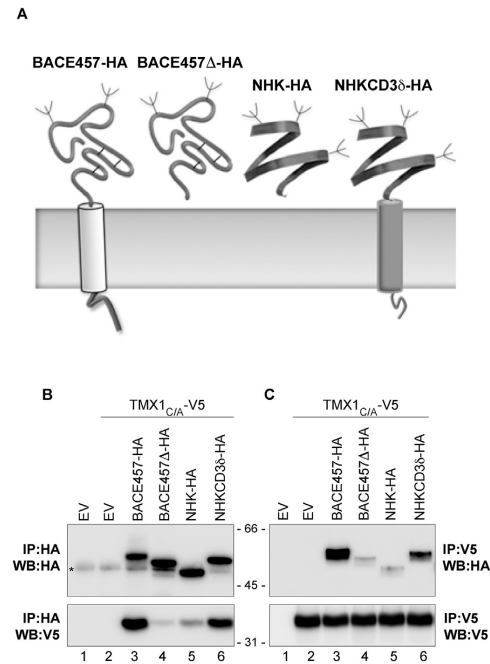


Fig. 1. TMX1 association with ERAD substrates. (A) Schematic of model folding-defective substrates used in this work. (B) HEK293 cells were transfected with an empty vector (EV, lane 1), V5-tagged TMX1_{C/A} (lane 2), or with V5-tagged TMX1_{C/A} in combination with HA-tagged BACE457, BACE457Δ, NHK or NHKCD3δ (lanes 3–6). Upper panel, the HA-tagged substrates were immunoprecipitated from PNS and revealed by WB with an anti-HA antibody. Lower panel, anti-V5 antibody revealed TMX1_{C/A} co-precipitation. (C) Same as B, but V5-tagged TMX1_{C/A} was immunoprecipitated from the same PNS with an anti-V5 antibody conjugated agarose beads to check the presence of the model folding-defective proteins in the immunocomplexes. *, antibody heavy chain recognized by the secondary antibody in WB.

conjugated agarose beads to capture TMX1 (Fig. 1C, lower panel). Probing the upper part of the PVDF membrane with the anti-HA antibody reveals the selective co-precipitation of the membrane-bound substrates BACE457 (lane 3) and NHKCD3δ (lane 6). Their soluble variants BACE457Δ (lane 4) and NHK (lane 5) are very inefficiently trapped by TMX1_{C/A}, again confirming the preference of TMX1 for membrane-bound polypeptides.

3.2. TMX1 establishes mixed disulfides with BACE457 and NHKCD3δ

Functional interactions between oxidoreductases and their substrates require transient formation of mixed disulfides i.e., of intermolecular disulfide-bonded complexes [17,18]. To verify the formation of mixed disulfides with ERAD substrates, the complexes immunoprecipitated with an antibody to the V5 tag of TMX1_{C/A} (as in Fig. 1C) were separated in non-reducing SDS polyacrylamide gel electrophoresis to preserve disulfide bonds' integrity and were then transferred on a PVDF membrane (Fig. 2A and B). Incubation of

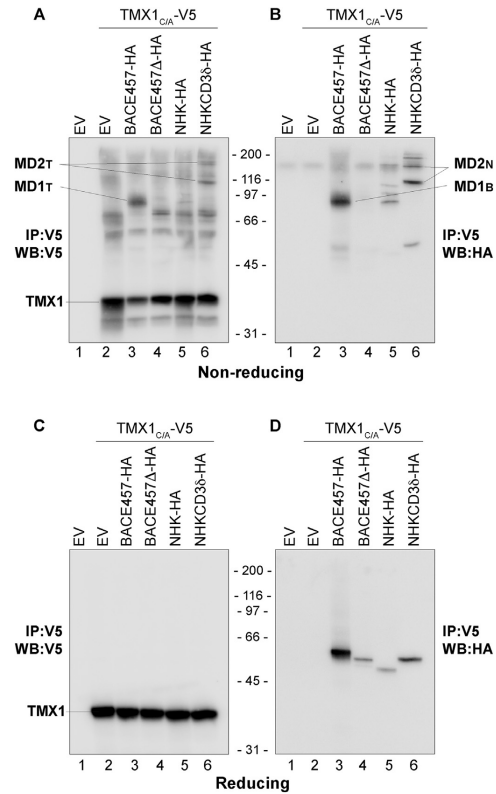
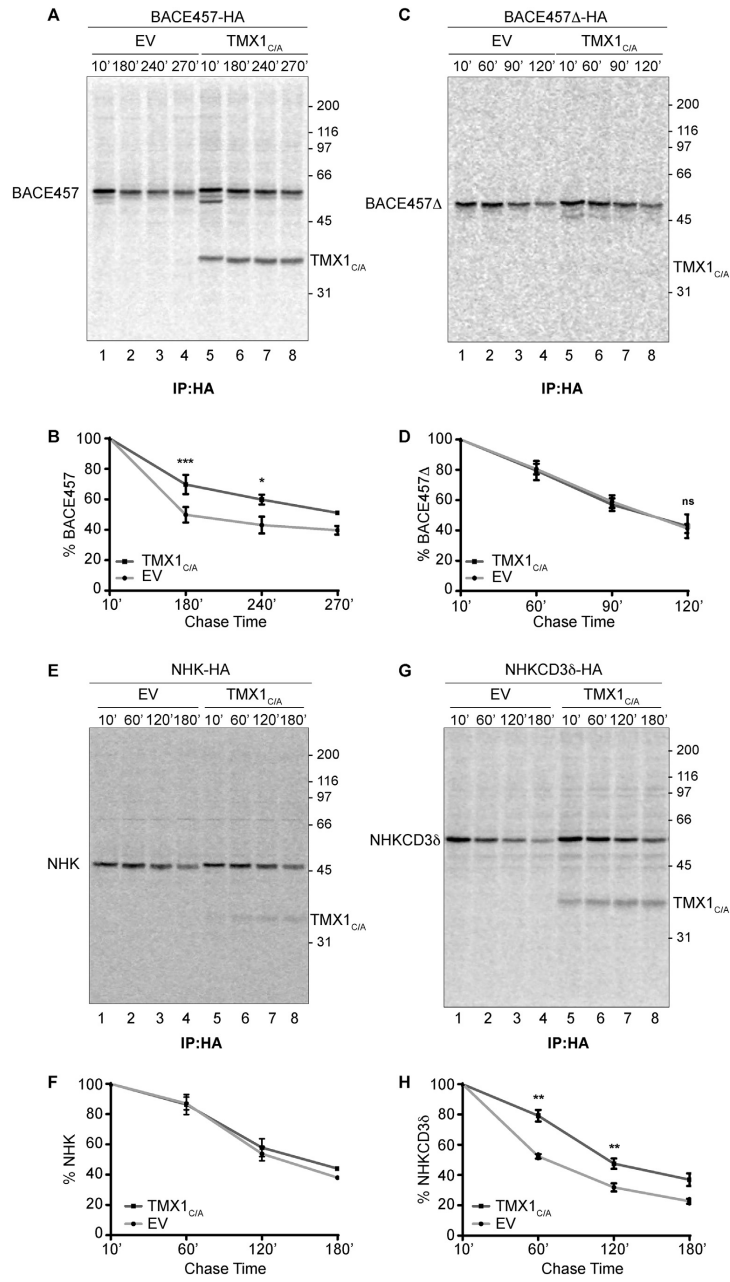


Fig. 2. TMX1_{C/A} establishes mixed disulfides with BACE457 and NHKCD3δ. (A) HEK293 cells were transfected with an empty vector (EV, lane 1), V5-tagged TMX1_{C/A} (lane 2), or V5-tagged TMX1_{C/A} in combination with HA-tagged BACE457, BACE457Δ, NHK, NHKCD3δ (lanes 3–6). V5-tagged TMX1_{C/A}-containing complexes were immunoprecipitated from PNS using anti-V5 conjugated agarose beads. The immunocomplexes were separated in non-reducing SDS polyacrylamide gel electrophoresis and analyzed by WB using an anti-V5 antibody. (B) Same membrane as in A was analyzed by WB with an anti-HA antibody after stripping. (C) Same as A, but immunocomplexes were separated in reducing gels. (D) Same membrane as in C was analyzed by WB with an anti-HA antibody after stripping. MD1_T for BACE457 component (α) of Mixed Disulfide 1; MD1_B for BACE457 component (β) of Mixed Disulfide 1; MD2_T for TMX1 component (γ) of Mixed Disulfides 2; MD2_N for NHKCD3δ component (α) of Mixed Disulfides 2.

the PVDF membrane with an anti-V5 antibody confirms the immunoprecipitation of TMX1 (shown with a line in Fig. 2A) and of TMX1-containing disulfide-bonded complexes from lysates of cells transfected with the plasmid for TMX1_{C/A} expression (immunoreactive polypeptides above the 45 kDa MW marker, Fig. 2A, lanes 2–6). TMX1_{C/A} expressed alone engages endogenous polypeptides in stable disulfide-bonded complexes (Fig. 2A, lane 2). These are cysteine containing membrane polypeptides [3]. Co-expression of model ERAD substrates (Fig. 2A, lanes 3–6), changes the pattern of TMX1_{C/A}-containing disulfide-bonded complexes (Fig. 2A, lane 2 vs.



3–6). This is particularly evident on co-expression of BACE457 (lane 3) or of NHHKCD3 δ (lane 6), the two membrane tethered ERAD substrates analyzed in these experiments. In cells expressing HA-tagged BACE457, TMX1_{C/A} enters an intermolecular disulfide-bonded complex of about 80 kDa, which is stained both with the anti-V5 (Fig. 2A, lane 3, arrow MD1_T for TMX1 component (T) of Mixed Disulfide 1) and the anti-HA antibody (Fig. 2B, lane 3, arrow MD1_B for BACE457 component (B) of Mixed Disulfide 1). Both MD1_T and MD1_B disappear on analysis of the same sample under reducing conditions (Fig. 2, C and D, lane 3). Thus, MD1_T and MD1_B are the TMX1 and BACE457 component, respectively, of a TMX1-s-BACE457 mixed disulfide.

Likewise, in cells expressing NHHKCD3 δ , TMX1_{C/A} enters two clearly distinct intermolecular disulfide-bonded complexes of about 116 and 150 kDa, which are stained both with the anti-V5 (Fig. 2A, lane 6, arrows MD2_T for TMX1 component (T) of Mixed Disulfides 2) and the anti-HA antibody (Fig. 2B, lane 6, arrows MD2_N for NHHKCD3 δ component (B) of Mixed Disulfides 2). Here as well, MD2_T and MD2_N are disassembled on sample reduction (Fig. 2, C and D, lane 6). Thus, MD2_T and MD2_N are the TMX1 and NHHKCD3 δ components, respectively, of TMX1-s-s-NHHKCD3 δ and (based on electrophoretic mobility) TMX1-s-s-NHHKCD3 δ -s-s-NHHKCD3 δ mixed disulfides.

TMX1_{C/A} does not form distinct mixed disulfides with the soluble BACE457 Δ (Fig. 2A and B, lane 4) or NHHK (lane 5) that associate with the reductase only poorly (Fig. 1B and C and 2D, lanes 4 and 5). As specificity control, in mock-transfected cells and in cells transfected only with TMX1_{C/A}, no anti-HA immunoreactivity is visible (Fig. 2, B and D, lanes 1 and 2). Similarly, only in cells transfected with TMX1_{C/A} (i.e., lanes 2–6 in Fig. 2, A and C) probing the PVDF membrane with the anti-V5 antibody reveals ectopically expressed TMX1. All in all, the preferential association of TMX1 with membrane-bound folding-defective polypeptides involves the formation of a mixed disulfide intermediate.

3.3. TMX1 selectively intervenes in clearance of membrane-tethered ERAD substrates

Clearance of folding defective polypeptides from the ER may require reduction of intra- and inter-molecular disulfide bonds to facilitate dislocation across the ER membrane and proteasomal degradation [5,6]. The peculiar sequence of the TMX1 catalytic site with a proline residue at position 2 (CPAC), its prevalently reduced state in the ER lumen and the predicted role as an ER reductase [1,4], make TMX1 a likely candidate for a role as reductase in ERAD. To verify this, cells expressing the model ERAD substrates analyzed in this study were mock transfected (EV for empty vector in Fig. 3) or were transfected for expression of TMX1_{C/A}, where a mutation in the TMX1's catalytic site delays substrate release. Cells were metabolically labeled with ³⁵S-methionine/cysteine for 15 min and chased for the times indicated to monitor the decay of the radio-labeled, model ERAD substrates. These were immunoprecipitated from cell lysates with an anti-HA antibody and separated in reducing polyacrylamide gel electrophoresis. Decay of BACE457 (Fig. 3A, lanes 1–4 and 3B, EV) was significantly delayed on co-expression

of TMX1_{C/A} (Fig. 3A, lanes 5–8 and 3B). In contrast, co-expression of TMX1_{C/A} did not affect the clearance of BACE457 Δ (Fig. 3C, lanes 1–8 and 3D). Likewise, co-expression of TMX1_{C/A} did not affect the clearance of the soluble ERAD substrate NHHK (Fig. 3E lanes 1–8 and 3F), but significantly delayed the turnover of the same misfolded ectodomain when this was tethered at the ER membrane (Fig. 3G, lanes 1–8 and 3H). As previously shown (Figs. 1 and 2), TMX1 co-precipitates with BACE457 (Fig. 3A, lanes 5–8) and NHHKCD3 δ (Fig. 3G, lanes 5–8), but much more weakly with BACE457 Δ (Fig. 3C, lanes 5–8) and NHHK (Fig. 3E, lanes 5–8), testifying the preference of the reductase for membrane-tethered folding-defective polypeptides.

The mammalian ER contains over two dozens of highly divergent enzymes that share one or more thioredoxin-like domains and have been grouped in a so-called protein disulfide isomerase (PDI) superfamily [19]. The ER is site of protein synthesis and folding for about a third of the organism's proteome and the vast majority of these polypeptides displays one or many intra- or inter-molecular disulfide bonds to stabilize tertiary and quaternary structures. The heterogeneity of the cargo proteins entering the secretory pathway at the ER may explain the reason for the presence of so many enzymes ensuring oxidation, reduction, isomerization reactions. However, the precise function of individual members of the PDI superfamily is difficult to assess and is poorly understood. It is likely, for example, that the very same PDI acts as a reductase or as an oxidase depending on the ER subdomain, where the substrate is encountered or on the binding partners it is associated with. Similarly, the very same PDI could act in the folding pathway for some cargo proteins and in the degradation pathway for others, as shown in our works on TMX1. Studies in test tubes fail to recapitulate the complexity of the ER, which is an extremely crowded compartment organized in subdomains with distinct physico-chemical properties and proteinaceous content. On the other hand, studies *in vivo* are complicated by the high redundancy of the PDI world that may hamper the emergence of phenotypes upon individual gene ablations [20–24]. This has partially been solved by ectopic expression of trapping mutant versions of the select PDI family member [3,15,25–28]. In these mutants, the resolving cysteine residue is replaced with an alanine thereby substantially prolonging the functional interaction of the PDI family member with the substrates. This experimental approach led to the identification of endogenous substrates for Erp18, Erp46, Erp57, Erp72, PDI, P5, ERdj5 and, in a previous work by our group, for TMX1. Here, the use of the TMX1 trapping mutant showed that the preference of TMX1 for membrane-tethered substrates recently reported for folding-competent polypeptides [3] remains valid for folding-defective polypeptides. Significantly, TMX1_{C/A} selectively engages membrane-tethered ERAD substrates in mixed disulfides, ignoring the same misfolded ectodomains when expressed as luminal polypeptides. Consistently, the trapping mutant selectively delays clearance from the ER of membrane-bound misfolded proteins, leaving unaffected degradation of soluble misfolded proteins. As such, TMX1 is the first example of a topology-specific reductase involved in ERAD.

Fig. 3. TMX1 selectively controls membrane protein ERAD. (A) HEK293 cells were transfected with HA-tagged BACE457 in combination with an empty vector (EV, lanes 1–4), or V5-tagged TMX1_{C/A} (lanes 5–8). Transfected cells were pulsed with [³⁵S]methionine/cysteine for 15 min and chased for 10, 180, 240, or 270 min. The degradation of radiolabeled BACE457-HA was analyzed upon immunoprecipitation with an anti-HA antibody. (B) Quantification of A. Error bars: SDs of six independent experiments for 180 min, three independent experiments for 240 and two for 270 min chase. For 180 and 240 min chase points, significance analyzed by unpaired t-test; *p < 0.05; ***p < 0.001. (C) Same as A for HA-tagged BACE457 Δ . (D) Quantification of C. Error bars: SDs of two independent experiments for 60 and 90 min chase, and three independent experiments for 120 min chase time. For 120 min chase point, significance analyzed by unpaired t-test; (E) Same as A for HA-tagged NHHK. (F) Quantification of E. Error bars show SDs of two independent experiments for 60 and 120 min chase points. (G) Same as A for HA-tagged NHHKCD3 δ . (H) Quantification of G. Error bars: SDs of three independent experiments for 60 and 120 min chase, and two independent experiments for 180 min chase time. For 60 and 120 min chase points, significance analyzed by unpaired t-test. *p < 0.05; **p < 0.01; ***p < 0.001; ns, not significant.

Acknowledgements

M.M. is supported by the Swiss National Science Foundation (31003A_163063), Signora Alessandra, AlphaONE Foundation, Foundation for Research on Neurodegenerative Diseases, the Novartis Foundation, the Comel Foundation and the Gelu Foundation.

References

- [1] Y. Matsuo, N. Akiyama, H. Nakamura, J. Yodoi, M. Noda, S. Kizaka-Kondoh, Identification of a novel thioredoxin-related transmembrane protein, *J. Biol. Chem.* 276 (2001) 10032–10038.
- [2] Y. Matsuo, H. Masutani, A. Son, S. Kizaka-Kondoh, J. Yodoi, Physical and functional interaction of transmembrane thioredoxin-related protein with major histocompatibility complex class I heavy chain: redox-based protein quality control and its potential relevance to immune responses, *Mol. Biol. Cell* 20 (2009) 4552–4562.
- [3] G.B. Pisoni, L.W. Ruddock, N. Bulleid, M. Molinari, Division of labor among oxidoreductases: TMX1 preferentially acts on transmembrane polypeptides, *Mol. Biol. Cell* 26 (2015) 3390–3400.
- [4] Y. Matsuo, K. Hirota, Transmembrane thioredoxin-related protein TMX1 is reversibly oxidized in response to protein accumulation in the endoplasmic reticulum, *FEBS Open Bio* 7 (2017) 1768–1777.
- [5] G.B. Pisoni, M. Molinari, Five questions (with their answers) on ER-associated degradation, *Traffic* 17 (2016) 341–350.
- [6] Y. Suzuki, M.J. Schmitt, Redox diversity in ERAD-mediated protein retrotranslocation from the endoplasmic reticulum: a complex puzzle, *Biol. Chem.* 396 (2015) 539–554.
- [7] K.Y. He, C.N. Cunningham, N. Manickam, M. Liu, P. Arvan, B. Tsai, PDI reductase acts on Akita mutant proinsulin to initiate retrotranslocation along the Hrd1/SecE-p97 axis, *Mol. Biol. Cell* 26 (2015) 3413–3423.
- [8] M. Molinari, C. Galli, V. Piccaluga, M. Pieren, P. Paganetti, Sequential assistance of molecular chaperones and transient formation of covalent complexes during protein degradation from the ER, *J. Cell Biol.* 158 (2002) 247–257.
- [9] R. Ushioda, J. Haseki, K. Araki, G. Jansen, D.Y. Thomas, K. Nagata, ERdj5 is required as a disulfide reductase for degradation of misfolded proteins in the ER, *Science* 321 (2008) 569–572.
- [10] S. Grubb, L. Guo, E.A. Fisher, J.L. Brodsky, Protein disulfide isomerases contribute differentially to the endoplasmic reticulum-associated degradation of apolipoprotein B and other substrates, *Mol. Biol. Cell* 23 (2012) 520–532.
- [11] R.T. Timms, S.A. Menzies, I.A. Tchasovnikarova, L.C. Christensen, J.C. Williamson, R. Antrosius, G. Dougan, L. Ellgaard, P.J. Lehner, Genetic dissection of mammalian ERAD through comparative haploid and CRISPR forward genetic screens, *Nat. Commun.* 7 (2016).
- [12] D.G. Gorasia, N.L. Dudek, H. Safavi-Hemami, R.A. Perez, R.B. Schittenhelm, P.M. Saunders, S. Wee, J.E. Mangum, M.J. Hubbard, A.W. Purcell, A prominent role of PDIA6 in processing of misfolded proinsulin, *Bba-Proteins Proteom* 1864 (2016) 715–723.
- [13] L. Ellgaard, S.S. Sevier, N.J. Bulleid, How are proteins reduced in the endoplasmic reticulum? *Trends Biochem. Sci.* 43 (2018) 32–43.
- [14] F. Hatahet, L.W. Ruddock, Substrate recognition by the protein disulfide isomerases, *FEBS J.* 274 (2007) 5223–5234.
- [15] C.E. Jessop, R.H. Watkins, J.J. Simmons, M. Tasab, N.J. Bulleid, Protein disulfide isomerase family members show distinct substrate specificity: P5 is targeted to BiP client proteins, *J. Cell Sci.* 122 (2009) 4287–4295.
- [16] J. Merulla, T. Solda, M. Molinari, A novel UGGT1 and p97-dependent checkpoint for native ectodomains with ionizable intramembrane residue, *Mol. Biol. Cell* 26 (2015) 1532–1542.
- [17] M. Molinari, A. Helenius, Glycoproteins form mixed disulphides with oxidoreductases during folding in living cells, *Nature* 402 (1999) 90–93.
- [18] J.B. Huppa, H.L. Ploegh, The eS-Sence of -SH in the ER, *Cell* 92 (1998) 145–148.
- [19] N.J. Bulleid, Disulfide bond formation in the mammalian endoplasmic reticulum, *Csh Perspect Biol* 4 (2012).
- [20] T. Solda, N. Garbi, G.J. Hammerling, M. Molinari, Consequences of Erp57 deletion on oxidative folding of obligate and facultative clients of the calnexin cycle, *J. Biol. Chem.* 281 (2006) 6219–6226.
- [21] C. Appenzeller-Herzog, L. Ellgaard, The human PDI family: versatility packed into a single fold, *Biochim. Biophys. Acta* 1783 (2008) 535–548.
- [22] Y. Zhang, G. Kozlov, C.L. Pocanski, U. Brockmeier, B.S. Ireland, P. Maattanen, C. Howe, T. Elliott, K. Gehring, D.B. Williams, Erp57 does not require interactions with calnexin and calreticulin to promote assembly of class I histocompatibility molecules, and it enhances peptide loading independently of its redox activity, *J. Biol. Chem.* 284 (2009) 10160–10173.
- [23] K. Kang, B. Park, K. Oh, K. Cho, K. Ahn, A role for protein disulfide isomerase in the early folding and assembly of MHC class I molecules, *Antioxidants Redox Signal.* 11 (2009) 2553–2561.
- [24] L.A. Rutkevich, M.F. Cohen-Doyle, U. Brockmeier, D.B. Williams, Functional relationship between protein disulfide isomerase family members during the oxidative folding of human secretory proteins, *Mol. Biol. Cell* 21 (2010) 3093–3105.
- [25] T.P. Dick, P. Cresswell, Thiol oxidation and reduction in major histocompatibility complex class I-restricted antigen processing and presentation, *Protein Sensors and Reactive Oxygen Species*, Pt B, *Thiol Enzymes and Proteins* 348 (2002) 49–54.
- [26] C.E. Jessop, S. Chakravarthi, N. Garbi, G.J. Hammerling, S. Lovell, N.J. Bulleid, Erp57 is essential for efficient folding of glycoproteins sharing common structural domains, *EMBO J.* 26 (2007) 28–40.
- [27] S. Schulman, B. Wang, W. Li, T.A. Rapoport, Vitamin K epoxide reductase prefers ER membrane-anchored thioredoxin-like redox partners, *P Natl Acad Sci USA* 107 (2010) 15027–15032.
- [28] O.B. Oka, M.A. Pringle, I.M. Schopp, I. Braakman, N.J. Bulleid, ERdj5 is the ER reductase that catalyzes the removal of non-native disulfides and correct folding of the LDL receptor, *Mol. Cell* 50 (2013) 793–804.

Review Article

Eat it right: ER-phagy and recover-phagy

Marisa Loi^{1,2,3}, Ilaria Fregno^{1,2,3}, Concetta Guerra^{1,2} and Maurizio Molinari^{1,2,4}

¹Università della Svizzera italiana, Via G. Buffi, CH-6900 Lugano, Switzerland, ²Institute for Research in Biomedicine, Via V. Vita 6, CH-6500 Bellinzona, Switzerland, ³Department of Biology, Swiss Federal Institute of Technology, Wolfgang Pauli Strasse 27, CH-8093 Zurich, Switzerland, ⁴École Polytechnique Fédérale de Lausanne, School of Life Sciences, EPFL Station 19, CH-1015 Lausanne, Switzerland

Correspondence: Maurizio Molinari (maurizio.molinari@epfl.ch)



The endoplasmic reticulum (ER) is the site of protein, lipid, phospholipid, steroid and oligosaccharide synthesis and modification, calcium ion storage, and detoxification of endogenous and exogenous products. Its volume (and activity) must be maintained under normal growth conditions, must be expanded in a controlled manner on activation of ER stress programs and must be reduced to pre-stress size during the recovery phase that follows ER stress termination. ER-phagy is the constitutive or regulated fragmentation and delivery of ER fragments to lysosomal compartments for clearance. It gives essential contribution to the maintenance of cellular homeostasis, proteostasis, lipidostasis and oligosaccharidostasis (i.e. the capacity to produce the proteome, lipidome and oligosaccharidome in appropriate quality and quantity). ER turnover is activated on ER stress, nutrient deprivation, accumulation of misfolded polypeptides, pathogen attack and by activators of macroautophagy. The selectivity of these poorly characterized catabolic pathways is ensured by proteins displayed at the limiting membrane of the ER subdomain to be removed from cells. These proteins are defined as ER-phagy receptors and engage the cytosolic macroautophagy machinery via specific modules that associate with ubiquitin-like, cytosolic proteins of the Atg8/LC3/GABARAP family. In this review, we give an overview on selective ER turnover and on the yeast and mammalian ER-phagy receptors identified so far.

Autophagy, the discovery

The term autophagy, literally 'self-eating', was first used in 1963 by Christian de Duve, during the CIBA Foundation Symposium on Lysosomes [1]. It now defines constitutive and regulated catabolic processes characterized by delivery of cytosolic material and organelles within the lysosomal compartment for clearance [2]. It was soon established that these self-eating pathways are enhanced by glucagon treatment or nutrient deprivation [3,4]. Initially, autophagy was merely studied in mammalian cells at morphological level. Transient intermediate autophagic structures (i.e. double membranes surrounding the cytosolic material that eventually fuse with lysosomes for degradation) were described [5]. The molecular mechanisms regulating autophagy were uncovered in the 1990s, when the process was first reported to exist also in the yeast *Saccharomyces cerevisiae* [6] and when genetic screens in this organism identified the first autophagy gene APG1 (now ATG1) [7]. To date, 140 autophagy-related (ATG) genes have been discovered. ATG genes are highly conserved from yeast to mammals to the point that yeast orthologs may functionally replace mammalian genes and vice versa [8].

Selective autophagy of organelles

From the very beginning, besides the observation of a bulk 'self-eating' process, the idea of selective degradation of intracellular components emerged. In fact, early morphological studies revealed the presence of whole organelles and organelle portions such as endoplasmic reticulum (ER), mitochondria and peroxisomes in lysosomes (or in the yeast vacuole) [9–11]. These selective degradative mechanisms may reflect the cellular need to control the size of organelles, to eliminate damaged organelles or to remove organelle subdomains containing toxic material. Based on the cargo delivered to

Received 11 April 2018
Revised 28 April 2018
Accepted 2 May 2018

Version of Record published
25 May 2018

lysosomal compartments for clearance, these processes have been named aggrephagy for cytosolic protein aggregates, ER-phagy or reticulophagy for ER, mitophagy for mitochondria, pexophagy for peroxisomes, ribophagy for ribosomes and xenophagy for intracellular pathogens [12].

Selective autophagy of the ER

The ER is a dynamic organelle, whose volume is adapted to fluctuations in the protein and lipid biosynthetic demand, to changes of developmental and environmental conditions, to pharmacologic intervention or chemical insult and to attack by pathogens. First evidences of lysosomal degradation of the ER were observed in insect's fat body during the formation of storage granules [13] and in rat hepatocytes upon cessation of phenobarbital treatment [9]. *Constitutive* ER clearance maintains the volume of the organelle under normal growth conditions [14]. *Regulated* ER turnover is activated on nutrient deprivation [14–16], prevents excessive ER expansion in cells exposed to physiologic or pathologic stresses that elicit transcriptional and translational programs named unfolded protein responses (UPRs) [16,17] or terminates such ER stresses to re-establish pre-stress ER volume, content and activity [18]. ER-phagy may also be induced to remove subdomains containing faulty proteins and lipids [19] and by pathogen attack [20]. ER turnover requires ER vesiculation and capture of ER-derived vesicles by double-membrane autophagosomes that eventually fuse with lysosomes to clear their content. Alternatively, ER-derived vesicles may directly fuse with lysosomal compartments to deliver their luminal content for destruction. Most of these events eventually leading to ER clearance are mechanistically poorly understood. Paradoxically, the term 'ER-phagy' was coined by the group of Peter Walter to define the selective delivery of ER to the vacuole in yeast cells experiencing a dithiothreitol (DTT)-induced ER stress [17,21]. However, DTT-induced, yeast 'ER-phagy' cannot be considered representative for the catabolic processes regulating lysosomal ER turnover as described in this review. In fact, it results in the formation of ER whorls that are engulfed by the vacuolar membrane in a process that is topologically equivalent to microautophagy and does not require intervention of autophagy genes. Moreover, and significantly, the ER whorls are not degraded and accumulate in the vacuolar lumen. DTT-induced yeast ER-phagy has subsequently been defined as 'micro-ER-phagy' to distinguish it from another type of selective ER delivery to the yeast vacuole that has been defined as 'macro-ER-phagy'. The latter is triggered by the overexpression of membrane proteins, requires conventional autophagy genes, small GTPases and results in *de facto* ER degradation [19]. The autophagy gene *Atg9* plays a role in the exit of macro-ER-phagy cargo from the ER, being required for the formation of ER-to-autophagy membranes (ERAM). The small GTPase *Ypt1* is involved in the assembly of ERAM with pre-autophagosomal proteins *Atg1*, *Atg8* and *Atg11*. The small GTPase *Ypt51* mediates the delivery of autophagosomes to the vacuole. *Atg2* plays an uncharacterized role in this process as its deletion impairs the removal of the membrane-bound cargo proteins. It is likely that macro-ER-phagy as defined in ref. [19] involves ER-phagy receptors that regulate the selective clearance of ER subdomains containing excess membrane proteins. However, these receptors remain to be characterized.

Autophagy receptors

Selectivity in autophagic processes implies the involvement of receptors bridging the cargo or the organelle to be degraded and the autophagic machinery. Autophagy receptors are defined by their capability (1) to recognize the cargo and/or to define the organelle or organelle portion to be degraded and (2) to interact with the autophagy modifier proteins of the *Atg8/LC3* (light chain 3)/GABARAP (γ -aminobutyric acid receptor-associated protein) family via an *Atg8*-interacting motif (AIM) in yeast and via a *LC3*-interacting region *LC3*-interacting region (LIR) in mammals [22,23]. In the following sections, we will summarize the current knowledge on ER-resident, *Atg8/LC3*-binding proteins that ensure constitutive and regulated clearance of the ER by acting as ER-phagy receptors.

ER-phagy receptors in yeast

Atg39 and *Atg40*

In the budding yeast, ER-phagy is triggered by overexpression of integral membrane proteins (macro-ER-phagy) [19], by target of rapamycin (TOR) inhibition on nitrogen deprivation or on incubation with the macrolide compound rapamycin [24,25]. As written above, receptors that regulate delivery of ER portions containing excess membrane proteins to the yeast vacuole (i.e. macro-ER-phagy receptors) have not been identified [19].

In contrast, ER-phagy receptors have been characterized for starvation- and rapamycin-induced ER-phagy. Here, the Atg8-binding proteins Atg39 and Atg40 decorate the membrane of ER and nuclear envelope subdomains to be delivered to the vacuole for clearance [26]. Atg39 and a small fraction of Atg40 localize in (and regulate turnover of) the nuclear envelope, which in *S. cerevisiae* is equivalent to the mammalian perinuclear ER. Atg40 mainly localizes to (and regulates turnover of) the cytoplasmic and cortical ER. Both Atg39 and Atg40 are transcriptionally and translationally induced in response to nitrogen deprivation- or rapamycin-induced TOR inactivation. Atg40 (but not Atg39) contains a domain similar to the mammalian reticulon-homology domain (RHD; Figure 1) required for membrane shaping and probably facilitating ER fragmentation. Both Atg39 and Atg40 contain an AIM (Figure 1) that engages phagophore membrane-bound Atg8. They both also interact with Atg11, an autophagy mediator that recruits the autophagosome biogenesis machinery at the receptor–cargo complex [27], but only Atg39 displays a consensus Atg11-binding sequence (Atg11BR, Figure 1) [26]. So far, it has been established that Atg39- and Atg40-mediated ER-phagy require Atg1, Atg8, Atg11 and Atg17, the vacuolar peptidase Pep4 and the small GTPase Ypt7 (Table 1) [26].

ER-phagy receptors in mammalian cells

FAM134B

FAM134B [family with sequence similarity 134; also known as RETREG1 (reticulophagy regulator 1)] is a member of the FAM134 reticulon protein family [14,28,29]. It harbors a RHD, which promotes curvature of ER membranes, and a LIR at the cytosolic C-terminus (Figure 1) that engages LC3 and/or GABARAP displayed at the limiting membrane of growing phagophores. This hints at a role of FAM134B as an ER-phagy receptor. Consistently, the RHD and the LIR are required for ER fragmentation, capture of ER fragments

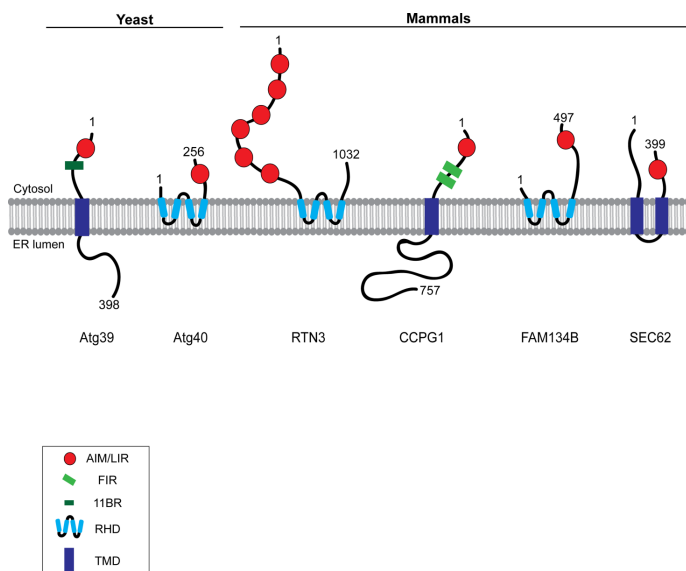


Figure 1. ER-phagy receptors in yeast and mammals.

The figure illustrates the yeast ER-phagy receptors Atg39 and Atg40 and the mammalian ER-phagy receptors FAM134B, SEC62, RTN3 and CCPG1. Number of residues in protein topology is shown. AIM: Atg8-interacting motif; LIR: LC3-interacting region; FIR: FIP200-interacting region; 11BR: Atg11-binding region; RHD: Reticulon-homology domain; TMD: transmembrane domain.

Table 1 ER-phagy receptors in yeast and mammals: cargos and requirements

The table shows a list of the yeast and mammalian ER-phagy receptors reported so far in the literature, the ER subdomain and the ER-resident proteins cleared on their intervention and the gene products reported to be involved in the given ER-phagy pathway.

Receptors	Cargo degraded	Cargo excluded	Gene products required	Gene products not required
Yeast				
Atg39	Perinuclear ER Hmg1, Kar2, Src1, Nop1, Sec63	Rtn1	Atg1, Atg8, Atg11, Atg17, Ypt7, Pep4	ND
Atg40	Cytosolic/cortical ER Rtn1, Sec63	Kar2	Atg1, Atg8, Atg11, Atg17, Ypt7, Pep4	ND
Mammals				
FAM134B	ER sheets SEC61B, CLIMP63, TRAP- α , RTN4	RTN3, RTN1, Reep5	LC3/GABARAP ATG5, Beclin1, FIP200	RTN3
SEC62	ER chaperones (e.g. CNX, CRT, BiP,...) Folding enzymes (e.g. ERp72, ERp57,...)	ERAD factors	LC3 ATG5, ATG7	ND
RTN3L	ER tubuli (RTN1, RTN4, Reep5)	CLIMP63, TRAP- α FAM134B	LC3/GABARAP ATG5, ATG7, FIP200	FAM134B
CCPG1	Peripheral/tubular ER (RTN3)	FAM134B	LC3/GABARAP, ATG5, FIP200	ND

Abbreviation: ND: not determined.

within autophagosomes and their subsequent delivery to lysosomal compartments for clearance. Ablation of FAM134B or sensory neuropathy-causing loss-of-function FAM134B mutations cause ER expansion as a consequence of defective ER clearance [14,28]. This reveals a constitutive role of FAM134B in the maintenance of mammalian ER size [14]. FAM134B-mediated ER clearance is enhanced in cells subjected to nutrient deprivation. FAM134B co-localizes with SEC61B, CLIMP-63, TRAP- α (translocon-associated protein subunit alpha) and to a lesser extent with reticulon (RTN)4 to the edge of ER sheets, which are the ER subdomains found to be selectively cleared by FAM134B-regulated ER-phagy. This requires the autophagy gene products LC3/GABARAP, ATG5, Beclin1 and FIP200 (FAK family kinase-interacting protein of 200 kDa) (Table 1) [14,15].

SEC62

SEC62 (translocation protein SEC62) is an ER-resident transmembrane component of the SEC61/SEC62/SEC63 translocation machinery involved in the import of newly synthesized proteins into the ER lumen [30–32]. SEC62 was identified as the ER-phagy receptor that regulates ER turnover after conclusion of a transient ER stress. SEC62-regulated catabolic processes re-establish pre-stress ER volume and ER content and have been defined as recover-phagy [18]. Bioinformatics analysis revealed a LIR at the C-terminus of SEC62 (Figure 1), which is conserved in Metazoa, not in yeast. This functional region is required for the function of SEC62 in recover-phagy, but is dispensable for its role in protein translocation. The LIR-mediated interaction of SEC62 with LC3 was validated *in vitro* (surface plasmon resonance, nuclear magnetic resonance spectroscopy and peptide array analyses) and *in cellulo* [18]. SEC62-mediated recover-phagy is activated on resolution of a transient ER stress to ensure the clearance of specific ER subdomains and restore ER homeostasis. Mass spectrometry analyses confirmed the selectivity of this process. In fact, recover-phagy clears ER fragments, leaving unaffected mitochondria. More important, the catabolic activity targets ER subdomains containing molecular chaperones and folding enzymes [e.g. calnexin, calreticulin, BiP, PDI (protein disulfide isomerase), ERp72 and ERp57], but not factors that regulate ER-associated degradation (ERAD) [18]. This finding supports the notion

that different luminal activities (in this case, protein folding and selection for protein disposal) are compartmentalized in distinct ER subdomains. Interestingly, tumors expressing increased levels of SEC62 show a higher ER stress tolerance and drug resistance, which directly correlate with higher malignancy [33–36]. This new identified role of SEC62 in clearance of excess and damaged ER may explain why cancer cells with increased levels of SEC62 better tolerate ER stresses [37]. So far, it has been reported that SEC62-mediated recover-ER-phagy relies on the autophagy proteins LC3, ATG5 and ATG7 (Table 1) [18].

Reticulon3

RTN3 belongs to the RHD-containing proteins (RTN1–4), which are curving-membrane proteins highly enriched in tubular ER [38]. Among the numerous splice variants, only the longest (RTN3L) functions as the ER-phagy receptor [15]. It contains six LIRs in the N-terminal cytosolic domain of the protein (Figure 1), which interact with LC3 and GABARAP. Like FAM134B, the role of RTN3L in ER-phagy is activated on amino acid deprivation. However, in contrast with FAM134B that regulates turnover of ER sheets [14], RTN3L regulates the selective fragmentation and autophagic degradation of ER tubules containing RTN1, RTN4, REEP5 and RTN3 [15]. This process requires the oligomerization of RTN3L as well as the association of LC3/GABARAP and is abolished on disruption of all six LIRs. LC3/GABARAP, ATG5, ATG7 and FIP200 are required for starvation-induced ER tubules turnover (Table 1) [15].

CCPG1

Cell-cycle progression gene 1 (CCPG1) is a receptor for ER stress-induced ER-phagy [16]. CCPG1 localizes to perinuclear ER and in small foci at the ER periphery. It contains a LIR at the N-terminal cytosolic domain engaging LC3/GABARAP. However, it is defined as a non-canonical ER-phagy receptor because it also contains two FIP200-interacting regions, defined as FIRs (Figure 1). FIR shows similarity to the Atg11BR displayed by the yeast Atg39 protein, which facilitates the recruitment of the autophagic machinery. During ER stress, endogenous CCPG1 is induced and drives the autophagic degradation of peripheral ER. In cells lacking CCPG1, the starvation-induced degradation of the peripheral/tubular ER marker RTN3 was impaired, while degradation of a marker of ER sheets, FAM134B, was not affected. *In vivo*, CCPG1 plays an important role in maintaining the proteostasis of the pancreas protecting against aggregation of ER luminal proteins and consequent UPR activation, thus sustaining tissue health. CCPG1-mediated ER-phagy requires LC3/GABARAP, ATG5 and FIP200 (Table 1) [16].

Involvement of promiscuous LC3-binding proteins in ER turnover: BNIP3 and p62

BNIP3 (BCL2/adenovirus E1B 19 kDa protein-interacting protein 3) and p62 regulate removal of the ER via autophagy [39,40]. BNIP3 is a transmembrane protein involved in apoptosis signaling, which contains a LIR at its N-terminal region. Endogenous BNIP3 localizes at the mitochondria, but during hypoxia, small amounts can relocate at the ER. Overexpression of BNIP3 enhances both mitophagy and reticulophagy via BNIP3-mediated engagement of autophagosome-localized LC3 [41]. However, disruption of BNIP3–LC3 interaction does not completely abolish autophagy of the ER, indicating the contribution of other ER-phagy receptors [39]. The autophagy receptor p62 has also been proposed to play a role in ER turnover [40]. p62 is a cytosolic, LIR-containing protein that regulates lysosomal clearance of polyubiquitylated polypeptides. Its involvement in ER clearance can be ascribed to the recognition of ER proteins polyubiquitylated at their cytosolic domains. After withdrawal of the xenobiotics 1,4-bis[2-(3,5-dichloropyridyloxy)]benzene (TCPOBOP), mouse liver cells lacking p62 fail to degrade excess ER, indicating the relevance of p62 in ER clearance [40].

Concluding remarks

ER misfunction causes severe disease conditions. For that reason, intense research has been devoted to characterize the pathways that maintain ER homeostasis. The transcriptional/translational ER stress responses [42], as well as the pathways delivering misfolded polypeptides from the ER to the cytosol for degradation by the ubiquitin proteasome system [43], have been elucidated in molecular details. Pharmacologic modulation of the UPR [44–46] and the ubiquitin proteasome system [47] are expected to affect on protein misfolding diseases, cognitive disorders and tumors to mention just a few pathologic states resulting from proteostasis impairment. In sharp contrast, only recently the characterization of the molecular mechanisms ensuring lysosomal clearance

of ER fragments or subdomains has attracted the interest of cell biologists. The identification of ER-phagy receptors, both in yeast and in mammalian cells, paves the way to the characterization of constitutive and regulated ER turnover and clearly shows that ER subdomains can specifically be selected for disposal. A limitation of studies published so far is that ER turnover is activated on cells exposure to unspecific stimuli such as chemically induced ER stresses, nutrient deprivation or autophagy modulators. Such stimuli certainly led to the identification of few ER-phagy receptors both in yeast and in mammalian cells. However, they certainly have pleiotropic effects as shown by the fact that the same experimental conditions have been used to investigate conventional autophagic pathways as well as other types of organelle-specific macroautophagies, all of which are possibly simultaneously induced. More physiologic stimuli eliciting exclusive activation of clearance of select ER subdomains and leaving unaffected the turnover of other subdomains, other cargos or other organelles are actively sought after and must be the focus of future research. It is likely, in fact, that individual ER-phagy receptors are displayed in particular subdomains of the ER that sense the luminal and membrane environment and eventually send alert signals on accumulation of faulty proteins, lipids, otherwise toxic material or pathogens to the autophagy machineries located in the cytosolic space.

Abbreviations

AIM, Atg8-interacting motif; ATG, autophagy-related; BiP, binding immunoglobulin protein; BNIP3, BCL2/adenovirus E1B 19 kDa protein-interacting protein 3; CCPG1, cell-cycle progression gene 1; DTT, dithiothreitol; ER, endoplasmic reticulum; ERAD, ER-associated degradation; ERAM, ER-to-autophagy membranes; FAM134, family with sequence similarity 134; FIP200, FAK family kinase-interacting protein of 200 kDa; FIR, FIP200-interacting regions; GABARAP, γ -aminobutyric acid receptor-associated protein; LC3, light chain 3; LIIR, LC3-interacting region; RHD, reticulon-homology domain; RTN, reticulon; SEC62, translocation protein SEC62; TOR, target of rapamycin; TRAP- α , translocon-associated protein subunit alpha; UPR, unfolded protein response.

Funding

M.M. is supported by the SNF, Signora Alessandra, AlphaONE Foundation, Foundation for Research on Neurodegenerative Diseases, the Novartis Foundation, Swiss National Science Foundation (SNF), the Comel and Gelu Foundations.

Acknowledgements

We thank members of the M.M.'s laboratory for discussions and inputs during the preparation of this manuscript.

Competing Interests

The Authors declare that there are no competing interests associated with the manuscript.

References

- De Duve, C. and Wattiaux, R. (1966) Functions of lysosomes. *Annu. Rev. Physiol.* **28**, 435–492 <https://doi.org/10.1146/annurev.ph.28.030166.002251>
- Yu, L., Chen, Y. and Tooze, S.A. (2018) Autophagy pathway: cellular and molecular mechanisms. *Autophagy* **14**, 207–215 <https://doi.org/10.1080/15548627.2017.1378838>
- Deter, R.L., Baudhuin, P. and De Duve, C. (1967) Participation of lysosomes in cellular autophagy induced in rat liver by glucagon. *J. Cell Biol.* **35**, C11–C16 <https://doi.org/10.1083/jcb.35.2.C11>
- Novikoff, A.B., Essner, E. and Quintana, N. (1964) Golgi apparatus and lysosomes. *Fed. Proc.* **23**, 1010–1022 PMID:14209792
- Arstilla, A.U. and Trump, B.F. (1968) Studies on cellular autophagocytosis. The formation of autophagic vacuoles in the liver after glucagon administration. *Am. J. Pathol.* **53**, 687–733 PMID:4300890
- Takehige, K., Baba, M., Tsuboi, S., Noda, T. and Ohsumi, Y. (1992) Autophagy in yeast demonstrated with proteinase-deficient mutants and conditions for its induction. *J. Cell Biol.* **119**, 301–311 <https://doi.org/10.1083/jcb.119.2.301>
- Matsuura, A., Tsukada, M., Wada, Y. and Ohsumi, Y. (1997) Apg1p, a novel protein kinase required for the autophagic process in *Saccharomyces cerevisiae*. *Gene* **192**, 245–250 [https://doi.org/10.1016/S0378-1119\(97\)00084-X](https://doi.org/10.1016/S0378-1119(97)00084-X)
- Bento, C.F., Penna, M., Ghislat, G., Puri, C., Ashkenazi, A., Vicinanza, M. et al. (2016) Mammalian autophagy: how does it work? *Annu. Rev. Biochem.* **85**, 685–713 <https://doi.org/10.1146/annurev-biochem-060815-014556>
- Bolender, R.P. and Weibel, E.R. (1973) A morphometric study of the removal of phenobarbital-induced membranes from hepatocytes after cessation of treatment. *J. Cell Biol.* **56**, 746–761 <https://doi.org/10.1083/jcb.56.3.746>
- Beaulaton, J. and Lockshin, R.A. (1977) Ultrastructural study of the normal degeneration of the intersegmental muscles of *Antheraea polyphemus* and *Manduca sexta* (Insecta, Lepidoptera) with particular reference to cellular autophagy. *J. Morphol.* **154**, 39–57 <https://doi.org/10.1002/jmor.1051540104>

- 11 Veenhuis, M., Douma, A., Harder, W. and Osumi, M. (1983) Degradation and turnover of peroxisomes in the yeast *Hansenula polymorpha* induced by selective inactivation of peroxisomal enzymes. *Arch. Microbiol.* **134**, 193–203 <https://doi.org/10.1007/BF00407757>
- 12 Stolz, A., Ernst, A. and Dikic, I. (2014) Cargo recognition and trafficking in selective autophagy. *Nat. Cell Biol.* **16**, 495–501 <https://doi.org/10.1038/ncb2979>
- 13 Locke, M. and Collins, J.V. (1965) The structure and formation of protein granules in the fat body of an insect. *J. Cell Biol.* **26**, 857–884 <https://doi.org/10.1083/jcb.26.3.857>
- 14 Khaminets, A., Heinrich, T., Mari, M., Grumati, P., Huebner, A.K., Akutsu, M. et al. (2015) Regulation of endoplasmic reticulum turnover by selective autophagy. *Nature* **522**, 354–358 <https://doi.org/10.1038/nature14498>
- 15 Grumati, P., Morozzi, G., Holper, S., Mari, M., Harwardt, M.J., Yan, R. et al. (2017) Full length RTN3 regulates turnover of tubular endoplasmic reticulum via selective autophagy. *eLife* **6**, 911 <https://doi.org/10.7554/eLife.25555>
- 16 Smith, M.D., Harley, M.E., Kemp, A.J., Wills, J., Lee, M., Arends, M. et al. (2018) CCPG1 is a non-canonical autophagy cargo receptor essential for ER-phagy and pancreatic ER proteostasis. *Dev. Cell* **44**, 217–232 <https://doi.org/10.1016/j.devcel.2017.11.024>
- 17 Schuck, S., Gallagher, C.M. and Walter, P. (2014) ER-phagy mediates selective degradation of endoplasmic reticulum independently of the core autophagy machinery. *J. Cell Sci.* **127**, 4078–4088 <https://doi.org/10.1242/jcs.154716>
- 18 Fumagalli, F., Noack, J., Bergmann, T.J., Cebollero, E., Pisoni, G.B., Fasana, E. et al. (2016) Translocon component Sec62 acts in endoplasmic reticulum turnover during stress recovery. *Nat. Cell Biol.* **18**, 1173–1184 <https://doi.org/10.1038/ncb3423>
- 19 Lipatova, Z. and Segev, N. (2015) A role for macro-ER-phagy in ER quality control. *PLoS Genet.* **11**, e1005390 <https://doi.org/10.1371/journal.pgen.1005390>
- 20 Moretti, J., Roy, S., Bozec, D., Martinez, J., Chapman, J.R., Ueberheide, B. et al. (2017) STING senses microbial viability to orchestrate stress-mediated autophagy of the endoplasmic reticulum. *Cell* **171**, 809–823 <https://doi.org/10.1016/j.cell.2017.09.034>
- 21 Bernales, S., McDonald, K.L. and Walter, P. (2006) Autophagy counterbalances endoplasmic reticulum expansion during the unfolded protein response. *PLoS Biol.* **4**, e423 <https://doi.org/10.1371/journal.pbio.0040423>
- 22 Popelka, H. and Klionsky, D.J. (2015) Analysis of the native conformation of the LIR/AM motif in the Atg9/LC3/GABARAP-binding proteins. *Autophagy* **11**, 2153–2159 <https://doi.org/10.1080/15548627.2015.1111503>
- 23 Birgisdotir, A.B., Lamark, T. and Johansen, T. (2013) The LIR motif — crucial for selective autophagy. *J. Cell Sci.* **126**(Pt 15), 3237–3247
- 24 Hamasaki, M., Noda, T., Baba, M. and Osumi, Y. (2005) Starvation triggers the delivery of the endoplasmic reticulum to the vacuole via autophagy in yeast. *Traffic* **6**, 56–65 <https://doi.org/10.1111/j.1600-0854.2004.00245.x>
- 25 Klionsky, D.J., Abdelmohsen, K., Abe, A., Abedin, M.J., Abeliovich, H., Acevedo Arozena, A. et al. (2016) Guidelines for the use and interpretation of assays for monitoring autophagy (3rd edition). *Autophagy* **12**, 1–222 <https://doi.org/10.1080/15548627.2015.1100356>
- 26 Mochida, K., Oikawa, Y., Kimura, Y., Kirisako, H., Hirano, H., Osumi, Y. et al. (2015) Receptor-mediated selective autophagy degrades the endoplasmic reticulum and the nucleus. *Nature* **522**, 359–362 <https://doi.org/10.1038/nature14506>
- 27 Okamoto, K. (2014) Organellephagy: eliminating cellular building blocks via selective autophagy. *J. Cell Biol.* **205**, 435–445 <https://doi.org/10.1083/jcb.201402054>
- 28 Kurth, L., Pamming, T., Hennings, J.C., Soehendra, D., Huebner, A.K., Rothier, A. et al. (2009) Mutations in FAM134B, encoding a newly identified Golgi protein, cause severe sensory and autonomic neuropathy. *Nat. Genet.* **41**, 1179–1181 <https://doi.org/10.1038/ng.464>
- 29 Islam, F., Gopalan, V. and Lam, A.K. (2018) *RETREG1 (FAM134B)*: a new player in human diseases: 15 years after the discovery in cancer. *J. Cell. Physiol.* **233**, 4479–4489 <https://doi.org/10.1002/jcp.26384>
- 30 Meyer, H.A., Grau, H., Kraft, R., Kostka, S., Prehn, S., Kalies, K.U. et al. (2000) Mammalian Sec61 is associated with Sec62 and Sec63. *J. Biol. Chem.* **275**, 14550–14557 <https://doi.org/10.1074/jbc.275.19.14550>
- 31 Conti, B.J., Devaraneni, P.K., Yang, Z., David, L.L. and Skach, W.R. (2015) Cotranslational stabilization of Sec62/63 within the ER Sec61 translocon is controlled by distinct substrate-driven translocation events. *Mol. Cell* **58**, 269–283 <https://doi.org/10.1016/j.molcel.2015.02.018>
- 32 Lang, S., Benedix, J., Fedeles, S.V., Schorr, S., Schirra, C., Schauble, N. et al. (2012) Different effects of Sec61 α , Sec62 and Sec63 depletion on transport of polypeptides into the endoplasmic reticulum of mammalian cells. *J. Cell Sci.* **125**(Pt 8), 1958–1969 <https://doi.org/10.1242/jcs.096727>
- 33 Greiner, M., Kreutzer, B., Jung, V., Grobholz, R., Hasenfuß, A., Stohr, R.F. et al. (2011) Silencing of the SEC62 gene inhibits migratory and invasive potential of various tumor cells. *Int. J. Cancer* **128**, 2284–2295 <https://doi.org/10.1002/ijc.25580>
- 34 Hagerstrand, D., Tong, A., Schumacher, S.E., Ilic, N., Shen, R.R., Cheung, H.W. et al. (2013) Systematic interrogation of 3q26 identifies TLOC1 and SKL1 as cancer drivers. *Cancer Discov.* **3**, 1044–1057 <https://doi.org/10.1158/2159-8290.CD-12-0592>
- 35 Linxweiler, M., Linxweiler, J., Barth, M., Benedix, J., Jung, V., Kim, Y.J. et al. (2012) Sec62 bridges the gap from 3q amplification to molecular cell biology in non-small cell lung cancer. *Am. J. Pathol.* **180**, 473–483 <https://doi.org/10.1016/j.ajpath.2011.10.039>
- 36 Weng, L., Du, J., Zhou, Q., Cheng, B., Li, J., Zhang, D. et al. (2012) Identification of cyclin B1 and Sec62 as biomarkers for recurrence in patients with HBV-related hepatocellular carcinoma after surgical resection. *Mol. Cancer* **11**, 39 <https://doi.org/10.1186/1476-4598-11-39>
- 37 Bergmann, T.J., Fumagalli, F., Loi, M. and Molinari, M. (2017) Role of SEC62 in ER maintenance: a link with ER stress tolerance in SEC62-overexpressing tumors? *Mol. Cell. Oncol.* **4**, e1264351 <https://doi.org/10.1080/23723556.2016.1264351>
- 38 Yang, Y.S. and Strittmatter, S.M. (2007) The reticulons: a family of proteins with diverse functions. *Genome Biol.* **8**, 234 <https://doi.org/10.1186/gb-2007-8-12-234>
- 39 Glick, D., Zhang, W., Beaton, M., Marsboom, G., Gruber, M., Simon, M.C. et al. (2012) Bnip3 regulates mitochondrial function and lipid metabolism in the liver. *Mol. Cell. Biol.* **32**, 2570–2584 <https://doi.org/10.1128/MCB.00167-12>
- 40 Yang, H., Ni, H.M., Guo, F., Ding, Y., Shi, Y.H., Lahiri, P. et al. (2016) Sequestosome 1/p62 protein is associated with autophagic removal of excess hepatic endoplasmic reticulum in mice. *J. Biol. Chem.* **291**, 18663–18674 <https://doi.org/10.1074/jbc.M116.739821>
- 41 Hanna, R.A., Quinsay, M.N., Orogo, A.M., Giang, K., Rikka, S. and Gustafsson, A.B. (2012) Microtubule-associated protein 1 light chain 3 (LC3) interacts with Bnip3 protein to selectively remove endoplasmic reticulum and mitochondria via autophagy. *J. Biol. Chem.* **287**, 19094–19104 <https://doi.org/10.1074/jbc.M111.322933>
- 42 Walter, P. and Ron, D. (2011) The unfolded protein response: from stress pathway to homeostatic regulation. *Science* **334**, 1081–1086 <https://doi.org/10.1126/science.1209038>

- 43 Preston, G.M. and Brodsky, J.L. (2017) The evolving role of ubiquitin modification in endoplasmic reticulum-associated degradation. *Biochem. J.* **474**, 445–469 <https://doi.org/10.1042/BCJ20160582>
- 44 Hughes, D. and Mallucci, G.R. (2018) The unfolded protein response in neurodegenerative disorders — therapeutic modulation of the PERK pathway. *FEBS J.* <https://doi.org/10.1111/febs.14422>
- 45 Hetz, C., Chevet, E. and Harding, H.P. (2013) Targeting the unfolded protein response in disease. *Nat. Rev. Drug Discov.* **12**, 703–719 <https://doi.org/10.1038/nrd3976>
- 46 Obacz, J., Avril, T., Le Reste, P.J., Urta, H., Quillien, V., Hetz, C. et al. (2017) Endoplasmic reticulum proteostasis in glioblastoma—from molecular mechanisms to therapeutic perspectives. *Sci. Signal.* **10**, eaal2323 <https://doi.org/10.1126/scisignal.aal2323>
- 47 Myeku, N. and Duff, K.E. (2018) Targeting the 26S proteasome to protect against proteotoxic diseases. *Trends Mol. Med.* **24**, 18–29 <https://doi.org/10.1016/j.molmed.2017.11.006>

9 REFERENCES

- 1 Schwarz, D. S. & Blower, M. D. The endoplasmic reticulum: structure, function and response to cellular signaling. *Cell Mol Life Sci* **73**, 79-94, doi:10.1007/s00018-015-2052-6 (2016).
- 2 Palade, G. E. The endoplasmic reticulum. *J Biophys Biochem Cytol* **2**, 85-98, doi:10.1083/jcb.2.4.85 (1956).
- 3 Shemesh, T. *et al.* A model for the generation and interconversion of ER morphologies. *Proc Natl Acad Sci U S A* **111**, E5243-5251, doi:10.1073/pnas.1419997111 (2014).
- 4 Palade, G. E. & Siekevitz, P. Liver microsomes; an integrated morphological and biochemical study. *J Biophys Biochem Cytol* **2**, 171-200, doi:10.1083/jcb.2.2.171 (1956).
- 5 Dallner, G., Orrenius, S. & Bergstrand, A. Isolation and properties of rough and smooth vesicles from rat liver. *J Cell Biol* **16**, 426-430, doi:10.1083/jcb.16.2.426 (1963).
- 6 Lynes, E. M. & Simmen, T. Urban planning of the endoplasmic reticulum (ER): how diverse mechanisms segregate the many functions of the ER. *Biochim Biophys Acta* **1813**, 1893-1905, doi:10.1016/j.bbamcr.2011.06.011 (2011).
- 7 Sitia, R. & Meldolesi, J. Endoplasmic reticulum: a dynamic patchwork of specialized subregions. *Mol Biol Cell* **3**, 1067-1072, doi:10.1091/mbc.3.10.1067 (1992).
- 8 Wu, H., Carvalho, P. & Voeltz, G. K. Here, there, and everywhere: The importance of ER membrane contact sites. *Science* **361**, doi:10.1126/science.aan5835 (2018).
- 9 Levine, T. & Rabouille, C. Endoplasmic reticulum: one continuous network compartmentalized by extrinsic cues. *Curr Opin Cell Biol* **17**, 362-368, doi:10.1016/j.ceb.2005.06.005 (2005).
- 10 Costantini, L. & Snapp, E. Probing endoplasmic reticulum dynamics using fluorescence imaging and photobleaching techniques. *Curr Protoc Cell Biol* **60**, Unit 21 27, doi:10.1002/0471143030.cb2107s60 (2013).
- 11 Shibata, Y., Voeltz, G. K. & Rapoport, T. A. Rough sheets and smooth tubules. *Cell* **126**, 435-439, doi:10.1016/j.cell.2006.07.019 (2006).
- 12 English, A. R. & Voeltz, G. K. Endoplasmic reticulum structure and interconnections with other organelles. *Cold Spring Harb Perspect Biol* **5**, a013227, doi:10.1101/cshperspect.a013227 (2013).
- 13 Fagone, P. & Jackowski, S. Membrane phospholipid synthesis and endoplasmic reticulum function. *J Lipid Res* **50 Suppl**, S311-316, doi:10.1194/jlr.R800049-JLR200 (2009).
- 14 Galteau, M. M., Antoine, B. & Reggio, H. Epoxide hydrolase is a marker for the smooth endoplasmic reticulum in rat liver. *EMBO J* **4**, 2793-2800 (1985).
- 15 Orrenius, S. On the Mechanism of Drug Hydroxylation in Rat Liver Microsomes. *J Cell Biol* **26**, 713-723, doi:10.1083/jcb.26.3.713 (1965).
- 16 Palade, G. Intracellular aspects of the process of protein synthesis. *Science* **189**, 347-358, doi:10.1126/science.1096303 (1975).
- 17 Ghaemmaghami, S. *et al.* Global analysis of protein expression in yeast. *Nature* **425**, 737-741, doi:10.1038/nature02046 (2003).
- 18 Chen, Y. *et al.* SPD--a web-based secreted protein database. *Nucleic Acids Res* **33**, D169-173, doi:10.1093/nar/gki093 (2005).
- 19 Uhlen, M. *et al.* Proteomics. Tissue-based map of the human proteome. *Science* **347**, 1260419, doi:10.1126/science.1260419 (2015).

- 20 Aviram, N. & Schuldiner, M. Targeting and translocation of proteins to the endoplasmic reticulum at a glance. *J Cell Sci* **130**, 4079-4085, doi:10.1242/jcs.204396 (2017).
- 21 Fewell, S. W. & Brodsky, J. L. in *Trafficking Inside Cells* Ch. Chapter 7, 119-142 (2009).
- 22 von Heijne, G. Patterns of amino acids near signal-sequence cleavage sites. *Eur J Biochem* **133**, 17-21, doi:10.1111/j.1432-1033.1983.tb07424.x (1983).
- 23 von Heijne, G. Analysis of the distribution of charged residues in the N-terminal region of signal sequences: implications for protein export in prokaryotic and eukaryotic cells. *EMBO J* **3**, 2315-2318 (1984).
- 24 von Heijne, G. How signal sequences maintain cleavage specificity. *J Mol Biol* **173**, 243-251, doi:10.1016/0022-2836(84)90192-x (1984).
- 25 von Heijne, G. Signal sequences. The limits of variation. *J Mol Biol* **184**, 99-105, doi:10.1016/0022-2836(85)90046-4 (1985).
- 26 von Heijne, G. A new method for predicting signal sequence cleavage sites. *Nucleic Acids Res* **14**, 4683-4690, doi:10.1093/nar/14.11.4683 (1986).
- 27 Duffy, J., Patham, B. & Mensa-Wilmot, K. Discovery of functional motifs in h-regions of trypanosome signal sequences. *Biochem J* **426**, 135-145, doi:10.1042/BJ20091277 (2010).
- 28 Zimmermann, R., Eyrisch, S., Ahmad, M. & Helms, V. Protein translocation across the ER membrane. *Biochim Biophys Acta* **1808**, 912-924, doi:10.1016/j.bbamem.2010.06.015 (2011).
- 29 Lingappa, V. R., Lingappa, J. R. & Blobel, G. Signal sequences for early events in protein secretion and membrane assembly. *Ann N Y Acad Sci* **343**, 356-361, doi:10.1111/j.1749-6632.1980.tb47264.x (1980).
- 30 Walter, P. & Blobel, G. Purification of a membrane-associated protein complex required for protein translocation across the endoplasmic reticulum. *Proc Natl Acad Sci U S A* **77**, 7112-7116, doi:10.1073/pnas.77.12.7112 (1980).
- 31 Walter, P. & Blobel, G. Disassembly and reconstitution of signal recognition particle. *Cell* **34**, 525-533, doi:10.1016/0092-8674(83)90385-9 (1983).
- 32 Walter, P. & Blobel, G. Signal recognition particle: a ribonucleoprotein required for cotranslational translocation of proteins, isolation and properties. *Methods Enzymol* **96**, 682-691, doi:10.1016/s0076-6879(83)96057-3 (1983).
- 33 Egea, P. F. *et al.* Substrate twinning activates the signal recognition particle and its receptor. *Nature* **427**, 215-221, doi:10.1038/nature02250 (2004).
- 34 Rapoport, T. A., Li, L. & Park, E. Structural and Mechanistic Insights into Protein Translocation. *Annu Rev Cell Dev Biol* **33**, 369-390, doi:10.1146/annurev-cellbio-100616-060439 (2017).
- 35 Chirico, W. J., Waters, M. G. & Blobel, G. 70K heat shock related proteins stimulate protein translocation into microsomes. *Nature* **332**, 805-810, doi:10.1038/332805a0 (1988).
- 36 Ngosuwan, J., Wang, N. M., Fung, K. L. & Chirico, W. J. Roles of cytosolic Hsp70 and Hsp40 molecular chaperones in post-translational translocation of presecretory proteins into the endoplasmic reticulum. *J Biol Chem* **278**, 7034-7042, doi:10.1074/jbc.M210544200 (2003).
- 37 Crowley, K. S., Liao, S., Worrell, V. E., Reinhart, G. D. & Johnson, A. E. Secretory proteins move through the endoplasmic reticulum membrane via an aqueous, gated pore. *Cell* **78**, 461-471, doi:10.1016/0092-8674(94)90424-3 (1994).
- 38 Van den Berg, B. *et al.* X-ray structure of a protein-conducting channel. *Nature* **427**, 36-44, doi:10.1038/nature02218 (2004).

- 39 Nguyen, T. H., Law, D. T. & Williams, D. B. Binding protein BiP is required for translocation of secretory proteins into the endoplasmic reticulum in *Saccharomyces cerevisiae*. *Proc Natl Acad Sci U S A* **88**, 1565-1569, doi:10.1073/pnas.88.4.1565 (1991).
- 40 Fons, R. D., Bogert, B. A. & Hegde, R. S. Substrate-specific function of the translocon-associated protein complex during translocation across the ER membrane. *J Cell Biol* **160**, 529-539, doi:10.1083/jcb.200210095 (2003).
- 41 Sommer, N., Junne, T., Kalies, K. U., Spiess, M. & Hartmann, E. TRAP assists membrane protein topogenesis at the mammalian ER membrane. *Biochim Biophys Acta* **1833**, 3104-3111, doi:10.1016/j.bbamcr.2013.08.018 (2013).
- 42 Sanders, S. L., Whitfield, K. M., Vogel, J. P., Rose, M. D. & Schekman, R. W. Sec61p and BiP directly facilitate polypeptide translocation into the ER. *Cell* **69**, 353-365, doi:10.1016/0092-8674(92)90415-9 (1992).
- 43 Brodsky, J. L. & Schekman, R. A Sec63p-BiP complex from yeast is required for protein translocation in a reconstituted proteoliposome. *J Cell Biol* **123**, 1355-1363, doi:10.1083/jcb.123.6.1355 (1993).
- 44 Weitzmann, A., Baldes, C., Dudek, J. & Zimmermann, R. The heat shock protein 70 molecular chaperone network in the pancreatic endoplasmic reticulum - a quantitative approach. *FEBS J* **274**, 5175-5187, doi:10.1111/j.1742-4658.2007.06039.x (2007).
- 45 Behnke, J., Feige, M. J. & Hendershot, L. M. BiP and its nucleotide exchange factors Grp170 and Sill: mechanisms of action and biological functions. *J Mol Biol* **427**, 1589-1608, doi:10.1016/j.jmb.2015.02.011 (2015).
- 46 Meyer, H. A. *et al.* Mammalian Sec61 is associated with Sec62 and Sec63. *J Biol Chem* **275**, 14550-14557, doi:10.1074/jbc.275.19.14550 (2000).
- 47 Voss, M., Schroder, B. & Fluhrer, R. Mechanism, specificity, and physiology of signal peptide peptidase (SPP) and SPP-like proteases. *Biochim Biophys Acta* **1828**, 2828-2839, doi:10.1016/j.bbamem.2013.03.033 (2013).
- 48 Mohorko, E., Glockshuber, R. & Aebi, M. Oligosaccharyltransferase: the central enzyme of N-linked protein glycosylation. *J Inherit Metab Dis* **34**, 869-878, doi:10.1007/s10545-011-9337-1 (2011).
- 49 Cali, T., Vanoni, O. & Molinari, M. The endoplasmic reticulum crossroads for newly synthesized polypeptide chains. *Prog Mol Biol Transl Sci* **83**, 135-179, doi:10.1016/S0079-6603(08)00604-1 (2008).
- 50 Aebi, M. N-linked protein glycosylation in the ER. *Biochim Biophys Acta* **1833**, 2430-2437, doi:10.1016/j.bbamcr.2013.04.001 (2013).
- 51 Aebi, M., Bernasconi, R., Clerc, S. & Molinari, M. N-glycan structures: recognition and processing in the ER. *Trends Biochem Sci* **35**, 74-82, doi:10.1016/j.tibs.2009.10.001 (2010).
- 52 Kelleher, D. J. & Gilmore, R. An evolving view of the eukaryotic oligosaccharyltransferase. *Glycobiology* **16**, 47R-62R, doi:10.1093/glycob/cwj066 (2006).
- 53 Ramírez, A. S., Kowal, J. & Locher, K. P. Cryo-electron microscopy structures of human oligosaccharyltransferase complexes OST-A and OST-B. *Science* **366**, 1372-1375, doi:10.1126/science.aaz3505 (2019).
- 54 Kelleher, D. J., Karaoglu, D., Mandon, E. C. & Gilmore, R. Oligosaccharyltransferase isoforms that contain different catalytic STT3 subunits have distinct enzymatic properties. *Mol Cell* **12**, 101-111, doi:10.1016/s1097-2765(03)00243-0 (2003).

- 55 Schwarz, F. & Aebi, M. Mechanisms and principles of N-linked protein glycosylation. *Curr Opin Struct Biol* **21**, 576-582, doi:10.1016/j.sbi.2011.08.005 (2011).
- 56 Helenius, A. & Aebi, M. Intracellular functions of N-linked glycans. *Science* **291**, 2364-2369, doi:10.1126/science.291.5512.2364 (2001).
- 57 Bieberich, E. Synthesis, Processing, and Function of N-glycans in N-glycoproteins. *Adv Neurobiol* **9**, 47-70, doi:10.1007/978-1-4939-1154-7_3 (2014).
- 58 Tannous, A., Pisoni, G. B., Hebert, D. N. & Molinari, M. N-linked sugar-regulated protein folding and quality control in the ER. *Semin Cell Dev Biol* **41**, 79-89, doi:10.1016/j.semcdb.2014.12.001 (2015).
- 59 Molinari, M. N-glycan structure dictates extension of protein folding or onset of disposal. *Nat Chem Biol* **3**, 313-320, doi:10.1038/nchembio880 (2007).
- 60 Parodi, A. J. Protein glucosylation and its role in protein folding. *Annu Rev Biochem* **69**, 69-93, doi:10.1146/annurev.biochem.69.1.69 (2000).
- 61 Chang, I. J., He, M. & Lam, C. T. Congenital disorders of glycosylation. *Ann Transl Med* **6**, 477, doi:10.21037/atm.2018.10.45 (2018).
- 62 Shailubhai, K., Pukazhenti, B. S., Saxena, E. S., Varma, G. M. & Vijay, I. K. Glucosidase I, a transmembrane endoplasmic reticular glycoprotein with a luminal catalytic domain. *J Biol Chem* **266**, 16587-16593 (1991).
- 63 Schallus, T., Feher, K., Sternberg, U., Rybin, V. & Muhle-Goll, C. Analysis of the specific interactions between the lectin domain of malectin and diglucosides. *Glycobiology* **20**, 1010-1020, doi:10.1093/glycob/cwq059 (2010).
- 64 Galli, C., Bernasconi, R., Solda, T., Calanca, V. & Molinari, M. Malectin participates in a backup glycoprotein quality control pathway in the mammalian ER. *PLoS One* **6**, e16304, doi:10.1371/journal.pone.0016304 (2011).
- 65 Qin, S. Y. *et al.* Malectin forms a complex with ribophorin I for enhanced association with misfolded glycoproteins. *J Biol Chem* **287**, 38080-38089, doi:10.1074/jbc.M112.394288 (2012).
- 66 Takeda, K., Qin, S. Y., Matsumoto, N. & Yamamoto, K. Association of malectin with ribophorin I is crucial for attenuation of misfolded glycoprotein secretion. *Biochem Biophys Res Commun* **454**, 436-440, doi:10.1016/j.bbrc.2014.10.102 (2014).
- 67 Trombetta, E. S., Simons, J. F. & Helenius, A. Endoplasmic reticulum glucosidase II is composed of a catalytic subunit, conserved from yeast to mammals, and a tightly bound noncatalytic HDEL-containing subunit. *J Biol Chem* **271**, 27509-27516, doi:10.1074/jbc.271.44.27509 (1996).
- 68 Hammond, C., Braakman, I. & Helenius, A. Role of N-linked oligosaccharide recognition, glucose trimming, and calnexin in glycoprotein folding and quality control. *Proc Natl Acad Sci U S A* **91**, 913-917, doi:10.1073/pnas.91.3.913 (1994).
- 69 Peterson, J. R., Ora, A., Van, P. N. & Helenius, A. Transient, lectin-like association of calreticulin with folding intermediates of cellular and viral glycoproteins. *Mol Biol Cell* **6**, 1173-1184, doi:10.1091/mbc.6.9.1173 (1995).
- 70 Leach, M. R. & Williams, D. B. in *Calreticulin Molecular Biology Intelligence Unit* Ch. Chapter 6, 49-62 (2003).
- 71 Wada, I. *et al.* SSR alpha and associated calnexin are major calcium binding proteins of the endoplasmic reticulum membrane. *J Biol Chem* **266**, 19599-19610 (1991).
- 72 Schrag, J. D. *et al.* The Structure of calnexin, an ER chaperone involved in quality control of protein folding. *Mol Cell* **8**, 633-644, doi:10.1016/s1097-2765(01)00318-5 (2001).

- 73 Ellgaard, L. *et al.* NMR structures of 36 and 73-residue fragments of the calreticulin P-domain. *J Mol Biol* **322**, 773-784, doi:10.1016/s0022-2836(02)00812-4 (2002).
- 74 Molinari, M. *et al.* Contrasting functions of calreticulin and calnexin in glycoprotein folding and ER quality control. *Mol Cell* **13**, 125-135, doi:10.1016/s1097-2765(03)00494-5 (2004).
- 75 Frickel, E. M. *et al.* TROSY-NMR reveals interaction between ERp57 and the tip of the calreticulin P-domain. *Proc Natl Acad Sci U S A* **99**, 1954-1959, doi:10.1073/pnas.042699099 (2002).
- 76 Kozlov, G. *et al.* Structural basis of cyclophilin B binding by the calnexin/calreticulin P-domain. *J Biol Chem* **285**, 35551-35557, doi:10.1074/jbc.M110.160101 (2010).
- 77 Schmid, F. X. & Baldwin, R. L. Acid catalysis of the formation of the slow-folding species of RNase A: evidence that the reaction is proline isomerization. *Proc Natl Acad Sci U S A* **75**, 4764-4768, doi:10.1073/pnas.75.10.4764 (1978).
- 78 Wedemeyer, W. J., Welker, E., Narayan, M. & Scheraga, H. A. Disulfide bonds and protein folding. *Biochemistry* **39**, 4207-4216, doi:10.1021/bi992922o (2000).
- 79 Hebert, D. N., Foellmer, B. & Helenius, A. Glucose trimming and reglucosylation determine glycoprotein association with calnexin in the endoplasmic reticulum. *Cell* **81**, 425-433, doi:10.1016/0092-8674(95)90395-x (1995).
- 80 Cannon, K. S. & Helenius, A. Trimming and readdition of glucose to N-linked oligosaccharides determines calnexin association of a substrate glycoprotein in living cells. *J Biol Chem* **274**, 7537-7544, doi:10.1074/jbc.274.11.7537 (1999).
- 81 Chen, B., Retzlaff, M., Roos, T. & Frydman, J. Cellular strategies of protein quality control. *Cold Spring Harb Perspect Biol* **3**, a004374, doi:10.1101/cshperspect.a004374 (2011).
- 82 Diaz-Villanueva, J. F., Diaz-Molina, R. & Garcia-Gonzalez, V. Protein Folding and Mechanisms of Proteostasis. *Int J Mol Sci* **16**, 17193-17230, doi:10.3390/ijms160817193 (2015).
- 83 Anelli, T., Sannino, S. & Sitia, R. Proteostasis and "redoxstasis" in the secretory pathway: Tales of tails from ERp44 and immunoglobulins. *Free Radic Biol Med* **83**, 323-330, doi:10.1016/j.freeradbiomed.2015.02.020 (2015).
- 84 Ellgaard, L., Molinari, M. & Helenius, A. Setting the standards: quality control in the secretory pathway. *Science* **286**, 1882-1888, doi:10.1126/science.286.5446.1882 (1999).
- 85 Balchin, D., Hayer-Hartl, M. & Hartl, F. U. In vivo aspects of protein folding and quality control. *Science* **353**, aac4354, doi:10.1126/science.aac4354 (2016).
- 86 Aguzzi, A. & O'Connor, T. Protein aggregation diseases: pathogenicity and therapeutic perspectives. *Nat Rev Drug Discov* **9**, 237-248, doi:10.1038/nrd3050 (2010).
- 87 Shamsi, T. N., Athar, T., Parveen, R. & Fatima, S. A review on protein misfolding, aggregation and strategies to prevent related ailments. *Int J Biol Macromol* **105**, 993-1000, doi:10.1016/j.ijbiomac.2017.07.116 (2017).
- 88 Sousa, M. & Parodi, A. J. The molecular basis for the recognition of misfolded glycoproteins by the UDP-Glc:glycoprotein glucosyltransferase. *EMBO J* **14**, 4196-4203 (1995).
- 89 Arnold, S. M. & Kaufman, R. J. The noncatalytic portion of human UDP-glucose: glycoprotein glucosyltransferase I confers UDP-glucose binding and transferase function to the catalytic domain. *J Biol Chem* **278**, 43320-43328, doi:10.1074/jbc.M305800200 (2003).

- 90 Caramelo, J. J. & Parodi, A. J. A sweet code for glycoprotein folding. *FEBS Lett* **589**, 3379-3387, doi:10.1016/j.febslet.2015.07.021 (2015).
- 91 Ferris, S. P., Jaber, N. S., Molinari, M., Arvan, P. & Kaufman, R. J. UDP-glucose:glycoprotein glucosyltransferase (UGGT1) promotes substrate solubility in the endoplasmic reticulum. *Mol Biol Cell* **24**, 2597-2608, doi:10.1091/mbc.E13-02-0101 (2013).
- 92 Alberini, C. M., Bet, P., Milstein, C. & Sitia, R. Secretion of immunoglobulin M assembly intermediates in the presence of reducing agents. *Nature* **347**, 485-487, doi:10.1038/347485a0 (1990).
- 93 Reddy, P., Sparvoli, A., Fagioli, C., Fassina, G. & Sitia, R. Formation of reversible disulfide bonds with the protein matrix of the endoplasmic reticulum correlates with the retention of unassembled Ig light chains. *EMBO J* **15**, 2077-2085 (1996).
- 94 Merulla, J., Solda, T. & Molinari, M. A novel UGGT1 and p97-dependent checkpoint for native ectodomains with ionizable intramembrane residue. *Mol Biol Cell* **26**, 1532-1542, doi:10.1091/mbc.E14-12-1615 (2015).
- 95 Kurokawa, K. & Nakano, A. The ER exit sites are specialized ER zones for the transport of cargo proteins from the ER to the Golgi apparatus. *J Biochem* **165**, 109-114, doi:10.1093/jb/mvy080 (2019).
- 96 Lord, C., Ferro-Novick, S. & Miller, E. A. The highly conserved COPII coat complex sorts cargo from the endoplasmic reticulum and targets it to the golgi. *Cold Spring Harb Perspect Biol* **5**, doi:10.1101/cshperspect.a013367 (2013).
- 97 Jensen, D. & Schekman, R. COPII-mediated vesicle formation at a glance. *J Cell Sci* **124**, 1-4, doi:10.1242/jcs.069773 (2011).
- 98 Bannykh, S. I., Rowe, T. & Balch, W. E. The organization of endoplasmic reticulum export complexes. *J Cell Biol* **135**, 19-35, doi:10.1083/jcb.135.1.19 (1996).
- 99 Stephens, D. J. & Pepperkok, R. Illuminating the secretory pathway: when do we need vesicles? *J Cell Sci* **114**, 1053-1059 (2001).
- 100 Geva, Y. & Schuldiner, M. The back and forth of cargo exit from the endoplasmic reticulum. *Curr Biol* **24**, R130-136, doi:10.1016/j.cub.2013.12.008 (2014).
- 101 Gonzalez, D. S., Karaveg, K., Vandersall-Nairn, A. S., Lal, A. & Moremen, K. W. Identification, expression, and characterization of a cDNA encoding human endoplasmic reticulum mannosidase I, the enzyme that catalyzes the first mannose trimming step in mammalian Asn-linked oligosaccharide biosynthesis. *J Biol Chem* **274**, 21375-21386, doi:10.1074/jbc.274.30.21375 (1999).
- 102 Kamiya, Y. *et al.* Molecular basis of sugar recognition by the human L-type lectins ERGIC-53, VIPL, and VIP36. *J Biol Chem* **283**, 1857-1861, doi:10.1074/jbc.M709384200 (2008).
- 103 Klumperman, J. Transport between ER and Golgi. *Curr Opin Cell Biol* **12**, 445-449, doi:10.1016/s0955-0674(00)00115-0 (2000).
- 104 Thor, F., Gautschi, M., Geiger, R. & Helenius, A. Bulk flow revisited: transport of a soluble protein in the secretory pathway. *Traffic* **10**, 1819-1830, doi:10.1111/j.1600-0854.2009.00989.x (2009).
- 105 Schubert, U. *et al.* Rapid degradation of a large fraction of newly synthesized proteins by proteasomes. *Nature* **404**, 770-774, doi:10.1038/35008096 (2000).
- 106 Kim, I., Xu, W. & Reed, J. C. Cell death and endoplasmic reticulum stress: disease relevance and therapeutic opportunities. *Nature Reviews Drug Discovery* **7**, 1013-1030, doi:10.1038/nrd2755 (2008).
- 107 Römisch, K. ENDOPLASMIC RETICULUM-ASSOCIATED DEGRADATION. *Annual Review of Cell and Developmental Biology* **21**, 435-456, doi:10.1146/annurev.cellbio.21.012704.133250 (2005).

- 108 Erbaykent Tepedelen, B. & Ballar Kirmizibayrak, P. in *Endoplasmic Reticulum* Ch. Chapter 3, (2019).
- 109 Olivari, S. *et al.* EDEM1 regulates ER-associated degradation by accelerating de-mannosylation of folding-defective polypeptides and by inhibiting their covalent aggregation. *Biochem Biophys Res Commun* **349**, 1278-1284, doi:10.1016/j.bbrc.2006.08.186 (2006).
- 110 Hosokawa, N. *et al.* EDEM1 accelerates the trimming of alpha1,2-linked mannose on the C branch of N-glycans. *Glycobiology* **20**, 567-575, doi:10.1093/glycob/cwq001 (2010).
- 111 Molinari, M., Calanca, V., Galli, C., Lucca, P. & Paganetti, P. Role of EDEM in the release of misfolded glycoproteins from the calnexin cycle. *Science* **299**, 1397-1400, doi:10.1126/science.1079474 (2003).
- 112 Mast, S. W. *et al.* Human EDEM2, a novel homolog of family 47 glycosidases, is involved in ER-associated degradation of glycoproteins. *Glycobiology* **15**, 421-436, doi:10.1093/glycob/cwi014 (2005).
- 113 Ninagawa, S. *et al.* EDEM2 initiates mammalian glycoprotein ERAD by catalyzing the first mannose trimming step. *J Cell Biol* **206**, 347-356, doi:10.1083/jcb.201404075 (2014).
- 114 Olivari, S., Galli, C., Alanen, H., Ruddock, L. & Molinari, M. A novel stress-induced EDEM variant regulating endoplasmic reticulum-associated glycoprotein degradation. *J Biol Chem* **280**, 2424-2428, doi:10.1074/jbc.C400534200 (2005).
- 115 Hirao, K. *et al.* EDEM3, a soluble EDEM homolog, enhances glycoprotein endoplasmic reticulum-associated degradation and mannose trimming. *J Biol Chem* **281**, 9650-9658, doi:10.1074/jbc.M512191200 (2006).
- 116 Christianson, J. C., Shaler, T. A., Tyler, R. E. & Kopito, R. R. OS-9 and GRP94 deliver mutant alpha1-antitrypsin to the Hrd1-SEL1L ubiquitin ligase complex for ERAD. *Nat Cell Biol* **10**, 272-282, doi:10.1038/ncb1689 (2008).
- 117 Groisman, B., Shenkman, M., Ron, E. & Lederkremer, G. Z. Mannose Trimming Is Required for Delivery of a Glycoprotein from EDEM1 to XTP3-B and to Late Endoplasmic Reticulum-associated Degradation Steps. *Journal of Biological Chemistry* **286**, 1292-1300, doi:10.1074/jbc.M110.154849 (2011).
- 118 Quan, E. M. *et al.* Defining the Glycan Destruction Signal for Endoplasmic Reticulum-Associated Degradation. *Molecular Cell* **32**, 870-877, doi:10.1016/j.molcel.2008.11.017 (2008).
- 119 Hebert, D. N., Bernasconi, R. & Molinari, M. ERAD substrates: Which way out? *Seminars in Cell & Developmental Biology* **21**, 526-532, doi:10.1016/j.semcdb.2009.12.007 (2010).
- 120 Hosokawa, N., Kamiya, Y., Kamiya, D., Kato, K. & Nagata, K. Human OS-9, a Lectin Required for Glycoprotein Endoplasmic Reticulum-associated Degradation, Recognizes Mannose-trimmed N-Glycans. *Journal of Biological Chemistry* **284**, 17061-17068, doi:10.1074/jbc.M809725200 (2009).
- 121 Bernasconi, R., Galli, C., Calanca, V., Nakajima, T. & Molinari, M. Stringent requirement for HRD1, SEL1L, and OS-9/XTP3-B for disposal of ERAD-LS substrates. *The Journal of Cell Biology* **188**, 223-235, doi:10.1083/jcb.200910042 (2010).
- 122 Hosokawa, N. *et al.* Human XTP3-B Forms an Endoplasmic Reticulum Quality Control Scaffold with the HRD1-SEL1L Ubiquitin Ligase Complex and BiP. *Journal of Biological Chemistry* **283**, 20914-20924, doi:10.1074/jbc.M709336200 (2008).

- 123 Hebert, D. N. & Molinari, M. In and Out of the ER: Protein Folding, Quality Control, Degradation, and Related Human Diseases. *Physiological Reviews* **87**, 1377-1408, doi:10.1152/physrev.00050.2006 (2007).
- 124 Paganetti, P., Pieren, M., Piccaluga, V., Galli, C. & Molinari, M. Sequential assistance of molecular chaperones and transient formation of covalent complexes during protein degradation from the ER. *Journal of Cell Biology* **158**, 247-257, doi:10.1083/jcb.200204122 (2002).
- 125 Shi, J. *et al.* A technique for delineating the unfolding requirements for substrate entry into retrotranslocons during endoplasmic reticulum-associated degradation. *Journal of Biological Chemistry* **294**, 20084-20096, doi:10.1074/jbc.RA119.010019 (2019).
- 126 Ushioda, R. *et al.* ERdj5 Is Required as a Disulfide Reductase for Degradation of Misfolded Proteins in the ER. *Science* **321**, 569-572, doi:10.1126/science.1159293 (2008).
- 127 Rutherford, S. *et al.* Cyclosporine A-Sensitive, Cyclophilin B-Dependent Endoplasmic Reticulum-Associated Degradation. *PLoS ONE* **5**, doi:10.1371/journal.pone.0013008 (2010).
- 128 Tirosch, B., Furman, M. H., Tortorella, D. & Ploegh, H. L. Protein Unfolding Is Not a Prerequisite for Endoplasmic Reticulum-to-Cytosol Dislocation. *Journal of Biological Chemistry* **278**, 6664-6672, doi:10.1074/jbc.M210158200 (2003).
- 129 Schekman, R. & Scott, D. C. Role of Sec61p in the ER-associated degradation of short-lived transmembrane proteins. *Journal of Cell Biology* **181**, 1095-1105, doi:10.1083/jcb.200804053 (2008).
- 130 Loureiro, J. *et al.* Signal peptide peptidase is required for dislocation from the endoplasmic reticulum. *Nature* **441**, 894-897, doi:10.1038/nature04830 (2006).
- 131 Lilley, B. N. & Ploegh, H. L. A membrane protein required for dislocation of misfolded proteins from the ER. *Nature* **429**, 834-840, doi:10.1038/nature02592 (2004).
- 132 Ye, Y., Shibata, Y., Yun, C., Ron, D. & Rapoport, T. A. A membrane protein complex mediates retro-translocation from the ER lumen into the cytosol. *Nature* **429**, 841-847, doi:10.1038/nature02656 (2004).
- 133 Carvalho, P., Stanley, A. M. & Rapoport, T. A. Retrotranslocation of a Misfolded Luminal ER Protein by the Ubiquitin-Ligase Hrd1p. *Cell* **143**, 579-591, doi:10.1016/j.cell.2010.10.028 (2010).
- 134 Schoebel, S. *et al.* Cryo-EM structure of the protein-conducting ERAD channel Hrd1 in complex with Hrd3. *Nature* **548**, 352-355, doi:10.1038/nature23314 (2017).
- 135 Wu, T. *et al.* HRD1, an Important Player in Pancreatic beta-Cell Failure and Therapeutic Target for Type 2 Diabetic Mice. *Diabetes* **69**, 940-953, doi:10.2337/db19-1060 (2020).
- 136 Christianson, J. C. & Ye, Y. Cleaning up in the endoplasmic reticulum: ubiquitin in charge. *Nat Struct Mol Biol* **21**, 325-335, doi:10.1038/nsmb.2793 (2014).
- 137 Komander, D. & Rape, M. The Ubiquitin Code. *Annual Review of Biochemistry* **81**, 203-229, doi:10.1146/annurev-biochem-060310-170328 (2012).
- 138 Neutzner, A. *et al.* A Systematic Search for Endoplasmic Reticulum (ER) Membrane-associated RING Finger Proteins Identifies Nixin/ZNRF4 as a Regulator of Calnexin Stability and ER Homeostasis. *Journal of Biological Chemistry* **286**, 8633-8643, doi:10.1074/jbc.M110.197459 (2011).

- 139 Wu, X. & Rapoport, T. A. Mechanistic insights into ER-associated protein degradation. *Current Opinion in Cell Biology* **53**, 22-28, doi:10.1016/j.ceb.2018.04.004 (2018).
- 140 Joshi, V., Upadhyay, A., Kumar, A. & Mishra, A. Gp78 E3 Ubiquitin Ligase: Essential Functions and Contributions in Proteostasis. *Frontiers in Cellular Neuroscience* **11**, doi:10.3389/fncel.2017.00259 (2017).
- 141 Sun, S. *et al.* Sel1L is indispensable for mammalian endoplasmic reticulum-associated degradation, endoplasmic reticulum homeostasis, and survival. *Proceedings of the National Academy of Sciences* **111**, E582-E591, doi:10.1073/pnas.1318114111 (2014).
- 142 Iida, Y. *et al.* SEL1L Protein Critically Determines the Stability of the HRD1-SEL1L Endoplasmic Reticulum-associated Degradation (ERAD) Complex to Optimize the Degradation Kinetics of ERAD Substrates. *Journal of Biological Chemistry* **286**, 16929-16939, doi:10.1074/jbc.M110.215871 (2011).
- 143 Mueller, B., Klemm, E. J., Spooner, E., Claessen, J. H. & Ploegh, H. L. SEL1L nucleates a protein complex required for dislocation of misfolded glycoproteins. *Proceedings of the National Academy of Sciences* **105**, 12325-12330, doi:10.1073/pnas.0805371105 (2008).
- 144 Cormier, J. H., Tamura, T., Sunryd, J. C. & Hebert, D. N. EDEM1 Recognition and Delivery of Misfolded Proteins to the SEL1L-Containing ERAD Complex. *Molecular Cell* **34**, 627-633, doi:10.1016/j.molcel.2009.05.018 (2009).
- 145 Leitman, J. *et al.* Herp coordinates compartmentalization and recruitment of HRD1 and misfolded proteins for ERAD. *Molecular Biology of the Cell* **25**, 1050-1060, doi:10.1091/mbc.e13-06-0350 (2014).
- 146 Schulze, A. *et al.* The Ubiquitin-domain Protein HERP forms a Complex with Components of the Endoplasmic Reticulum Associated Degradation Pathway. *Journal of Molecular Biology* **354**, 1021-1027, doi:10.1016/j.jmb.2005.10.020 (2005).
- 147 Huang, C.-H., Chu, Y.-R., Ye, Y. & Chen, X. Role of HERP and a HERP-related Protein in HRD1-dependent Protein Degradation at the Endoplasmic Reticulum. *Journal of Biological Chemistry* **289**, 4444-4454, doi:10.1074/jbc.M113.519561 (2014).
- 148 Ye, Y., Meyer, H. H. & Rapoport, T. A. The AAA ATPase Cdc48/p97 and its partners transport proteins from the ER into the cytosol. *Nature* **414**, 652-656, doi:10.1038/414652a (2001).
- 149 Stein, A., Ruggiano, A., Carvalho, P. & Rapoport, Tom A. Key Steps in ERAD of Luminal ER Proteins Reconstituted with Purified Components. *Cell* **158**, 1375-1388, doi:10.1016/j.cell.2014.07.050 (2014).
- 150 Schubert, C. & Buchberger, A. UBX domain proteins: major regulators of the AAA ATPase Cdc48/p97. *Cellular and Molecular Life Sciences* **65**, 2360-2371, doi:10.1007/s00018-008-8072-8 (2008).
- 151 Matyskiela, M. E. & Martin, A. Design Principles of a Universal Protein Degradation Machine. *Journal of Molecular Biology* **425**, 199-213, doi:10.1016/j.jmb.2012.11.001 (2013).
- 152 De Leonibus, C., Cinque, L. & Settembre, C. Emerging lysosomal pathways for quality control at the endoplasmic reticulum. *FEBS Letters* **593**, 2319-2329, doi:10.1002/1873-3468.13571 (2019).
- 153 Fregno, I. & Molinari, M. Proteasomal and lysosomal clearance of faulty secretory proteins: ER-associated degradation (ERAD) and ER-to-lysosome-associated

- degradation (ERLAD) pathways. *Crit Rev Biochem Mol Biol* **54**, 153-163, doi:10.1080/10409238.2019.1610351 (2019).
- 154 Noda, T. & Farquhar, M. G. A non-autophagic pathway for diversion of ER secretory proteins to lysosomes. *The Journal of Cell Biology* **119**, 85-97, doi:10.1083/jcb.119.1.85 (1992).
- 155 Teckman, J. H. & Perlmutter, D. H. Retention of mutant α 1-antitrypsin Z in endoplasmic reticulum is associated with an autophagic response. *American Journal of Physiology-Gastrointestinal and Liver Physiology* **279**, G961-G974, doi:10.1152/ajpgi.2000.279.5.G961 (2000).
- 156 Kamimoto, T. Intracellular Inclusions Containing Mutant 1-Antitrypsin Z Are Propagated in the Absence of Autophagic Activity. *Journal of Biological Chemistry* **281**, 4467-4476, doi:10.1074/jbc.M509409200 (2006).
- 157 Kroeger, H. *et al.* Endoplasmic Reticulum-associated Degradation (ERAD) and Autophagy Cooperate to Degrade Polymerogenic Mutant Serpins. *Journal of Biological Chemistry* **284**, 22793-22802, doi:10.1074/jbc.M109.027102 (2009).
- 158 Fregno, I. *et al.* ER-to-lysosome-associated degradation of proteasome-resistant ATZ polymers occurs via receptor-mediated vesicular transport. *EMBO J* **37**, doi:10.15252/embj.201899259 (2018).
- 159 Fujita, E. *et al.* Two endoplasmic reticulum-associated degradation (ERAD) systems for the novel variant of the mutant dysferlin: ubiquitin/proteasome ERAD(I) and autophagy/lysosome ERAD(II). *Human Molecular Genetics* **16**, 618-629, doi:10.1093/hmg/ddm002 (2007).
- 160 Ishida, Y. *et al.* Autophagic Elimination of Misfolded Procollagen Aggregates in the Endoplasmic Reticulum as a Means of Cell Protection. *Molecular Biology of the Cell* **20**, 2744-2754, doi:10.1091/mbc.e08-11-1092 (2009).
- 161 Omari, S. *et al.* Noncanonical autophagy at ER exit sites regulates procollagen turnover. *Proceedings of the National Academy of Sciences* **115**, E10099-E10108, doi:10.1073/pnas.1814552115 (2018).
- 162 Forrester, A. *et al.* A selective ER-phagy exerts procollagen quality control via a Calnexin-FAM134B complex. *EMBO J* **38**, doi:10.15252/embj.201899847 (2019).
- 163 Houck, Scott A. *et al.* Quality Control Autophagy Degrades Soluble ERAD-Resistant Conformers of the Misfolded Membrane Protein GnRHR. *Molecular Cell* **54**, 166-179, doi:10.1016/j.molcel.2014.02.025 (2014).
- 164 Schultz, M. L. *et al.* Coordinate regulation of mutant NPC1 degradation by selective ER autophagy and MARCH6-dependent ERAD. *Nature Communications* **9**, doi:10.1038/s41467-018-06115-2 (2018).
- 165 Cunningham, C. N. *et al.* Cells Deploy a Two-Pronged Strategy to Rectify Misfolded Proinsulin Aggregates. *Molecular Cell* **75**, 442-456.e444, doi:10.1016/j.molcel.2019.05.011 (2019).
- 166 Ramachandran, G. N. & Mitra, A. K. An explanation for the rare occurrence of cis peptide units in proteins and polypeptides. *J Mol Biol* **107**, 85-92, doi:10.1016/s0022-2836(76)80019-8 (1976).
- 167 Di Martino, G. P., Masetti, M., Cavalli, A. & Recanatini, M. Mechanistic insights into Pin1 peptidyl-prolylcis-transisomerization from umbrella sampling simulations. *Proteins: Structure, Function, and Bioinformatics* **82**, 2943-2956, doi:10.1002/prot.24650 (2014).
- 168 Schmidpeter, P. A. M. & Schmid, F. X. Prolyl Isomerization and Its Catalysis in Protein Folding and Protein Function. *Journal of Molecular Biology* **427**, 1609-1631, doi:10.1016/j.jmb.2015.01.023 (2015).

- 169 Schmid, F. X. Prolyl Isomerase: Enzymatic Catalysis of Slow Protein-Folding Reactions. *Annual Review of Biophysics and Biomolecular Structure* **22**, 123-143, doi:10.1146/annurev.bb.22.060193.001011 (1993).
- 170 Schmid, F. X., Mayr, L. M., Mucke, M. & Schonbrunner, E. R. Prolyl isomerases: role in protein folding. *Adv Protein Chem* **44**, 25-66, doi:10.1016/s0065-3233(08)60563-x (1993).
- 171 Määttänen, P., Gehring, K., Bergeron, J. J. M. & Thomas, D. Y. Protein quality control in the ER: The recognition of misfolded proteins. *Seminars in Cell & Developmental Biology* **21**, 500-511, doi:10.1016/j.semcdb.2010.03.006 (2010).
- 172 Fischer, G., Wittmann-Liebold, B., Lang, K., Kiefhaber, T. & Schmid, F. X. Cyclophilin and peptidyl-prolyl cis-trans isomerase are probably identical proteins. *Nature* **337**, 476-478, doi:10.1038/337476a0 (1989).
- 173 Lu, K. P., Finn, G., Lee, T. H. & Nicholson, L. K. Prolyl cis-trans isomerization as a molecular timer. *Nature Chemical Biology* **3**, 619-629, doi:10.1038/nchembio.2007.35 (2007).
- 174 Kang, C. B., Hong, Y., Dhe-Paganon, S. & Yoon, H. S. FKBP Family Proteins: Immunophilins with Versatile Biological Functions. *Neurosignals* **16**, 318-325, doi:10.1159/000123041 (2008).
- 175 Liu, J. *et al.* Calcineurin is a common target of cyclophilin-cyclosporin A and FKBP-FK506 complexes. *Cell* **66**, 807-815, doi:10.1016/0092-8674(91)90124-h (1991).
- 176 Kallen, J. *et al.* Structure of human cyclophilin and its binding site for cyclosporin A determined by X-ray crystallography and NMR spectroscopy. *Nature* **353**, 276-279, doi:10.1038/353276a0 (1991).
- 177 Schreiber, S. L. Chemistry and biology of the immunophilins and their immunosuppressive ligands. *Science* **251**, 283-287, doi:10.1126/science.1702904 (1991).
- 178 Jansen, G. *et al.* An Interaction Map of Endoplasmic Reticulum Chaperones and Foldases. *Molecular & Cellular Proteomics* **11**, 710-723, doi:10.1074/mcp.M111.016550 (2012).
- 179 Meunier, L., Usherwood, Y.-K., Chung, K. T., Hendershot, L. M. & Craig, E. A Subset of Chaperones and Folding Enzymes Form Multiprotein Complexes in Endoplasmic Reticulum to Bind Nascent Proteins. *Molecular Biology of the Cell* **13**, 4456-4469, doi:10.1091/mbc.e02-05-0311 (2002).
- 180 Feige, M. J. *et al.* An Unfolded CH1 Domain Controls the Assembly and Secretion of IgG Antibodies. *Molecular Cell* **34**, 569-579, doi:10.1016/j.molcel.2009.04.028 (2009).
- 181 Sevier, C. S. & Kaiser, C. A. Formation and transfer of disulphide bonds in living cells. *Nature Reviews Molecular Cell Biology* **3**, 836-847, doi:10.1038/nrm954 (2002).
- 182 Hwang, C., Sinskey, A. J. & Lodish, H. F. Oxidized redox state of glutathione in the endoplasmic reticulum. *Science* **257**, 1496-1502, doi:10.1126/science.1523409 (1992).
- 183 Paget, M. S. B. & Buttner, M. J. Thiol-Based Regulatory Switches. *Annual Review of Genetics* **37**, 91-121, doi:10.1146/annurev.genet.37.110801.142538 (2003).
- 184 Koehler, C. M., Beverly, K. N. & Leverich, E. P. Redox Pathways of the Mitochondrion. *Antioxidants & Redox Signaling* **8**, 813-822, doi:10.1089/ars.2006.8.813 (2006).

- 185 Wetlaufer, D. B. & Ristow, S. Acquisition of Three-Dimensional Structure of
Proteins. *Annual Review of Biochemistry* **42**, 135-158,
doi:10.1146/annurev.bi.42.070173.001031 (1973).
- 186 Ellgaard, L. & Ruddock, L. W. The human protein disulphide isomerase family:
substrate interactions and functional properties. *EMBO Rep* **6**, 28-32,
doi:10.1038/sj.embor.7400311 (2005).
- 187 Nagradova, N. Enzymes catalyzing protein folding and their cellular functions.
Curr Protein Pept Sci **8**, 273-282, doi:10.2174/138920307780831866 (2007).
- 188 Ellgaard, L., Sevier, C. S. & Bulleid, N. J. How Are Proteins Reduced in the
Endoplasmic Reticulum? *Trends in Biochemical Sciences* **43**, 32-43,
doi:10.1016/j.tibs.2017.10.006 (2018).
- 189 Kozlov, G., Maattanen, P., Thomas, D. Y. & Gehring, K. A structural overview of
the PDI family of proteins. *FEBS J* **277**, 3924-3936, doi:10.1111/j.1742-
4658.2010.07793.x (2010).
- 190 Klappa, P., Ruddock, L. W., Darby, N. J. & Freedman, R. B. The b' domain provides
the principal peptide-binding site of protein disulfide isomerase but all domains
contribute to binding of misfolded proteins. *EMBO J* **17**, 927-935,
doi:10.1093/emboj/17.4.927 (1998).
- 191 Hatahet, F. & Ruddock, L. W. Protein disulfide isomerase: a critical evaluation of
its function in disulfide bond formation. *Antioxid Redox Signal* **11**, 2807-2850,
doi:10.1089/ARS.2009.2466 (2009).
- 192 van Lith, M., Hartigan, N., Hatch, J. & Benham, A. M. PDILT, a Divergent Testis-
specific Protein Disulfide Isomerase with a Non-classical SXXC Motif That
Engages in Disulfide-dependent Interactions in the Endoplasmic Reticulum.
Journal of Biological Chemistry **280**, 1376-1383, doi:10.1074/jbc.M408651200
(2005).
- 193 Meng, X. *et al.* *Biochemical Genetics* **41**, 99-106, doi:10.1023/a:1022073917044
(2003).
- 194 Galligan, J. J. & Petersen, D. R. The human protein disulfide isomerase gene family.
Hum Genomics **6**, 6, doi:10.1186/1479-7364-6-6 (2012).
- 195 Yoshida, H., Haze, K., Yanagi, H., Yura, T. & Mori, K. Identification of the cis-
acting endoplasmic reticulum stress response element responsible for
transcriptional induction of mammalian glucose-regulated proteins. Involvement of
basic leucine zipper transcription factors. *J Biol Chem* **273**, 33741-33749,
doi:10.1074/jbc.273.50.33741 (1998).
- 196 Hatahet, F. & Ruddock, L. W. Substrate recognition by the protein disulfide
isomerases. *FEBS J* **274**, 5223-5234, doi:10.1111/j.1742-4658.2007.06058.x
(2007).
- 197 Matsuo, Y. *et al.* Identification of a novel thioredoxin-related transmembrane
protein. *J Biol Chem* **276**, 10032-10038, doi:10.1074/jbc.M011037200 (2001).
- 198 Akiyama, N., Matsuo, Y., Sai, H., Noda, M. & Kizaka-Kondoh, S. Identification of
a series of transforming growth factor beta-responsive genes by retrovirus-mediated
gene trap screening. *Mol Cell Biol* **20**, 3266-3273, doi:10.1128/mcb.20.9.3266-
3273.2000 (2000).
- 199 Roth, D. *et al.* A di-arginine motif contributes to the ER localization of the type I
transmembrane ER oxidoreductase TMX4. *Biochem J* **425**, 195-205,
doi:10.1042/BJ20091064 (2009).
- 200 Matsuo, Y. *et al.* TMX, a human transmembrane oxidoreductase of the thioredoxin
family: the possible role in disulfide-linked protein folding in the endoplasmic

- reticulum. *Arch Biochem Biophys* **423**, 81-87, doi:10.1016/j.abb.2003.11.003 (2004).
- 201 Pasetto, M. *et al.* Reductive activation of type 2 ribosome-inactivating proteins is promoted by transmembrane thioredoxin-related protein. *J Biol Chem* **287**, 7367-7373, doi:10.1074/jbc.M111.316828 (2012).
- 202 Matsuo, Y., Masutani, H., Son, A., Kizaka-Kondoh, S. & Yodoi, J. Physical and functional interaction of transmembrane thioredoxin-related protein with major histocompatibility complex class I heavy chain: redox-based protein quality control and its potential relevance to immune responses. *Mol Biol Cell* **20**, 4552-4562, doi:10.1091/mbc.E09-05-0439 (2009).
- 203 Matsuo, Y. & Hirota, K. Transmembrane thioredoxin-related protein TMX1 is reversibly oxidized in response to protein accumulation in the endoplasmic reticulum. *FEBS Open Bio* **7**, 1768-1777, doi:10.1002/2211-5463.12319 (2017).
- 204 Matsuo, Y. *et al.* The protective role of the transmembrane thioredoxin-related protein TMX in inflammatory liver injury. *Antioxid Redox Signal* **18**, 1263-1272, doi:10.1089/ars.2011.4430 (2013).
- 205 Schulman, S., Wang, B., Li, W. & Rapoport, T. A. Vitamin K epoxide reductase prefers ER membrane-anchored thioredoxin-like redox partners. *Proceedings of the National Academy of Sciences* **107**, 15027-15032, doi:10.1073/pnas.1009972107 (2010).
- 206 Pisoni, G. B., Ruddock, L. W., Bulleid, N. & Molinari, M. Division of labor among oxidoreductases: TMX1 preferentially acts on transmembrane polypeptides. *Mol Biol Cell* **26**, 3390-3400, doi:10.1091/mbc.E15-05-0321 (2015).
- 207 Lynes, E. M. *et al.* Palmitoylated TMX and calnexin target to the mitochondria-associated membrane. *The EMBO Journal* **31**, 457-470, doi:10.1038/emboj.2011.384 (2012).
- 208 Clark, H. F. The Secreted Protein Discovery Initiative (SPDI), a Large-Scale Effort to Identify Novel Human Secreted and Transmembrane Proteins: A Bioinformatics Assessment. *Genome Research* **13**, 2265-2270, doi:10.1101/gr.1293003 (2003).
- 209 Shaheen, R. *et al.* Characterizing the morbid genome of ciliopathies. *Genome Biology* **17**, doi:10.1186/s13059-016-1099-5 (2016).
- 210 Radhakrishnan, P., Nayak, S. S., Shukla, A., Lindstrand, A. & Girisha, K. M. Meckel syndrome: Clinical and mutation profile in six fetuses. *Clinical Genetics* **96**, 560-565, doi:10.1111/cge.13623 (2019).
- 211 Ridnői, K. *et al.* A prenatally diagnosed case of Meckel–Gruber syndrome with novel compound heterozygous pathogenic variants in the TXNDC15 gene. *Molecular Genetics & Genomic Medicine* **7**, doi:10.1002/mgg3.614 (2019).
- 212 Oguro, A. & Imaoka, S. Thioredoxin-related transmembrane protein 2 (TMX2) regulates the Ran protein gradient and importin-beta-dependent nuclear cargo transport. *Sci Rep* **9**, 15296, doi:10.1038/s41598-019-51773-x (2019).
- 213 Vandervore, L. V. *et al.* TMX2 Is a Crucial Regulator of Cellular Redox State, and Its Dysfunction Causes Severe Brain Developmental Abnormalities. *Am J Hum Genet* **105**, 1126-1147, doi:10.1016/j.ajhg.2019.10.009 (2019).
- 214 Kramer, N. J. *et al.* CRISPR–Cas9 screens in human cells and primary neurons identify modifiers of C9ORF72 dipeptide-repeat-protein toxicity. *Nature Genetics* **50**, 603-612, doi:10.1038/s41588-018-0070-7 (2018).
- 215 Ghosh, S. G. *et al.* Recurrent homozygous damaging mutation in TMX2, encoding a protein disulfide isomerase, in four families with microlissencephaly. *J Med Genet* **57**, 274-282, doi:10.1136/jmedgenet-2019-106409 (2020).

- 216 Haugstetter, J., Blicher, T. & Ellgaard, L. Identification and characterization of a novel thioredoxin-related transmembrane protein of the endoplasmic reticulum. *J Biol Chem* **280**, 8371-8380, doi:10.1074/jbc.M413924200 (2005).
- 217 Chen, R. *et al.* Glycoproteomics Analysis of Human Liver Tissue by Combination of Multiple Enzyme Digestion and Hydrazide Chemistry. *Journal of Proteome Research* **8**, 651-661, doi:10.1021/pr8008012 (2009).
- 218 Haugstetter, J. *et al.* Structure-Function Analysis of the Endoplasmic Reticulum Oxidoreductase TMX3 Reveals Interdomain Stabilization of the N-terminal Redox-active Domain. *Journal of Biological Chemistry* **282**, 33859-33867, doi:10.1074/jbc.M706442200 (2007).
- 219 Fox, J., Lu, Z. & Barrows, L. Thiol-disulfide Oxidoreductases TRX1 and TMX3 Decrease Neuronal Atrophy in a Lentiviral Mouse Model of Huntington's Disease. *PLoS Currents*, doi:10.1371/currents.hd.b966ec2eca8e2d89d2bb4d020be4351e (2016).
- 220 Sugiura, Y. *et al.* Novel thioredoxin-related transmembrane protein TMX4 has reductase activity. *J Biol Chem* **285**, 7135-7142, doi:10.1074/jbc.M109.082545 (2010).
- 221 Roos, G. *et al.* The Conserved Active Site Proline Determines the Reducing Power of Staphylococcus aureus Thioredoxin. *Journal of Molecular Biology* **368**, 800-811, doi:10.1016/j.jmb.2007.02.045 (2007).
- 222 Bergmann, T. J. & Molinari, M. Three branches to rule them all? UPR signalling in response to chemically versus misfolded proteins-induced ER stress. *Biology of the Cell* **110**, 197-204, doi:10.1111/boc.201800029 (2018).
- 223 Wang, M. & Kaufman, R. J. Protein misfolding in the endoplasmic reticulum as a conduit to human disease. *Nature* **529**, 326-335, doi:10.1038/nature17041 (2016).
- 224 Adams, C. J., Kopp, M. C., Larburu, N., Nowak, P. R. & Ali, M. M. U. Structure and Molecular Mechanism of ER Stress Signaling by the Unfolded Protein Response Signal Activator IRE1. *Frontiers in Molecular Biosciences* **6**, doi:10.3389/fmolb.2019.00011 (2019).
- 225 Taylor, R. C., Berendzen, K. M. & Dillin, A. Systemic stress signalling: understanding the cell non-autonomous control of proteostasis. *Nature Reviews Molecular Cell Biology* **15**, 211-217, doi:10.1038/nrm3752 (2014).
- 226 Hetz, C., Chevet, E. & Oakes, S. A. Proteostasis control by the unfolded protein response. *Nature Cell Biology* **17**, 829-838, doi:10.1038/ncb3184 (2015).
- 227 Martinon, F. & Aksentijevich, I. New players driving inflammation in monogenic autoinflammatory diseases. *Nature Reviews Rheumatology* **11**, 11-20, doi:10.1038/nrrheum.2014.158 (2014).
- 228 Jan Bergmann, T., Brambilla Pisoni, G. & Molinari, M. Quality control mechanisms of protein biogenesis: proteostasis dies hard. *AIMS Biophysics* **3**, 456-478, doi:10.3934/biophy.2016.4.456 (2016).
- 229 Hetz, C. & Papa, F. R. The Unfolded Protein Response and Cell Fate Control. *Molecular Cell* **69**, 169-181, doi:10.1016/j.molcel.2017.06.017 (2018).
- 230 Lee, A.-H., Iwakoshi, N. N. & Glimcher, L. H. XBP-1 Regulates a Subset of Endoplasmic Reticulum Resident Chaperone Genes in the Unfolded Protein Response. *Molecular and Cellular Biology* **23**, 7448-7459, doi:10.1128/mcb.23.21.7448-7459.2003 (2003).
- 231 Acosta-Alvear, D. *et al.* XBP1 Controls Diverse Cell Type- and Condition-Specific Transcriptional Regulatory Networks. *Molecular Cell* **27**, 53-66, doi:10.1016/j.molcel.2007.06.011 (2007).

- 232 Farhan, H., Weiss, M., Tani, K., Kaufman, R. J. & Hauri, H.-P. Adaptation of endoplasmic reticulum exit sites to acute and chronic increases in cargo load. *The EMBO Journal* **27**, 2043-2054, doi:10.1038/emboj.2008.136 (2008).
- 233 Hampton, R. Y. & Ron, D. Membrane biogenesis and the unfolded protein response. *Journal of Cell Biology* **167**, 23-25, doi:10.1083/jcb.200408117 (2004).
- 234 Bommasamy, H. *et al.* ATF6 induces XBP1-independent expansion of the endoplasmic reticulum. *Journal of Cell Science* **122**, 1626-1636, doi:10.1242/jcs.045625 (2009).
- 235 Schuck, S., Prinz, W. A., Thorn, K. S., Voss, C. & Walter, P. Membrane expansion alleviates endoplasmic reticulum stress independently of the unfolded protein response. *The Journal of Cell Biology* **187**, 525-536, doi:10.1083/jcb.200907074 (2009).
- 236 Harding, H. P., Zhang, Y. & Ron, D. Protein translation and folding are coupled by an endoplasmic-reticulum-resident kinase. *Nature* **397**, 271-274, doi:10.1038/16729 (1999).
- 237 Harding, H. P., Zhang, Y., Bertolotti, A., Zeng, H. & Ron, D. Perk is essential for translational regulation and cell survival during the unfolded protein response. *Mol Cell* **5**, 897-904, doi:10.1016/s1097-2765(00)80330-5 (2000).
- 238 Travers, K. J. *et al.* Functional and Genomic Analyses Reveal an Essential Coordination between the Unfolded Protein Response and ER-Associated Degradation. *Cell* **101**, 249-258, doi:10.1016/s0092-8674(00)80835-1 (2000).
- 239 Shore, G. C., Papa, F. R. & Oakes, S. A. Signaling cell death from the endoplasmic reticulum stress response. *Current Opinion in Cell Biology* **23**, 143-149, doi:10.1016/j.ceb.2010.11.003 (2011).
- 240 Tabas, I. & Ron, D. Integrating the mechanisms of apoptosis induced by endoplasmic reticulum stress. *Nature Cell Biology* **13**, 184-190, doi:10.1038/ncb0311-184 (2011).
- 241 Tirasophon, W., Welihinda, A. A. & Kaufman, R. J. A stress response pathway from the endoplasmic reticulum to the nucleus requires a novel bifunctional protein kinase/endoribonuclease (Ire1p) in mammalian cells. *Genes & Development* **12**, 1812-1824, doi:10.1101/gad.12.12.1812 (1998).
- 242 Haze, K., Yoshida, H., Yanagi, H., Yura, T. & Mori, K. Mammalian transcription factor ATF6 is synthesized as a transmembrane protein and activated by proteolysis in response to endoplasmic reticulum stress. *Mol Biol Cell* **10**, 3787-3799, doi:10.1091/mbc.10.11.3787 (1999).
- 243 Shen, J., Chen, X., Hendershot, L. & Prywes, R. ER stress regulation of ATF6 localization by dissociation of BiP/GRP78 binding and unmasking of Golgi localization signals. *Dev Cell* **3**, 99-111, doi:10.1016/s1534-5807(02)00203-4 (2002).
- 244 Shamu, C. E., Cox, J. S. & Walter, P. The unfolded-protein-response pathway in yeast. *Trends Cell Biol* **4**, 56-60, doi:10.1016/0962-8924(94)90011-6 (1994).
- 245 Bertolotti, A., Zhang, Y., Hendershot, L. M., Harding, H. P. & Ron, D. Dynamic interaction of BiP and ER stress transducers in the unfolded-protein response. *Nature Cell Biology* **2**, 326-332, doi:10.1038/35014014 (2000).
- 246 Okamura, K., Kimata, Y., Higashio, H., Tsuru, A. & Kohno, K. Dissociation of Kar2p/BiP from an ER Sensory Molecule, Ire1p, Triggers the Unfolded Protein Response in Yeast. *Biochemical and Biophysical Research Communications* **279**, 445-450, doi:10.1006/bbrc.2000.3987 (2000).

- 247 Carrara, M., Prischi, F., Nowak, P. R., Kopp, M. C. & Ali, M. M. U. Noncanonical binding of BiP ATPase domain to Ire1 and Perk is dissociated by unfolded protein CH1 to initiate ER stress signaling. *eLife* **4**, doi:10.7554/eLife.03522 (2015).
- 248 Kelly, J. W. *et al.* BiP Binding to the ER-Stress Sensor Ire1 Tunes the Homeostatic Behavior of the Unfolded Protein Response. *PLoS Biology* **8**, doi:10.1371/journal.pbio.1000415 (2010).
- 249 Credle, J. J., Finer-Moore, J. S., Papa, F. R., Stroud, R. M. & Walter, P. On the mechanism of sensing unfolded protein in the endoplasmic reticulum. *Proceedings of the National Academy of Sciences* **102**, 18773-18784, doi:10.1073/pnas.0509487102 (2005).
- 250 Gardner, B. M. & Walter, P. Unfolded Proteins Are Ire1-Activating Ligands That Directly Induce the Unfolded Protein Response. *Science* **333**, 1891-1894, doi:10.1126/science.1209126 (2011).
- 251 Promlek, T. *et al.* Membrane aberrancy and unfolded proteins activate the endoplasmic reticulum stress sensor Ire1 in different ways. *Molecular Biology of the Cell* **22**, 3520-3532, doi:10.1091/mbc.e11-04-0295 (2011).
- 252 Iwawaki, T., Akai, R., Yamanaka, S. & Kohno, K. Function of IRE1 alpha in the placenta is essential for placental development and embryonic viability. *Proceedings of the National Academy of Sciences* **106**, 16657-16662, doi:10.1073/pnas.0903775106 (2009).
- 253 Tsuru, A. *et al.* Negative feedback by IRE1 optimizes mucin production in goblet cells. *Proceedings of the National Academy of Sciences* **110**, 2864-2869, doi:10.1073/pnas.1212484110 (2013).
- 254 Bertolotti, A. *et al.* Increased sensitivity to dextran sodium sulfate colitis in IRE1 β -deficient mice. *Journal of Clinical Investigation* **107**, 585-593, doi:10.1172/jci11476 (2001).
- 255 Chen, Y. & Brandizzi, F. IRE1: ER stress sensor and cell fate executor. *Trends in Cell Biology* **23**, 547-555, doi:10.1016/j.tcb.2013.06.005 (2013).
- 256 Mori, K., Ma, W., Gething, M. J. & Sambrook, J. A transmembrane protein with a cdc2+/CDC28-related kinase activity is required for signaling from the ER to the nucleus. *Cell* **74**, 743-756, doi:10.1016/0092-8674(93)90521-q (1993).
- 257 Cox, J. S. & Walter, P. A novel mechanism for regulating activity of a transcription factor that controls the unfolded protein response. *Cell* **87**, 391-404, doi:10.1016/s0092-8674(00)81360-4 (1996).
- 258 Lee, K. P. K. *et al.* Structure of the Dual Enzyme Ire1 Reveals the Basis for Catalysis and Regulation in Nonconventional RNA Splicing. *Cell* **132**, 89-100, doi:10.1016/j.cell.2007.10.057 (2008).
- 259 Aragón, T. *et al.* Messenger RNA targeting to endoplasmic reticulum stress signalling sites. *Nature* **457**, 736-740, doi:10.1038/nature07641 (2008).
- 260 Korenykh, A. V. *et al.* The unfolded protein response signals through high-order assembly of Ire1. *Nature* **457**, 687-693, doi:10.1038/nature07661 (2008).
- 261 Sidrauski, C. & Walter, P. The Transmembrane Kinase Ire1p Is a Site-Specific Endonuclease That Initiates mRNA Splicing in the Unfolded Protein Response. *Cell* **90**, 1031-1039, doi:10.1016/s0092-8674(00)80369-4 (1997).
- 262 Uemura, A., Oku, M., Mori, K. & Yoshida, H. Unconventional splicing of XBP1 mRNA occurs in the cytoplasm during the mammalian unfolded protein response. *Journal of Cell Science* **122**, 2877-2886, doi:10.1242/jcs.040584 (2009).
- 263 Adamson, B. *et al.* A Multiplexed Single-Cell CRISPR Screening Platform Enables Systematic Dissection of the Unfolded Protein Response. *Cell* **167**, 1867-1882.e1821, doi:10.1016/j.cell.2016.11.048 (2016).

- 264 Yamamoto, K. Differential Contributions of ATF6 and XBP1 to the Activation of Endoplasmic Reticulum Stress-Responsive cis-Acting Elements ERSE, UPRE and ERSE-II. *Journal of Biochemistry* **136**, 343-350, doi:10.1093/jb/mvh122 (2004).
- 265 Yoshida, H. *et al.* A time-dependent phase shift in the mammalian unfolded protein response. *Dev Cell* **4**, 265-271, doi:10.1016/s1534-5807(03)00022-4 (2003).
- 266 Maurel, M., Chevet, E., Tavernier, J. & Gerlo, S. Getting RIDD of RNA: IRE1 in cell fate regulation. *Trends in Biochemical Sciences* **39**, 245-254, doi:10.1016/j.tibs.2014.02.008 (2014).
- 267 Iwawaki, T. *et al.* Translational control by the ER transmembrane kinase/ribonuclease IRE1 under ER stress. *Nature Cell Biology* **3**, 158-164, doi:10.1038/35055065 (2001).
- 268 Hollien, J. & Weissman, J. S. Decay of Endoplasmic Reticulum-Localized mRNAs During the Unfolded Protein Response. *Science* **313**, 104-107, doi:10.1126/science.1129631 (2006).
- 269 Hollien, J. *et al.* Regulated Ire1-dependent decay of messenger RNAs in mammalian cells. *The Journal of Cell Biology* **186**, 323-331, doi:10.1083/jcb.200903014 (2009).
- 270 Han, D. *et al.* IRE1 α Kinase Activation Modes Control Alternate Endoribonuclease Outputs to Determine Divergent Cell Fates. *Cell* **138**, 562-575, doi:10.1016/j.cell.2009.07.017 (2009).
- 271 Lerner, Alana G. *et al.* IRE1 α Induces Thioredoxin-Interacting Protein to Activate the NLRP3 Inflammasome and Promote Programmed Cell Death under Irremediable ER Stress. *Cell Metabolism* **16**, 250-264, doi:10.1016/j.cmet.2012.07.007 (2012).
- 272 Upton, J. P. *et al.* IRE1 Cleaves Select microRNAs During ER Stress to Derepress Translation of Proapoptotic Caspase-2. *Science* **338**, 818-822, doi:10.1126/science.1226191 (2012).
- 273 Ghosh, R. *et al.* Allosteric Inhibition of the IRE1 α RNase Preserves Cell Viability and Function during Endoplasmic Reticulum Stress. *Cell* **158**, 534-548, doi:10.1016/j.cell.2014.07.002 (2014).
- 274 Urano, F. Coupling of Stress in the ER to Activation of JNK Protein Kinases by Transmembrane Protein Kinase IRE1. *Science* **287**, 664-666, doi:10.1126/science.287.5453.664 (2000).
- 275 Nishitoh, H. ASK1 is essential for endoplasmic reticulum stress-induced neuronal cell death triggered by expanded polyglutamine repeats. *Genes & Development* **16**, 1345-1355, doi:10.1101/gad.992302 (2002).
- 276 Thuerauf, D. J., Morrison, L. & Glembotski, C. C. Opposing Roles for ATF6 α and ATF6 β in Endoplasmic Reticulum Stress Response Gene Induction. *Journal of Biological Chemistry* **279**, 21078-21084, doi:10.1074/jbc.M400713200 (2004).
- 277 Schindler, A. J. & Schekman, R. In vitro reconstitution of ER-stress induced ATF6 transport in COPII vesicles. *Proceedings of the National Academy of Sciences* **106**, 17775-17780, doi:10.1073/pnas.0910342106 (2009).
- 278 Ye, J. *et al.* ER Stress Induces Cleavage of Membrane-Bound ATF6 by the Same Proteases that Process SREBPs. *Molecular Cell* **6**, 1355-1364, doi:10.1016/s1097-2765(00)00133-7 (2000).
- 279 Kokame, K., Kato, H. & Miyata, T. Identification of ERSE-II, a New cis-Acting Element Responsible for the ATF6-dependent Mammalian Unfolded Protein Response. *Journal of Biological Chemistry* **276**, 9199-9205, doi:10.1074/jbc.M010486200 (2001).

- 280 McQuiston, A. & Diehl, J. A. Recent insights into PERK-dependent signaling from
the stressed endoplasmic reticulum. *F1000Research* **6**,
doi:10.12688/f1000research.12138.1 (2017).
- 281 Scheuner, D. *et al.* Translational control is required for the unfolded protein
response and in vivo glucose homeostasis. *Mol Cell* **7**, 1165-1176,
doi:10.1016/s1097-2765(01)00265-9 (2001).
- 282 Sonenberg, N. & Hinnebusch, A. G. Regulation of Translation Initiation in
Eukaryotes: Mechanisms and Biological Targets. *Cell* **136**, 731-745,
doi:10.1016/j.cell.2009.01.042 (2009).
- 283 Ron, D., Harding, H. P. & Lu, P. D. Translation reinitiation at alternative open
reading frames regulates gene expression in an integrated stress response. *Journal
of Cell Biology* **167**, 27-33, doi:10.1083/jcb.200408003 (2004).
- 284 Vattem, K. M. & Wek, R. C. Reinitiation involving upstream ORFs regulates ATF4
mRNA translation in mammalian cells. *Proceedings of the National Academy of
Sciences* **101**, 11269-11274, doi:10.1073/pnas.0400541101 (2004).
- 285 Harding, H. P. *et al.* An integrated stress response regulates amino acid metabolism
and resistance to oxidative stress. *Mol Cell* **11**, 619-633, doi:10.1016/s1097-
2765(03)00105-9 (2003).
- 286 Ye, J. & Koumenis, C. ATF4, an ER stress and hypoxia-inducible transcription
factor and its potential role in hypoxia tolerance and tumorigenesis. *Curr Mol Med*
9, 411-416, doi:10.2174/156652409788167096 (2009).
- 287 B'chir, W. *et al.* The eIF2 α /ATF4 pathway is essential for stress-induced autophagy
gene expression. *Nucleic Acids Research* **41**, 7683-7699, doi:10.1093/nar/gkt563
(2013).
- 288 Han, J. *et al.* ER-stress-induced transcriptional regulation increases protein
synthesis leading to cell death. *Nature Cell Biology* **15**, 481-490,
doi:10.1038/ncb2738 (2013).
- 289 Urrea, H., Dufey, E., Lisbona, F., Rojas-Rivera, D. & Hetz, C. When ER stress
reaches a dead end. *Biochimica et Biophysica Acta (BBA) - Molecular Cell
Research* **1833**, 3507-3517, doi:10.1016/j.bbamcr.2013.07.024 (2013).
- 290 Fawcett, T. W., Martindale, J. L., Guyton, K. Z., Hai, T. & Holbrook, N. J.
Complexes containing activating transcription factor (ATF)/cAMP-responsive-
element-binding protein (CREB) interact with the CCAAT/enhancer-binding
protein (C/EBP)-ATF composite site to regulate Gadd153 expression during the
stress response. *Biochem J* **339 (Pt 1)**, 135-141 (1999).
- 291 Marciniak, S. J. CHOP induces death by promoting protein synthesis and oxidation
in the stressed endoplasmic reticulum. *Genes & Development* **18**, 3066-3077,
doi:10.1101/gad.1250704 (2004).
- 292 Tsaytler, P., Harding, H. P., Ron, D. & Bertolotti, A. Selective Inhibition of a
Regulatory Subunit of Protein Phosphatase 1 Restores Proteostasis. *Science* **332**,
91-94, doi:10.1126/science.1201396 (2011).
- 293 Ma, Y. & Hendershot, L. M. Delineation of a Negative Feedback Regulatory Loop
That Controls Protein Translation during Endoplasmic Reticulum Stress. *Journal
of Biological Chemistry* **278**, 34864-34873, doi:10.1074/jbc.M301107200 (2003).
- 294 Liu, C. Y. The unfolded protein response. *Journal of Cell Science* **116**, 1861-1862,
doi:10.1242/jcs.00408 (2003).
- 295 Fregno, I. & Molinari, M. Endoplasmic reticulum turnover: ER-phagy and other
flavors in selective and non-selective ER clearance. *F1000Res* **7**, 454,
doi:10.12688/f1000research.13968.1 (2018).

- 296 Loi, M., Fregno, I., Guerra, C. & Molinari, M. Eat it right: ER-phagy and recoverER-phagy. *Biochem Soc Trans* **46**, 699-706, doi:10.1042/BST20170354 (2018).
- 297 Fumagalli, F. *et al.* Translocon component Sec62 acts in endoplasmic reticulum turnover during stress recovery. *Nat Cell Biol* **18**, 1173-1184, doi:10.1038/ncb3423 (2016).
- 298 Loi, M., Raimondi, A., Morone, D. & Molinari, M. ESCRT-III-driven piecemeal micro-ER-phagy remodels the ER during recovery from ER stress. *Nat Commun* **10**, 5058, doi:10.1038/s41467-019-12991-z (2019).
- 299 Huppa, J. B. & Ploegh, H. L. The eS-Sence of -SH in the ER. *Cell* **92**, 145-148, doi:10.1016/s0092-8674(00)80907-1 (1998).
- 300 Molinari, M. & Helenius, A. Glycoproteins form mixed disulphides with oxidoreductases during folding in living cells. *Nature* **402**, 90-93, doi:10.1038/47062 (1999).
- 301 Soldà, T., Garbi, N., Hämmerling, G. J. & Molinari, M. Consequences of ERp57 Deletion on Oxidative Folding of Obligate and Facultative Clients of the Calnexin Cycle. *Journal of Biological Chemistry* **281**, 6219-6226, doi:10.1074/jbc.M513595200 (2006).
- 302 Rutkevich, L. A., Cohen-Doyle, M. F., Brockmeier, U., Williams, D. B. & Glick, B. S. Functional Relationship between Protein Disulfide Isomerase Family Members during the Oxidative Folding of Human Secretory Proteins. *Molecular Biology of the Cell* **21**, 3093-3105, doi:10.1091/mbc.e10-04-0356 (2010).
- 303 Grubb, S., Guo, L., Fisher, E. A., Brodsky, J. L. & Gilmore, R. Protein disulfide isomerases contribute differentially to the endoplasmic reticulum-associated degradation of apolipoprotein B and other substrates. *Molecular Biology of the Cell* **23**, 520-532, doi:10.1091/mbc.e11-08-0704 (2012).
- 304 Pisoni, G. B. & Molinari, M. Five Questions (with their Answers) on ER-Associated Degradation. *Traffic* **17**, 341-350, doi:10.1111/tra.12373 (2016).
- 305 Wada, I. [Calnexin is involved in the quality-control mechanism of the ER]. *Seikagaku* **67**, 1133-1137 (1995).
- 306 Hebert, D. N., Zhang, J. X., Chen, W., Foellmer, B. & Helenius, A. The number and location of glycans on influenza hemagglutinin determine folding and association with calnexin and calreticulin. *J Cell Biol* **139**, 613-623, doi:10.1083/jcb.139.3.613 (1997).
- 307 Danilczyk, U. G., Cohen-Doyle, M. F. & Williams, D. B. Functional relationship between calreticulin, calnexin, and the endoplasmic reticulum luminal domain of calnexin. *J Biol Chem* **275**, 13089-13097, doi:10.1074/jbc.275.17.13089 (2000).
- 308 Ho, S. C. *et al.* Membrane anchoring of calnexin facilitates its interaction with its targets. *Mol Immunol* **36**, 1-12, doi:10.1016/s0161-5890(99)00018-8 (1999).
- 309 Ninagawa, S., Okada, T., Takeda, S. & Mori, K. SEL1L is required for endoplasmic reticulum-associated degradation of misfolded luminal proteins but not transmembrane proteins in chicken DT40 cell line. *Cell Struct Funct* **36**, 187-195, doi:10.1247/csf.11018 (2011).
- 310 Cunnea, P. M. *et al.* ERdj5, an Endoplasmic Reticulum (ER)-resident Protein Containing DnaJ and Thioredoxin Domains, Is Expressed in Secretory Cells or following ER Stress. *Journal of Biological Chemistry* **278**, 1059-1066, doi:10.1074/jbc.M206995200 (2003).
- 311 Chichiarelli, S. *et al.* The stress protein ERp57/GRP58 binds specific DNA sequences in HeLa cells. *Journal of Cellular Physiology* **210**, 343-351, doi:10.1002/jcp.20824 (2007).

- 312 Anelli, T. ERp44, a novel endoplasmic reticulum folding assistant of the
thioredoxin family. *The EMBO Journal* **21**, 835-844, doi:10.1093/emboj/21.4.835
(2002).
- 313 Osowski, C. M. & Urano, F. in *The Unfolded Protein Response and Cellular
Stress, Part B Methods in Enzymology* 71-92 (2011).
- 314 Otsu, M. *et al.* Dynamic Retention of Ero1 α and Ero1 β in the Endoplasmic
Reticulum by Interactions with PDI and ERp44. *Antioxidants & Redox Signaling* **8**,
274-282, doi:10.1089/ars.2006.8.274 (2006).
- 315 Anelli, T. *et al.* Thiol-mediated protein retention in the endoplasmic reticulum: the
role of ERp44. *EMBO J* **22**, 5015-5022, doi:10.1093/emboj/cdg491 (2003).
- 316 Hartill, V., Szymanska, K., Sharif, S. M., Wheway, G. & Johnson, C. A. Meckel-
Gruber Syndrome: An Update on Diagnosis, Clinical Management, and Research
Advances. *Frontiers in Pediatrics* **5**, doi:10.3389/fped.2017.00244 (2017).
- 317 Braakman, I. & Hebert, D. N. Protein folding in the endoplasmic reticulum. *Cold
Spring Harb Perspect Biol* **5**, a013201, doi:10.1101/cshperspect.a013201 (2013).
- 318 Ross, C. A. & Poirier, M. A. Protein aggregation and neurodegenerative disease.
Nature Medicine **10**, S10-S17, doi:10.1038/nm1066 (2004).
- 319 Wolff, S., Weissman, Jonathan S. & Dillin, A. Differential Scales of Protein Quality
Control. *Cell* **157**, 52-64, doi:10.1016/j.cell.2014.03.007 (2014).
- 320 England, C. G., Luo, H. & Cai, W. HaloTag technology: a versatile platform for
biomedical applications. *Bioconjug Chem* **26**, 975-986,
doi:10.1021/acs.bioconjchem.5b00191 (2015).
- 321 Neklesa, T. K. *et al.* Small-molecule hydrophobic tagging-induced degradation of
HaloTag fusion proteins. *Nature Chemical Biology* **7**, 538-543,
doi:10.1038/nchembio.597 (2011).
- 322 Ronchi, P., Colombo, S., Francolini, M. & Borgese, N. Transmembrane domain-
dependent partitioning of membrane proteins within the endoplasmic reticulum. *J
Cell Biol* **181**, 105-118, doi:10.1083/jcb.200710093 (2008).
- 323 Raina, K. *et al.* Targeted protein destabilization reveals an estrogen-mediated ER
stress response. *Nat Chem Biol* **10**, 957-962, doi:10.1038/nchembio.1638 (2014).
- 324 Pobre, K. F. R., Poet, G. J. & Hendershot, L. M. The endoplasmic reticulum (ER)
chaperone BiP is a master regulator of ER functions: Getting by with a little help
from ERdj friends. *Journal of Biological Chemistry* **294**, 2098-2108,
doi:10.1074/jbc.REV118.002804 (2019).
- 325 Bergmann, T. J. *et al.* Chemical stresses fail to mimic the unfolded protein response
resulting from luminal load with unfolded polypeptides. *J Biol Chem* **293**, 5600-
5612, doi:10.1074/jbc.RA117.001484 (2018).
- 326 Murray, L. A., Knight, D. A. & Laurent, G. J. in *Asthma and COPD* 193-200
(2009).
- 327 Ishikawa, Y., Ito, S., Nagata, K., Sakai, L. Y. & Bächinger, H. P. Intracellular
mechanisms of molecular recognition and sorting for transport of large extracellular
matrix molecules. *Proceedings of the National Academy of Sciences* **113**, E6036-
E6044, doi:10.1073/pnas.1609571113 (2016).
- 328 Martina, J. A., Diab, H. I., Brady, O. A. & Puertollano, R. TFEB and TFE3 are
novel components of the integrated stress response. *The EMBO Journal* **35**, 479-
495, doi:10.15252/embj.201593428 (2016).
- 329 Tejada-Muñoz, N., Albrecht, L. V., Bui, M. H. & De Robertis, E. M. Wnt canonical
pathway activates macropinocytosis and lysosomal degradation of extracellular

- proteins. *Proceedings of the National Academy of Sciences* **116**, 10402-10411, doi:10.1073/pnas.1903506116 (2019).
- 330 Karagöz, G. E., Acosta-Alvear, D. & Walter, P. The Unfolded Protein Response: Detecting and Responding to Fluctuations in the Protein-Folding Capacity of the Endoplasmic Reticulum. *Cold Spring Harbor Perspectives in Biology* **11**, doi:10.1101/cshperspect.a033886 (2019).
- 331 Iurlaro, R. & Muñoz-Pinedo, C. Cell death induced by endoplasmic reticulum stress. *The FEBS Journal* **283**, 2640-2652, doi:10.1111/febs.13598 (2016).
- 332 Brodsky, J. L. & Skach, W. R. Protein folding and quality control in the endoplasmic reticulum: Recent lessons from yeast and mammalian cell systems. *Curr Opin Cell Biol* **23**, 464-475, doi:10.1016/j.ceb.2011.05.004 (2011).
- 333 Sun, Z. & Brodsky, J. L. Protein quality control in the secretory pathway. *J Cell Biol* **218**, 3171-3187, doi:10.1083/jcb.201906047 (2019).
- 334 Okumura, M., Kadokura, H. & Inaba, K. Structures and functions of protein disulfide isomerase family members involved in proteostasis in the endoplasmic reticulum. *Free Radic Biol Med* **83**, 314-322, doi:10.1016/j.freeradbiomed.2015.02.010 (2015).
- 335 Hatahet, F. & Ruddock, L. W. Modulating proteostasis: peptidomimetic inhibitors and activators of protein folding. *Curr Pharm Des* **15**, 2488-2507, doi:10.2174/138161209788682343 (2009).
- 336 Neklesa, T. K. *et al.* Small-molecule hydrophobic tagging-induced degradation of HaloTag fusion proteins. *Nat Chem Biol* **7**, 538-543, doi:10.1038/nchembio.597 (2011).

10 ACKNOWLEDGEMENTS

Here, this journey comes to an end. This thesis would never exist without the contribution of many people that during these years supported me, in the good and in the bad times.

My biggest thank goes to Maurizio Molinari. I arrived in Bellinzona as a ‘little’ Master student with quite few ideas about what science could really mean. He gave me the opportunity to perform my PhD studies in his lab and to work on challenging and interesting projects. He guided and supported me through this journey, even when it was not so easy to do. Thank you.

Many thanks to the members of my PhD committee Prof. Kutay and Prof. Peter for insightful comments and stimulating discussions during the committee meetings.

For technical help and collaborations, I would like to thank Andrea Rinaldi, Manfredo Quadroni and Mathilde Perez.

To all the current and former members of the Molinari Lab. Marisa, Ilaria, Giorgia, Elisa, Carmela, Tatiana, Timothy, Fiorenza, Alessandro, thank you! From the very first day, Lab 403 felt like home for me. For the technical and moral help, for all the time that we spent together and for all the things that we went through, you are not just colleagues. Ah, and Marika, enjoy your time in 403!

Thank you, Cipressi. Even in the darkest moments, I never felt alone. Thank you for the laughs, the aperos, the dinners Chez Vicolo Muggiasca and wherever, the crazy holidays together, and for the parties, of course! These years would not have been so wonderful.

To this quarantine, that even if so difficult and strange, gave me the opportunity to think about myself and the world around.

Last, but not least. Grazie alla mia famiglia. Senza di voi, nulla di tutto questo sarebbe mai esistito. Grazie per avermi fatto sempre sentire il vostro supporto e il vostro amore, anche quando negli anni la lontananza faceva più paura. Siete stati sempre al mio fianco, in ogni mia scelta e decisione, e sono sicura che lo sarete sempre. Siamo un’unica realtà.

Ok, now I can stop crying! ;)